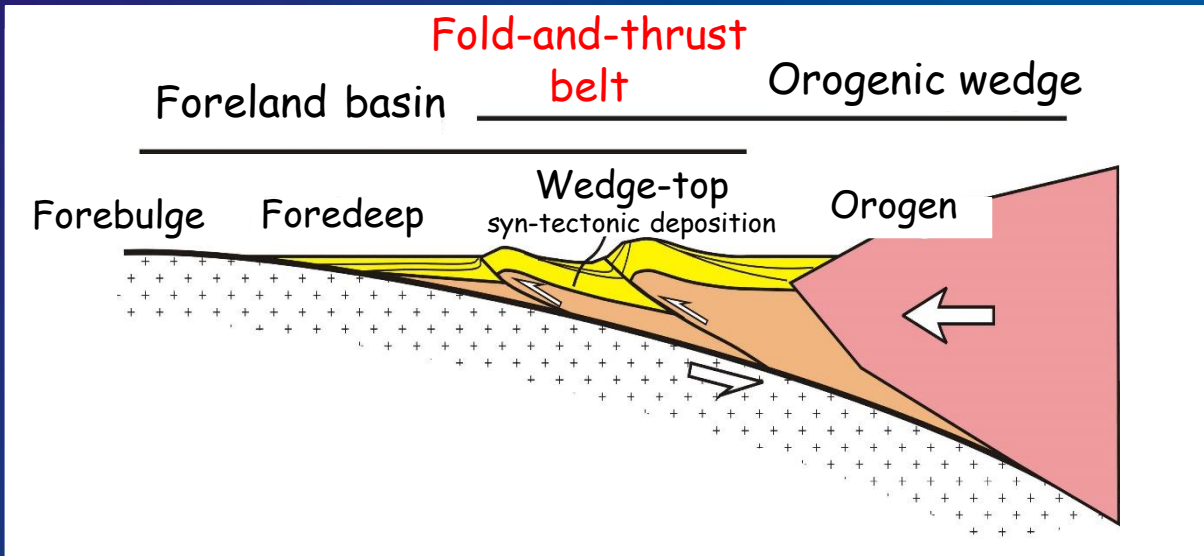
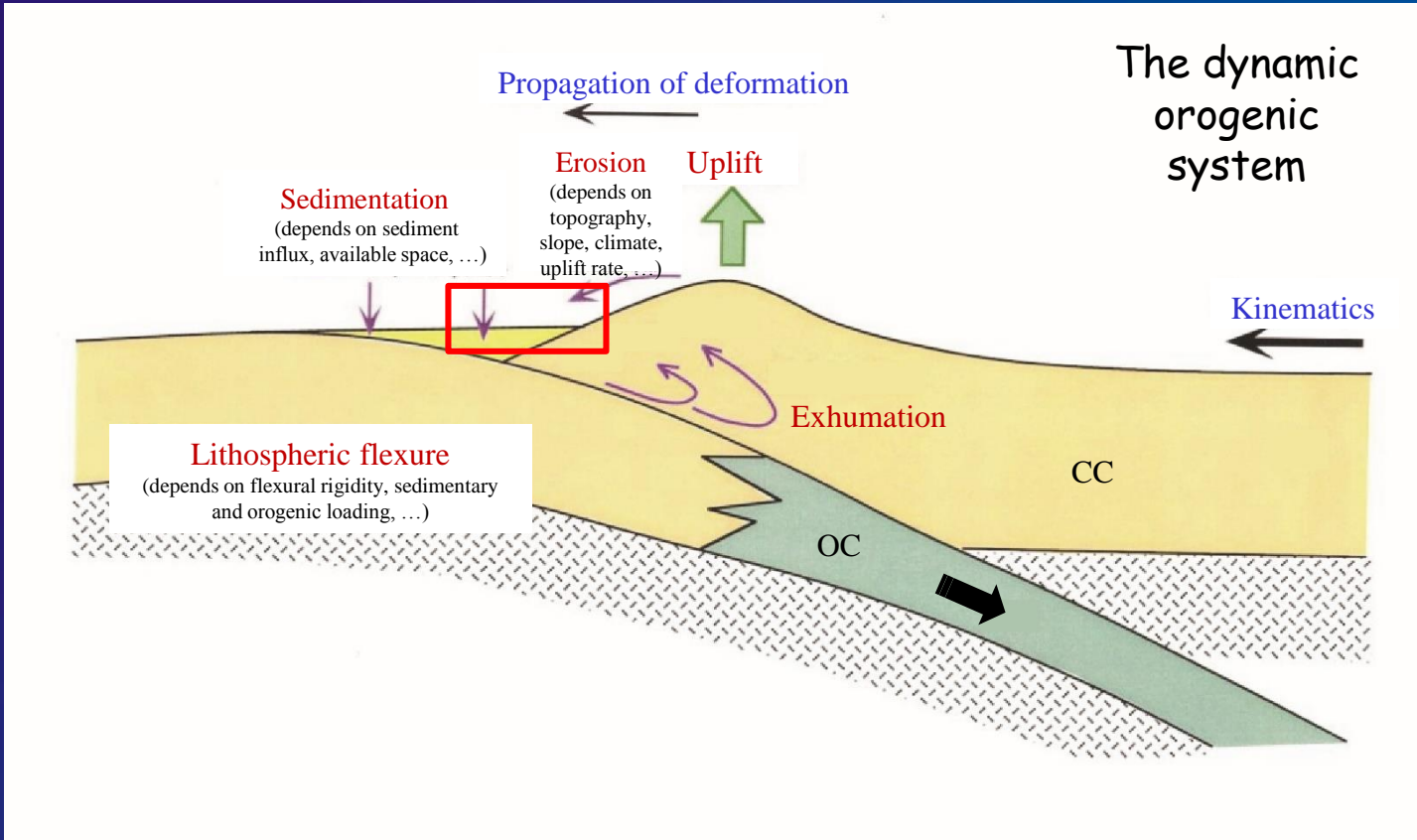


Foreland fold-and-thrust belts

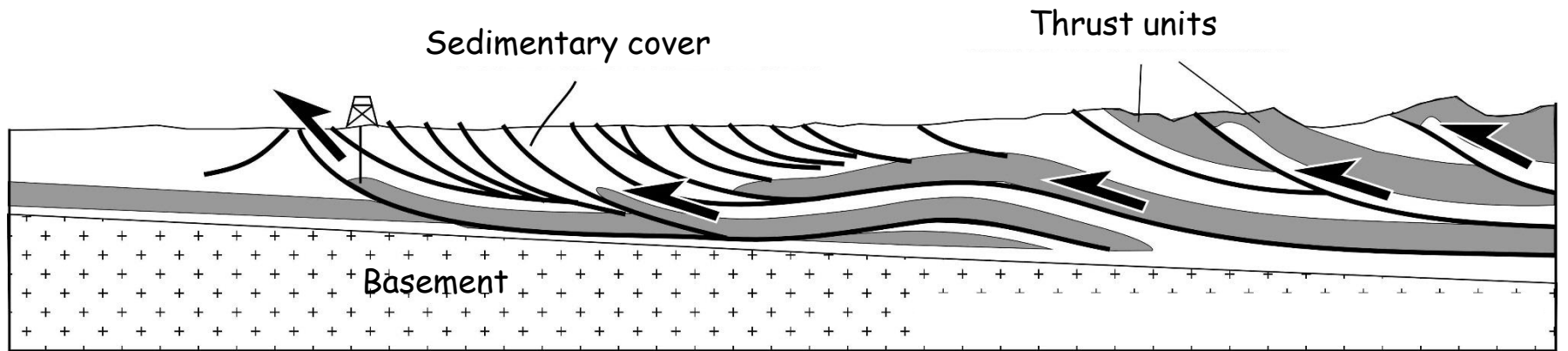
Part 1 : geometry, mechanics, structural styles and first-order controls

Olivier LACOMBE





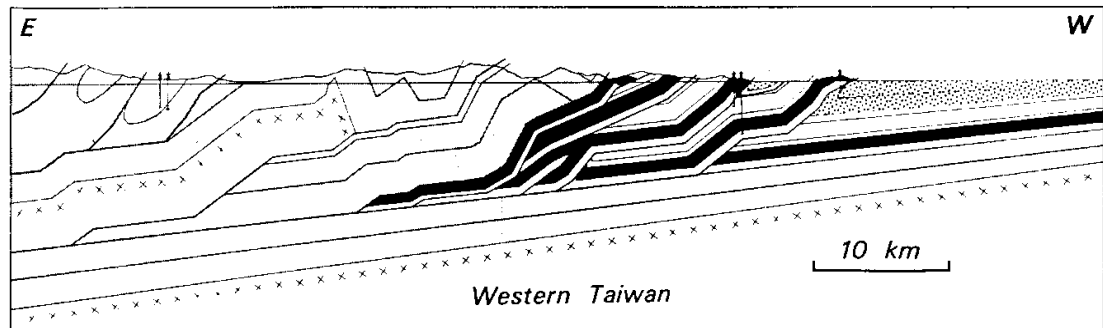
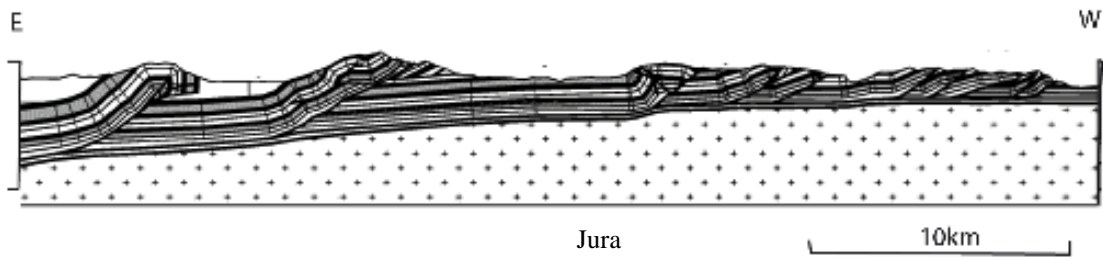
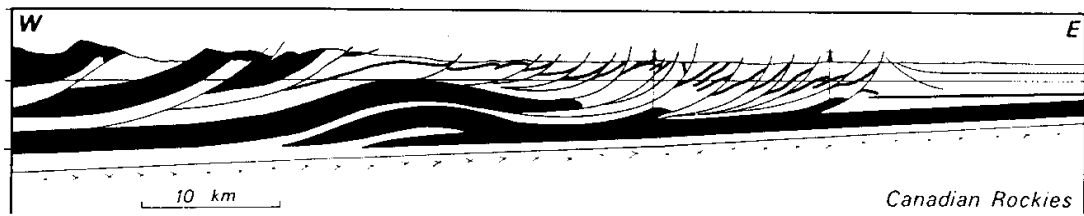
Fold-and-thrust belts and foreland basins, witnesses of interactions between deep and surface processes



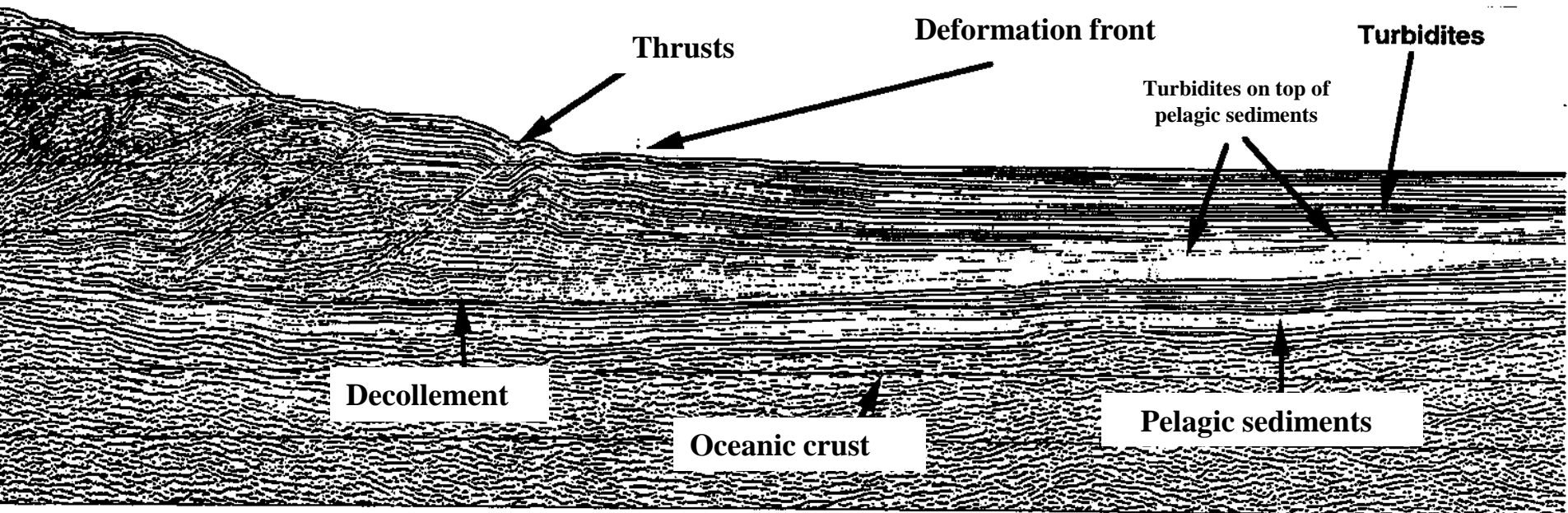
Shortening is usually accommodated in the upper part of the crust by stacking of thrust units above a basal décollement dipping toward the hinterland

Topographic slope and dip of basal décollement define the orogenic wedge

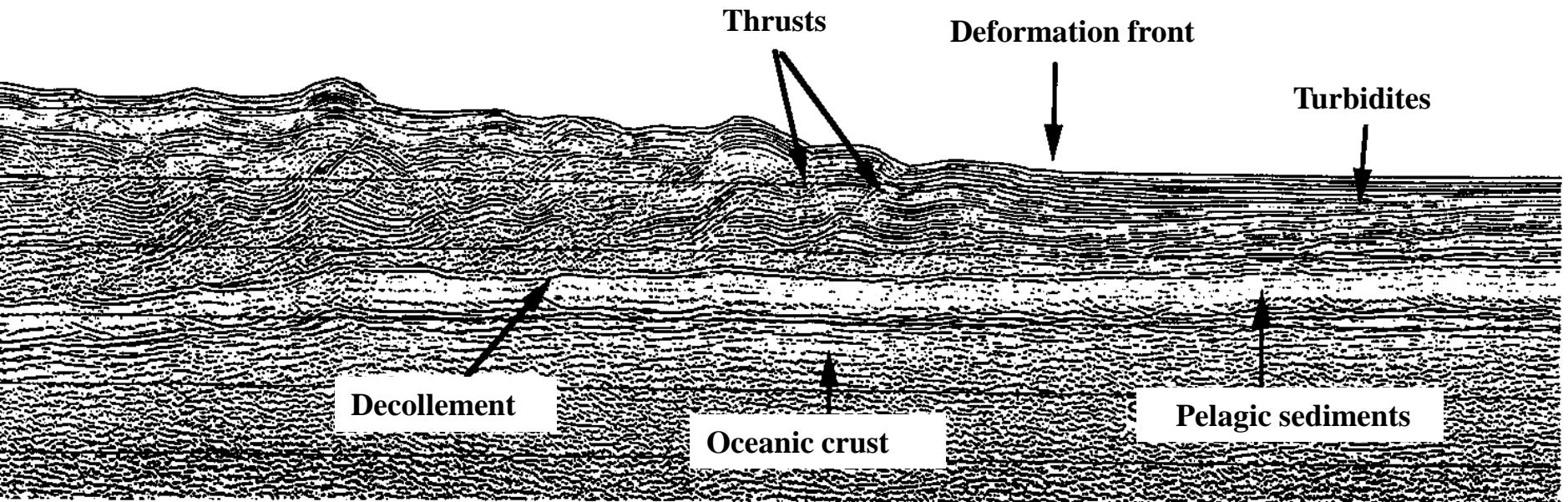
Usual implicit hypothesis of thin-skinned tectonics



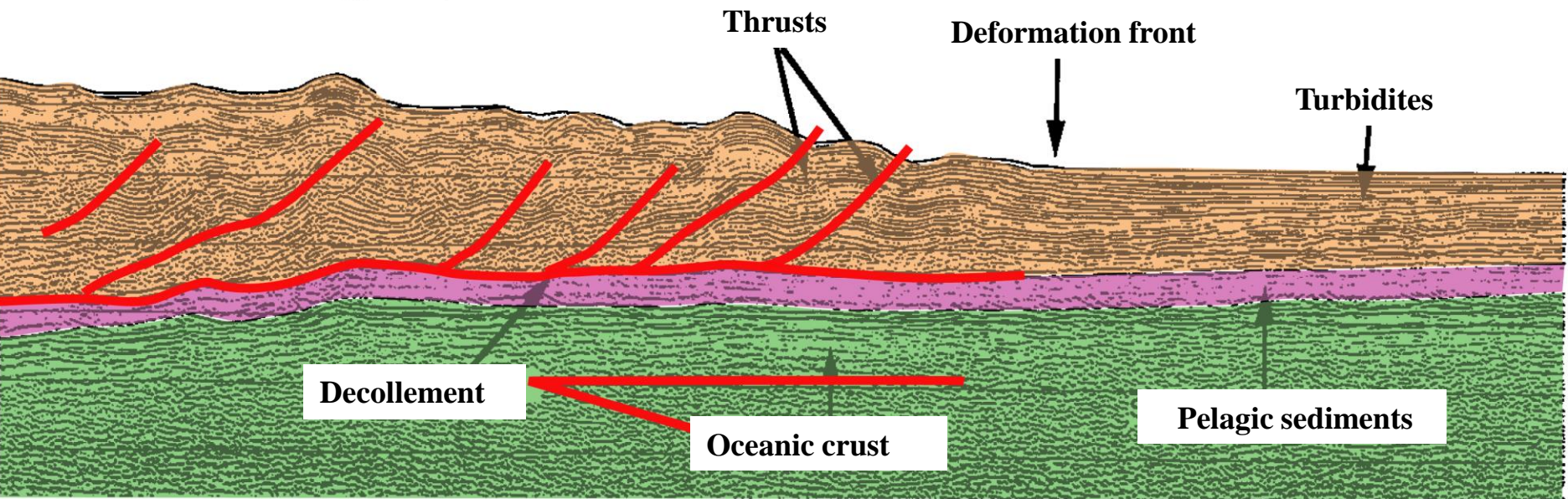
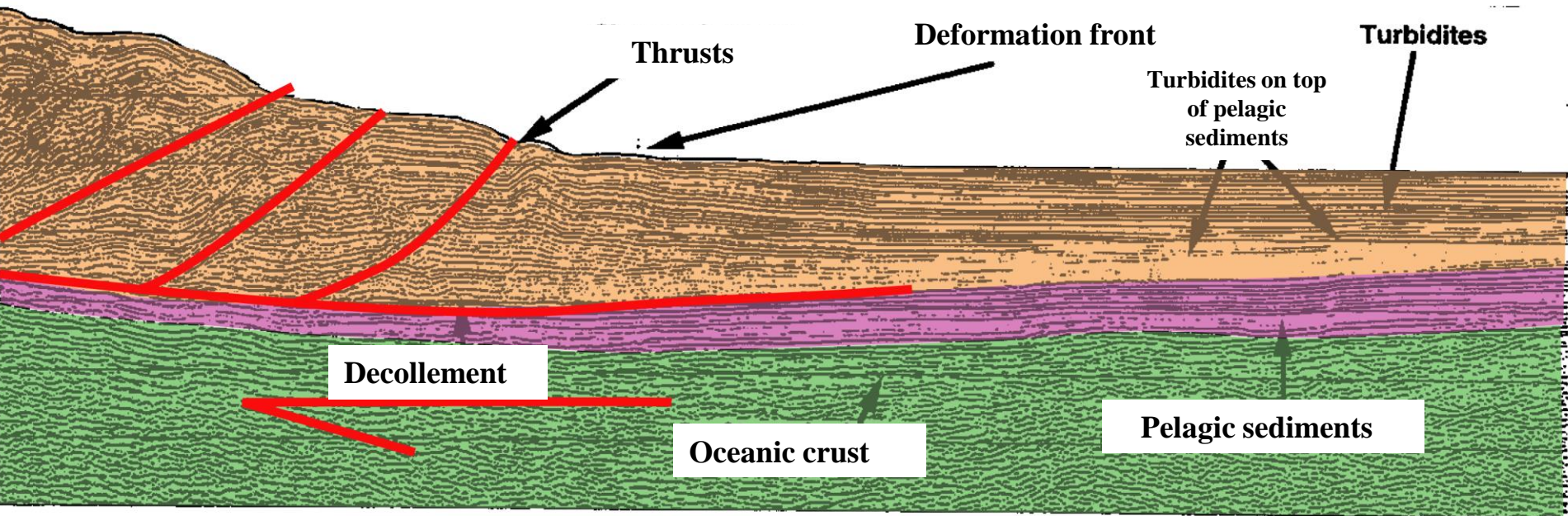
Analogue to oceanic sedimentary accretionary wedges



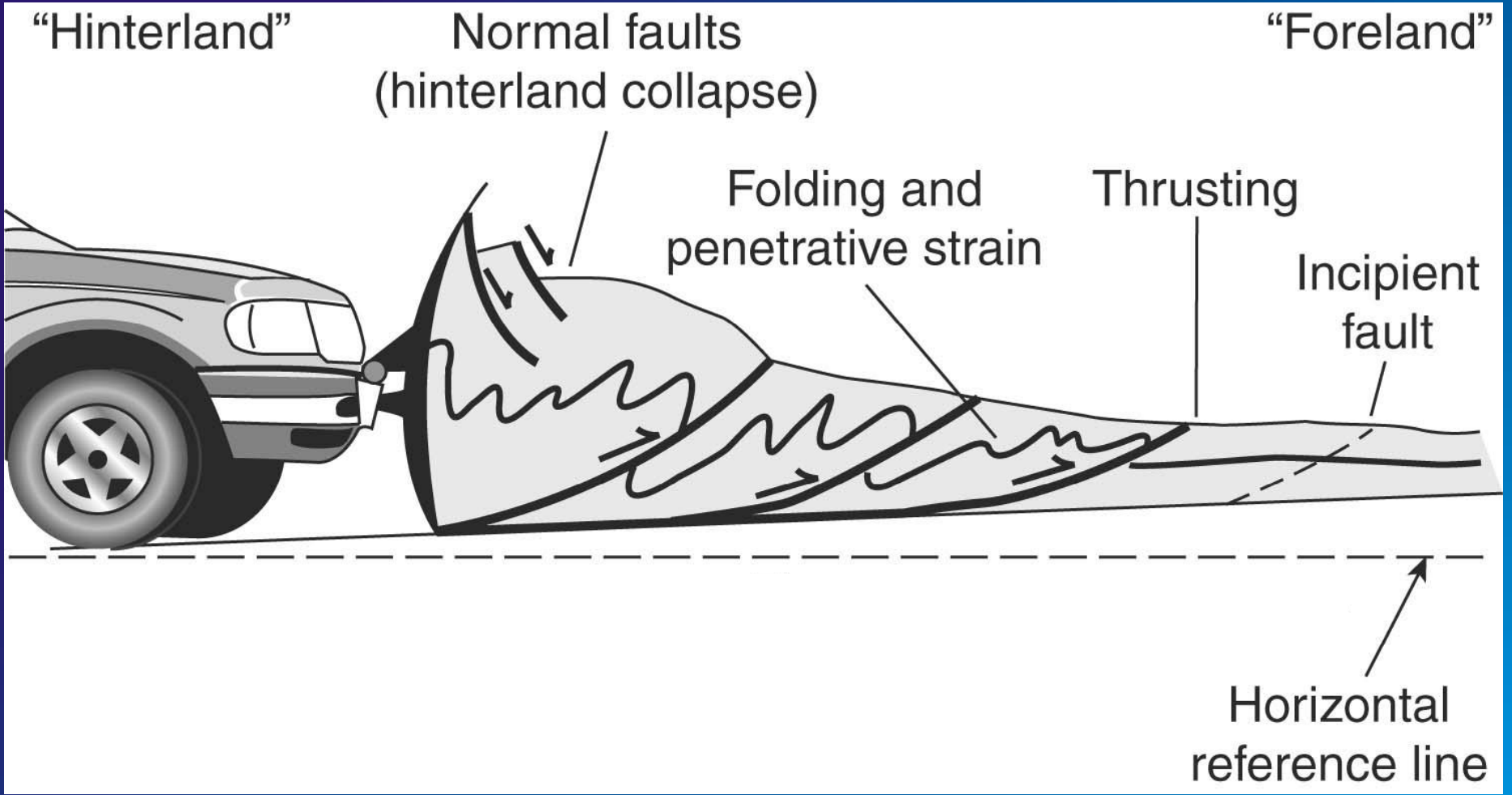
1 km



Analogue to oceanic sedimentary accretionary wedges

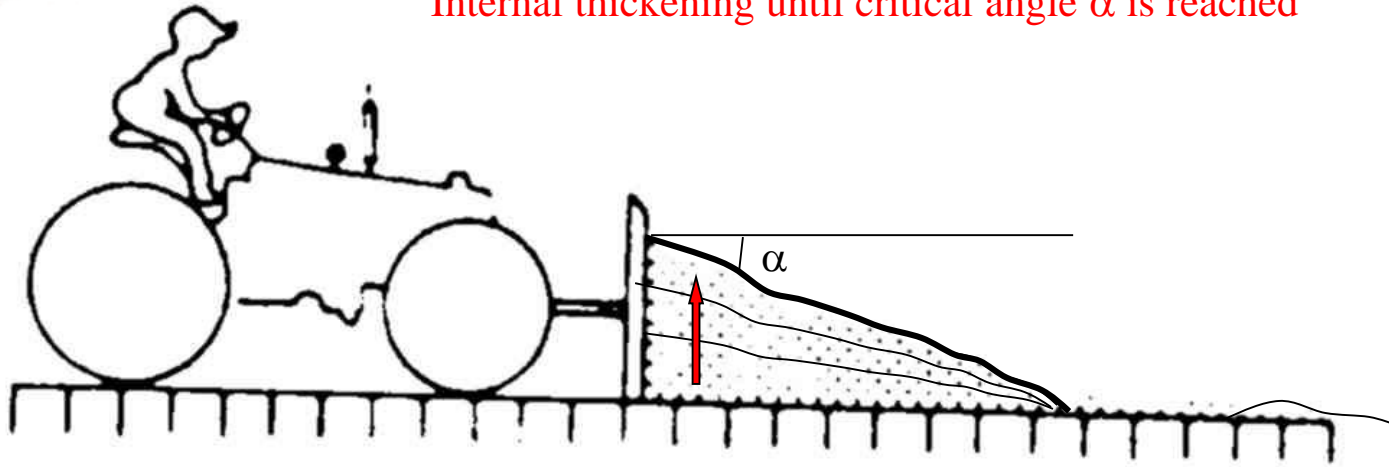


Mechanics of fold-and-thrust belts

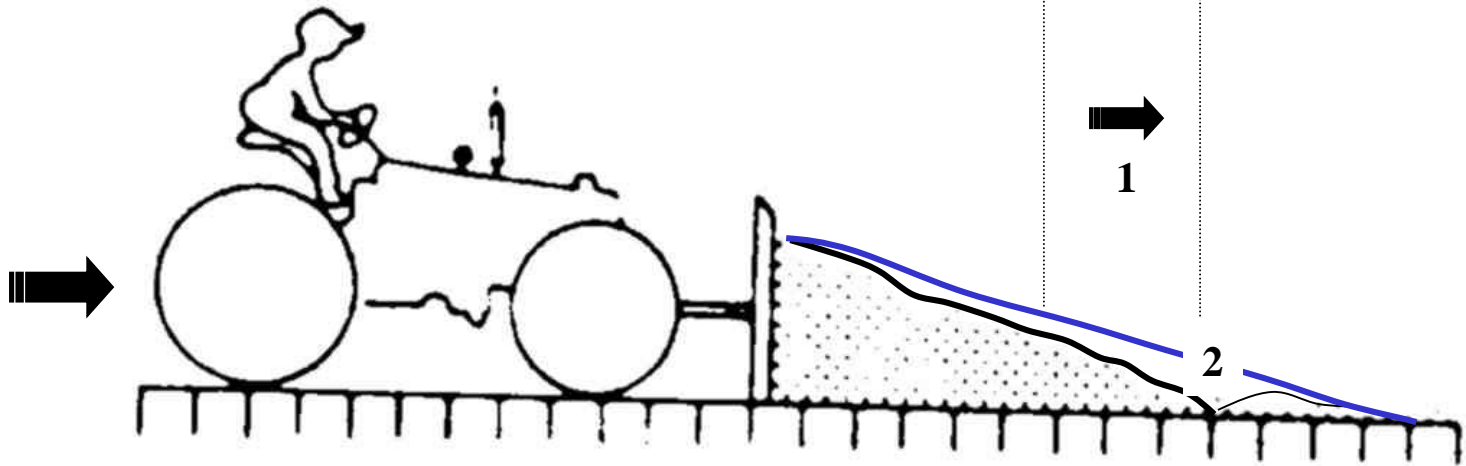




Internal thickening until critical angle α is reached



1. Basal sliding without internal thickening, then
2. New snow is incorporated in the wedge, α is lowered, then
3. The wedge will deform internally until α is reached again, and so on



The critical Taper

1983 : Davis et al. : Mechanics of wedge analogue to soil or snow in front of a moving bulldozer.

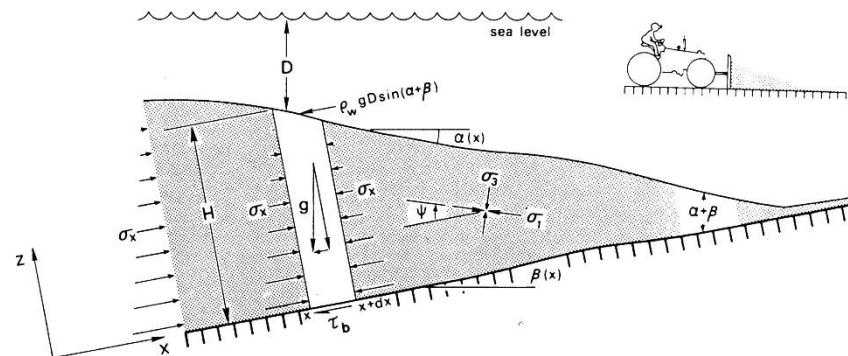
Mechanics of Fold-and-Thrust Belts and Accretionary Wedges

DAN DAVIS

Department of Earth and Planetary Sciences, Massachusetts Institute of Technology
Cambridge, Massachusetts 02139

JOHN SUPPE AND F. A. DAHLEN

The overall mechanics of fold-and-thrust belts and accretionary wedges along compressive plate boundaries is considered to be analogous to that of a wedge of soil or snow in front of a moving bulldozer. The material within the wedge deforms until a critical taper is attained, after which it slides stably, continuing to grow at constant taper as additional material is encountered at the toe. The critical taper is the shape for which the wedge is on the verge of failure under horizontal compression everywhere, including the basal decollement. A wedge of less than critical taper will not slide when pushed but will deform internally, steepening its surface slope until the critical taper is attained. Common silicate sediments and rocks in the upper 10–15 km of the crust have pressure-dependent brittle compressive strengths which can be approximately represented by the empirical Coulomb failure criterion, modified to account for the weakening effects of pore fluid pressure.



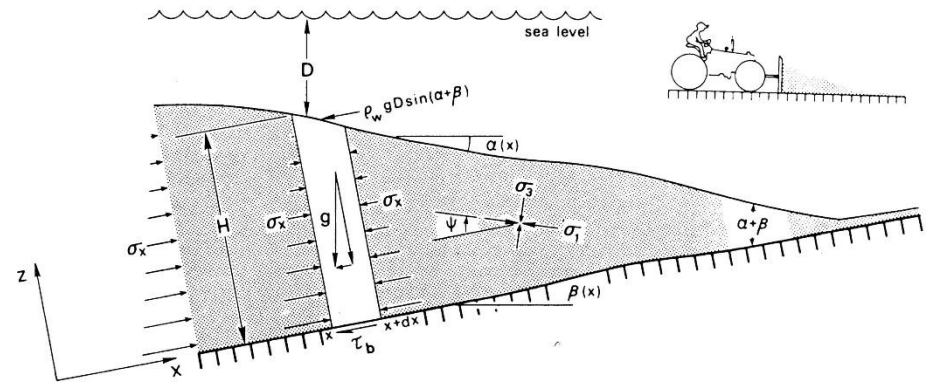
The critical Taper

Coulomb criterion : Rock deformation in the upper crust is governed by pressure dependent and time independent Coulomb behavior, ie by **brittle fracture** (Paterson, 1978) or **frictional sliding** (Byerlee, 1978).

$$|\tau| = S_0 + \mu(\sigma_n - p_f)$$

$$\sigma_n^* = \sigma_n - p_f$$

$$|\tau| = \mu\sigma_n^*$$



Force equilibrium : Gravitational body force, pressure of water, frictional resistance to sliding along the basal decollement, compressive push :

$$\rho g H \sin \beta + \rho_w g D \sin (\alpha + \beta) + \tau_b + \frac{d}{dx} \int_0^H \sigma_x dz = 0$$

Thin-skinned structures allow small angles approximations :

$$\rho g H \beta + \rho_w g D (\alpha + \beta) + \tau_b + \frac{d}{dx} \int_0^H \sigma_x dz = 0$$

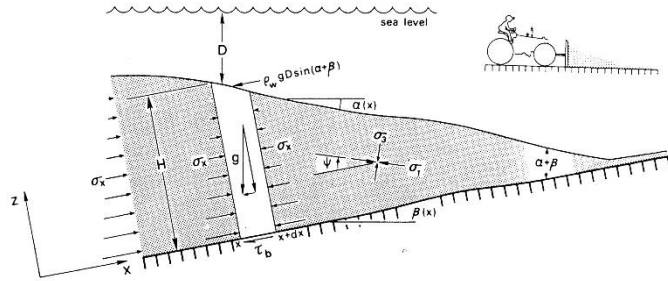
Weight of sedimentary column (lithostatic pressure)

Weight of water column

Basal frictional shear strength

Sum of lateral push forces

The critical Taper



$$\rho g H \beta + \rho_w g D (\alpha + \beta) + \tau_b + \frac{d}{dx} \int_0^H \sigma_x dz = 0$$

$$\int_0^H \sigma_x dz = \rho_w g D H + \frac{1}{2} \rho g H^2$$

$$+ 2 \rho g \int_0^H \frac{(1 - \lambda)(H - z)}{\csc \phi \sec 2\psi - 1} dz \quad (13)$$

Invoking the small-angle approximation once again, we set

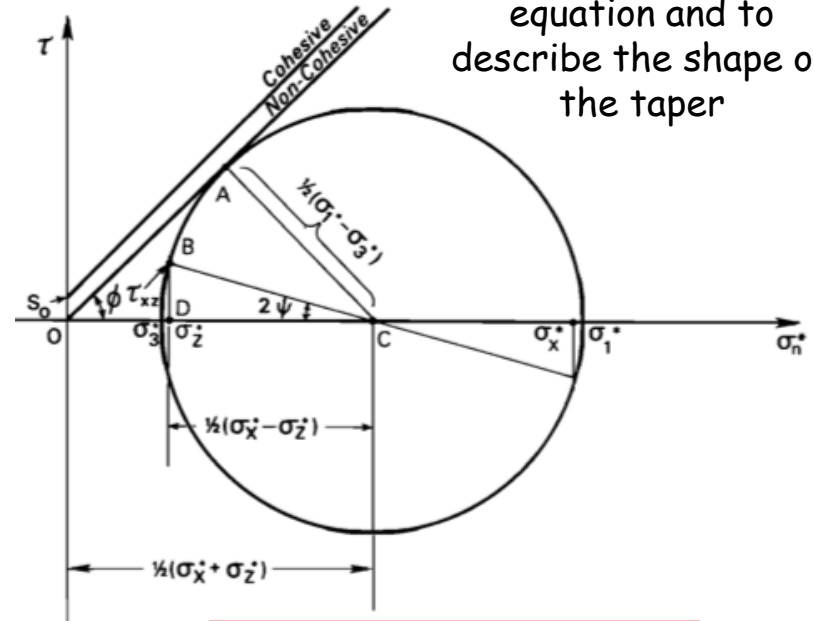
$$dH/dx = -(\alpha + \beta) \quad (14)$$

$$dD/dx = \alpha \quad (15)$$

$$K = 2H^{-1} \int_0^H \frac{dz}{\csc \phi \sec 2\psi(z) - 1}$$

$$\lambda = \frac{\rho_f - \rho_w g D}{|\sigma_z| - \rho_w g D}$$

The Mohr diagram is used to solve the equation and to describe the shape of the taper



$$\alpha + \beta = \frac{(1 - \lambda_b) \mu_b + (1 - \rho_w/\rho) \beta}{(1 - \rho_w/\rho) + (1 - \lambda) K} \quad (18)$$

It is noteworthy that this equation contains no explicit dependence on x so that a wedge with uniform properties and a planar base should have a constant surface slope. Note, in addition, that in the limit $\lambda_b \rightarrow \lambda \rightarrow 1$, (18) reduces to $\alpha \rightarrow 0$, which is the expected result for a wedge composed of material having negligible strength.

No length scale : scale independent

The critical Taper

Sandbox validation :



Formula for dry and cohesionless sand :

$$\alpha + \beta = \frac{\mu_b + \beta}{1 + K}$$

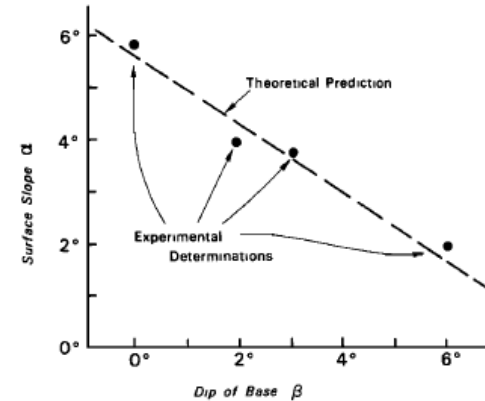


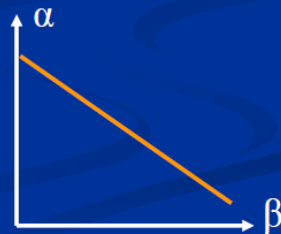
Fig. 8. Mean surface slope measured by linear regression off photographs versus dip of rigid base in sandbox experiments. Dots represent the average of eight experimental runs at $\beta = 0^\circ$, two at $\beta = 2^\circ$, fourteen at $\beta = 3^\circ$, and nine at $\beta = 6^\circ$. Line is theoretical prediction $\alpha = 5.9^\circ - 0.66\beta$.



$$\alpha + \beta = f(\mu, \mu_b, \lambda, \lambda_b)$$

$$\alpha + R\beta = F$$

Linear relationship
between α and β

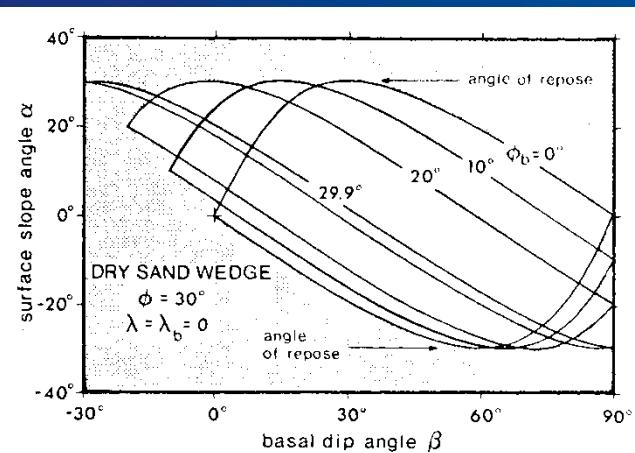
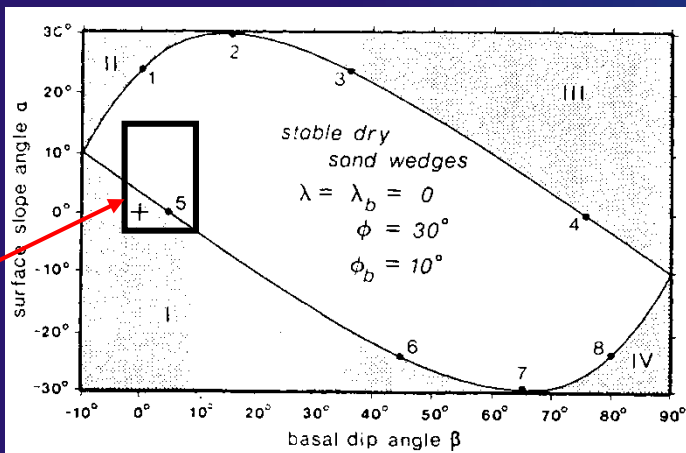


Force equilibrium results in a simple linear relation :

$$F = \alpha + \beta R$$

$$R = \frac{(1 - \lambda)K}{(1 - \rho_w / \rho) + (1 - \lambda)K}$$

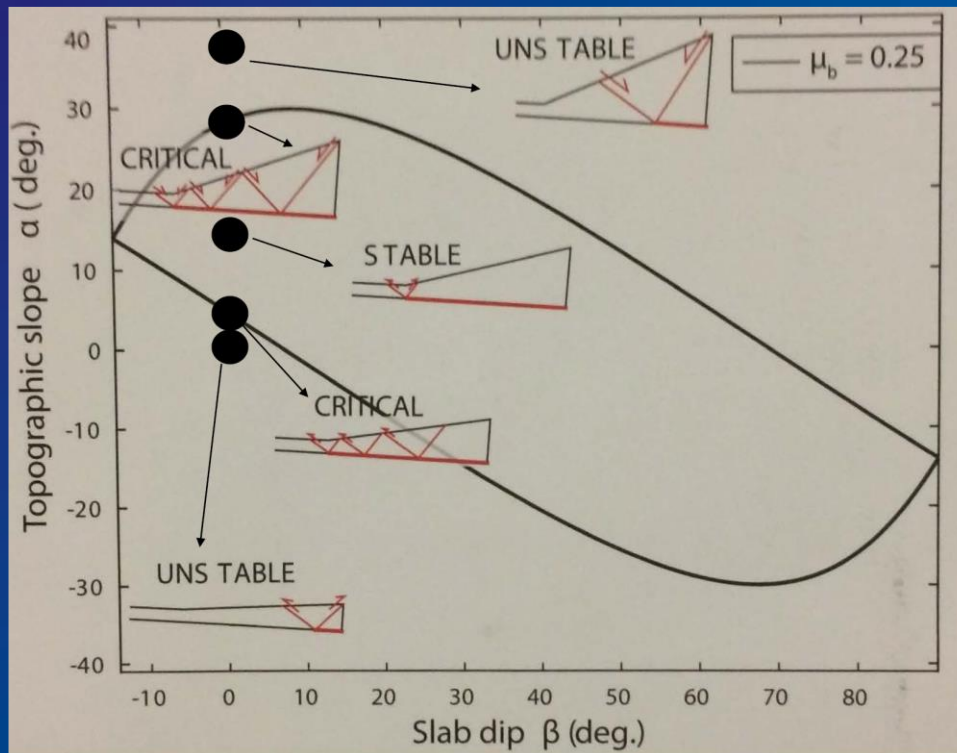
$$F = \frac{(1 - \lambda_b)\mu_b}{(1 - \rho_w / \rho) + (1 - \lambda)K}$$



Most accretionary wedges

The area inside the "lens shape" corresponds to the stability regime of the wedge, when it does not deform.

Along the envelope of the lens, the wedge is under critical conditions and is growing self-similarly. Outside of the lens, the wedge is in an under- or overcritical state. In the undercritical domain, compression is favoured, whereas extension occurs in the overcritical domain. Both types of adjustment tend to occur to restore the stability slope of the prism.



Critical taper : shape for which the wedge is on the verge of failure under horizontal compression everywhere, including the basal décollement

The stability domain is large for a weak basal friction and is reduced to a line when the basal friction of a dry wedge equals the internal friction.

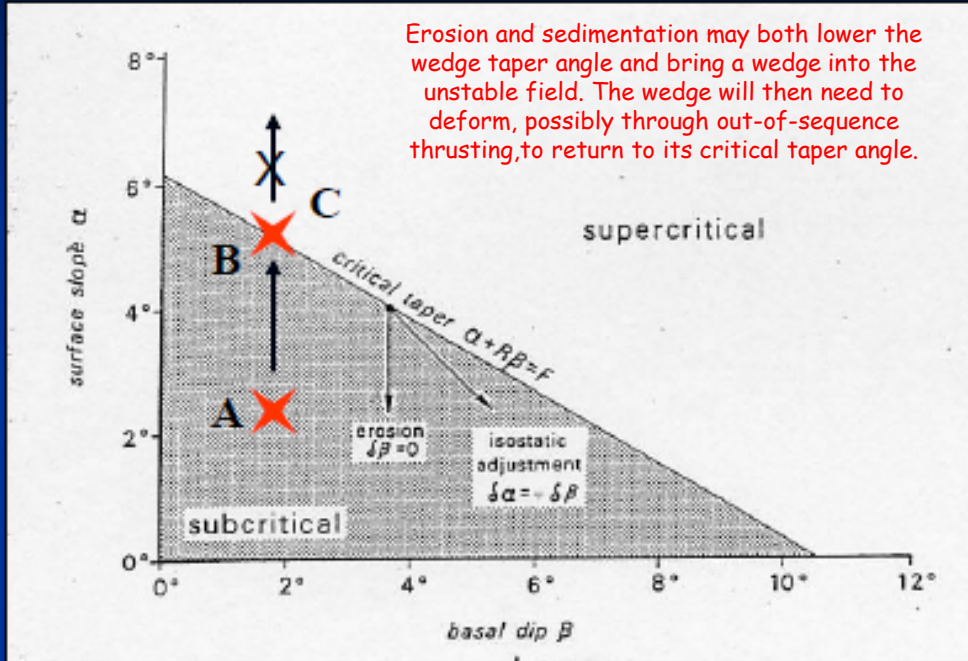
I, II, III and IV : unstable wedge.

I and III : the undercritical wedge has to shorten mainly by thrusting to reach equilibrium because basal friction is too great → increase/decrease taper in I/III

II and IV : the overcritical wedge has to extend by normal faulting to reach equilibrium because basal friction is too weak → decrease/increase taper in II/IV

Modification of the equilibrium

Erosion and sedimentation may both lower the wedge taper angle and bring a wedge into the unstable field. The wedge will then need to deform, possibly through out-of-sequence thrusting, to return to its critical taper angle.



Example: mountain building

A: subcritical $\rightarrow \alpha$ can increase.

B: critical taper. α cannot increase anymore. If $\alpha >$ critical value, the taper becomes supercritical / unstable and collapses.

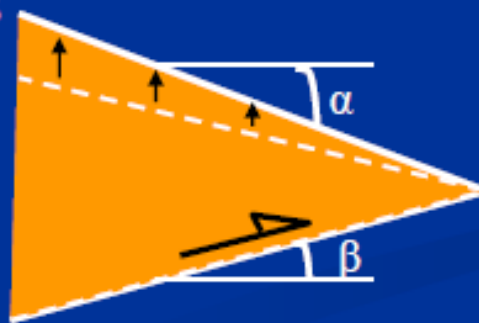
C: to carry on growing, the taper cannot steepen anymore so it has to “expand” horizontally as well as vertically.

= self-similarity

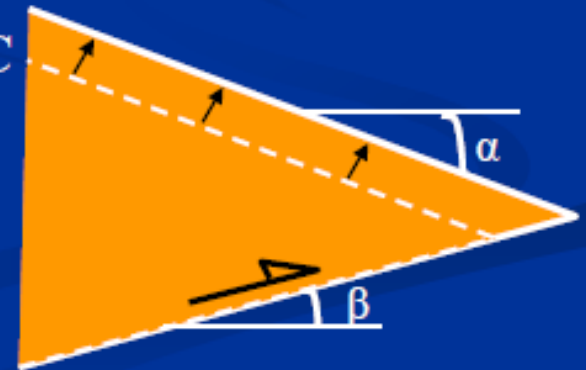
A



B



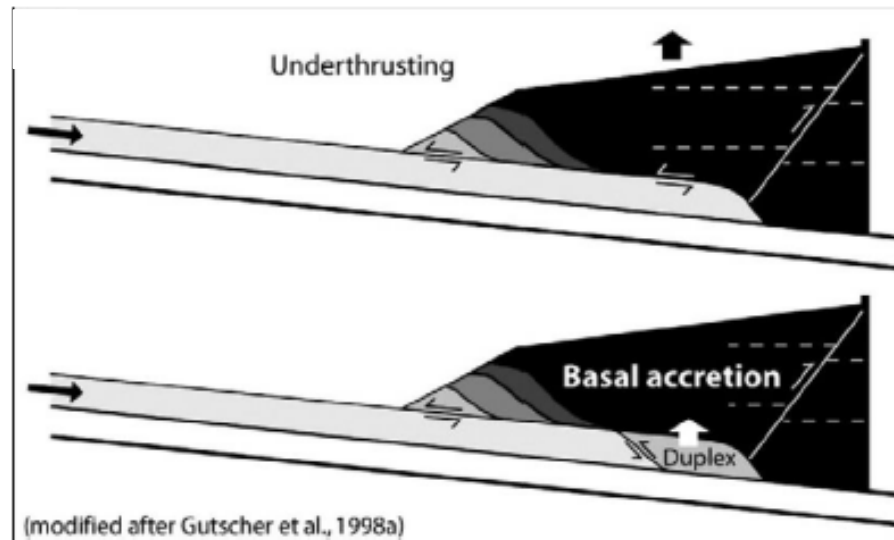
C



Limitations :

1. Assumptions of constant stress conditions and that wedges are at the verge of failure everywhere. The theory can, therefore, not account for wedges that are partly or transiently not at failure.
2. Materials are assumed homogeneous and isotropic and memory effects through, for example, reactivation of strain-weakened fault planes are not considered.
3. The stress state for wedges in the stable field is not defined.
4. Critical taper theory explains the present-day state and overall geometry of wedges (ie., a 'static' view), but does not show how the structures evolved to this state

An alternative
to frontal
accretion :
basal accretion
- underplating



Underplating occurs when the taper is low.

A long unit is generally underplated.

The taper increases during underplating

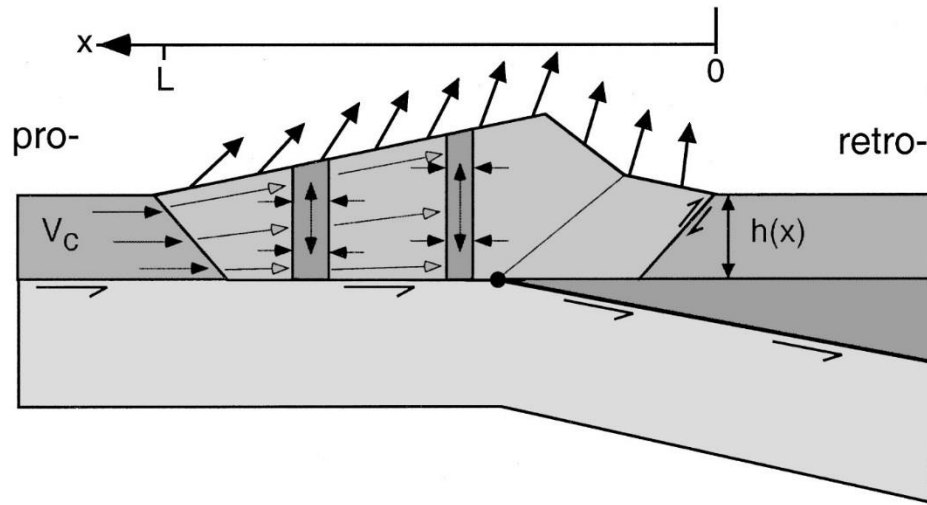
Friction on the intra-wedge decollement is higher than that along the basal decollement. The coupling changes the slope and the topography of the upper wedge.

When the taper is too high, the system switches to frontal accretion

→ Usual cyclical behaviour of thrust wedges with alternating frontal accretion and underplating

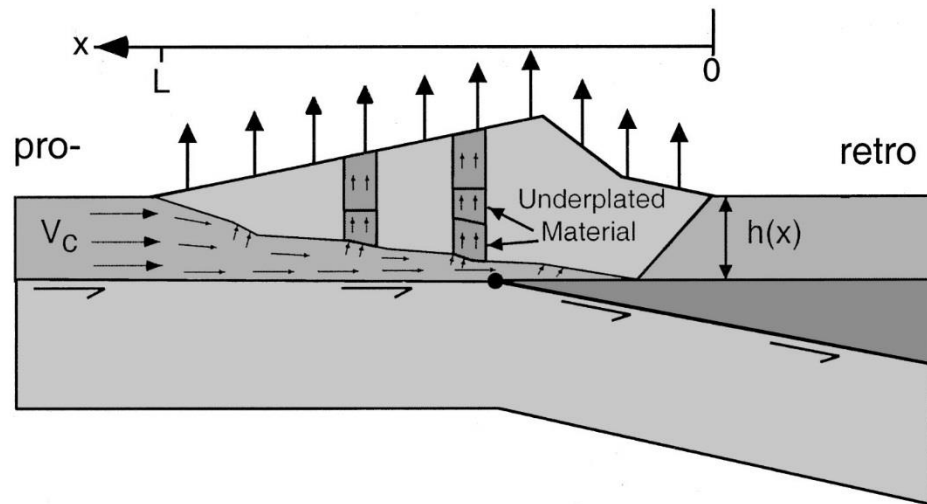
End-member kinematic models of orogenic wedge growth

A. Frontal Accretion



A) Frontal accretion. Wedge shortens such that a vertical column extends vertically and shortens horizontally. Vertical component of surface velocity is relatively constant.

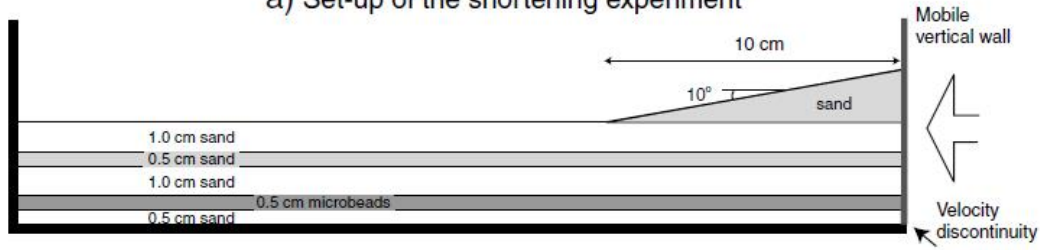
B. Underplating



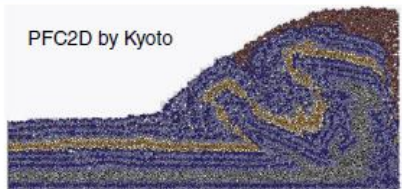
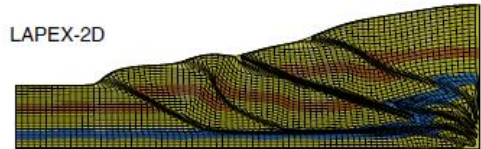
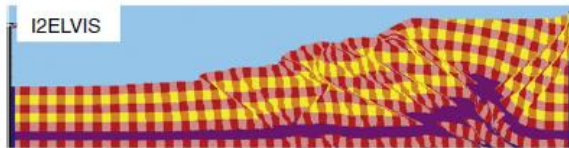
B) Underplating. Wedge does not shorten horizontally and thus has no horizontal velocity. Columns of rock move vertically at a constant rate in response to addition of new material at the base of the wedge.

The modeling approach

a) Set-up of the shortening experiment

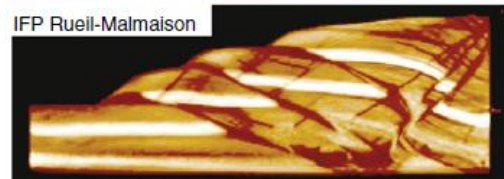
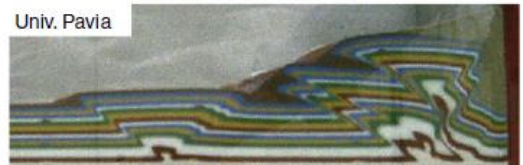


b) Numerical results



-40 -30 -20 cm

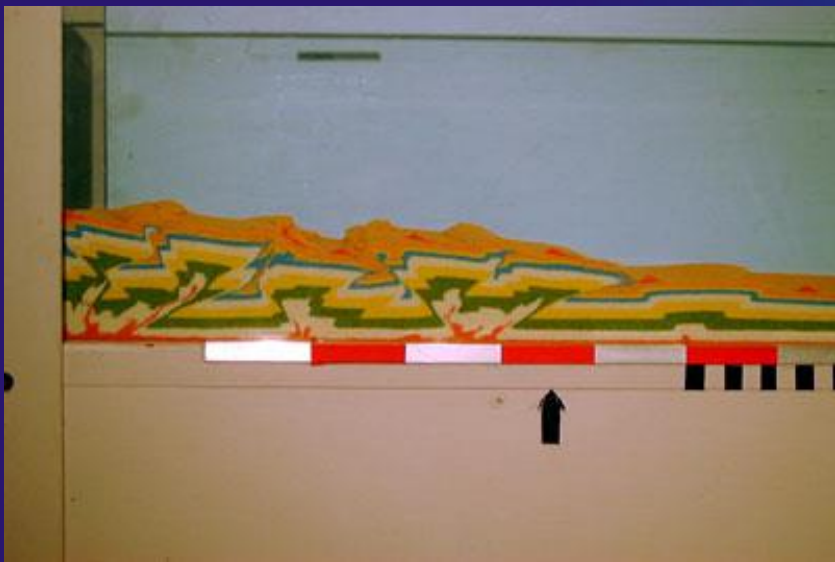
c) Analogue results



-40 -30 -20 cm

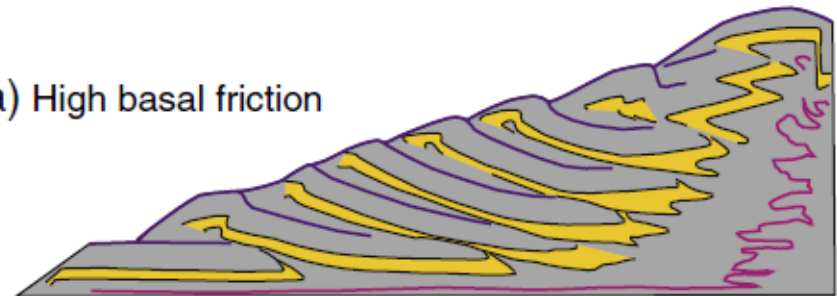
A wealth of attempts
at modelling
fold-and-thrust belts
by analogue and
numerical means

(Buiter, 2012)

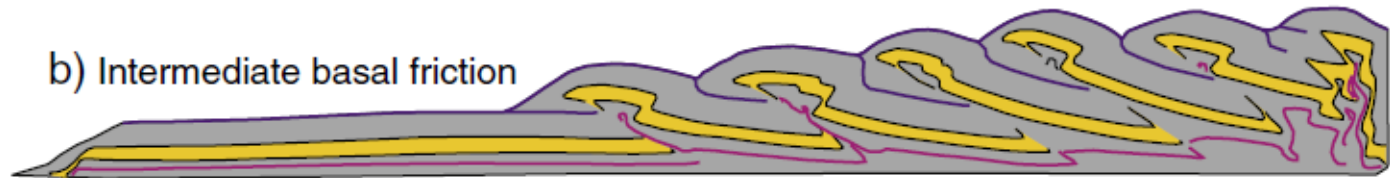


Influence of basal friction

a) High basal friction

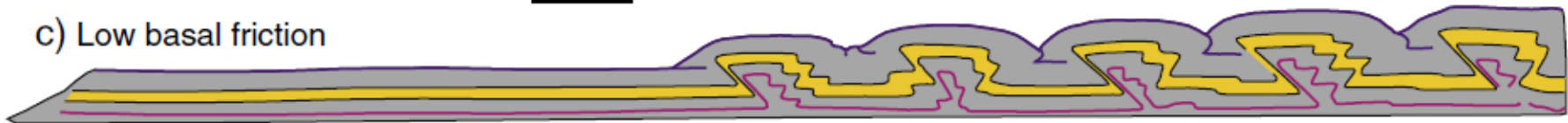


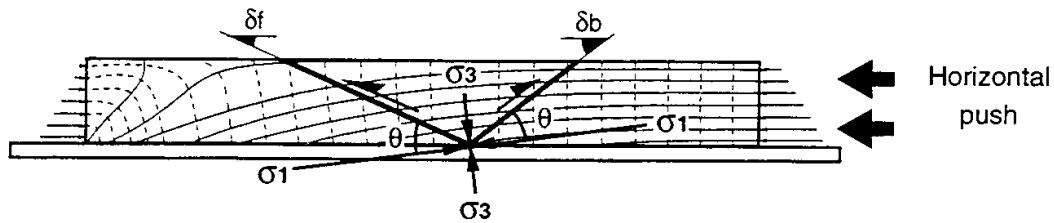
b) Intermediate basal friction



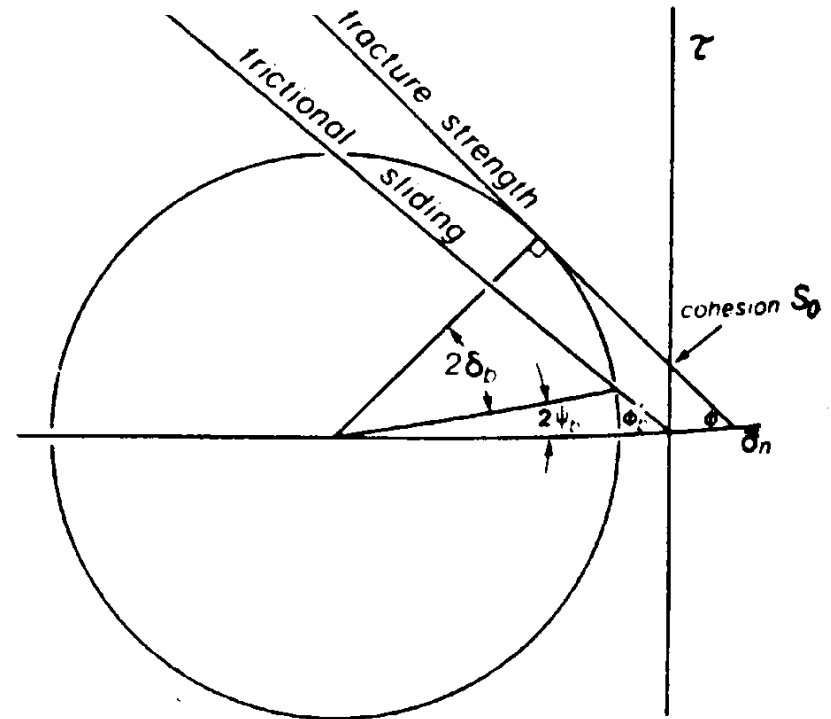
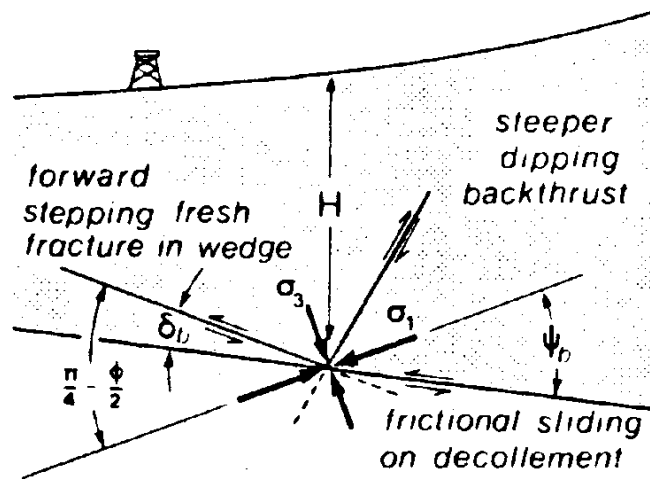
5 cm

c) Low basal friction





$$\text{tg } 2\theta = 2 \cdot \tau_b / (\sigma_h - \sigma_v)$$



- Thrust dip is higher for low basal friction wedges
- Backthrusts are more frequent in low basal friction wedges

The initial dip of the shear bands at the wedge toe is independent of the décollement strength because σ_1 is close to horizontal in the undeformed rock pile, in front of the wedge toe.

The new conjugate shear bands mark the location of the next ramping thrust only if the friction angle in the basal décollement is low.

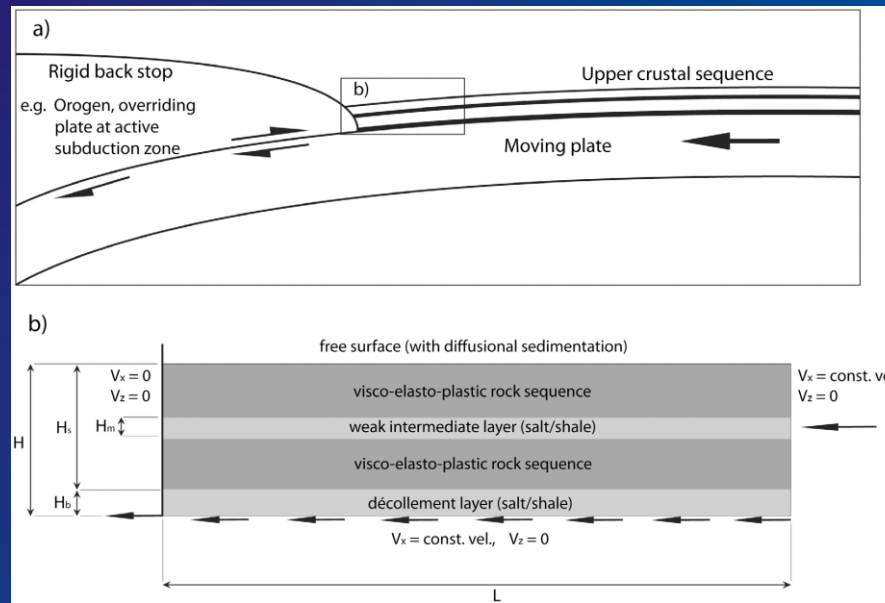
For larger basal friction angles, the deformation front is more dynamic and constantly generates new shear bands dipping toward the wedge,

σ_1 within the wedge produces ramp thrusts that are shallower dipping with increasing basal friction angle. Backthrusts are steeper than forward verging ramps depending on the dip of σ_1

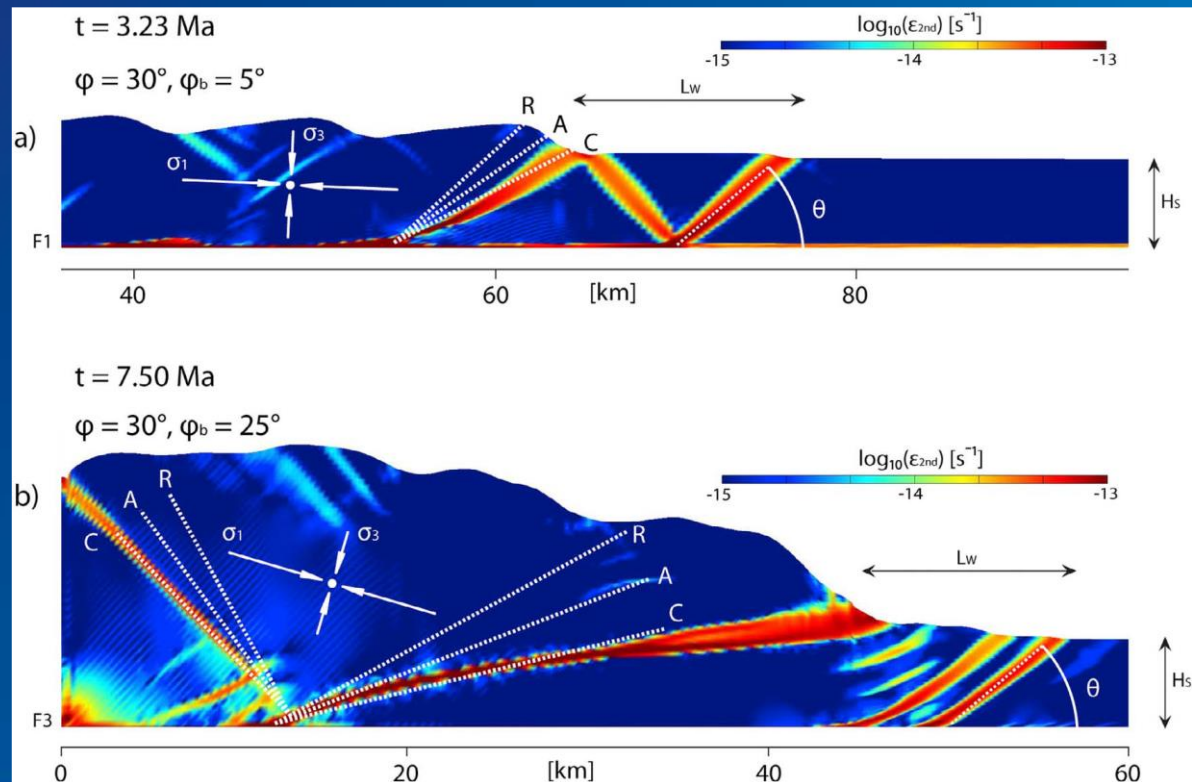
σ_1 is close to horizontal for compressional wedges with a very weak décollement. For wedges with a higher basal friction angle, σ_1 is steeper. This is due to a stronger asymmetric gravitational potential in large-tapered wedges.

The numerical model results agree with the angles between the horizontal décollement and σ_1 predicted by the critical wedge theory.

Ramp and back thrust dipping angles within the wedge follow Coulomb orientations

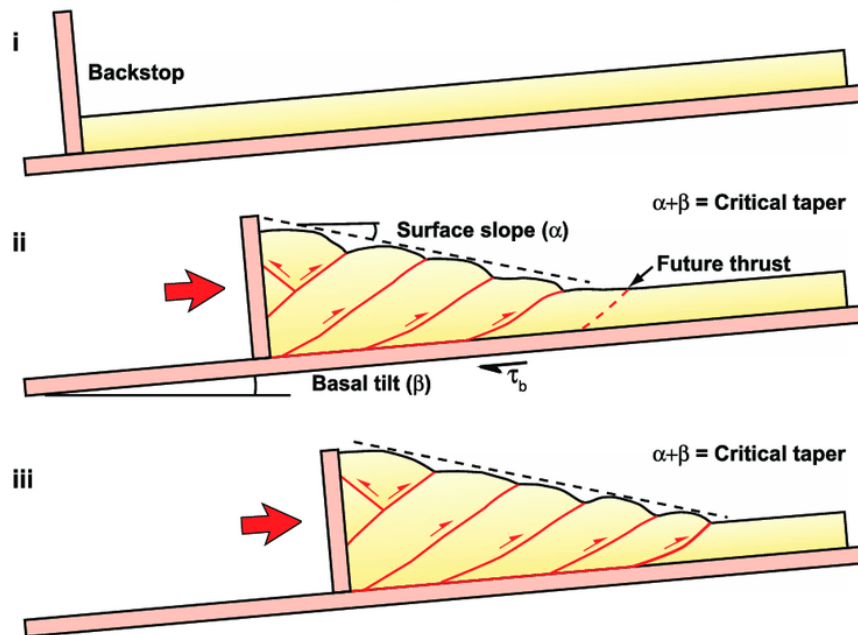


(Ruh et al., 2012)

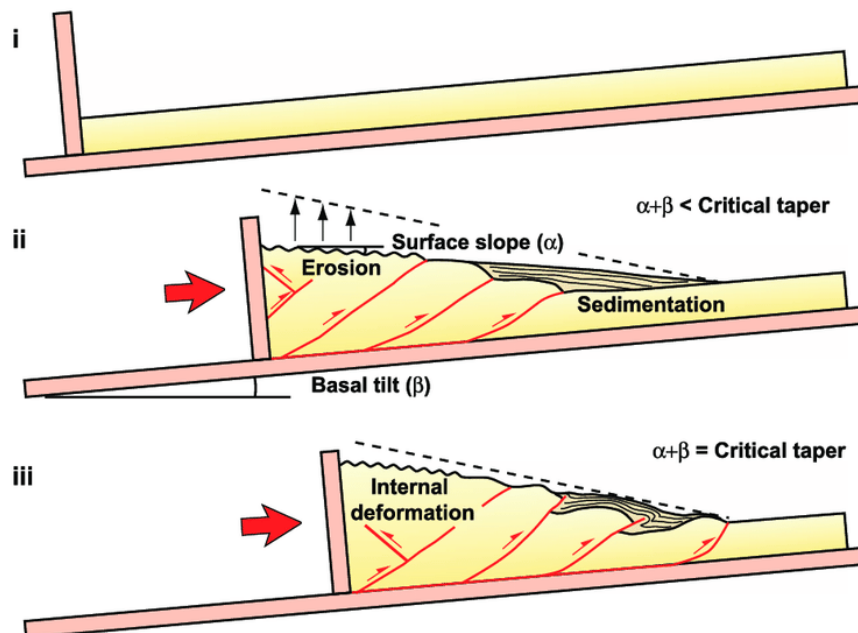


Syn-kinematic
erosion/sedimentation

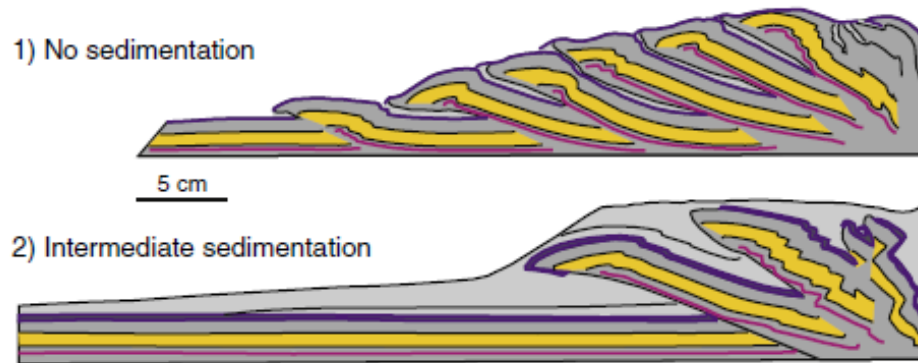
(a) Progressive evolution of a simple critical Coulomb wedge



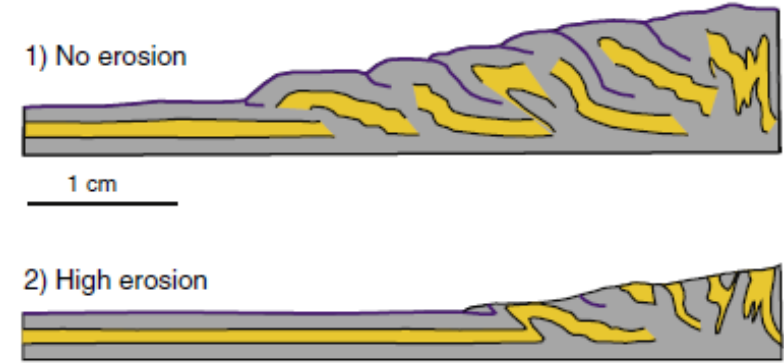
(b) Progressive evolution of a critical Coulomb wedge with synkinematic erosion and sedimentation



a) Effect of sedimentation (Storti and McClay, 1995)



b) Effect of erosion (Cruz et al., 2010)

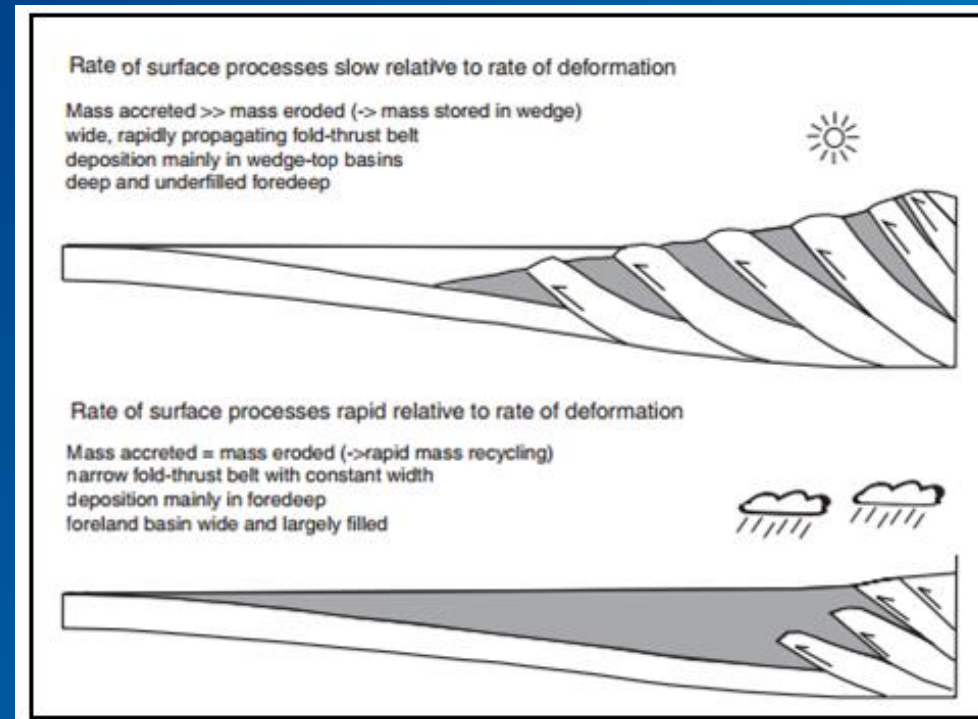


(Buiter, 2012)

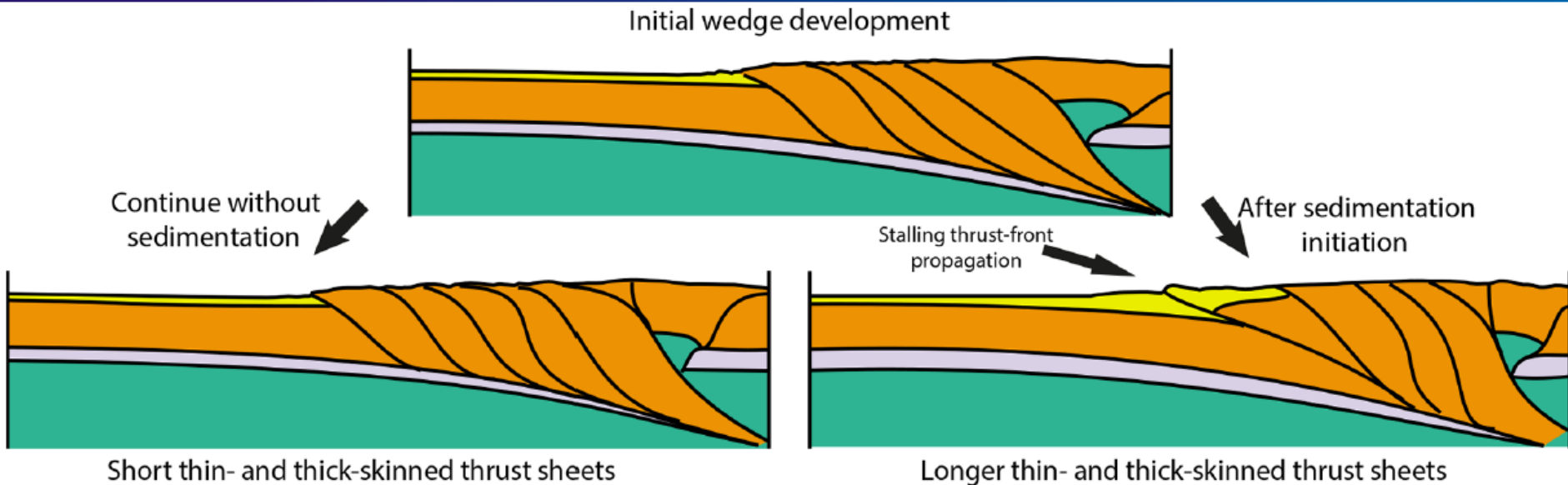
Surface processes can change the taper angle of brittle wedges through the addition or removal of material at the surface and through an isostatic response of the base to changes in the overburden.

Erosion and sedimentation may both lower the wedge taper angle and bring a wedge into the unstable field. The wedge will then need to deform, possibly through out-of-sequence thrusting, to return to its critical taper angle.

Erosion localises deformation in the eroding domain, focuses exhumation and promotes narrower thrust belts



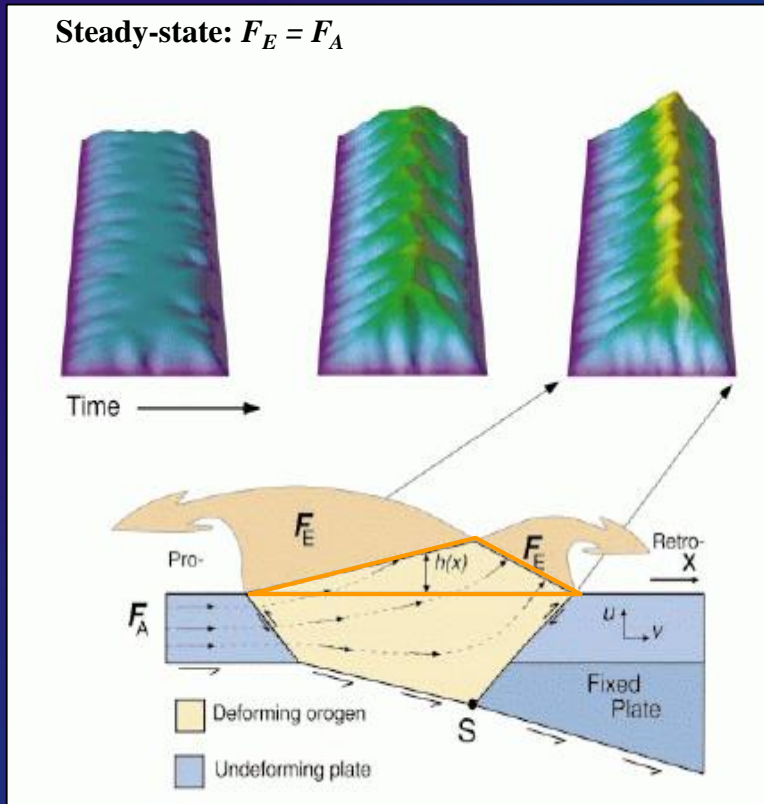
Difference between the evolution of a mountain belt with and without intensive late-stage sedimentation.



(Erdos et al., 2019)

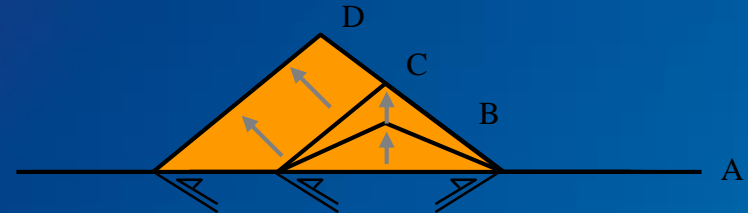
Surface processes affect gravitational stresses through a change of the overburden. For brittle wedges, this can lead to an increase in basal stresses for sedimentation (and a decrease for the case of erosion).

Erosion controls the geometry of mountains



(Willett & Brandon, 2002)

F_A = flux of material accreted,
 F_E = flux of material eroded.

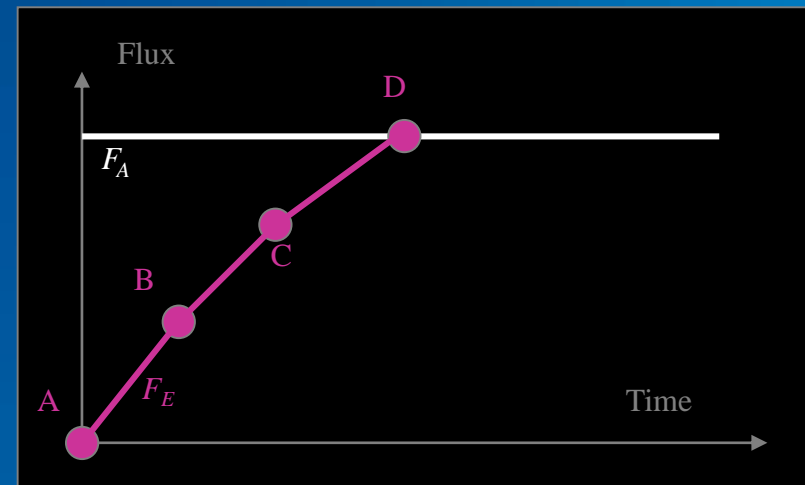


A: no topography, $F_E = 0$.

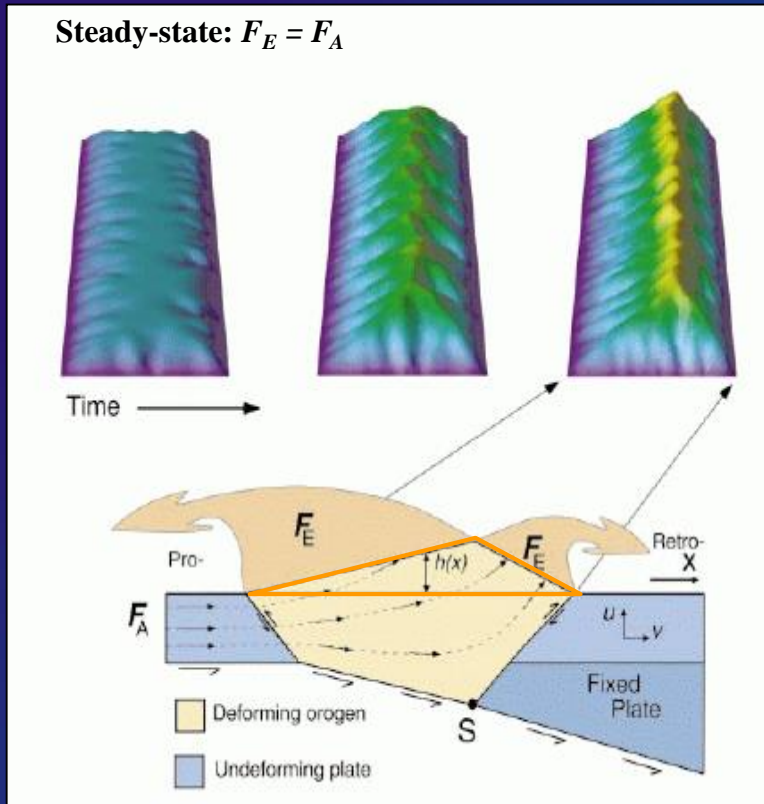
B: mountain grows → F_E increases.

C: critical taper stage, slope α cannot increase anymore.

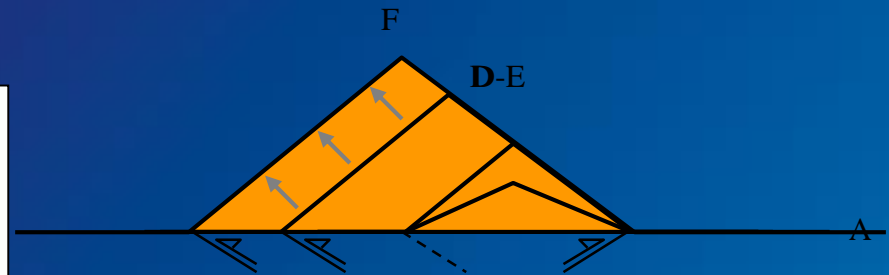
D: $F_A = F_E$ → steady-state. The topography does not evolve anymore.



Erosion controls the geometry of mountains



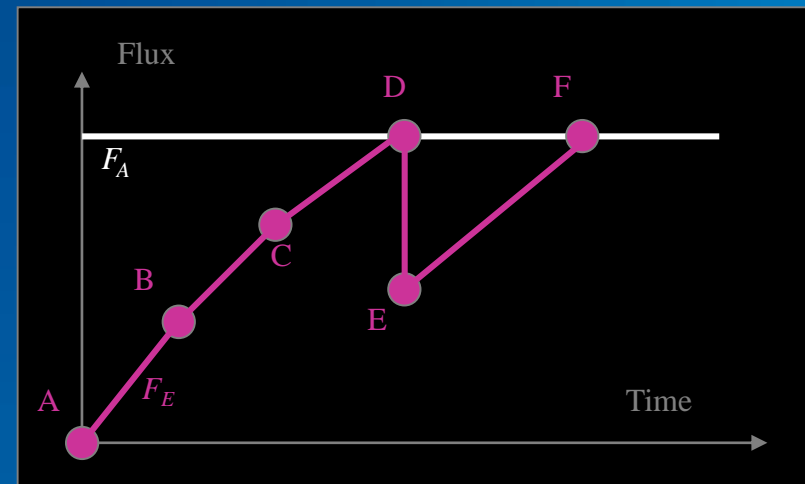
F_A = flux of material accreted,
 F_E = flux of material eroded.



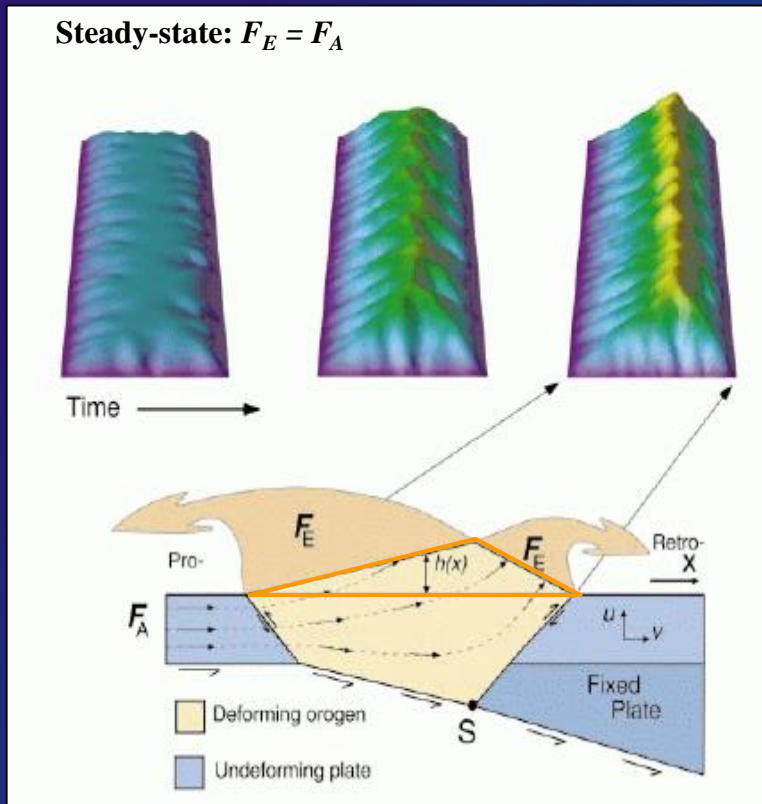
D: $F_A = F_E \rightarrow$ steady-state.

E: drop in F_E (e.g., climate change with less rain) \rightarrow erosion rate decreases \rightarrow the topography is not at steady-state anymore.

F: mountain grows again $\rightarrow F_E$ increases until a new steady-state is reached ($F_A = F_E$)



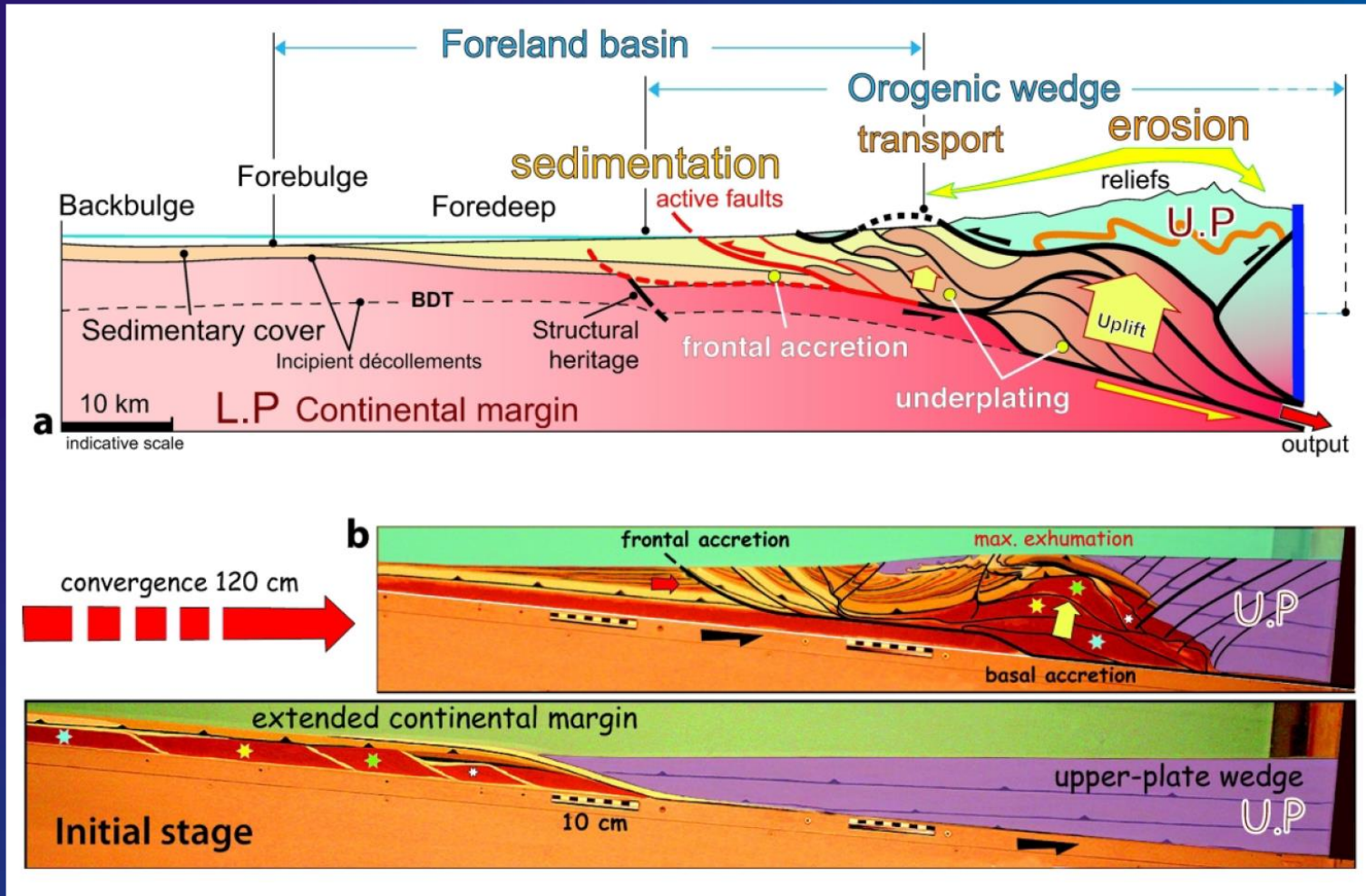
Erosion controls the geometry of mountains



However, “real” mountains are more complex:

- presence of discontinuities (e.g. faults),
- different lithologies (more resistant in the core of the range),
- change in crust rheology (basal friction)...

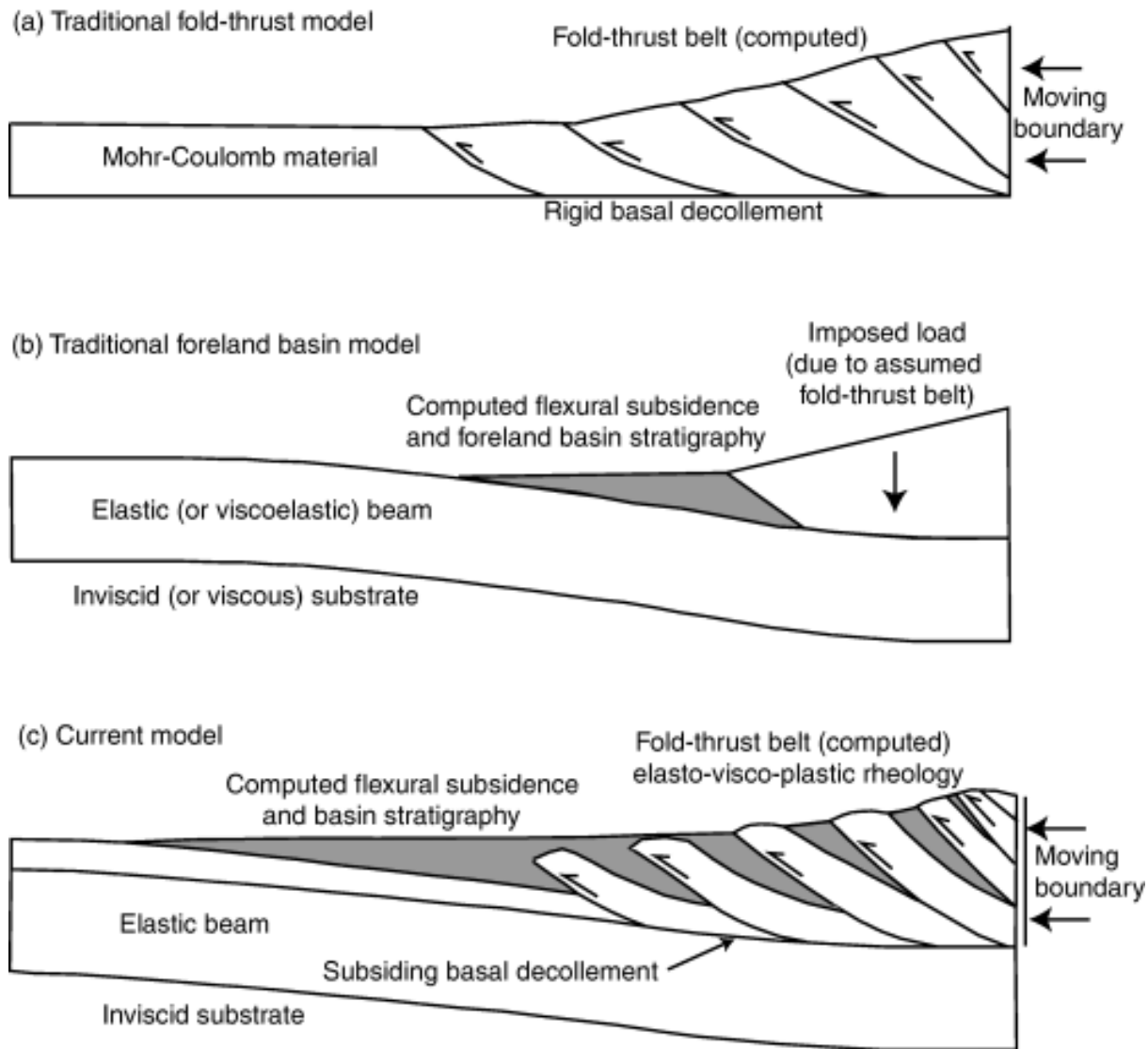
F_A = flux of material accreted,
 F_E = flux of material eroded.



(a) Main features and processes involved in mountain building during continental subduction.

(b) Analogue model (final and initial stages) depicting the impact of erosion, sedimentation and structural inheritance of a subducted continental margin on deformation partitioning. The structure of the model margin accounts for rheological layering of the sedimentary cover and for the presence of inherited normal faults.

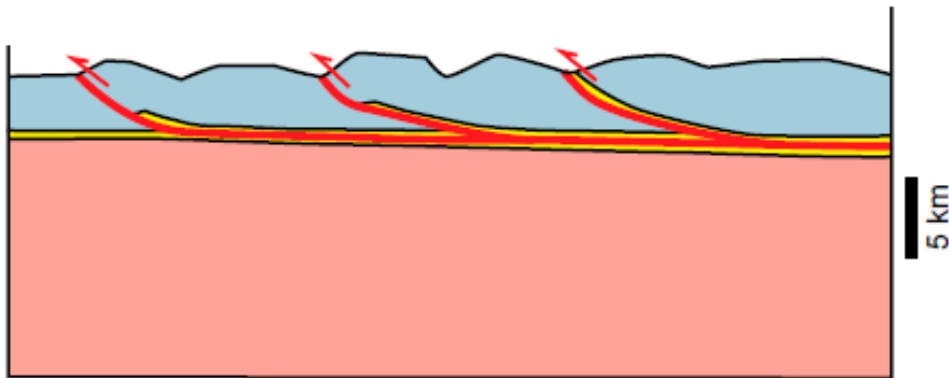
From simple models of fold-thrust belts to reality



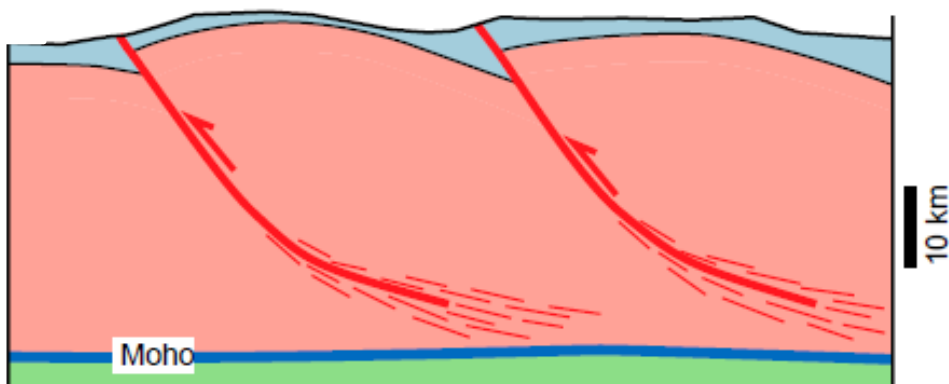
Tectonic styles in fold-and-thrust belts

Defining the structural style of fold-and-thrust belts and understanding the controlling factors are necessary steps toward prediction of their long-term and short-term dynamics, including seismic hazard, and to assess their potential in terms of hydrocarbon exploration.

Thin-skinned style



Thick-skinned style

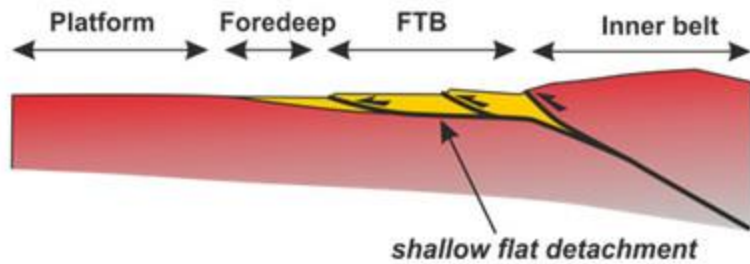


The depth (and degree) of décollement (mechanical decoupling) within the continental crust during (collisional) deformation has been widely debated for many years.

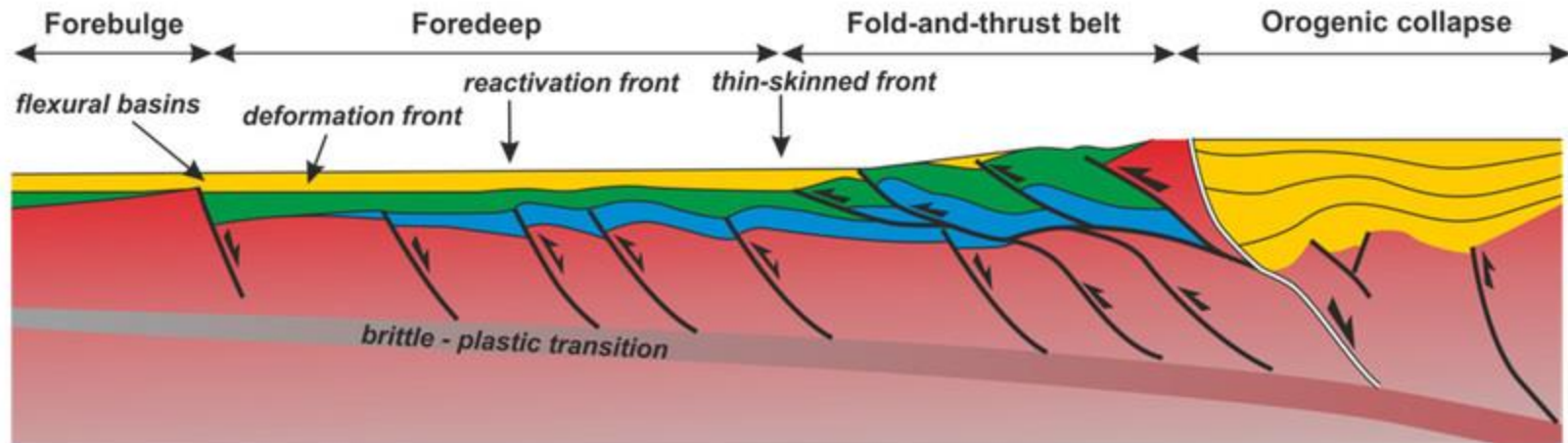
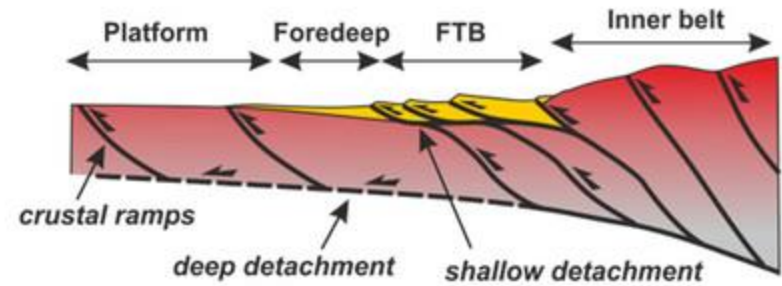
One view states that the sedimentary cover is detached from the underlying basement along a shallow, low-strength décollement and deformed by thrusts with ramp-flat geometries rooting into the décollement (thin-skinned tectonic style). This thin-skinned style supposes large-scale displacements and duplication of the sedimentary sequence, the underlying basement remaining undeformed.

The alternative view states that shortening involves a significant part of the crust along crustal-scale ramps above a deep ductile detachment (thick-skinned tectonic style).

Weak horizon at the bottom of the cover
Strong upper crust

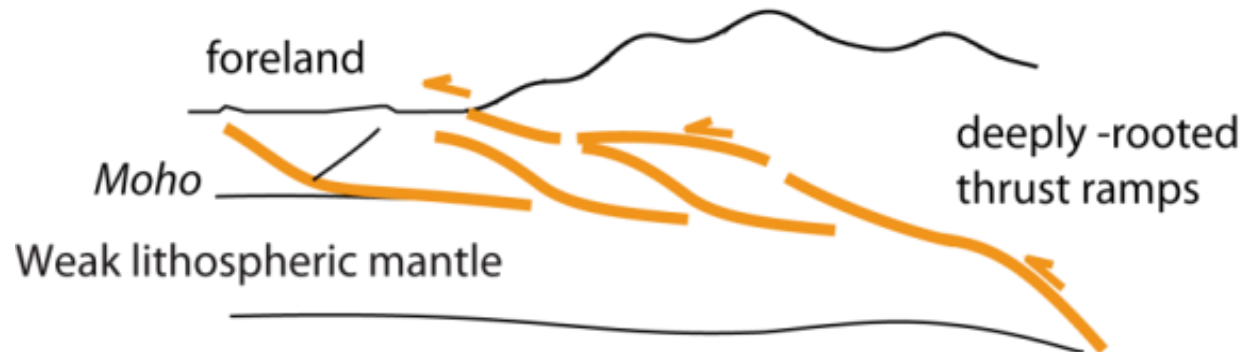
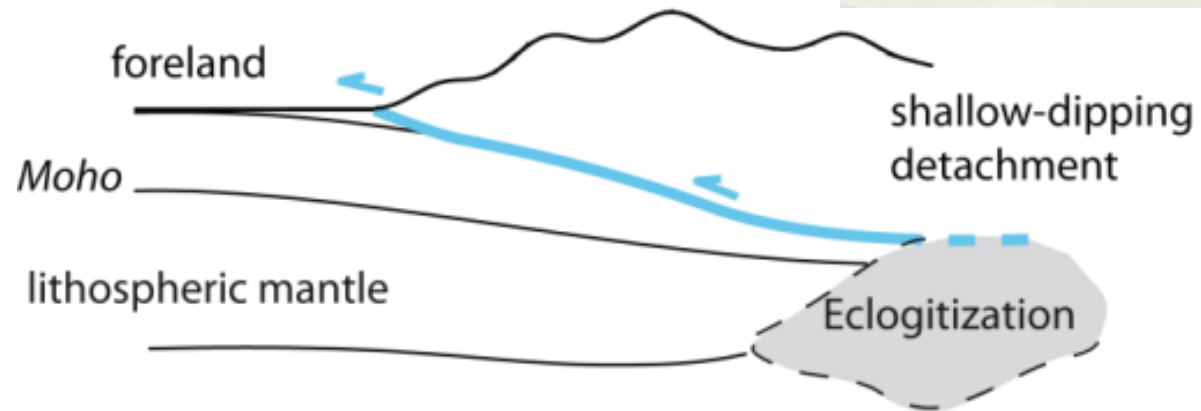


Favourably oriented inherited structures
Weak faults



(Modified after Lacombe and Mouthereau, 2002)

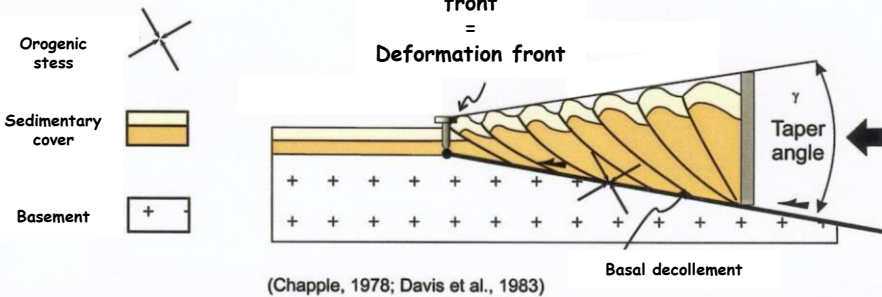
*simple-shear
style "subduction"*



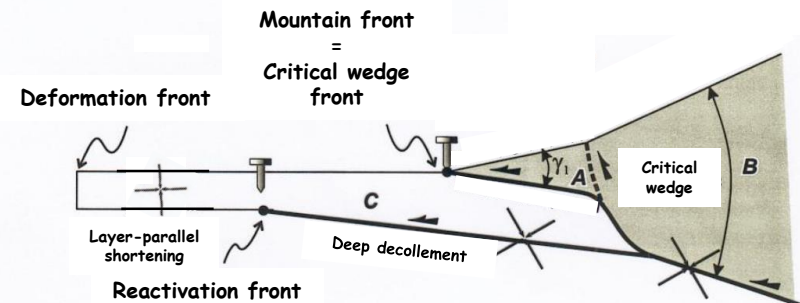
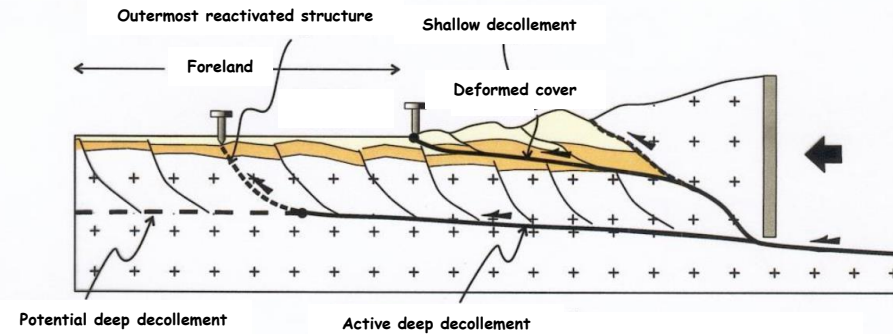
*pure-shear
style "inversion"*

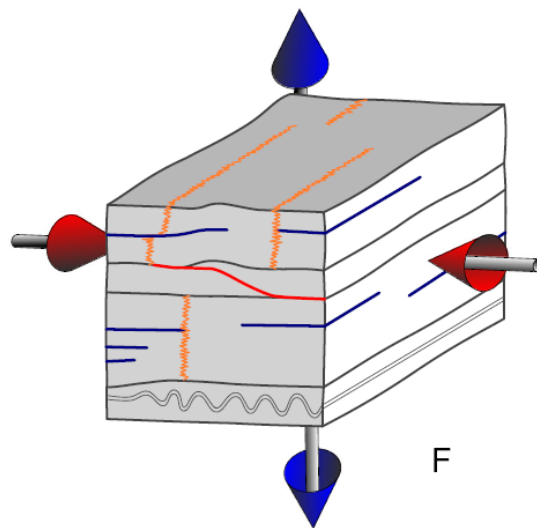
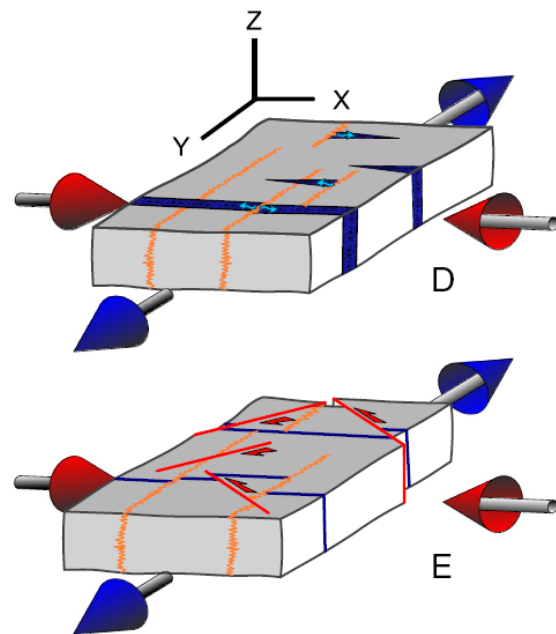
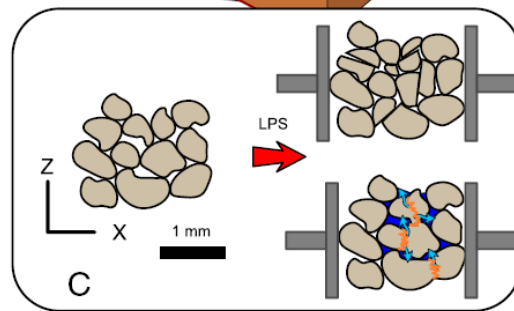
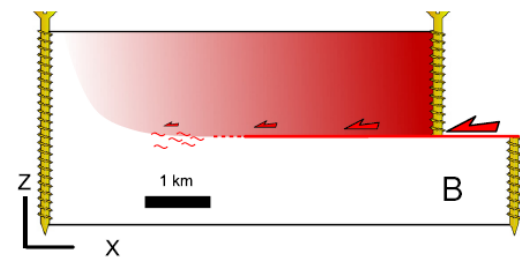
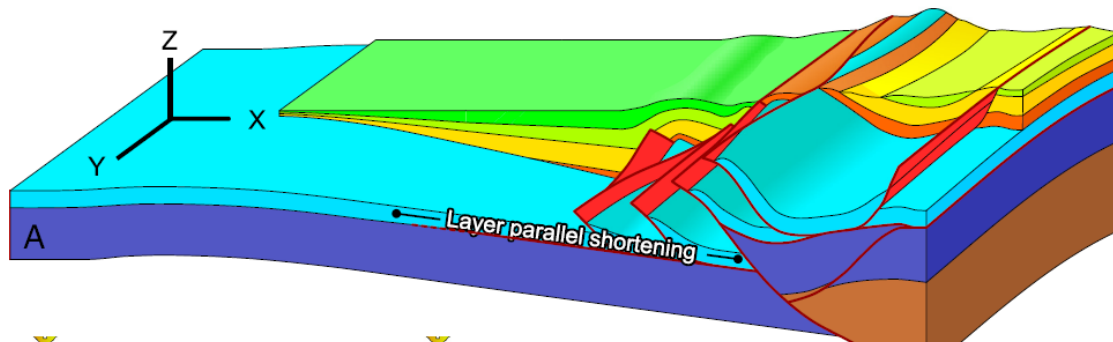
What is the real 'front' of orogens ?

Classical wedge model



Imbricate wedge model





What happens at the front of the wedge ?

Layer-Parallel Shortening (LPS) stimulates pressure-solution, inducing lateral changes in the compaction, decrease in porosity and permeability.

The main episode of LPS occurs in the footwall of frontal thrusts at the time of their nucleation, when the evolving thrust belt and its foreland are mechanically strongly coupled.

LPS contributes to the development of overpressures and tectonically controlled squeegee episode of forelandward expulsion of compaction water.

Inversion tectonics in fold-and-thrust belts

*Fault inversion is a complex and selective process that depends on :

-the orientation and steepness of the fault plane

-the friction along the fault plane

-the contrast of this frictional strength with respect to the surrounding medium.

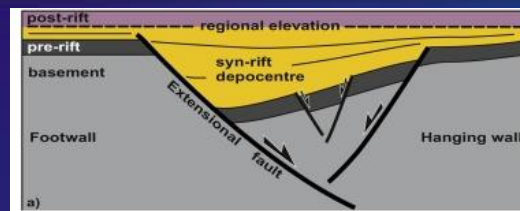
*Even when they are not reactivated, pre-existing faults are important mechanical discontinuities that can generate stress concentration and buttressing effects and often localize thrust ramps.

A key process by which basement becomes involved is the inversion of pre-existing extensional faults.

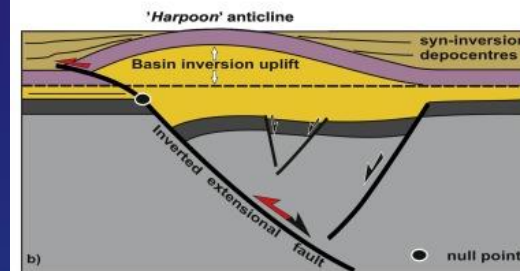
*Reactivation/inversion of basement faults widely occurs during orogenic evolution of collided passive margins and this process is known to exert a strong control on the evolution of orogens, including FTBs.

*Reactivated basement faults may induce localization of thrusts and folds in the developing shallow thrust wedge, development of basement uplifts or crystalline thrust sheets, out-of-sequence thrusting and refolding of shallow, nappes or development of accommodation structures such as lateral ramps, among others.

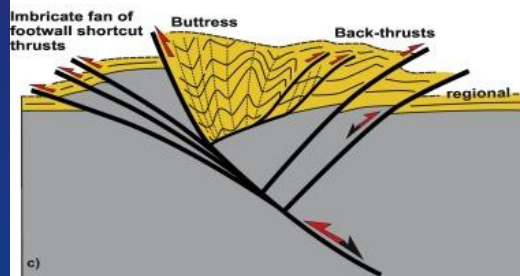
Multiple geometries resulting from inversion tectonics



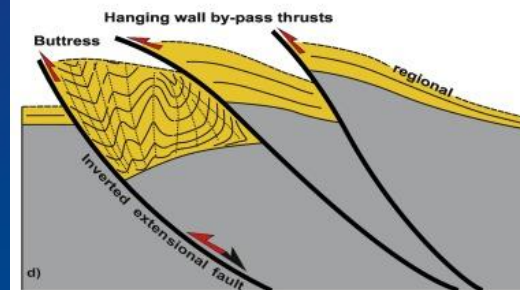
a) Starting half-graben basin; the regional elevation of the top syn-rift is taken as reference



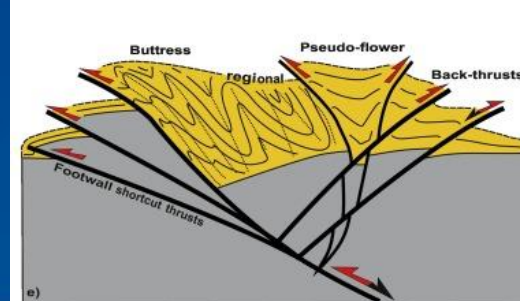
b) Inverted half-graben with mild reactivation of the extensional fault causing hanging wall uplift and shift of depocentres. The null point separates extensional offsets below from contractional offsets above.



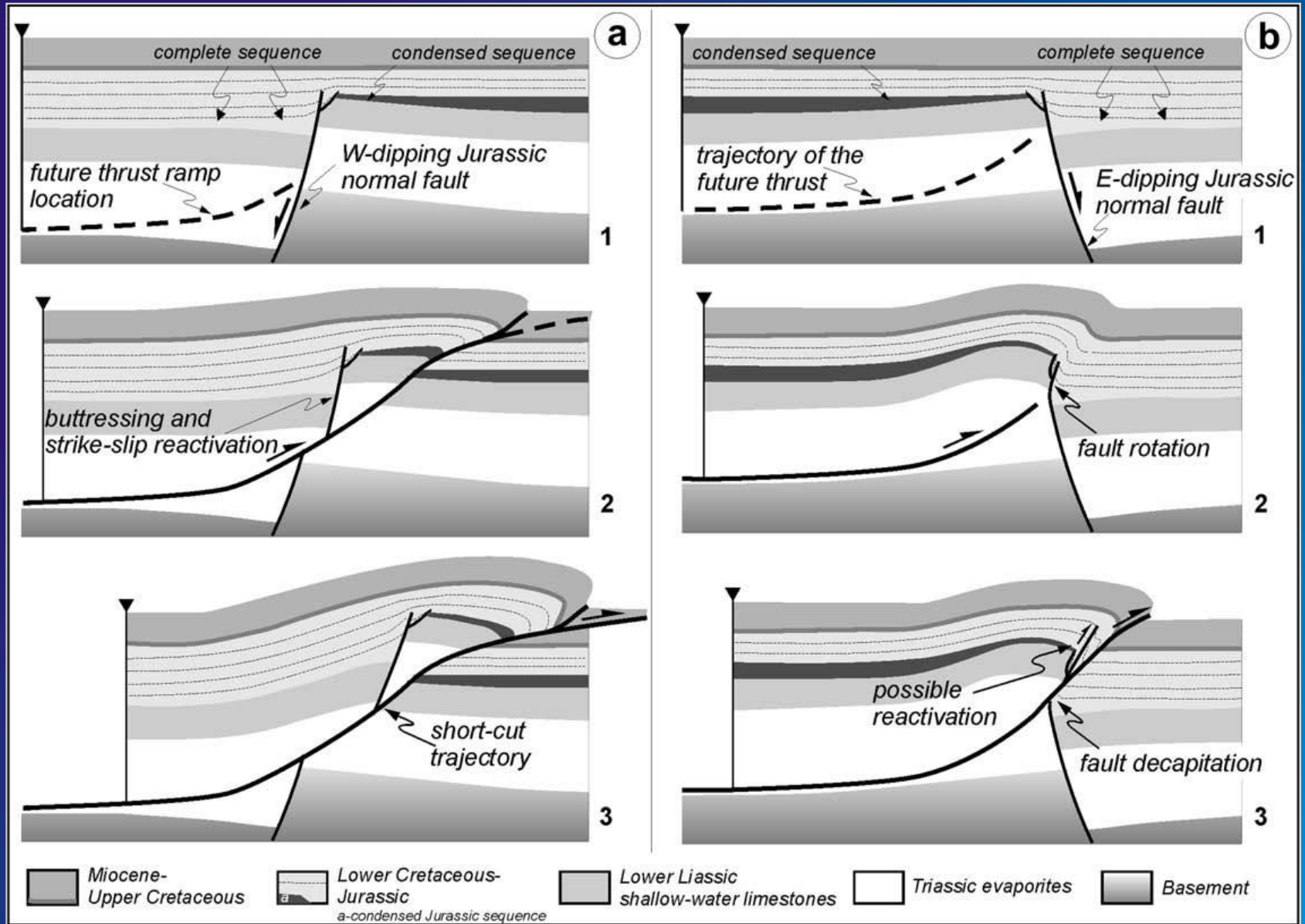
c) Inverted half-graben showing an imbricate fan of footwall shortcuts and back-thrusts; the syn-rift is internally deformed against the footwall block forming a buttress structure.



d) Inverted half-graben with basement-involved hanging wall by-pass thrusts.

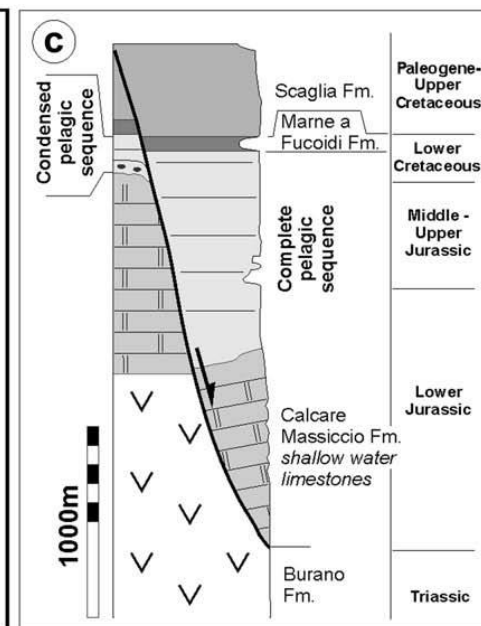
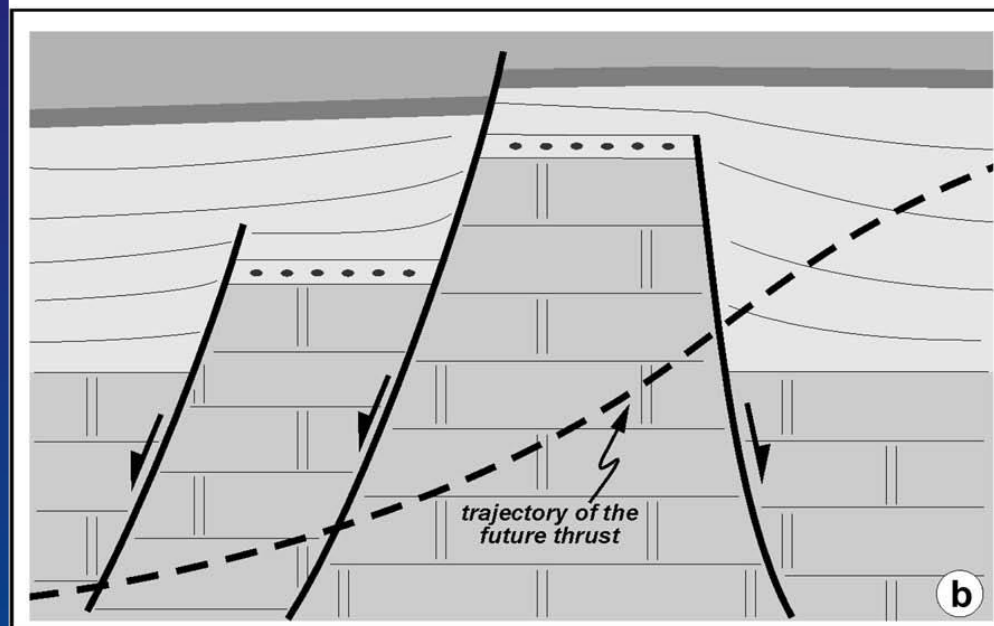
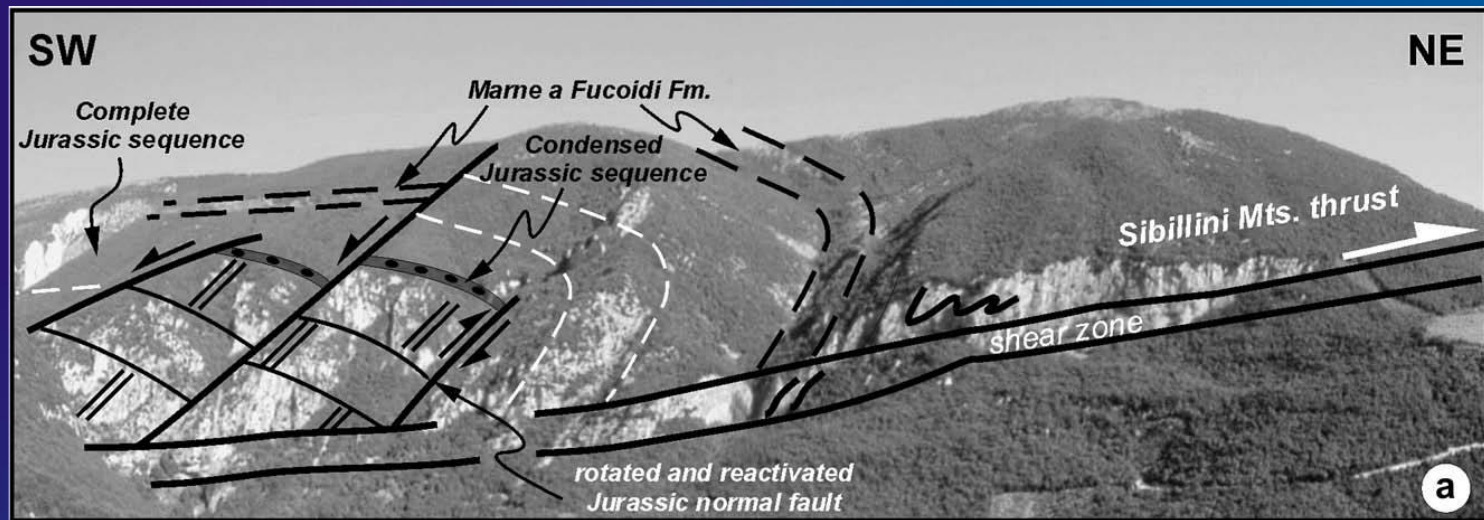


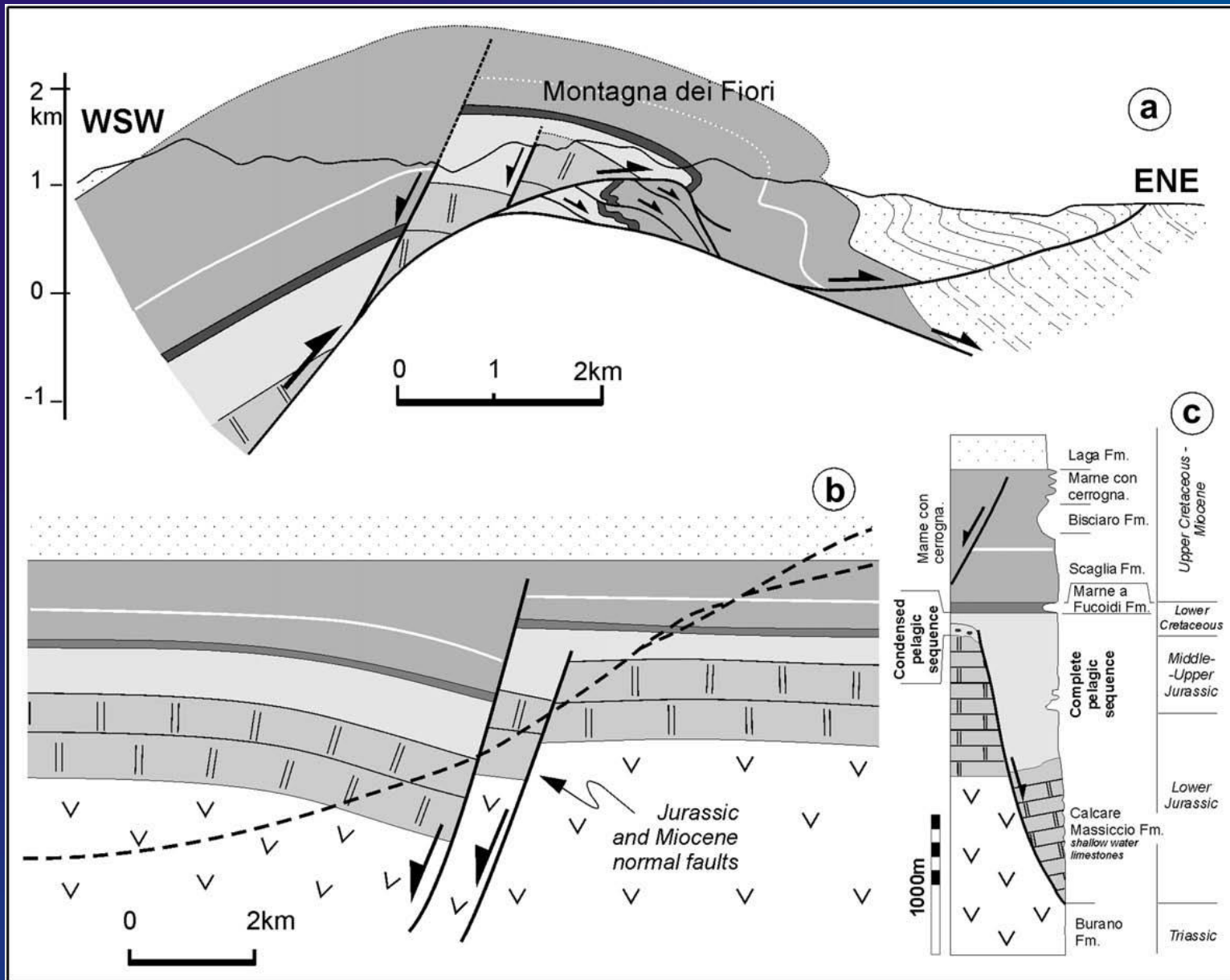
e) Inverted half-graben with footwall shortcuts, back-thrusts and a pseudo-flower structure formed after reactivation of hanging wall extensional faults.



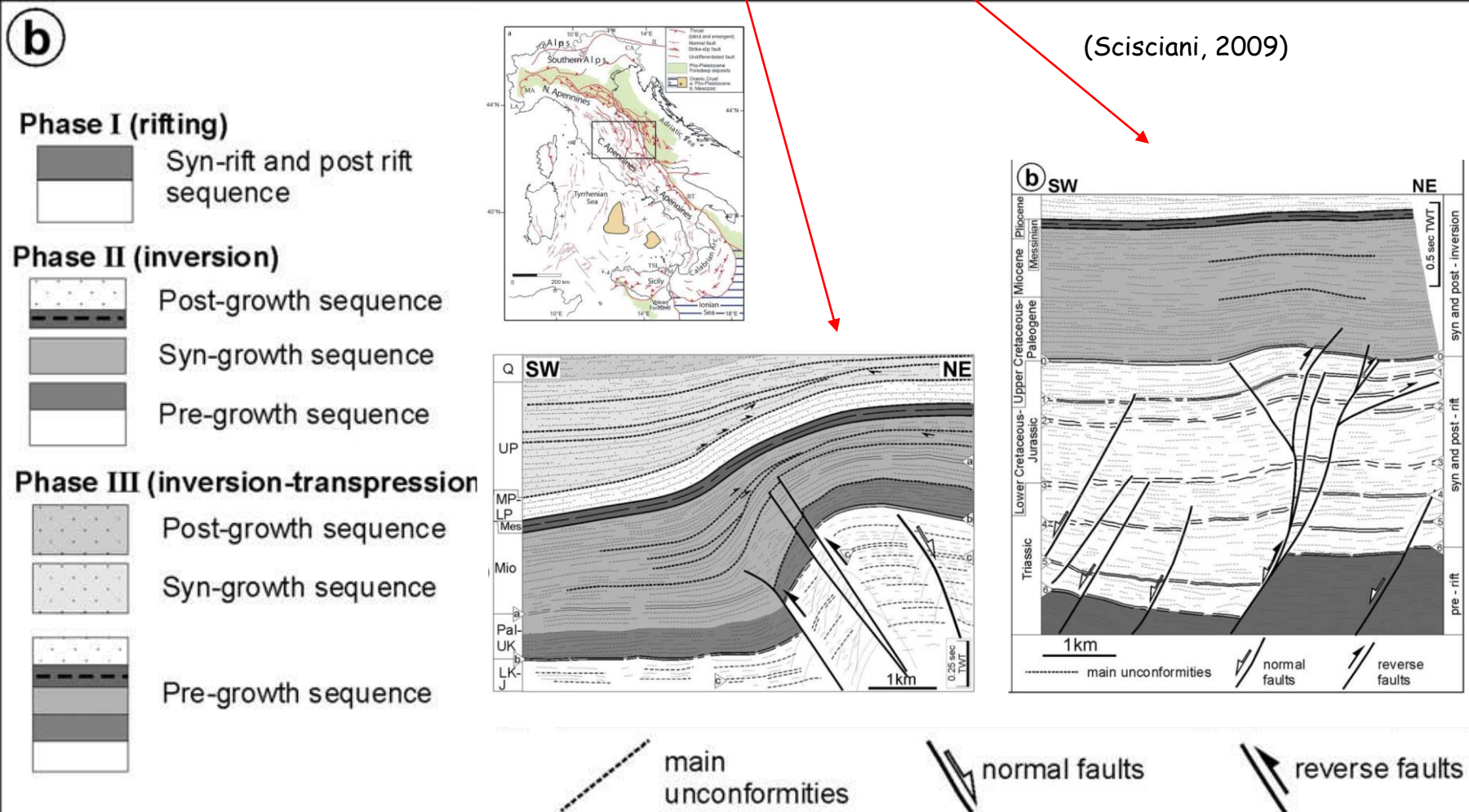
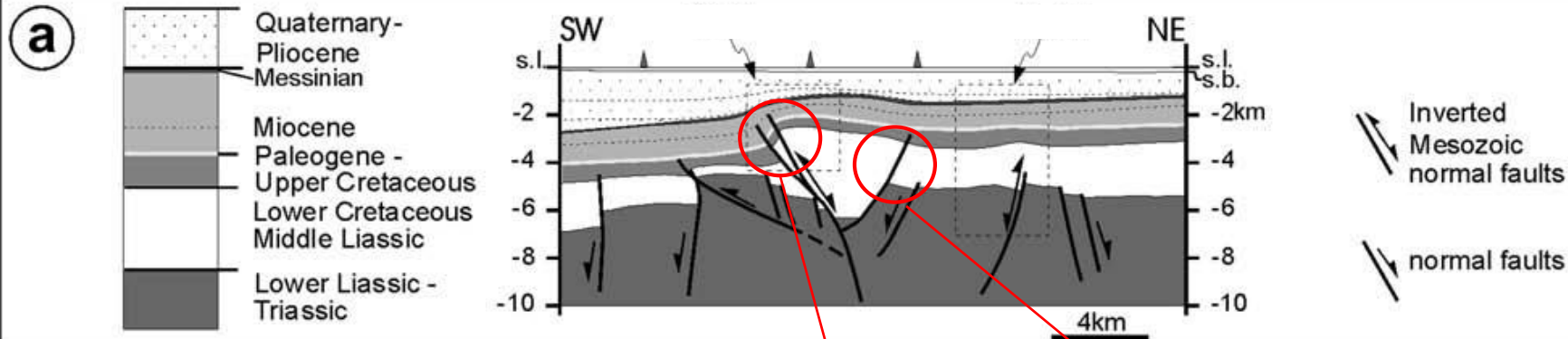
Interaction between the inherited extensional structures and subsequent thrusting. The pre-existing discontinuities promote the thrust-ramp localisation and they are decapitated by the later thrust faults that propagate with short-cut trajectories

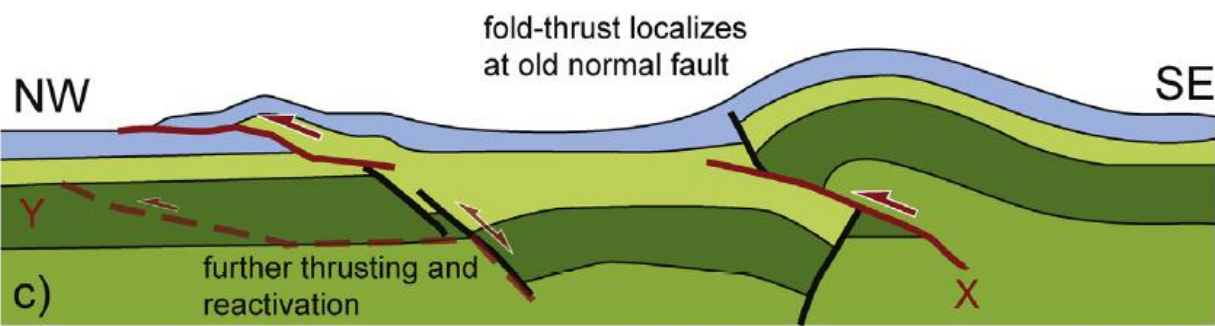
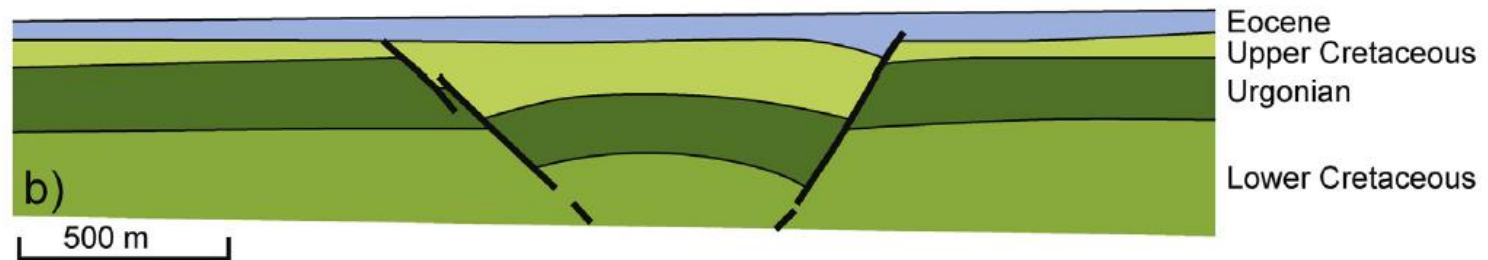
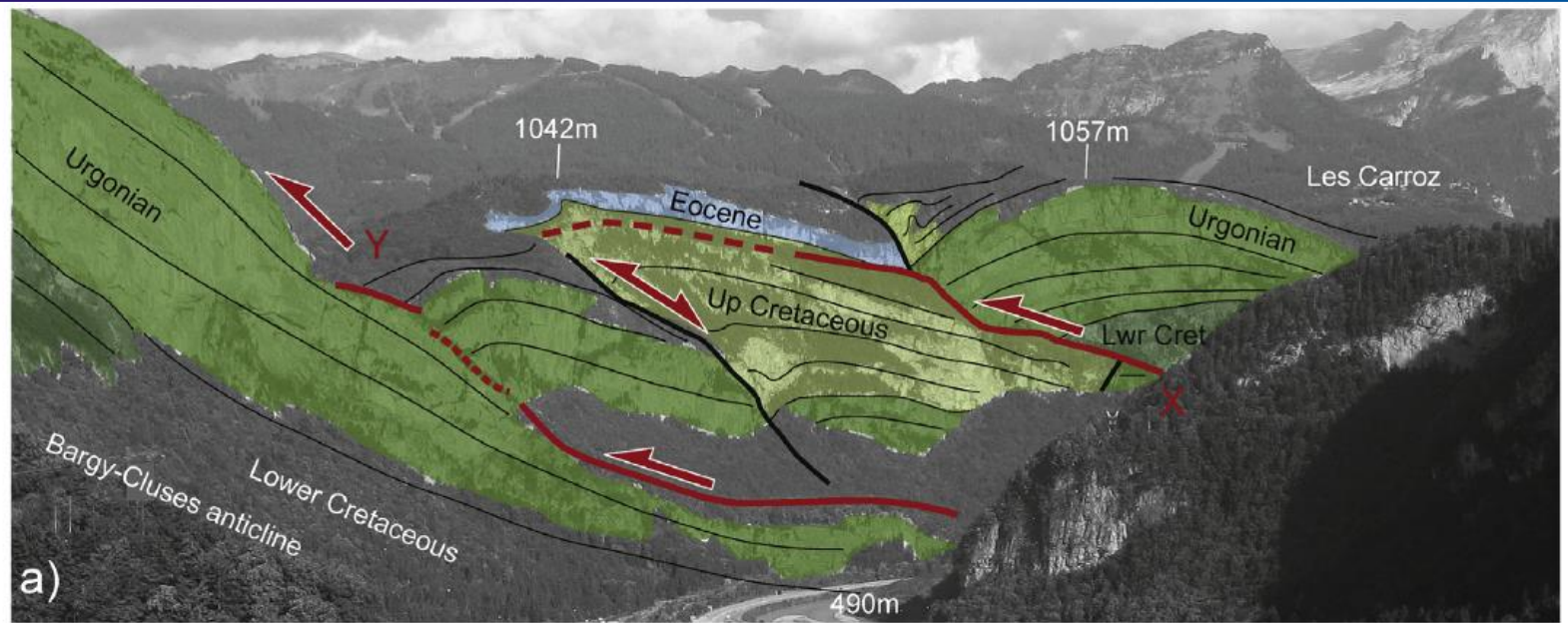
Jurassic horst later truncated and passively transported in the hangingwall block of subsequent thrust (Sibillini Mts. Thrust)(Scisciani, 2009).



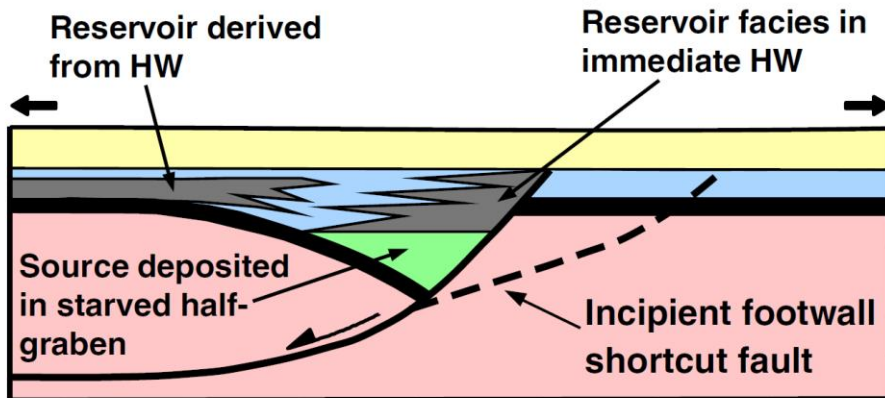


Pre-existing west dipping normal faults truncated by later thrust propagating with a short-cut trajectory.
 Montagna dei Fiori anticline (Scisciari, 2009)

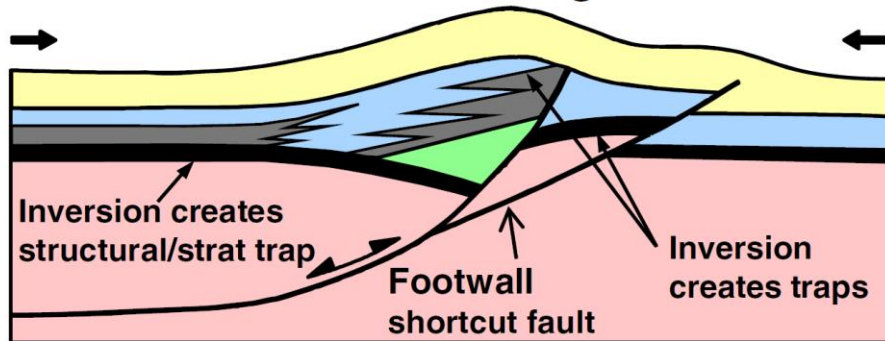




Extensional half-graben



Inverted half-graben



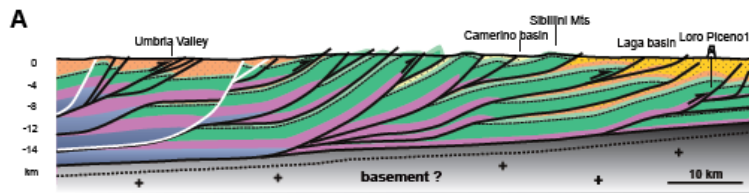
The compressional inversion of the extensional fault system will principally affect structural trap configurations, creating new trap geometries such as footwall shortcut structures and the inversion anticline.

The inversion can also modify older structural trap geometries which could result in the re-migration of pre-inversion hydrocarbon accumulations.

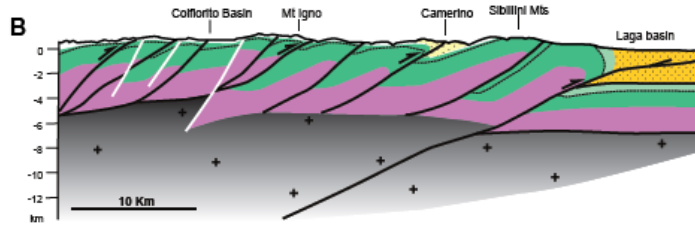
Inversion can also create new trap geometries by turning a facies change from reservoir to seal in a down dip direction into a viable stratigraphic trap that occurs in an updip direction.

However, the uplift above regional elevation that is a product of inversion, if significant, can result in erosion of one or more critical components of the petroleum system.

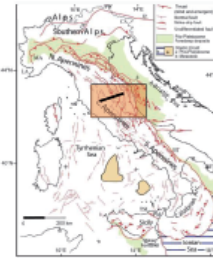
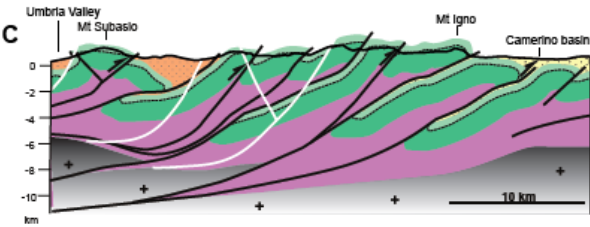
Evolution of ideas and views
on the structural style of fold-and-thrust belts



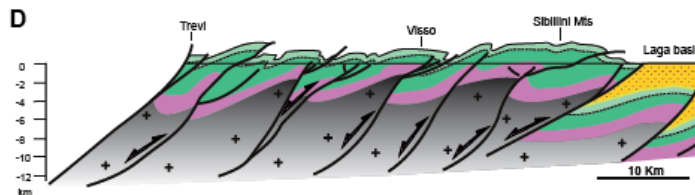
Thin-skinned style



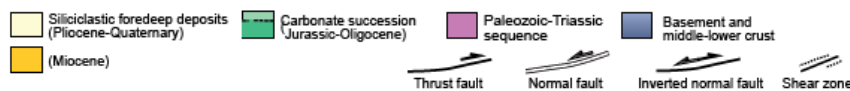
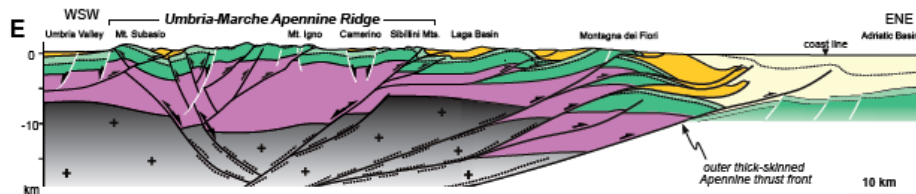
Thick-skinned style

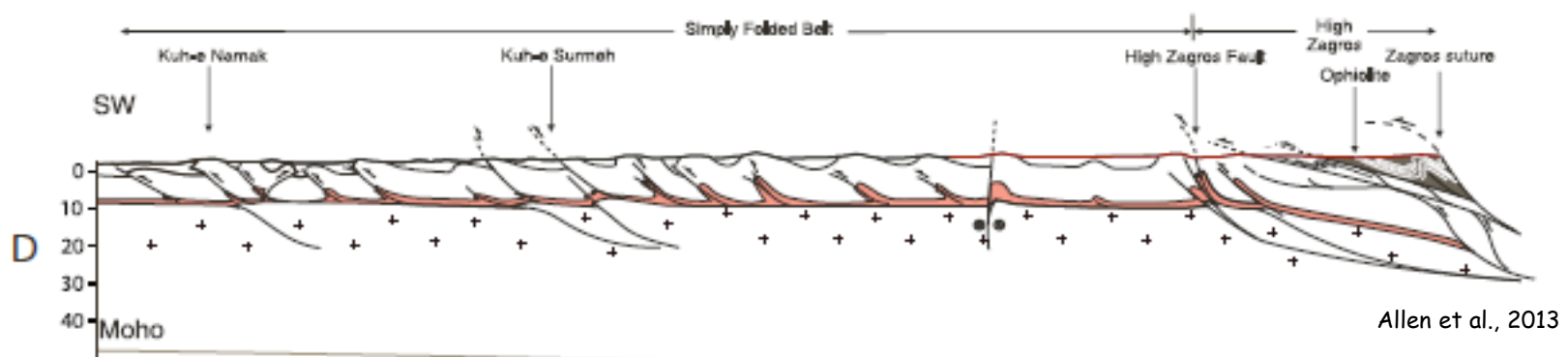
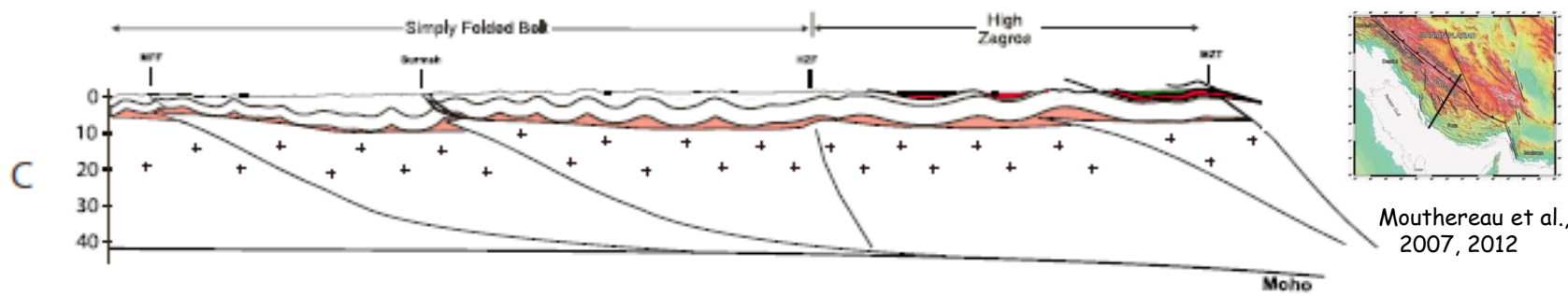
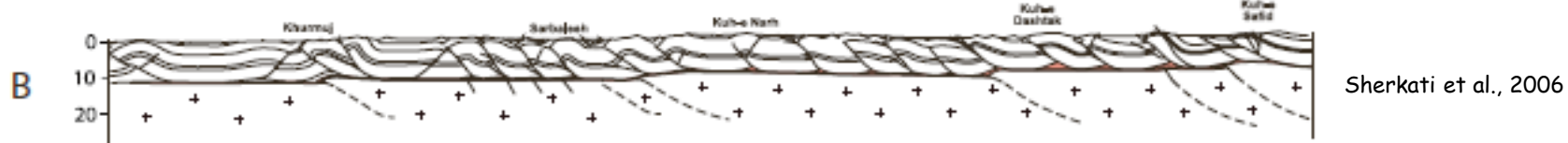
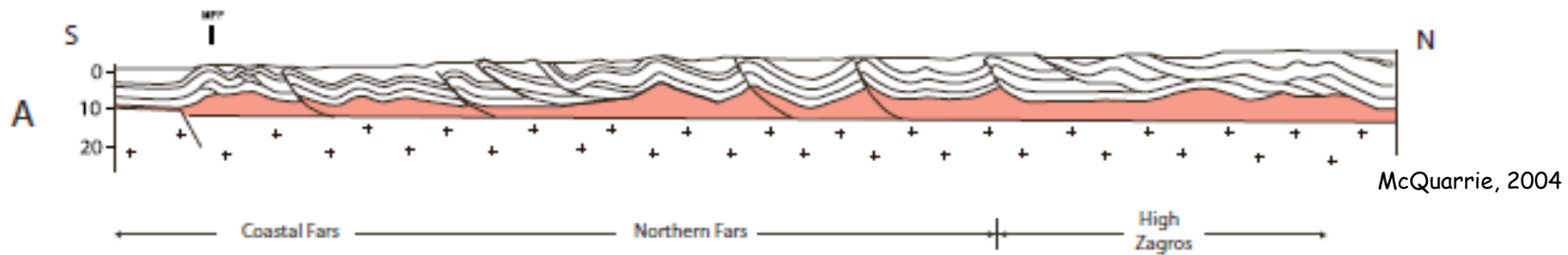


Changing interpretations through time of the structural style of the Umbria-Marches belt (Central Apennines)



Thick-skinned style with inversion tectonics

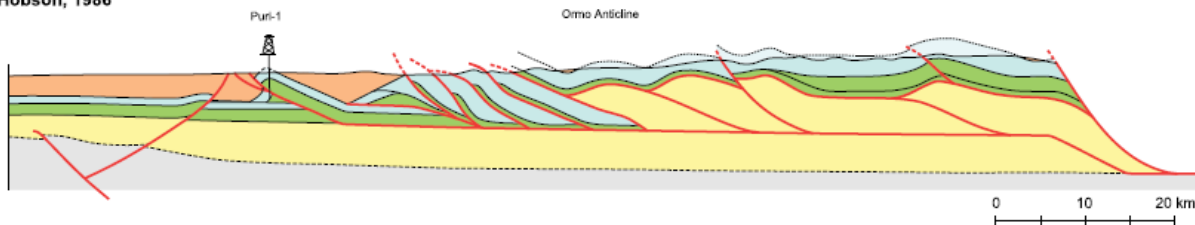




(Lacombe and Bellahsen, 2016)

Changing interpretations through time of the structural style of the Zagros Simply Folded belt (Fars)

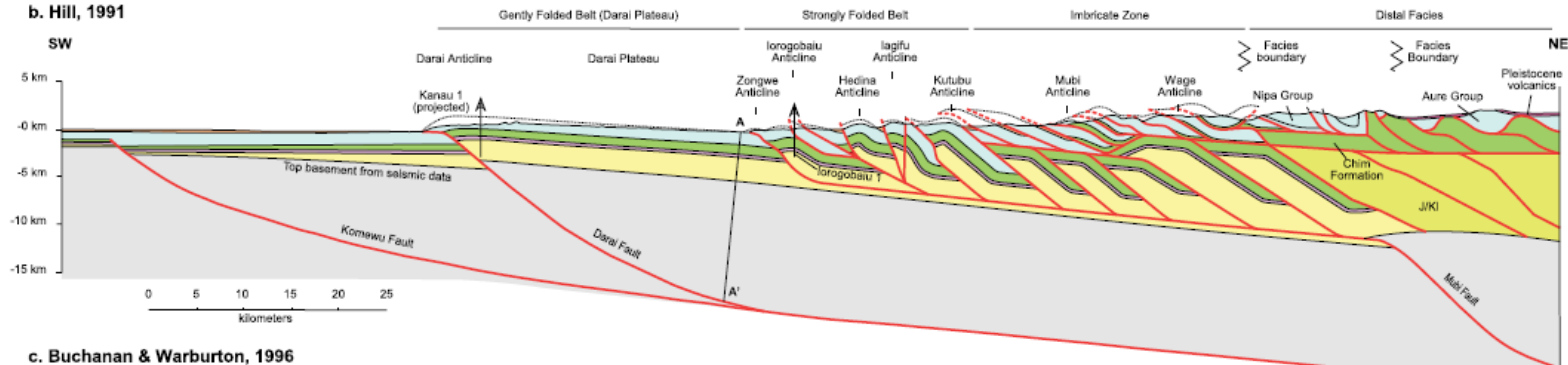
a. Hobson, 1986



Thin-skinned style

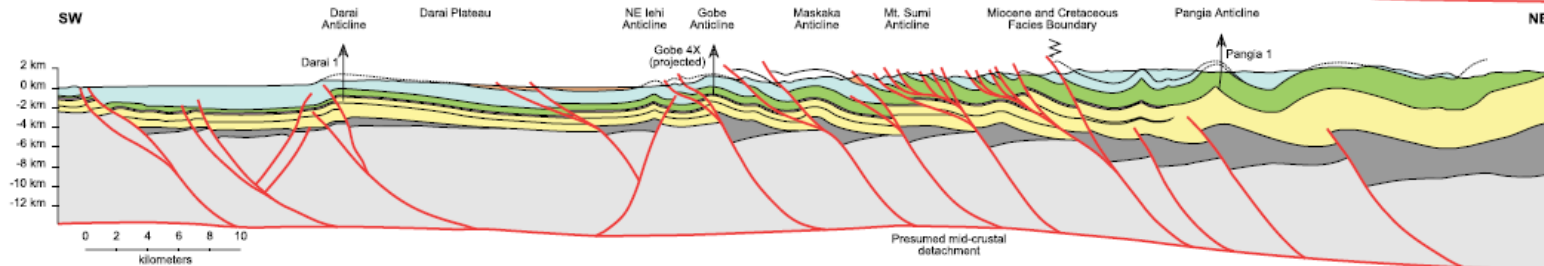
Superimposed thin-skinned and thick-skinned styles

b. Hill, 1991

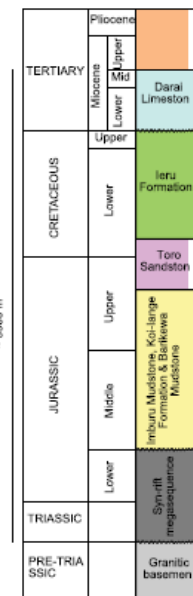


Thick-skinned style with inversion tectonics

c. Buchanan & Warburton, 1996

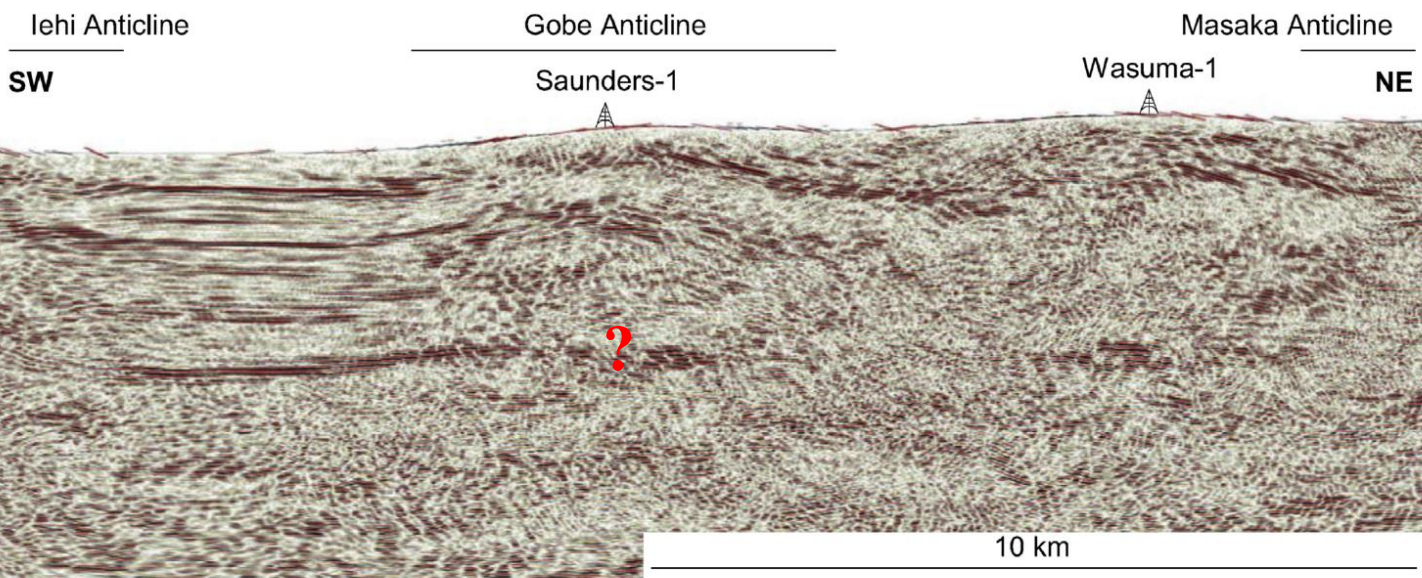


d. Simplified stratigraphic column

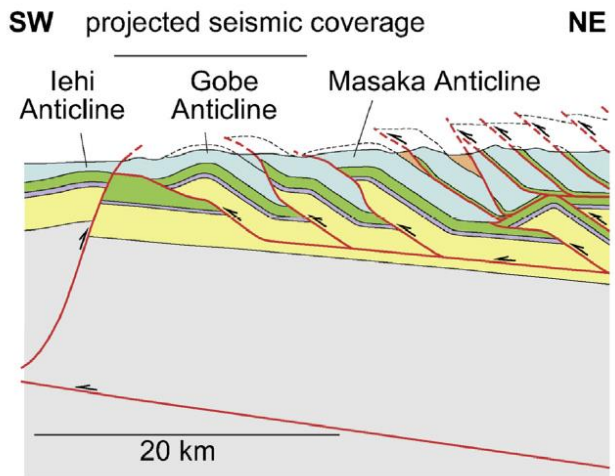


Changing interpretations through time of the structural style of the Papua New Guinea belt (Butler et al., 2018)

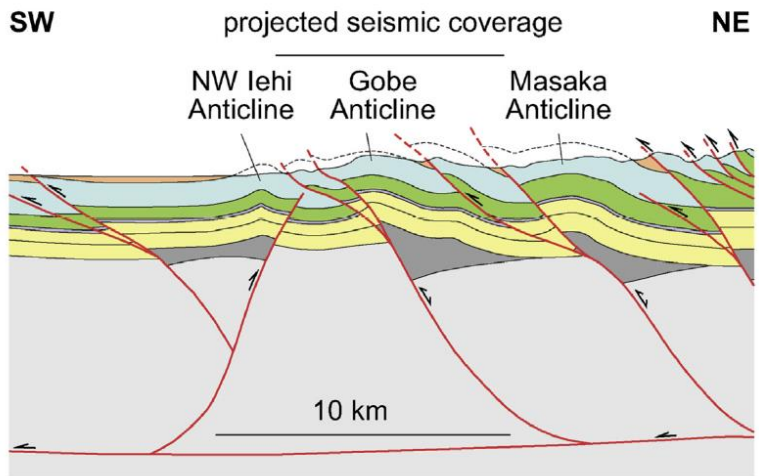
a.



b. Superimposed thin-skinned and thick-skinned styles

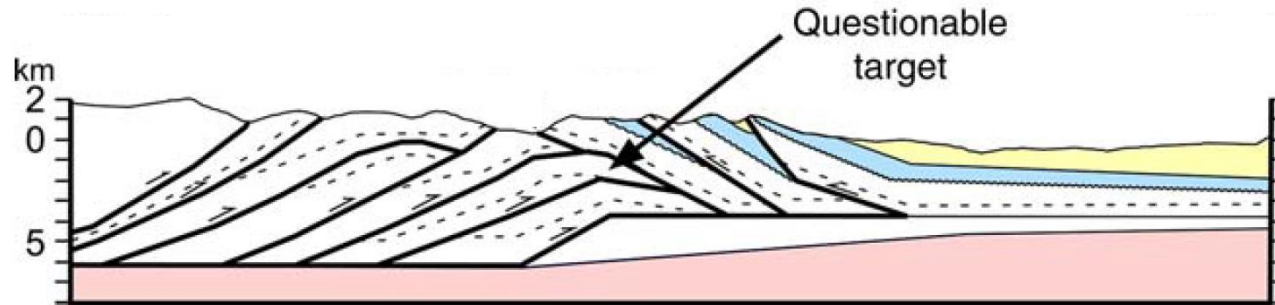


c. Thick-skinned style with inversion tectonics

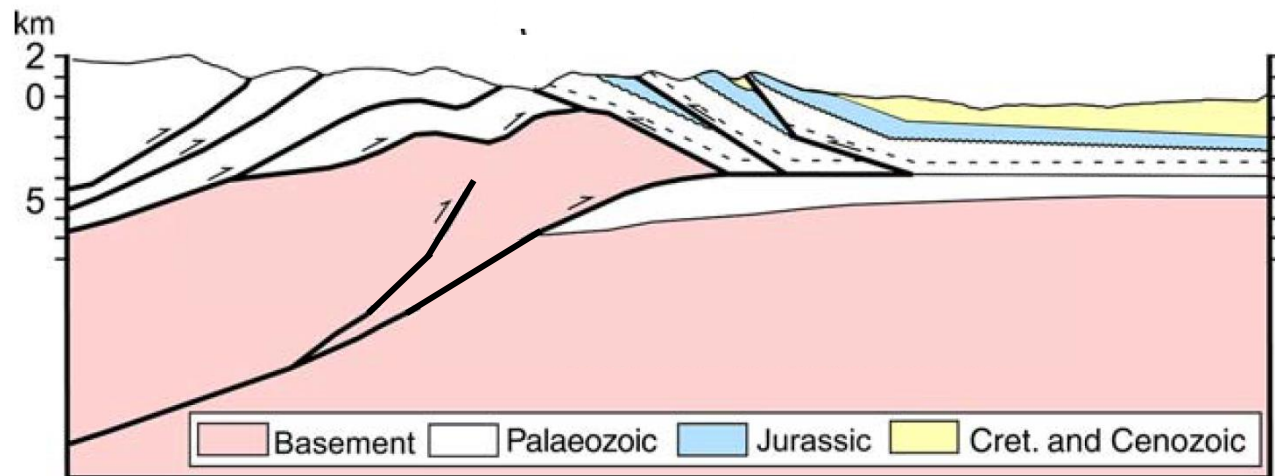


Contrasting interpretations of the structural style of the Gobe anticline (Papua New Guinea belt) (Butler et al., 2018)

Passive roof duplex model

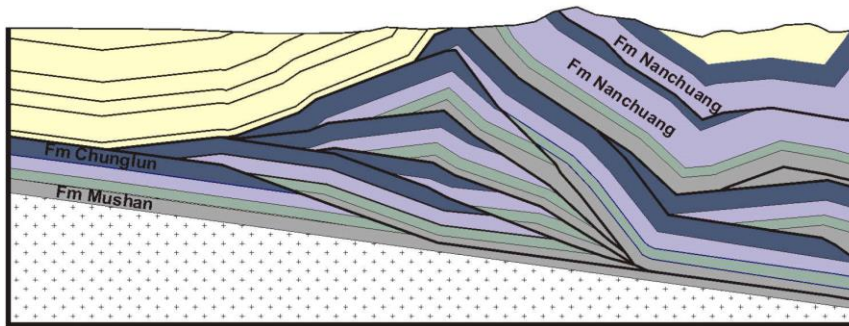


Inversion model alternative



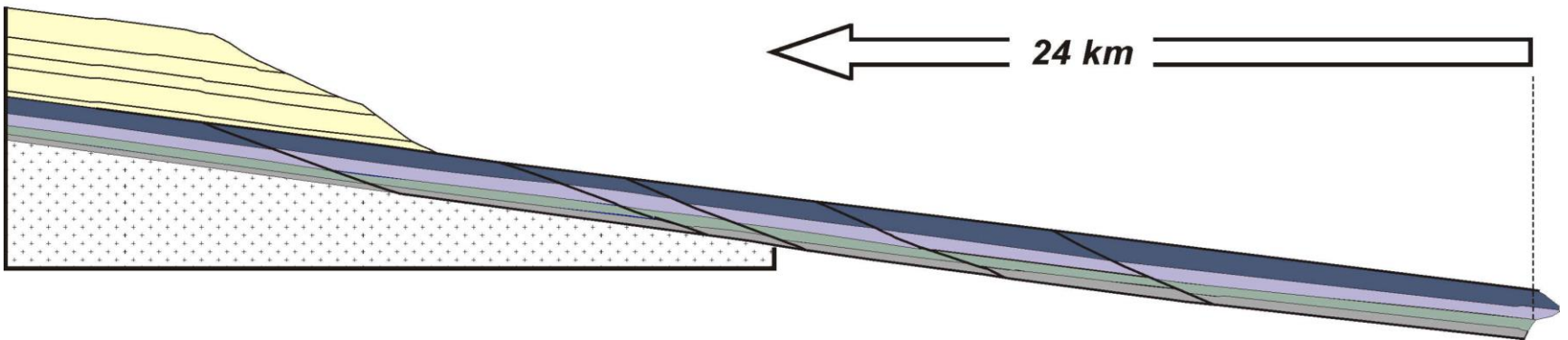
Chunglun

Tingpinglin



Thin-skinned hypothesis

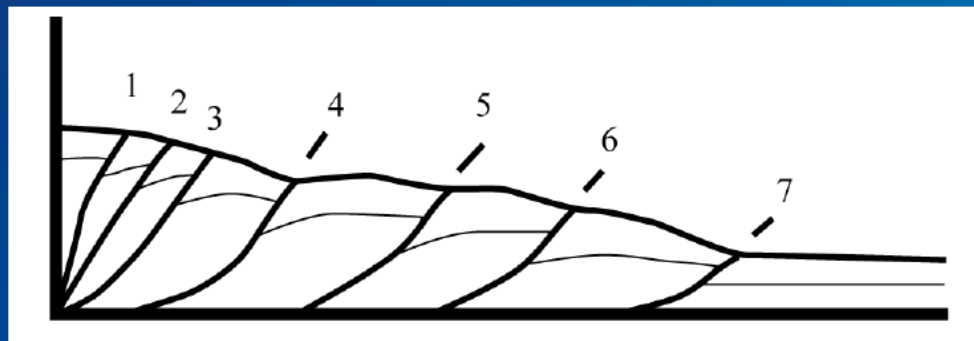
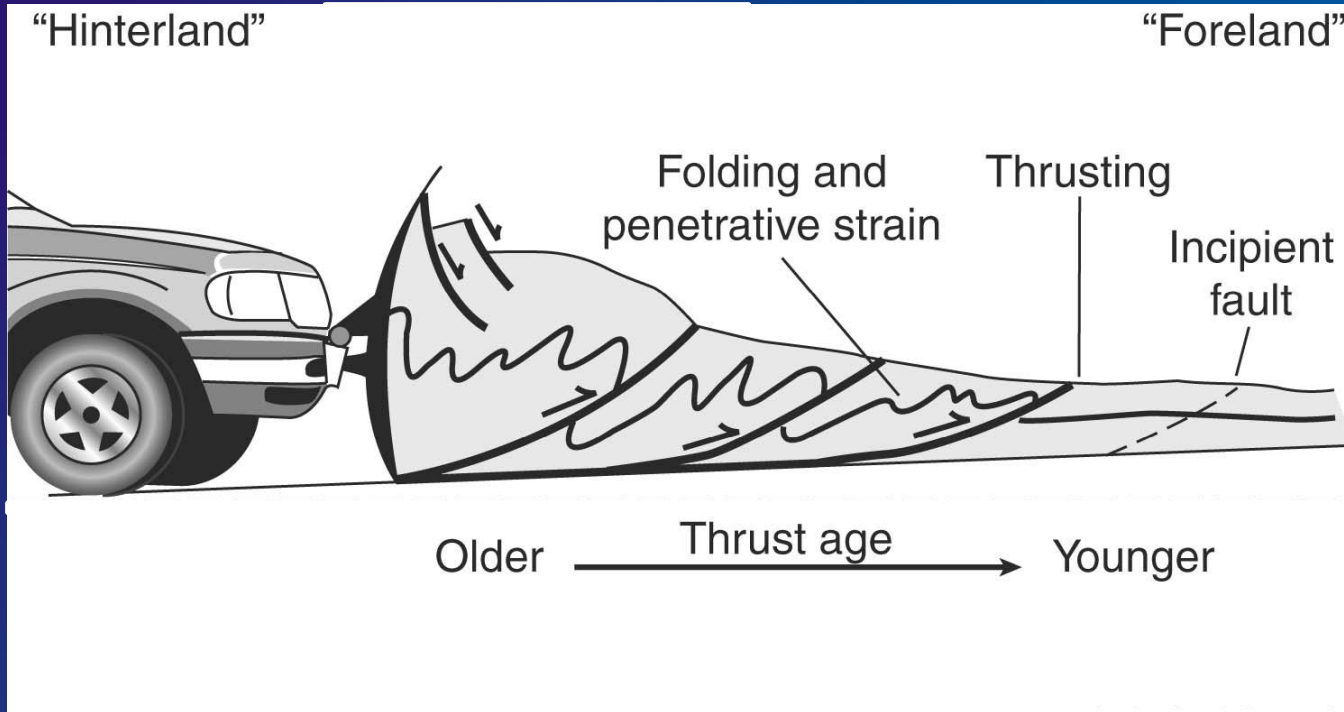
*Large shortening
of the sedimentary cover*

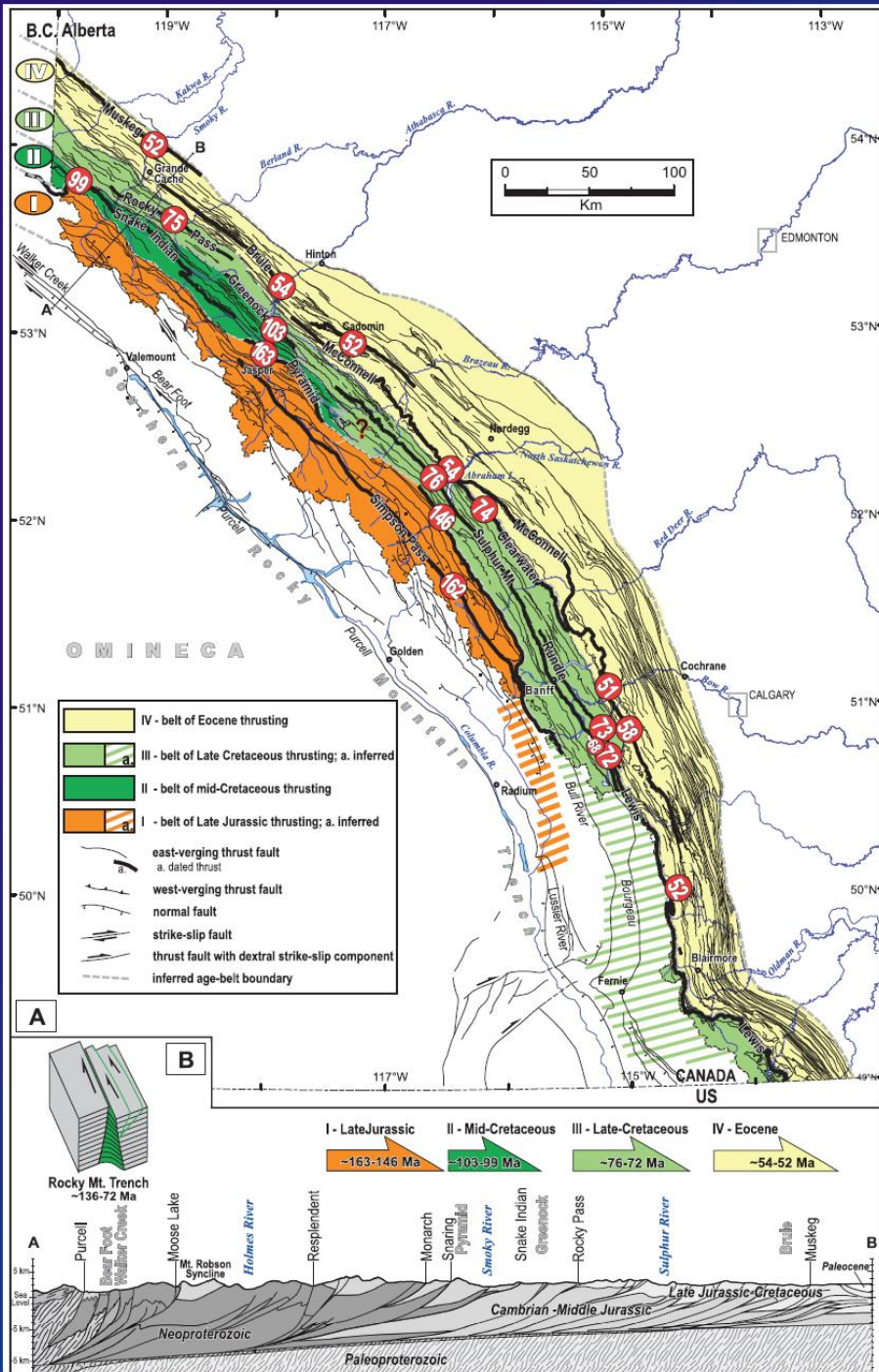


The amount of shortening is generally high in thin-skinned context, while it is much more conservative in a thick-skinned context, especially if inversion tectonics is involved.

**Sequence of deformation
in fold-and-thrust belts**

How does deformation distribute and propagate during thick-skinned tectonics?
Is the sequence of deformation the same than for thin-skinned style?



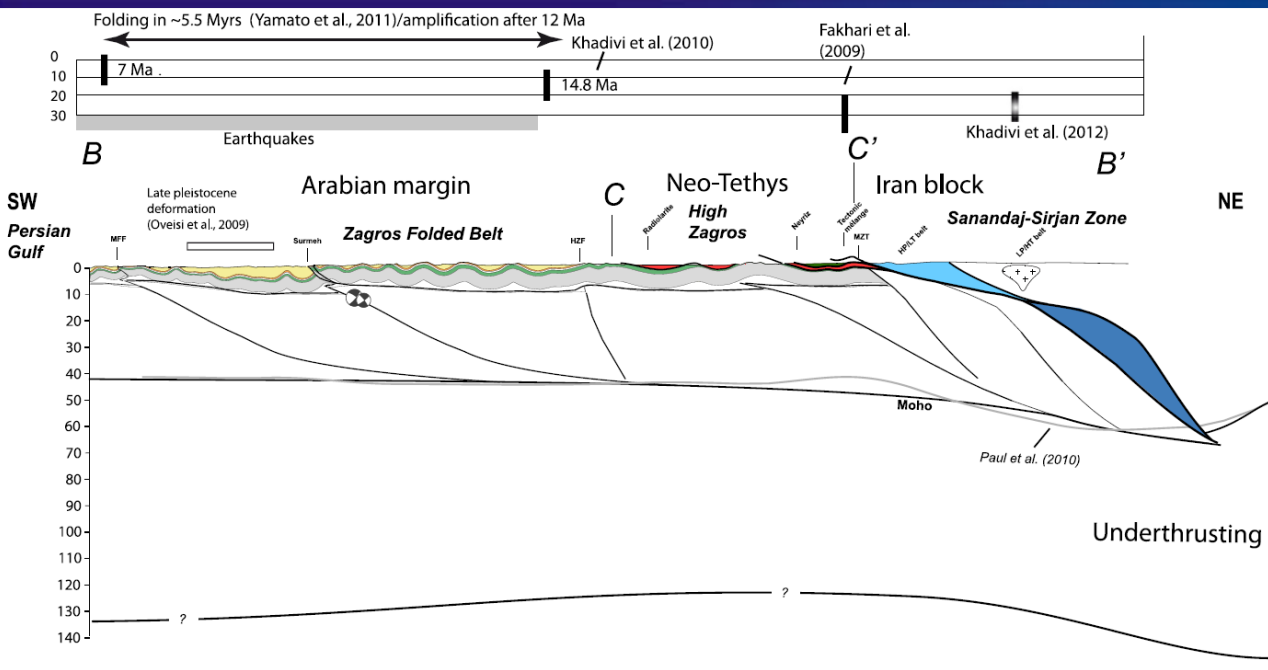


(Pana and Van der Pluijm, 2015)

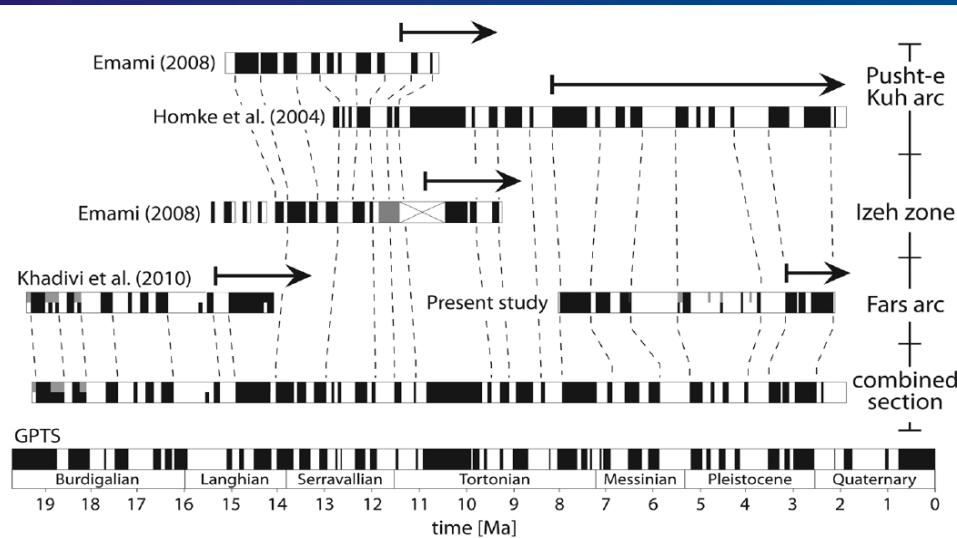
Evidence for orogenic pulses and outward sequence of Sevier deformation in the thin-skinned Alberta Rocky Mountains by $^{40}\text{Ar}/^{39}\text{Ar}$ dating of illites from gouges of major fault zones

Mouthereau et al., 2007, 2012

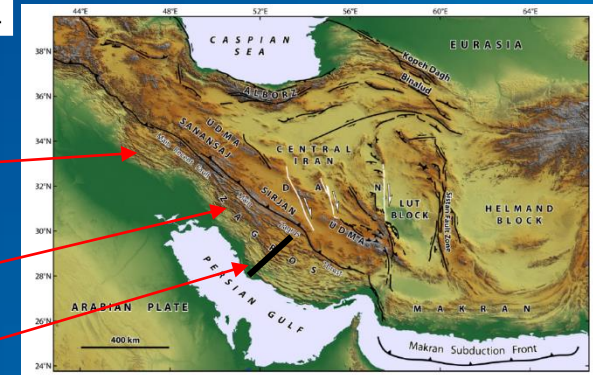
Evidence for outward sequence of folding in the Zagros belt by magnetostratigraphic dating of syn-folding formations



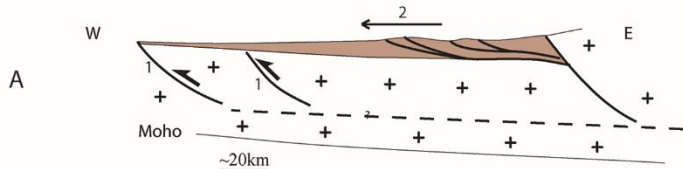
Ruh et al. 2014



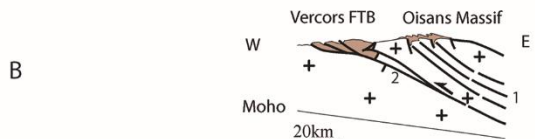
Combined magnetostratigraphic section of studies conducted in the Simply Folded Belt of the Zagros. Black arrows indicate onset of deformation inferred by progressive unconformities. Folding in the outer Pusht-e Kuh arc [Homke et al., 2004] is triggered by the Mountain Front Flexure.



Early inversion of inherited normal faults / early high angle basement thrusting in the foreland (Zagros, Taiwan)

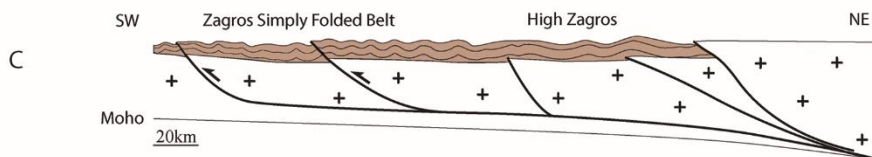


Basement shortening at the rear then exhumation and forelandward propagation above basement ramps activating cover shallow decollement (Western Alps)

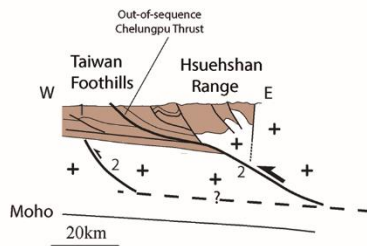
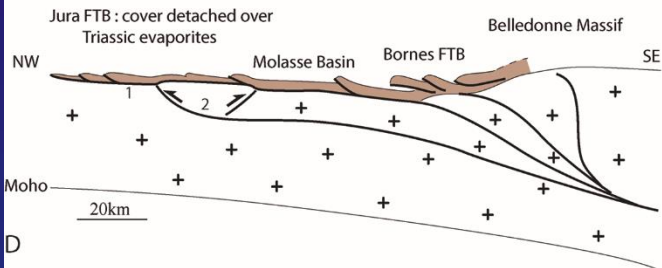


Coeval thin-skinned and thick-skinned tectonics.

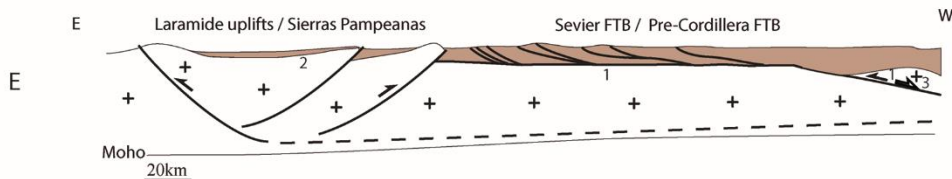
The cover is detached mainly above the low-viscosity Hormuz salt layer while the basement deforms by both seismogenic faulting and ductile aseismic shearing (Zagros)



Late basement thrusting : refolding of shallow nappes by high angle thrusts reactivating inherited normal faults (e.g. Jura, Provence) /out-of-sequence seismogenic basement thrusting



Basement-involved shortening occurring forelandward after thin-skinned tectonics : Laramide uplifts / Sevier FTB and Sierras Pampeanas / Pre-Cordillera FTB of Argentina



Sequence of thick-skinned versus thin-skinned tectonics in FTBs

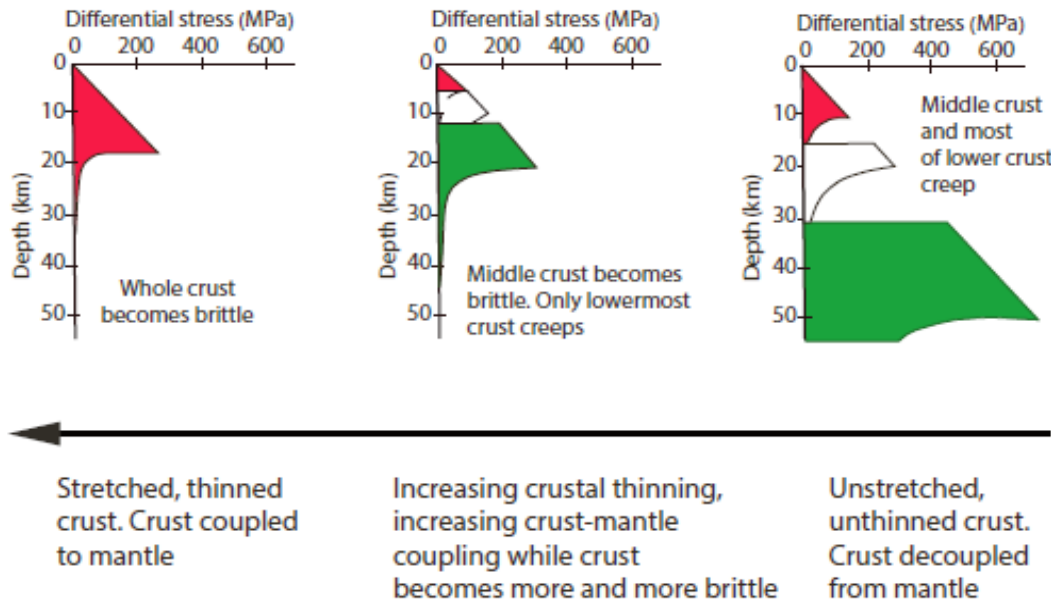
→ Thin-skinned orogenic wedges often develop through a progressive outward (forelandward) propagation of deformation through time.

→ Thick-skinned systems show a more erratic sequence owing to the reactivation of basement heterogeneities that govern the stress field in the overlying sedimentary cover.

→ Complex sequence may be encountered when both structural styles are superimposed

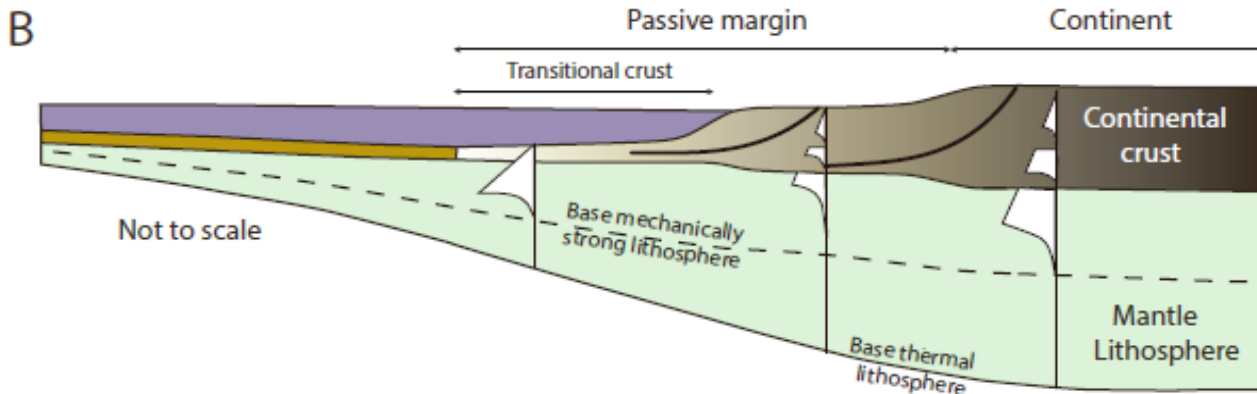
**Some first-order rheological controls
of the structure of fold-and-thrust belts**

Differential stretching of the lithosphere modifies its rheological properties which will subsequently control deformation style during collision.



As the crust thins and cools during progressive rifting, the reduction in overburden pressure and temperature makes the rocks which originally deformed by plastic creep gradually become more prone to brittle failure.

The result is that the initial weak zones in the middle crust and deep crust disappear and that the entire crust becomes brittle.



The important consequences of the progressive embrittlement of originally ductile rocks during lithospheric extension are :

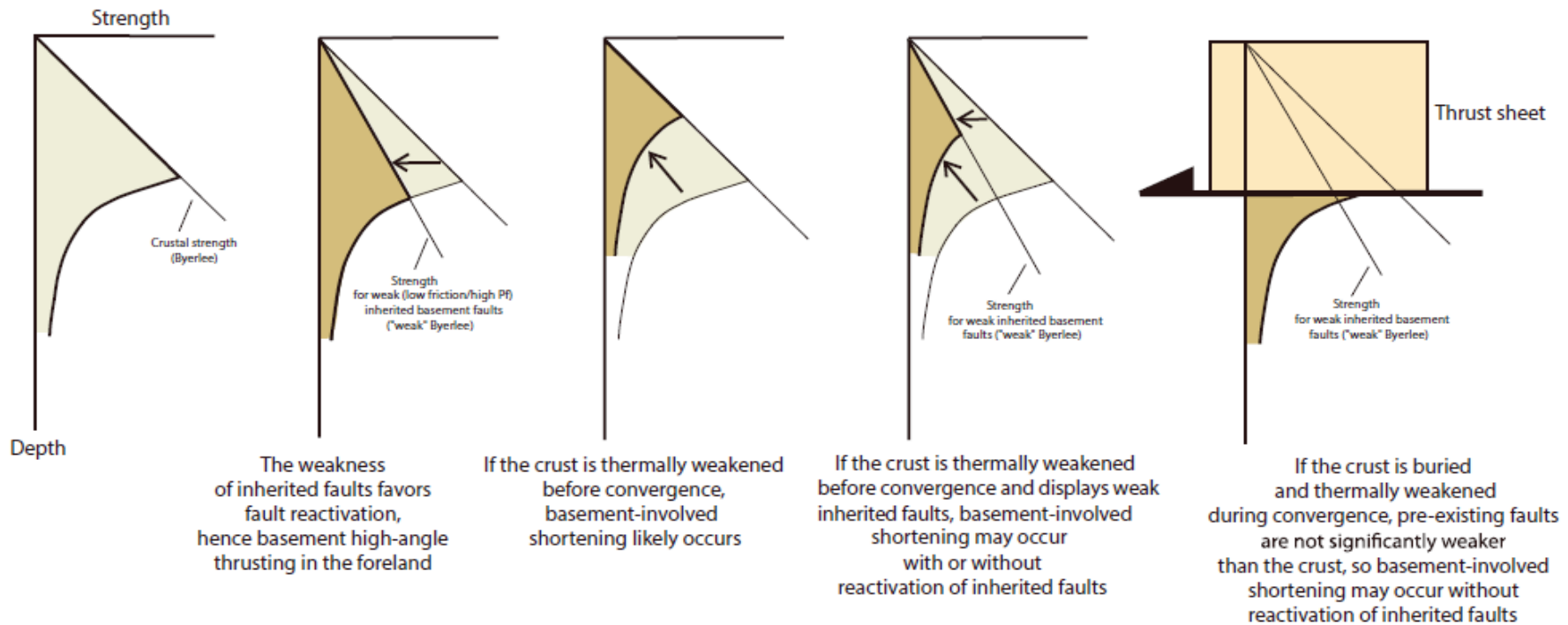
- (1) that lateral flow or displacement of particular layers within the crust should become progressively more difficult as rifting proceeds, and
- (2) that the upper crust becomes coupled to the mantle.

Passive margins are key players in the collisional processes as the arrival of their proximal, poorly thinned parts into the subduction zone mark the onset of collision.

For FTBs that developed from former passive margins, the occurrence of weak mechanical layers within the proximal margin lithosphere (the middle and most of the lower crust are expectedly ductile) may explain that contractional deformation be distributed within most of the crust, giving rise to basement- involved, collisional tectonic style.

In contrast, because these weak crustal levels are usually lacking in distal parts of the margins as a result of thinning, these stronger lithospheric domains are more prone to localized deformation in a thin-skinned, continental subduction style.

Thick-skinned tectonics with or without inversion tectonics : rheology (weakening) does matter

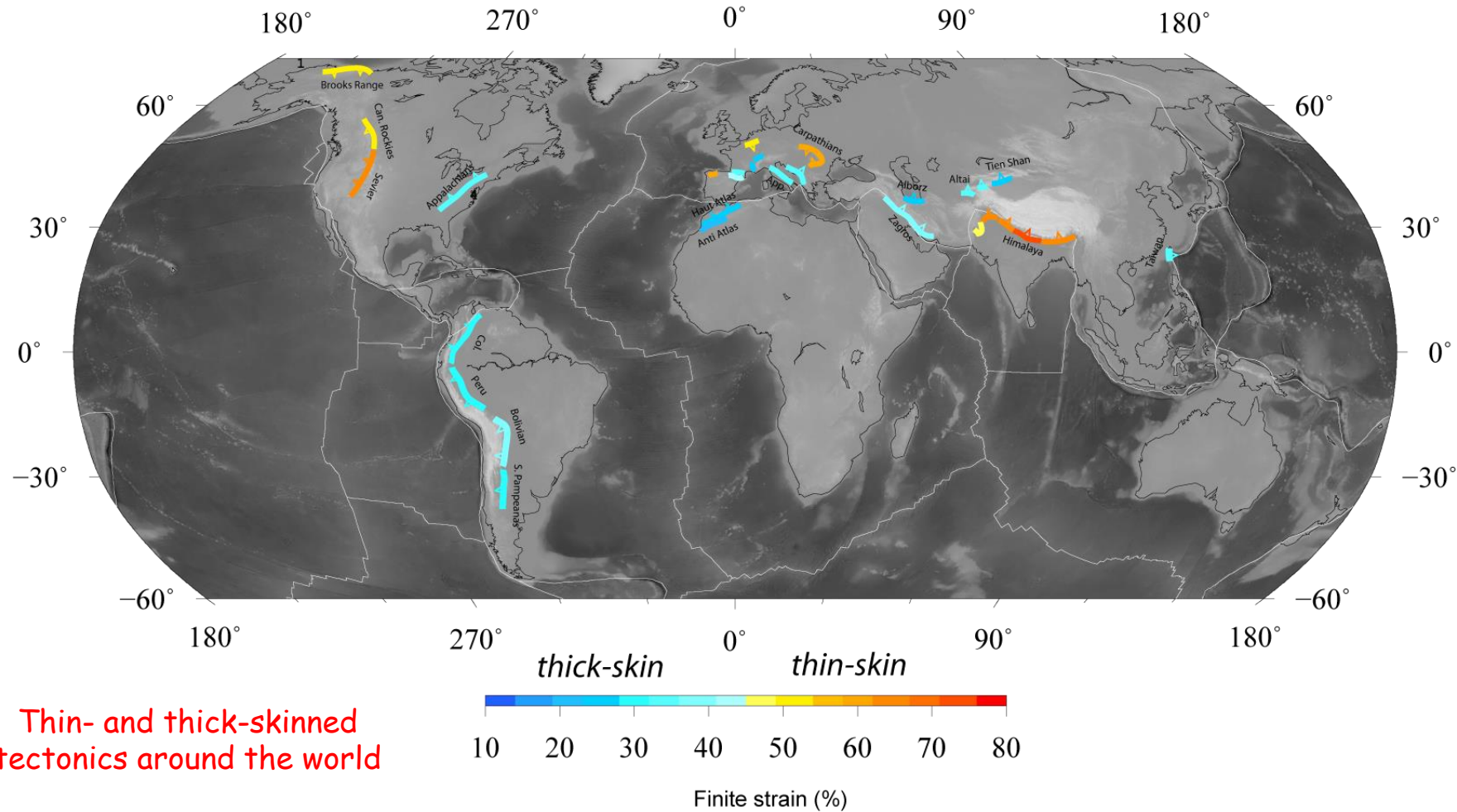


(Lacombe and Bellahsen, 2016)

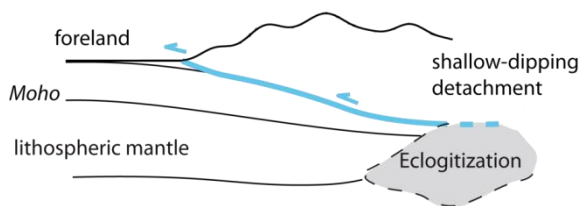
Correlation between spatial variations of the flexural rigidity of the lithosphere and the nature and amount of foreland deformation has been suggested for the Andes FTB and Taiwan.

Regions with low T_e correlate with thick-skinned deformation whereas regions with high T_e correlate with thin-skinned deformation :
a strong lithosphere is less easily deformed so that shortening is localized in a narrow zone at shallow depth, while a weaker lithosphere enables crust-mantle decoupling and shortening of the whole crust.

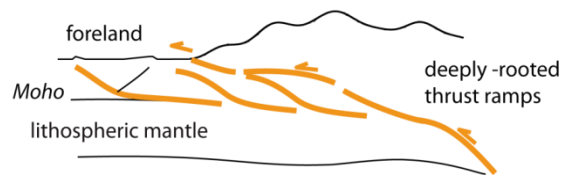
The local increase of plate coupling and inhomogeneities in a prefractured margin can affect the rigidity of the layered continental lithosphere, supporting a mechanical relationship between its strength and the structural style.



$h < 10$ km



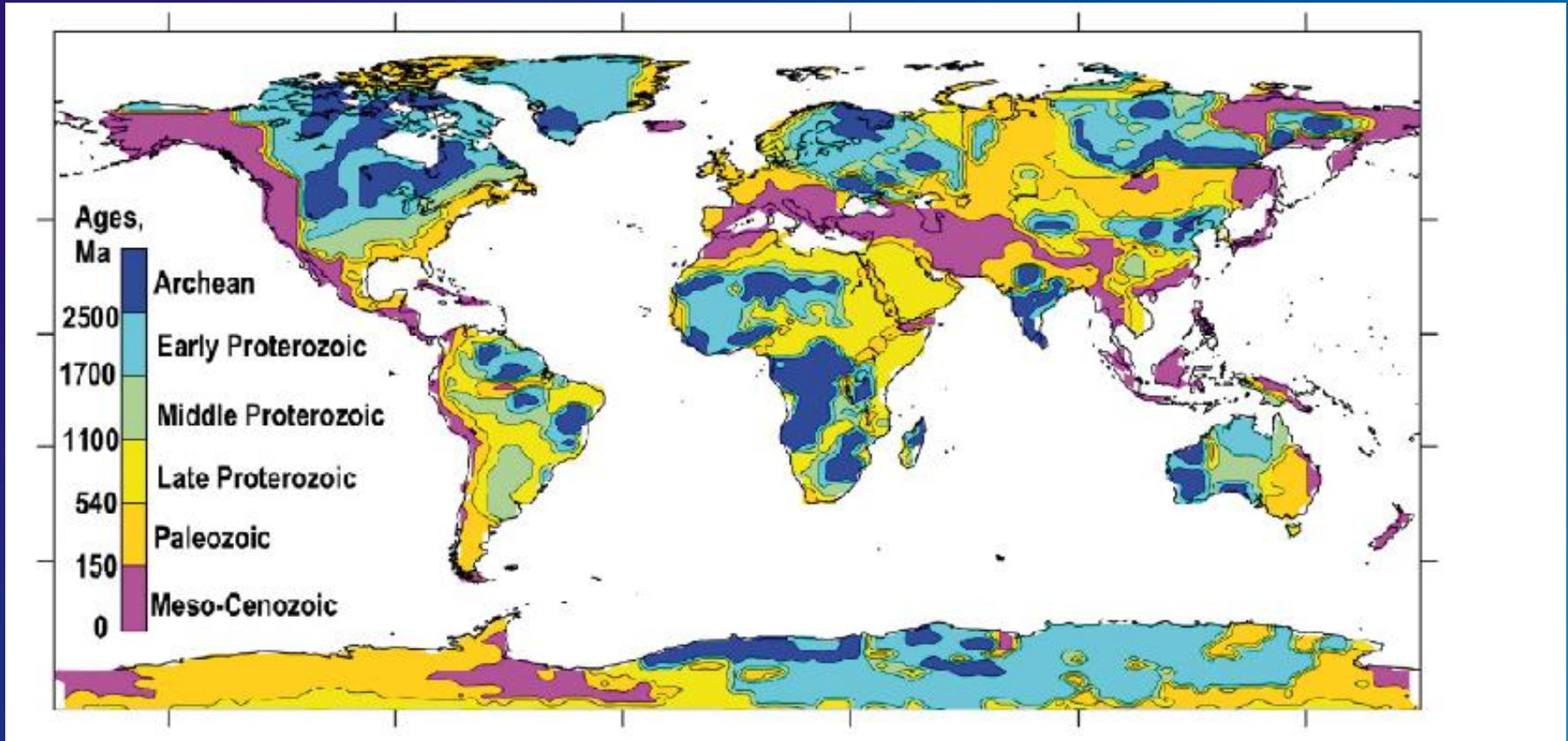
$h > 15-20$ km



Thin-skinned
~40-75%

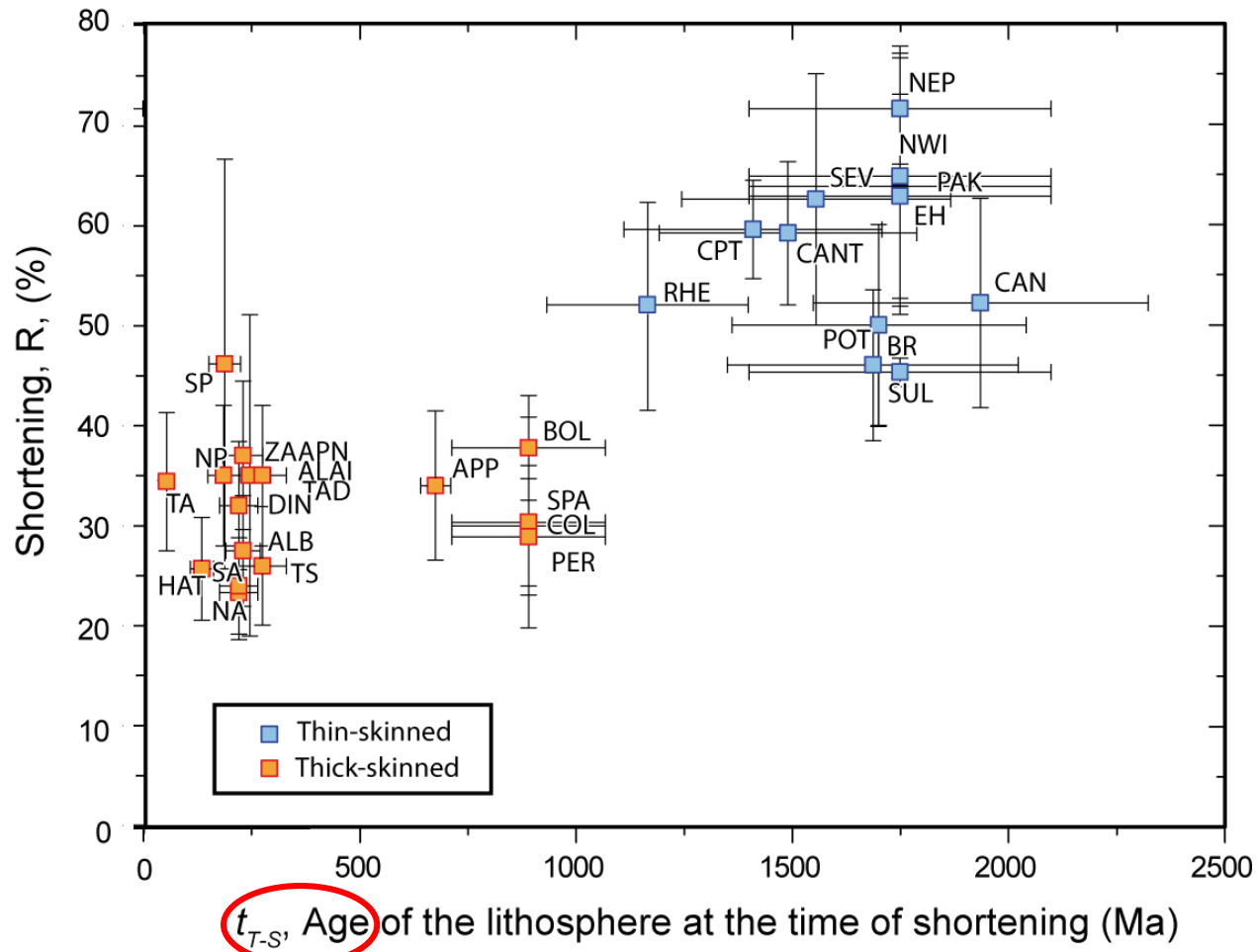
Thick-skinned ~20-40%

Thermotectonic age of continents
= age of the last 'rejuvenating' tectono-magmatic event



(Artemieva, 2006)

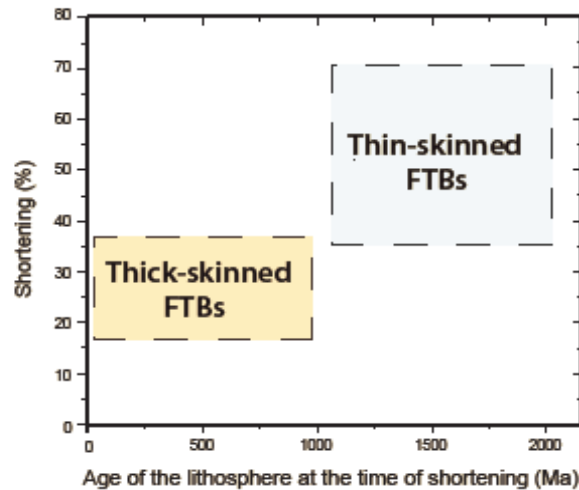
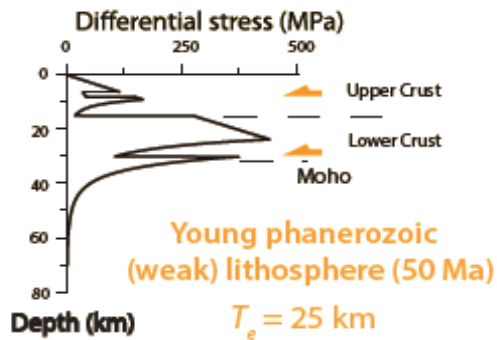
(Mouthereau et al., 2013)



Thick-skinned fold-thrust belts



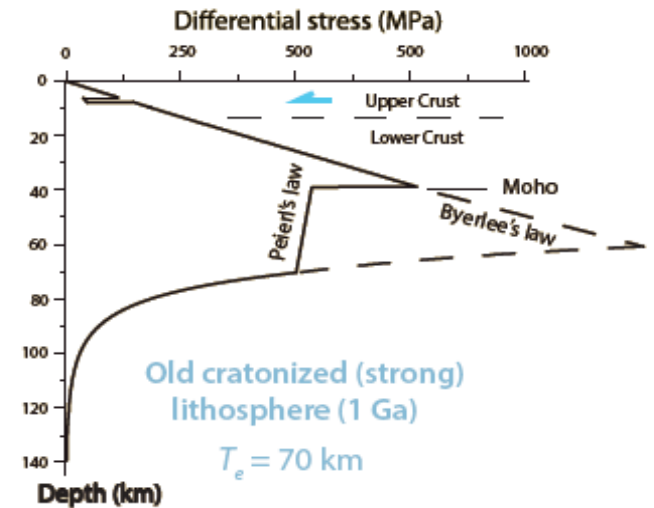
Pure-shear ('inversion/collision') style



Thin-skinned fold-thrust belts



Simple-shear ('subduction') style



1. There are increasing lines of evidence of basement-involved shortening in FTBs, even in the 'archetypal' thin-skinned belts. This basement involvement is often associated with basement inversion tectonics.

2. The pre-orogenic deformation of the basement may control the geometry, kinematics and mechanics of FTBs, either at the scale of the whole belt (e.g., belt curvature, segmentation and along-strike variations of structural styles, sequence of deformation, localization of contractional deformation and % of shortening) or at the scale of tectonic units (reactivation of inherited basement faults, basement-cored folding).

In some cases however, inherited basement (normal) faults are not reactivated whereas newly-formed compressional shear zones develop, which brings into question the bulk rheology of the crust vs the rheology of preexisting fault zones available for reactivation.

3. In basement-involved, thick-skinned FTBs, shortening is distributed throughout the whole crust and is usually lower than in their thin-skinned counterparts, which likely requires/reflects a specific thermo-mechanical behavior of the underlying lithosphere (e.g, hot and young, hence weak).

In FTBs resulting from inversion of former proximal passive margins, basement thrusting that occurs in a rather localized way in their inner parts requires structural inheritance and/or a hot crustal temperature either inherited from a recent (pre-orogenic) rifting event or resulting from syn-orogenic underthrusting and heating.

4. Basement-involvement in FTBs specifically raises the question of the way the orogen is mechanically coupled to the foreland and how orogenic stresses are transmitted through the heterogeneous basement of the foreland/plate interior.

Development of thick-skinned belts within cratons remains somewhat enigmatic and likely requires specific boundary conditions (strong interplate coupling, such as provided by flat-slab subduction) ensuring efficient transmission of stresses (crustal/lithospheric stress guide) and propagation of deformation in the pro- and retro-foreland by crustal/lithospheric buckling or deep crustal decollement, in addition to local structural and/or possible physical/compositional weakening.

Foreland fold-and-thrust belts

Part 2 : Case studies

Olivier LACOMBE

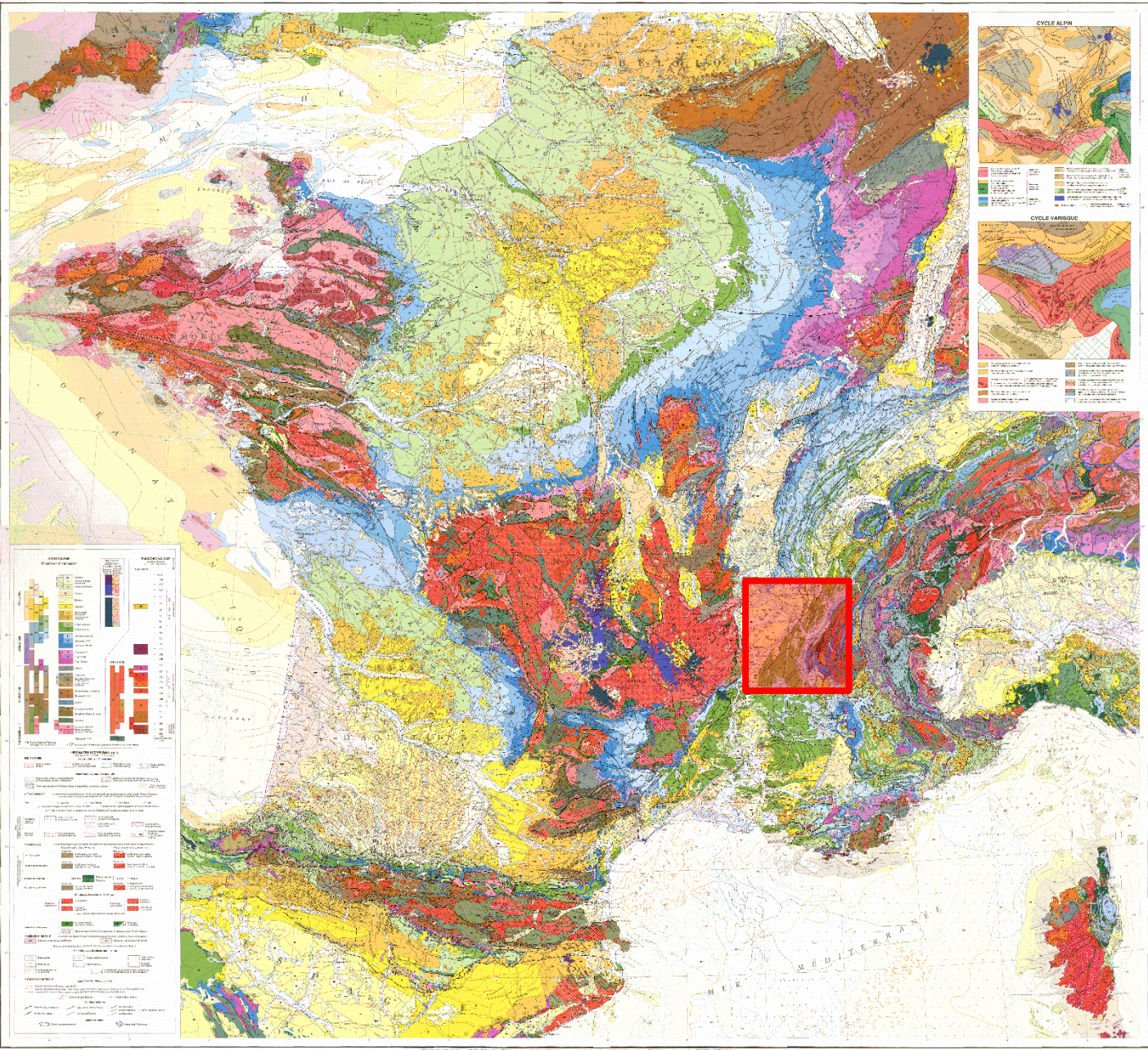


Alpine fold-thrust belts

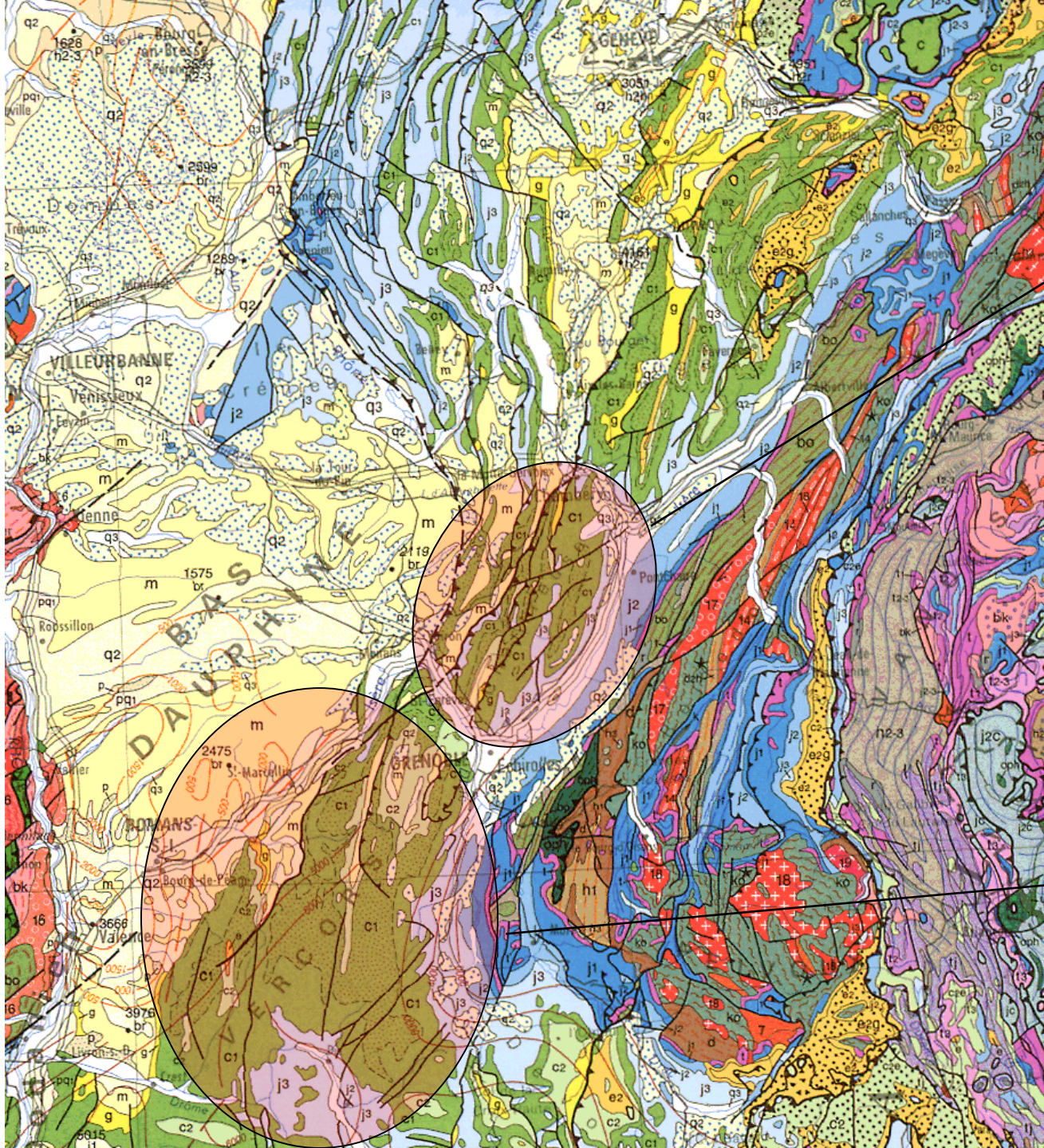
**Control of pre-orogenic sequences on structural style :
Vercors/Chartreuse**

CARTE GÉOLOGIQUE DE LA FRANCE

à l'échelle du millionième
 D'Alsace

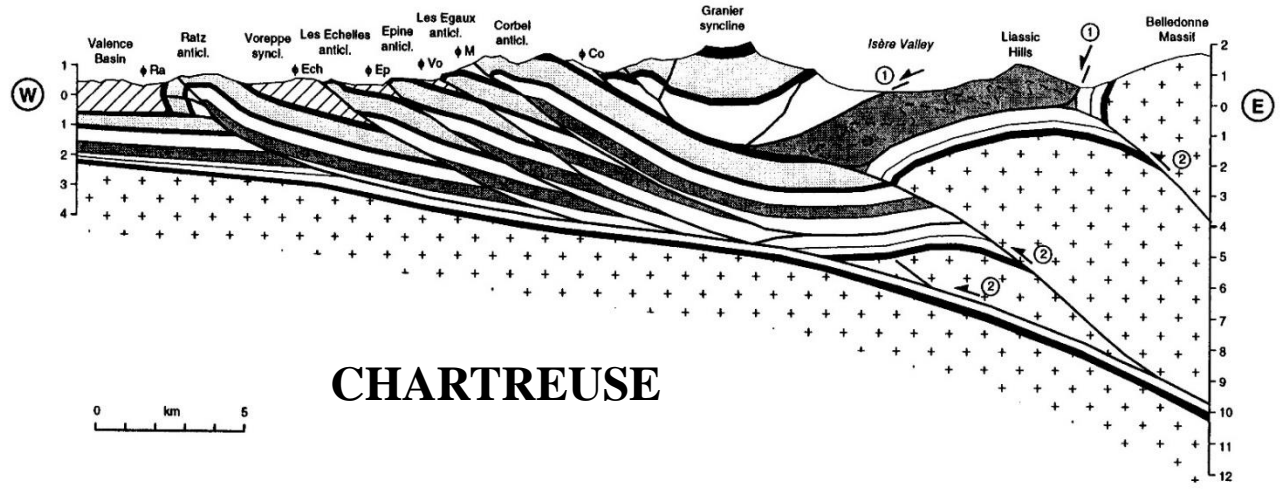
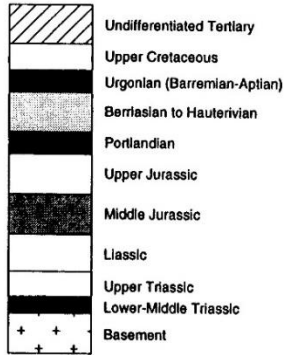


BRGM
 BUREAU BRASIER GÉOLOGIQUE
 MINISTÈRE DES PÊCHES, DE LA PÊCHE, DE LA FAUNE ET DE LA FAUCONNERIE
 17, AVENUE DE LA RÉPUBLIQUE, 93100 LA PLAINE SAINT-DENIS
 Tél. 01 49 39 39 39
 Fax 01 49 39 39 38
 Courriel : brgm@brgm.fr
 Site Internet : www.brgm.fr

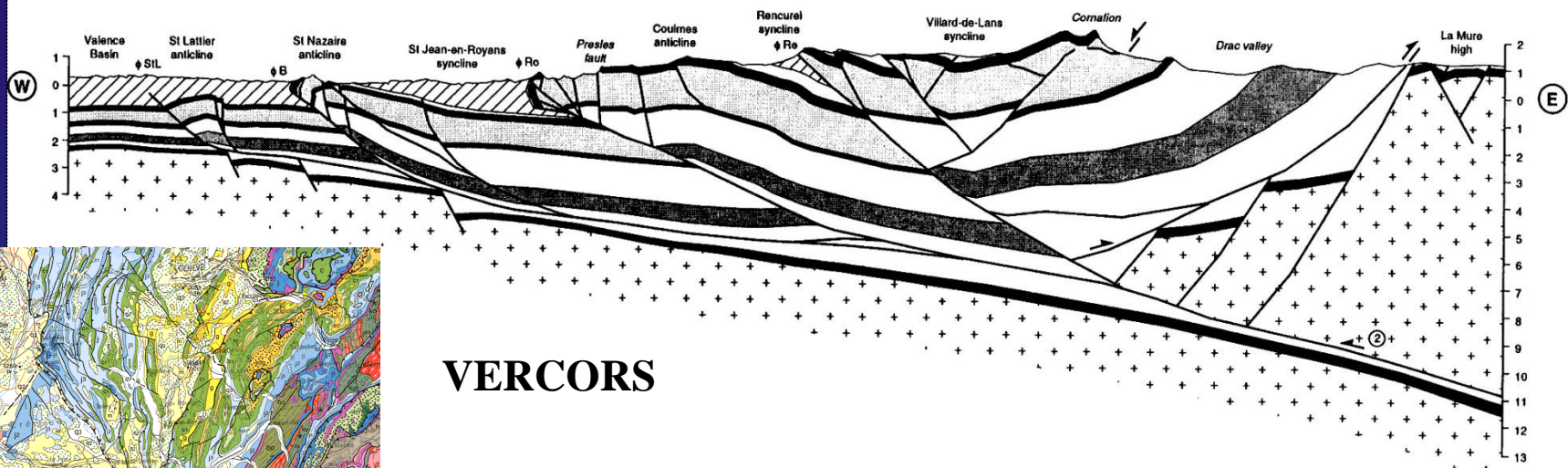


CHARTREUSE

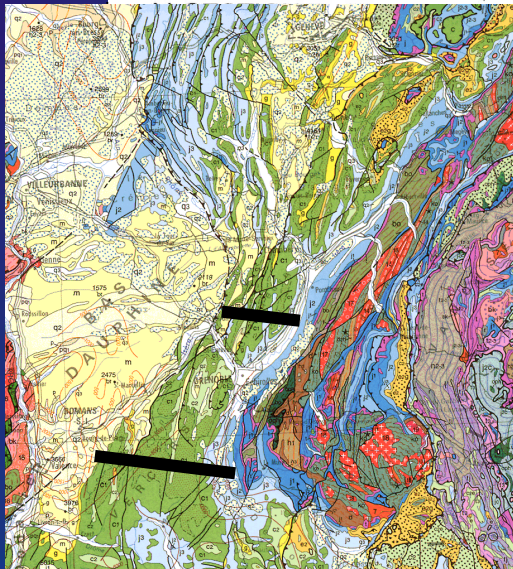
VERCORS



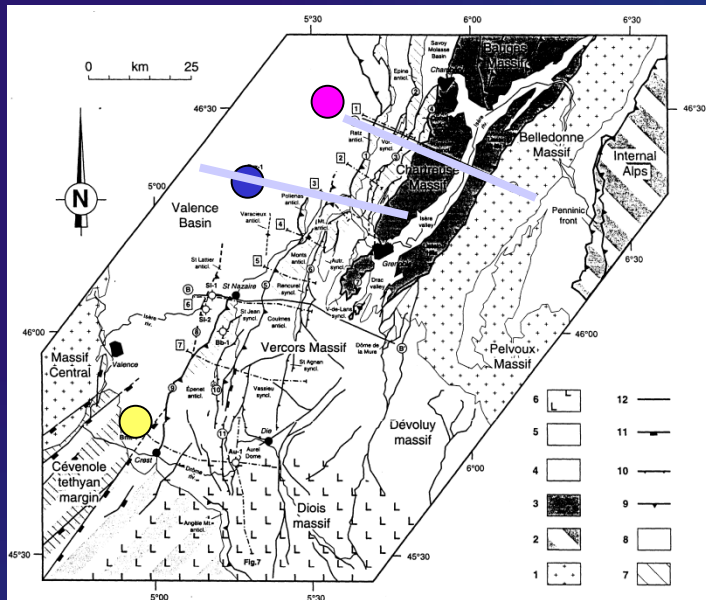
CHARTREUSE



VERCORS

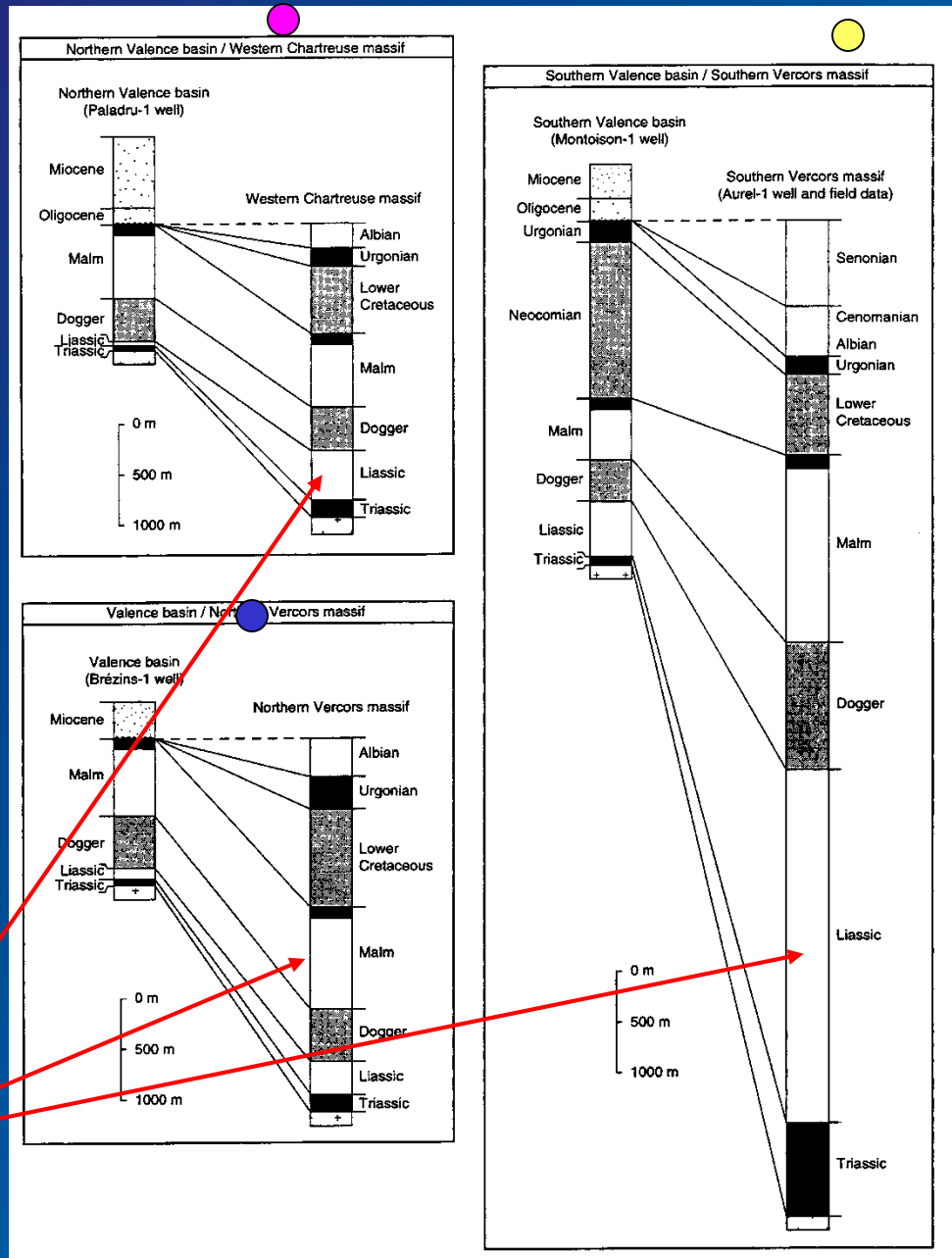


Sedimentary cover thickness in the Chartreuse and the Vercors



- The overall thickness of the pre-orogenic Mesozoic succession increases from N (Chartreuse) to S (Vercors)
- The thickness of the Liassic marls = décollement level increases from N (Chartreuse) to S (Vercors)

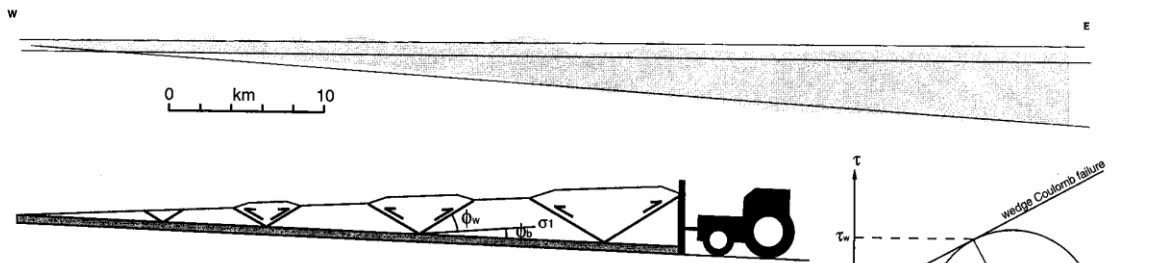
$$\tau_b = \eta \frac{V}{T_d}$$



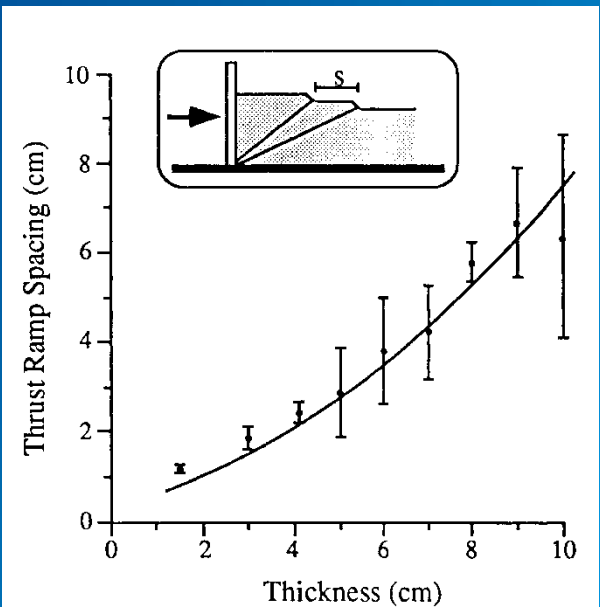
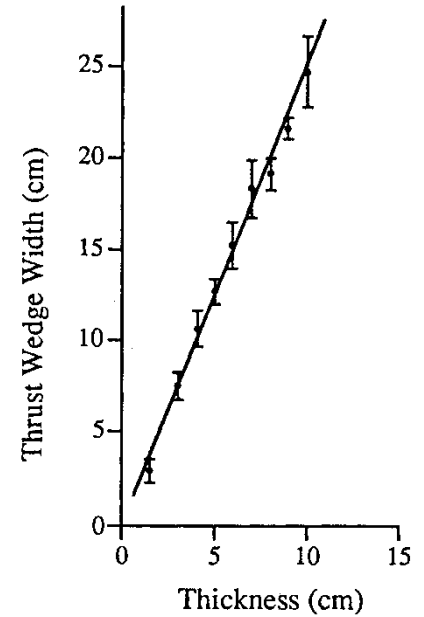
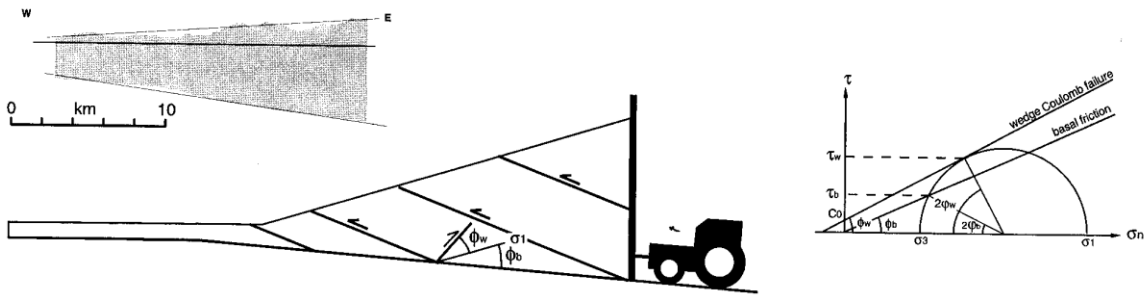
(Philippe, 1995)

Interpretation of the Vercors/Chartreuse tectonic style in terms of critical wedge (basal friction and thickness of deformed material)

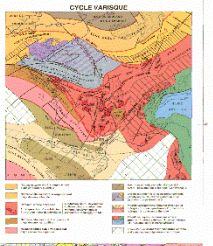
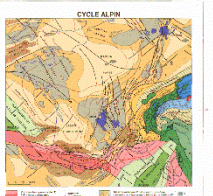
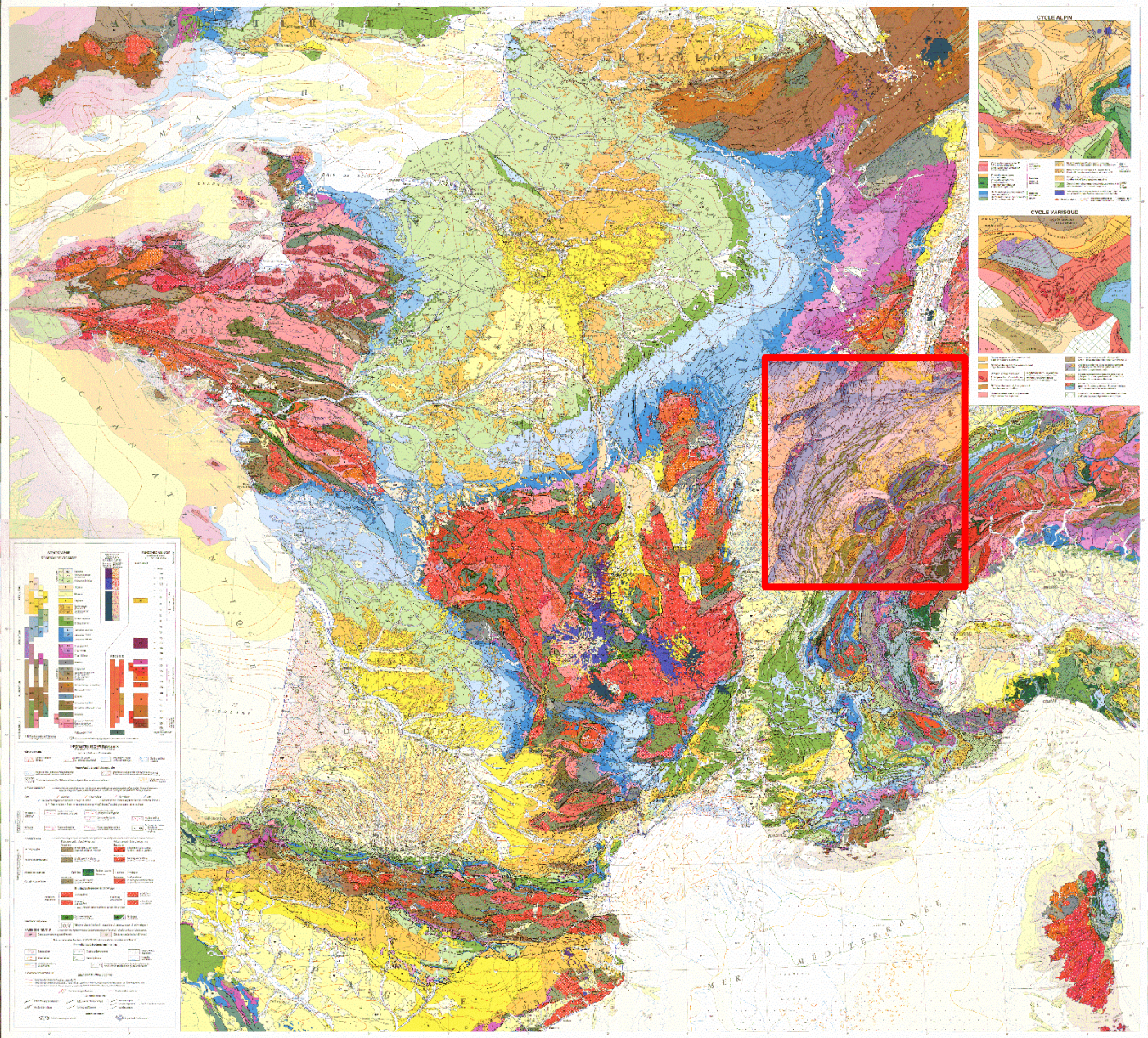
(a) Jura fold-and-thrust belt and Molasse Basin: / Vercors



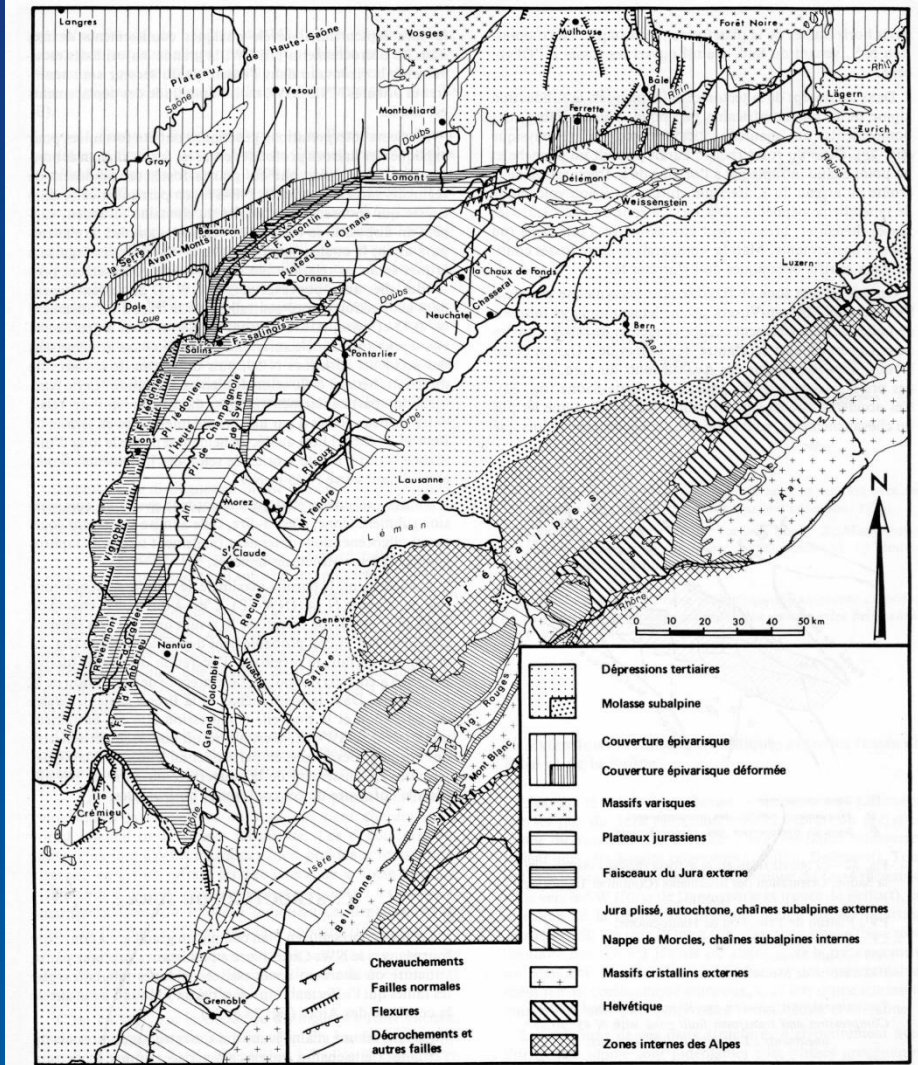
(b) Chartreuse fold-and-thrust belt:

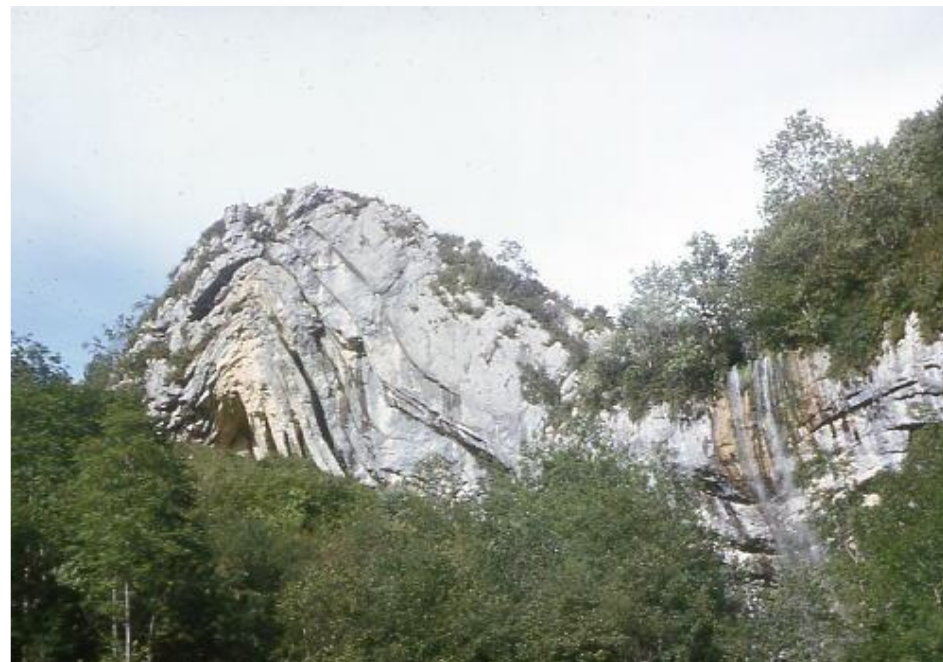


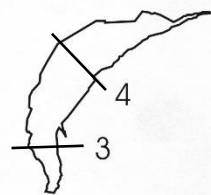
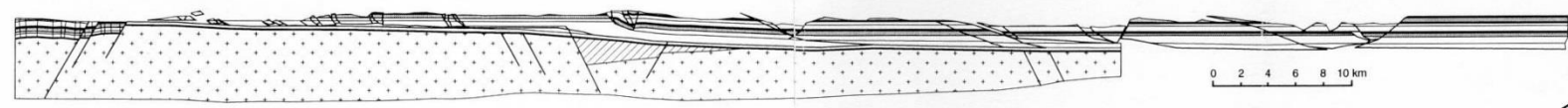
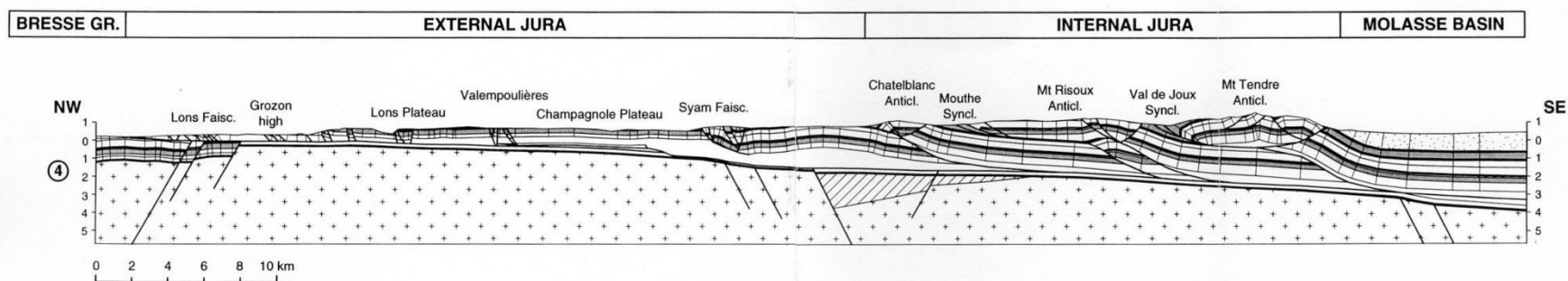
**Change from thin-skinned to thick-skinned
style though time : the Jura**



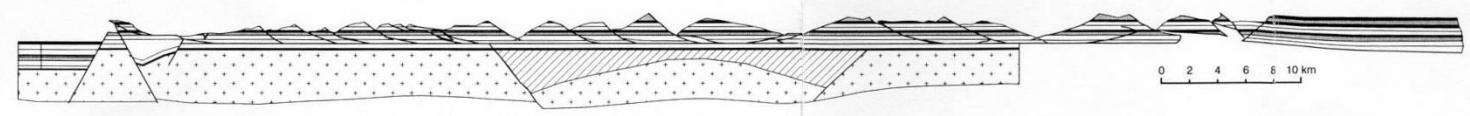
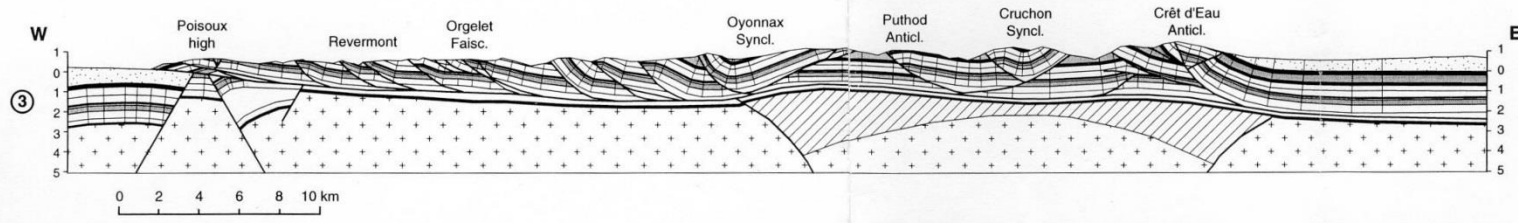
The famous, crescent-like Jura fold-and-thrust belt



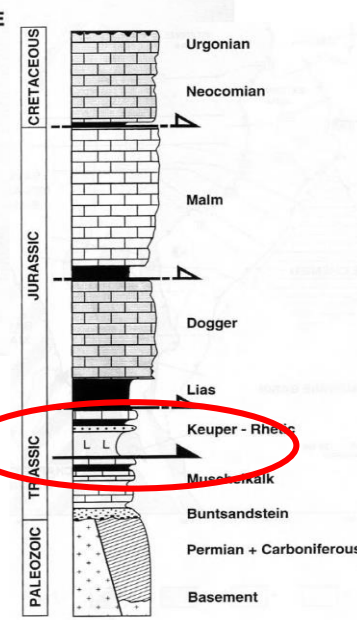




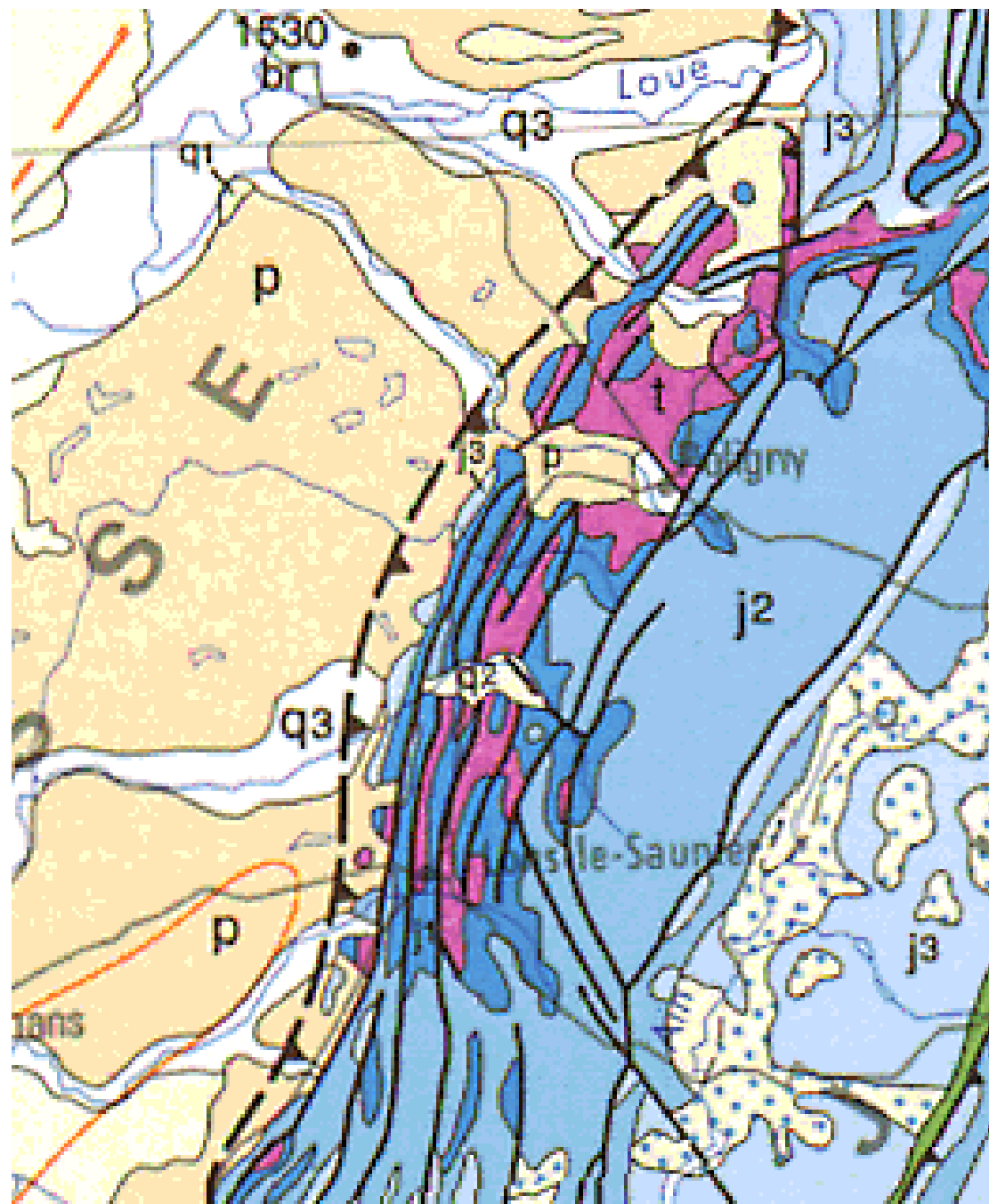
BRESSE GRABEN **EXTERNAL JURA** **INTERNAL JURA** **MOLASSE BASIN**



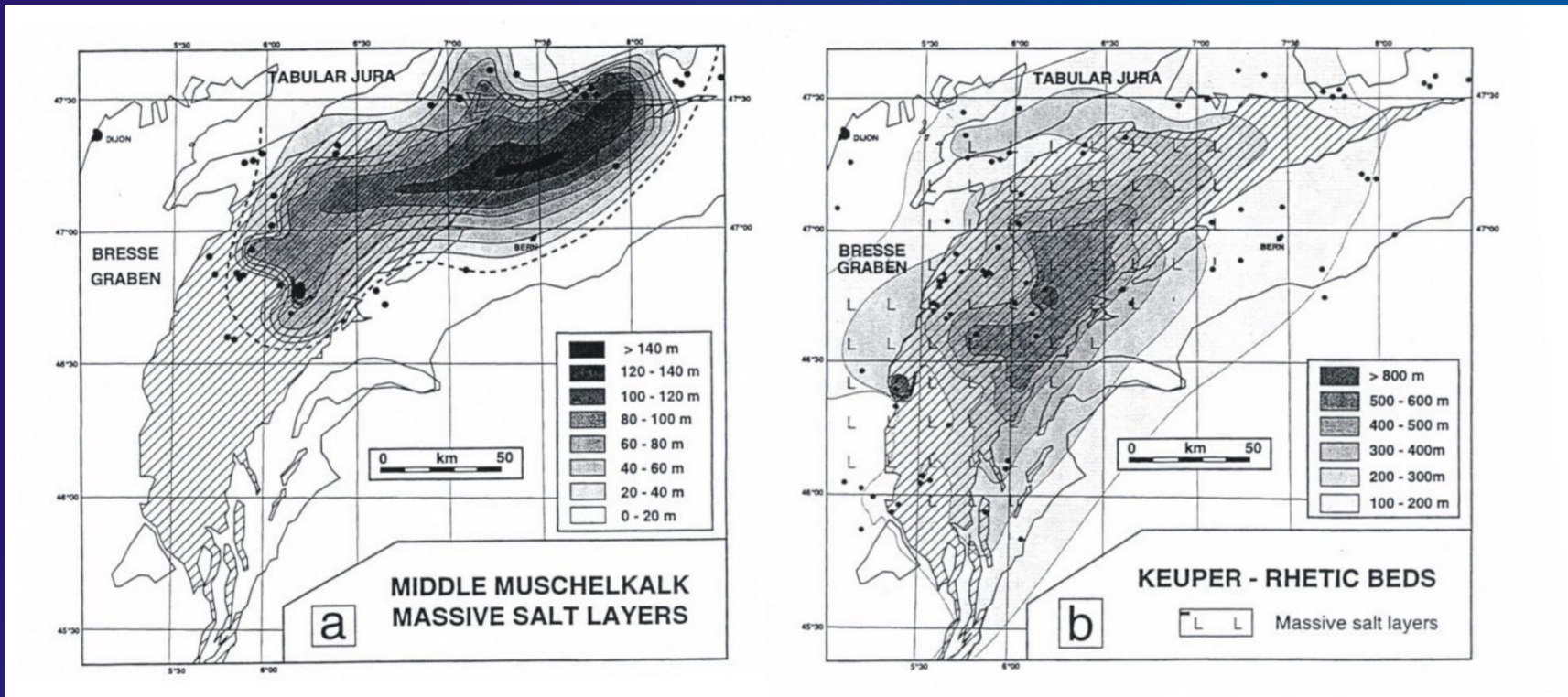
(Philippe, 1995)



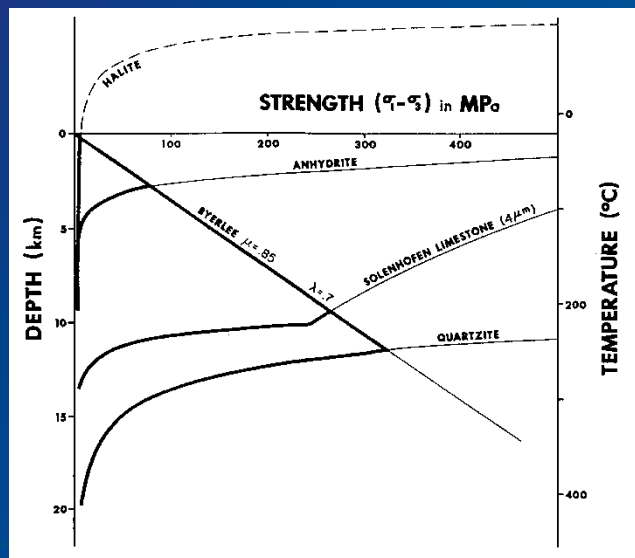
Thin-skinned tectonics in the Jura :
a rather short-lived event : 14-10Ma → 4-3Ma



Distribution of Triassic evaporites below the Jura

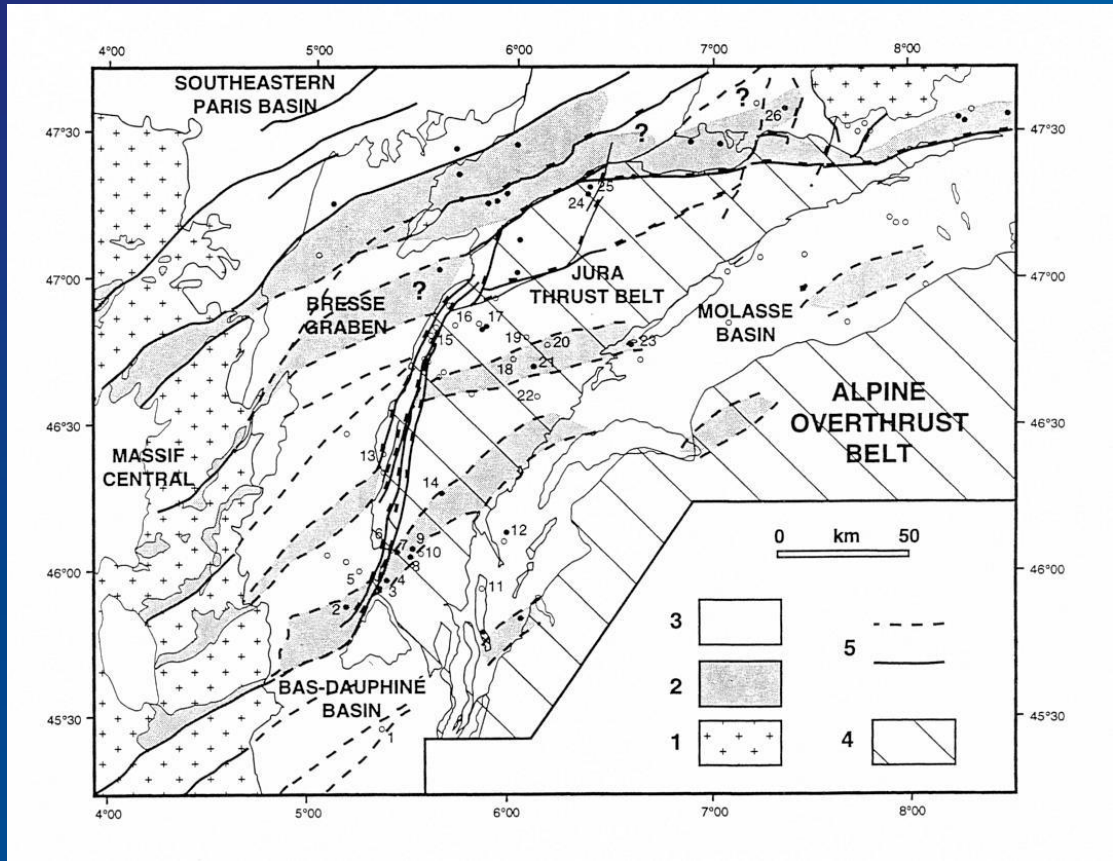
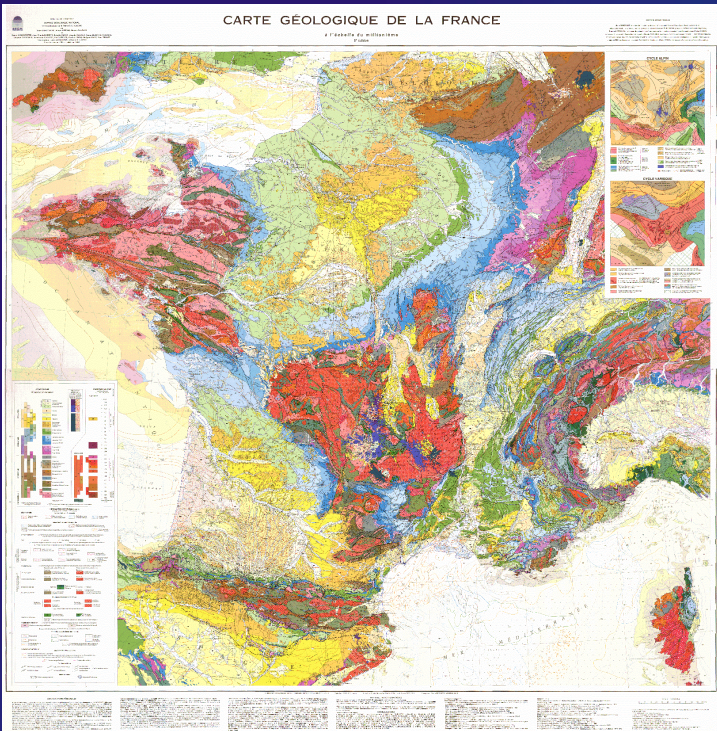


(Lienhard, 1984)

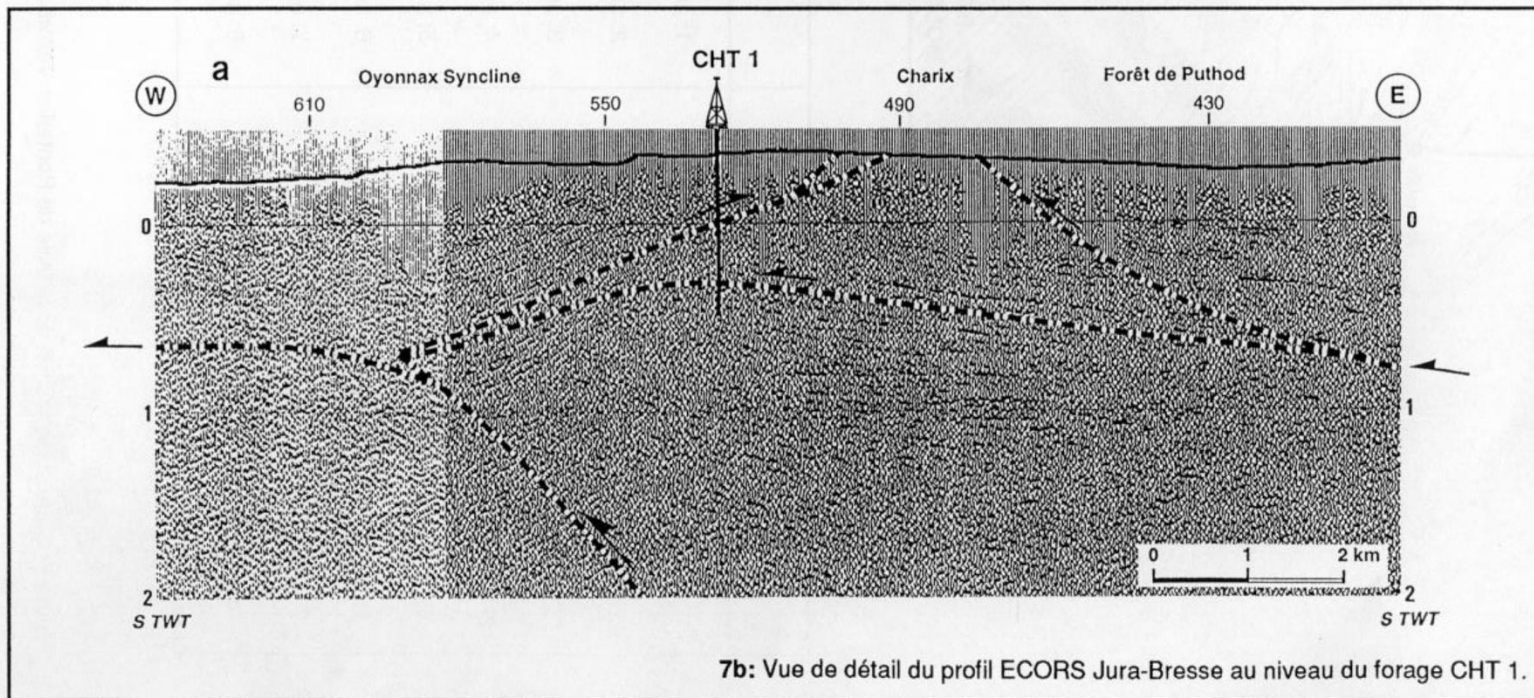
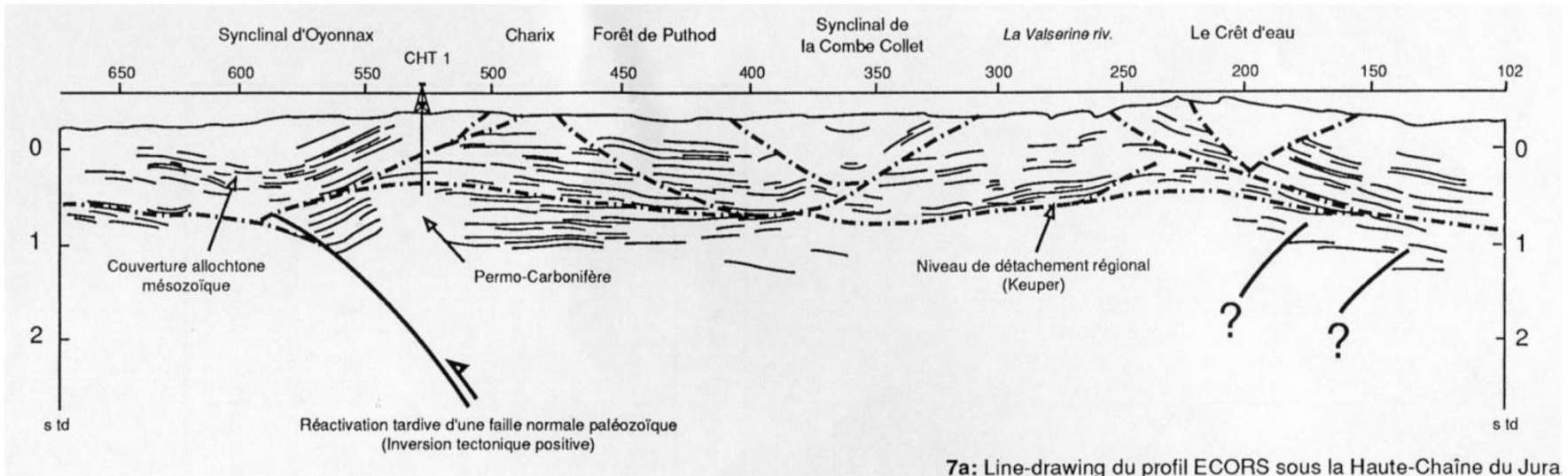


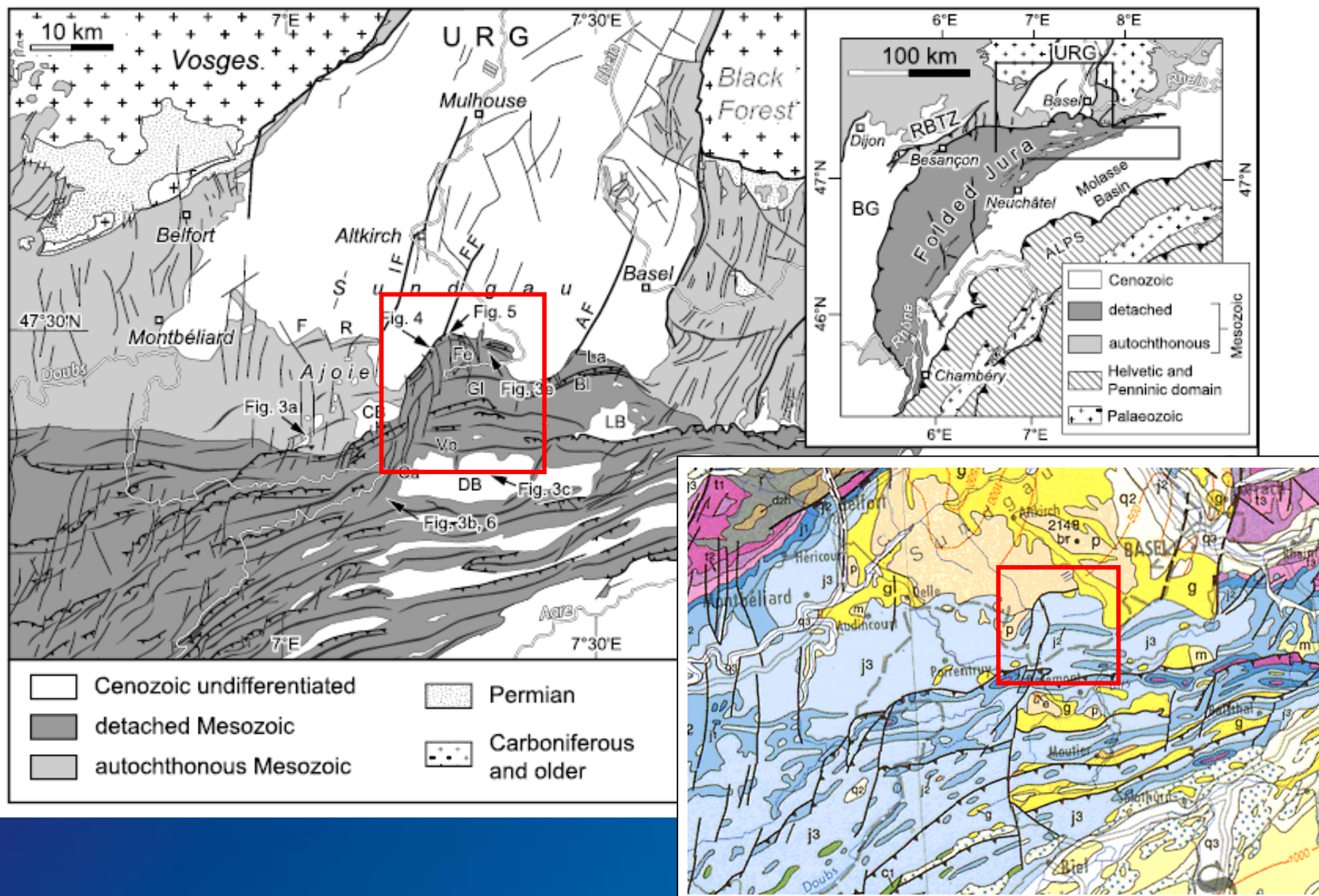
Rheological behaviour of evaporites

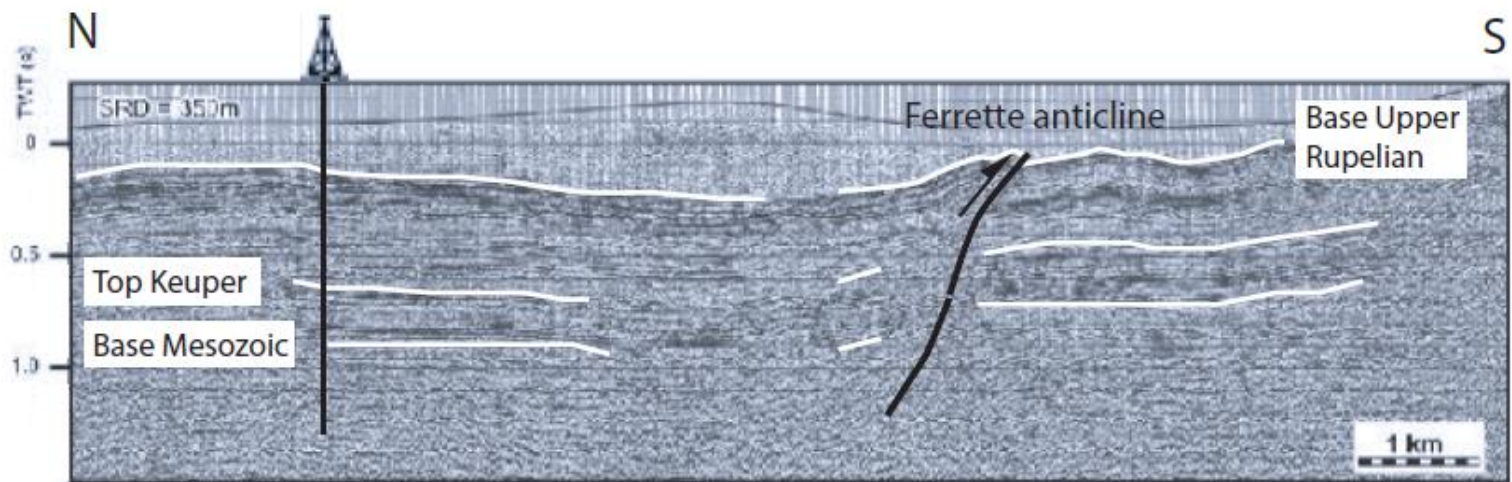
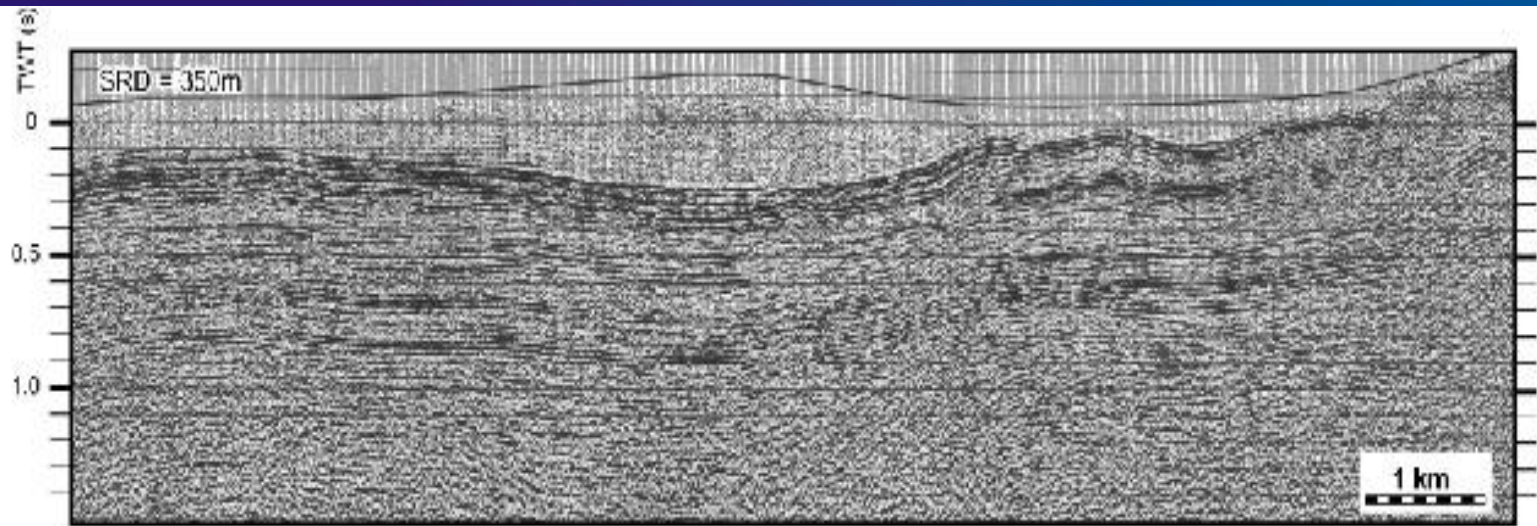
Note : in the case of a viscous décollement made of evaporites (Jura, Zagros, ...), the wedge is no longer frictional at its base, so the earlier equations must be adapted (Davis and Engelder, 1985)



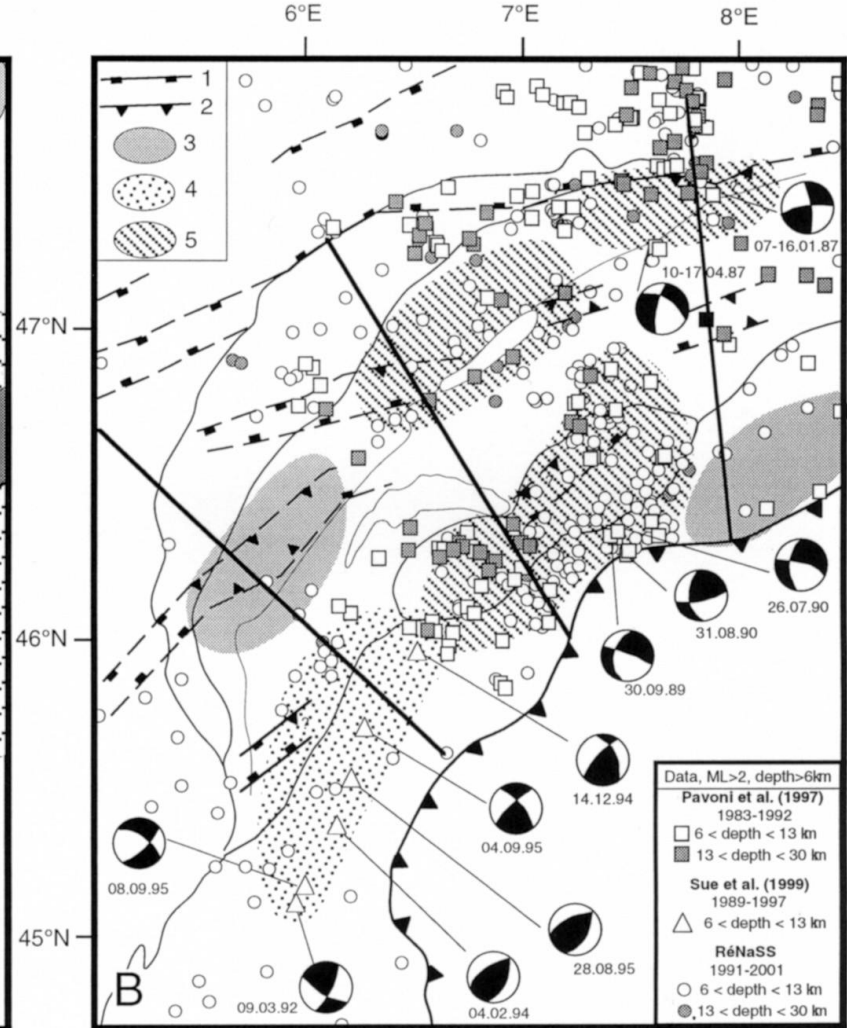
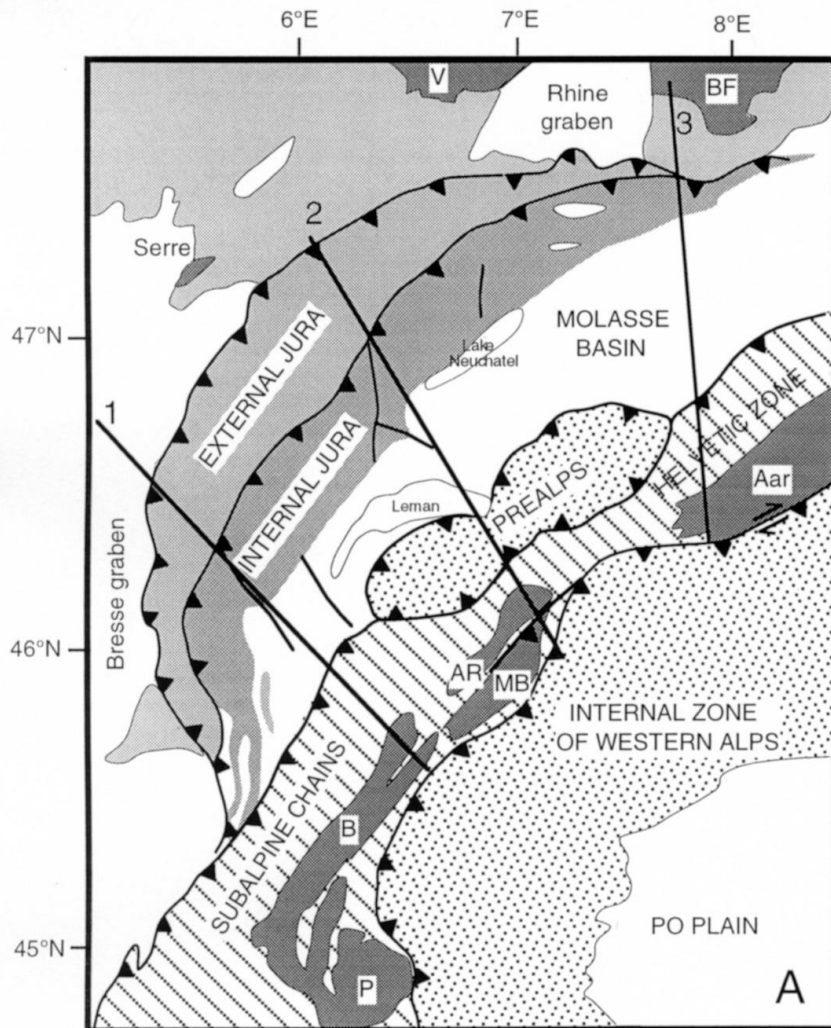
(BRGM, 1980; Truffert et al., 1990)



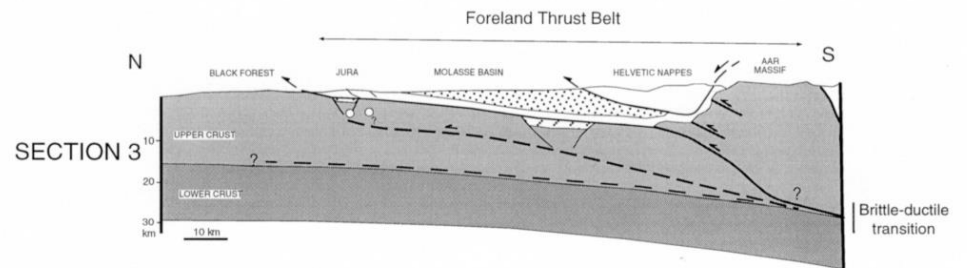
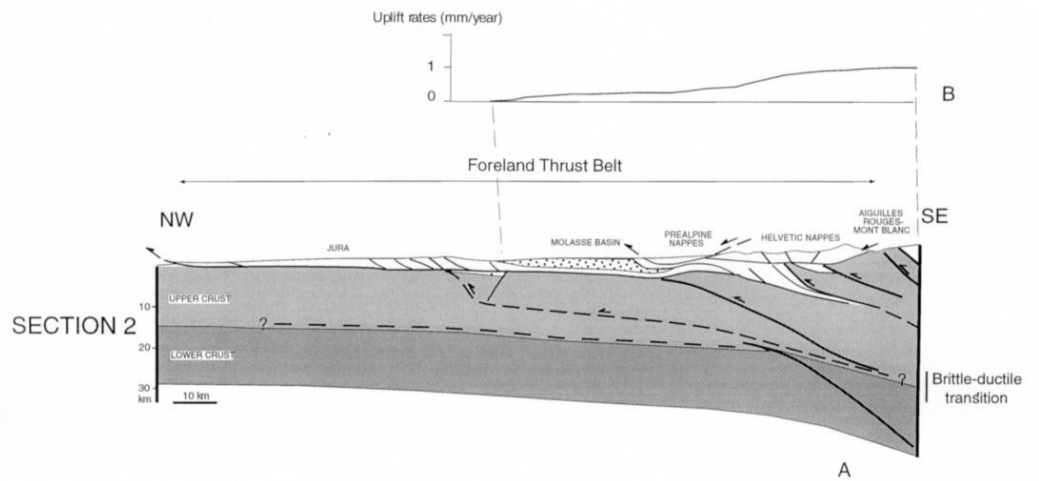
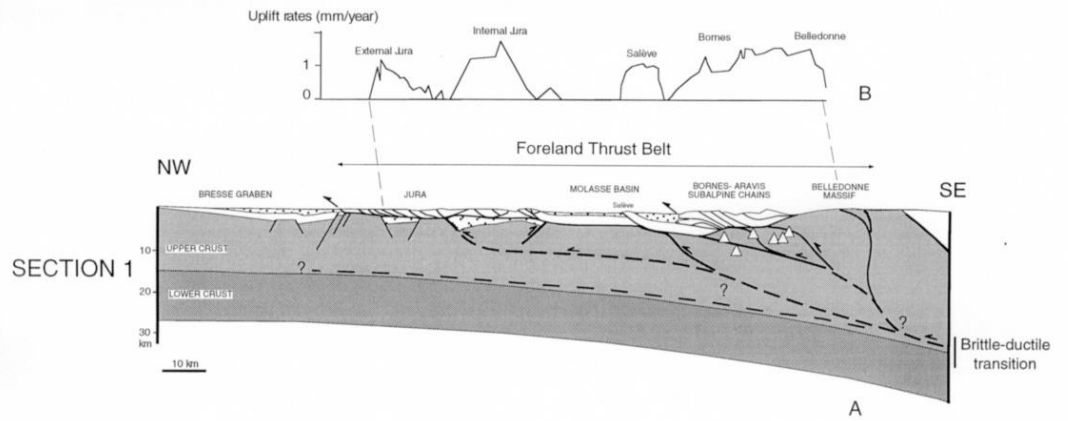




(Ustaszewski and Schmid, 2006)

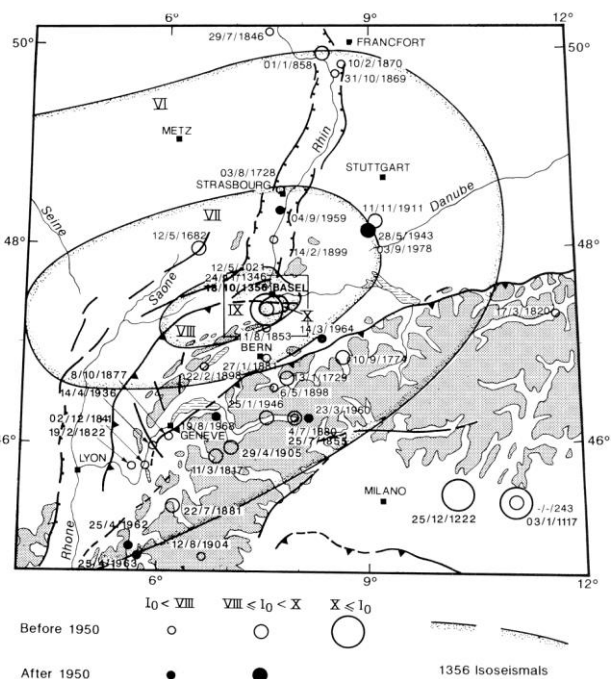


Areas of present-day basement-involved shortening inferred from :
3 : high present-day uplift rates 4 : high present-day uplift rates and seismicity 5 : seismicity

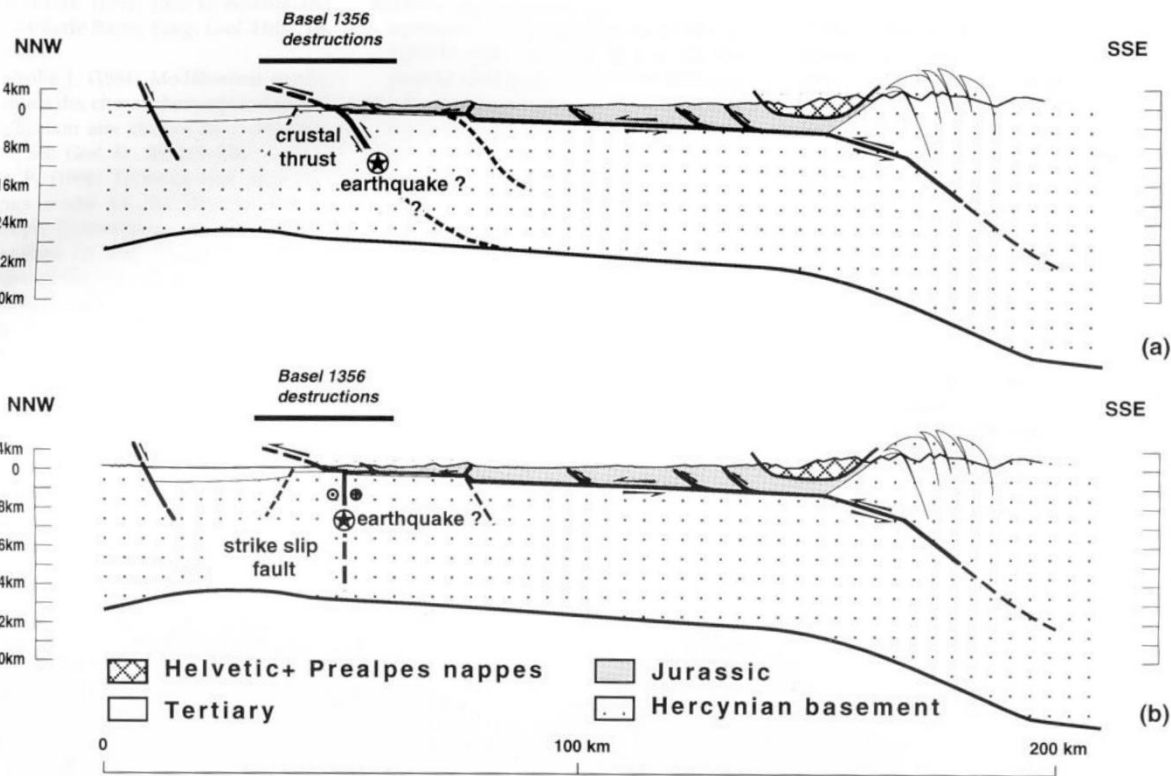


Cenozoic deposits
 Mesozoic cover
 Permo-Carboniferous grabens

The 1356 Basel earthquake : which fault produced it ?

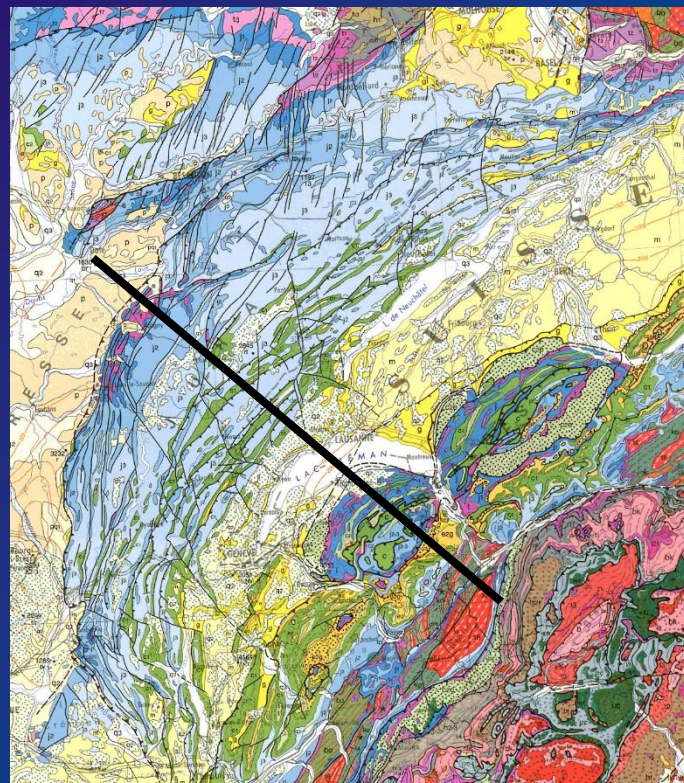


Seismotectonic map of NW Europe and Western Alps. Seismicity, active faults, and elevation contour line 1000 m are from Armijo et al. (1986). Altitudes greater than 1000 m are shaded. Isoseismals of Basel 1356 earthquake are from Mayer-Rosa and Cadot (1979). Box for Fig. 2b.

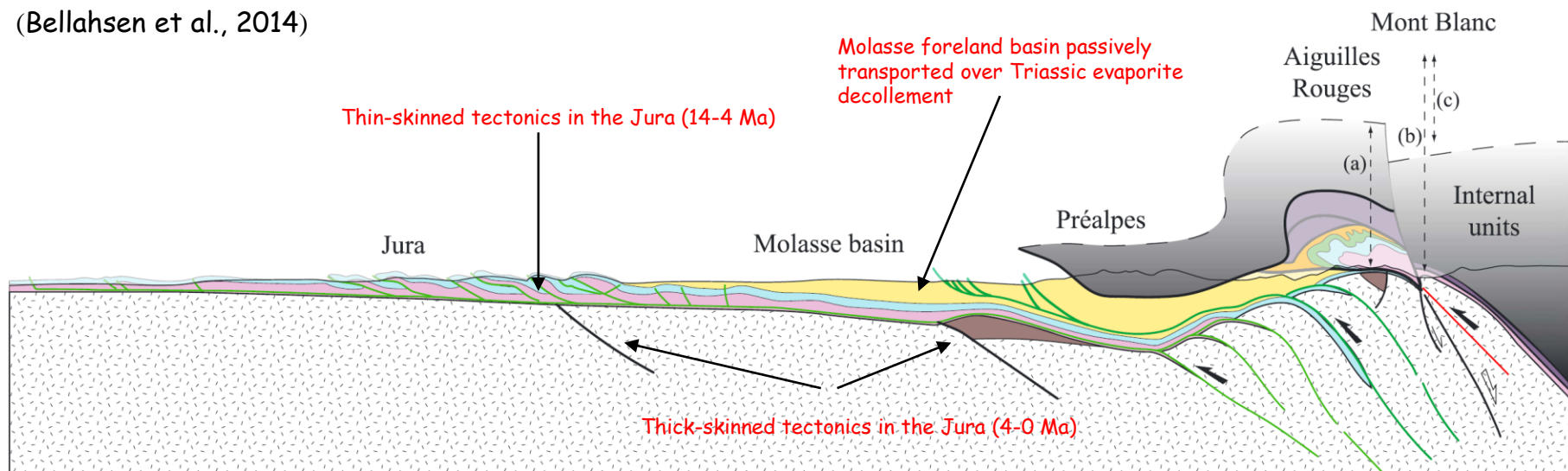


Plausible fault plane geometries for the Basel 1356 earthquake. (a) reactivation of a basement thrust fault beneath the detachment; (b) reactivation of a basement strike-slip fault beneath the detachment.

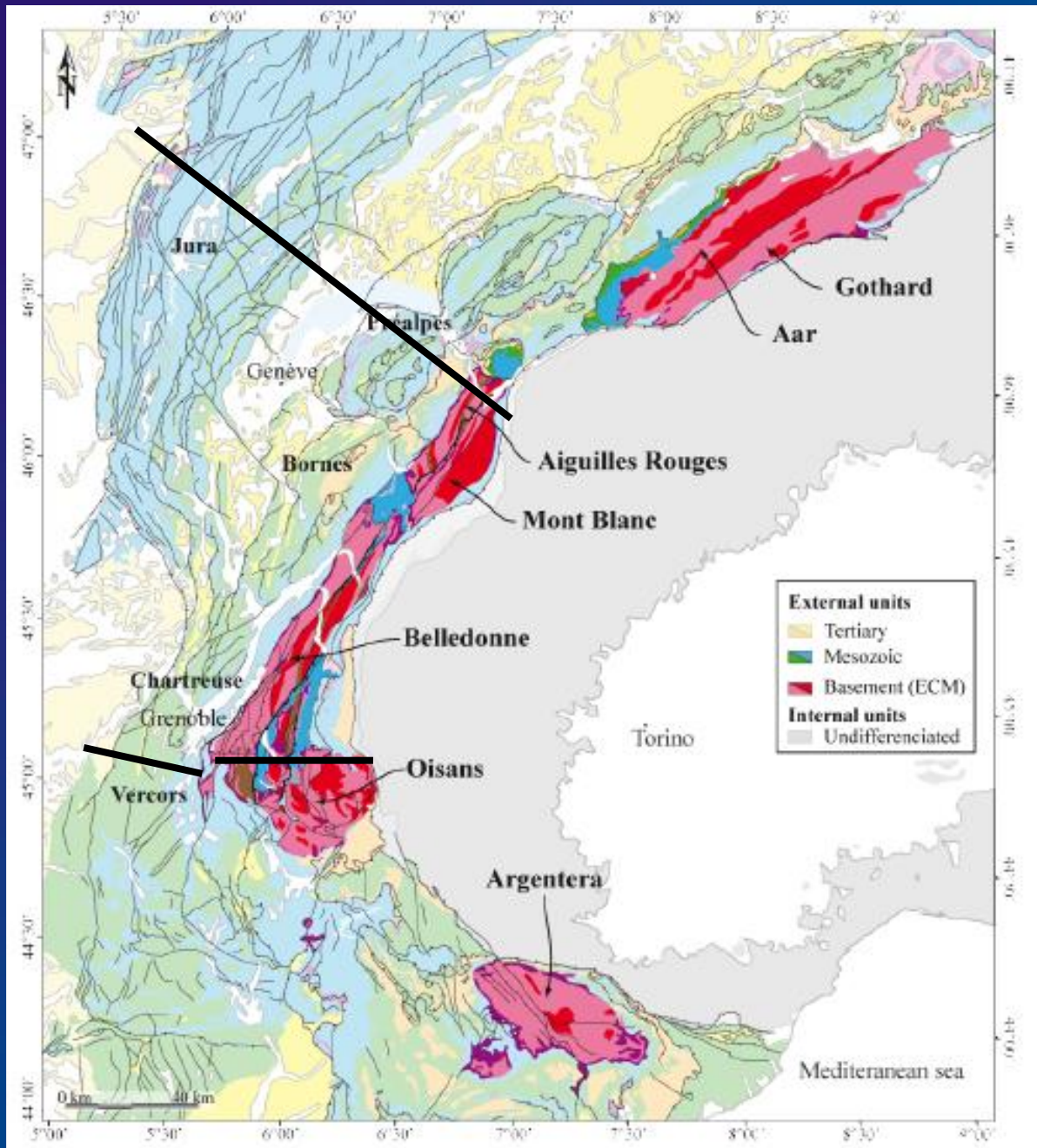
(Meyer et al., 1994)

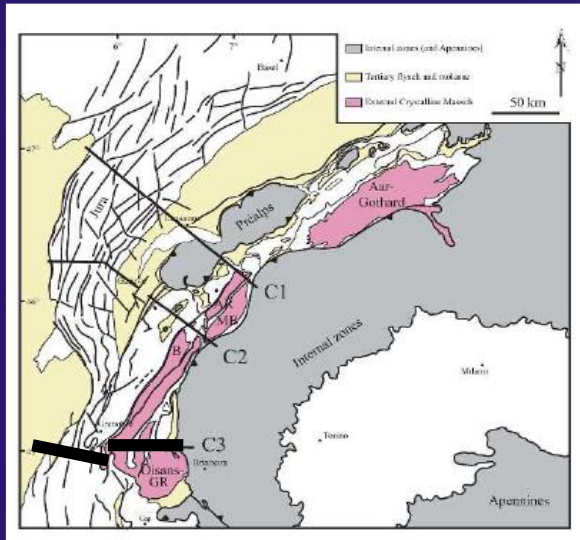


(Bellahsen et al., 2014)



**Along-strike variations
in basement-involved shortening :
the Alpine External Crystalline Massifs**

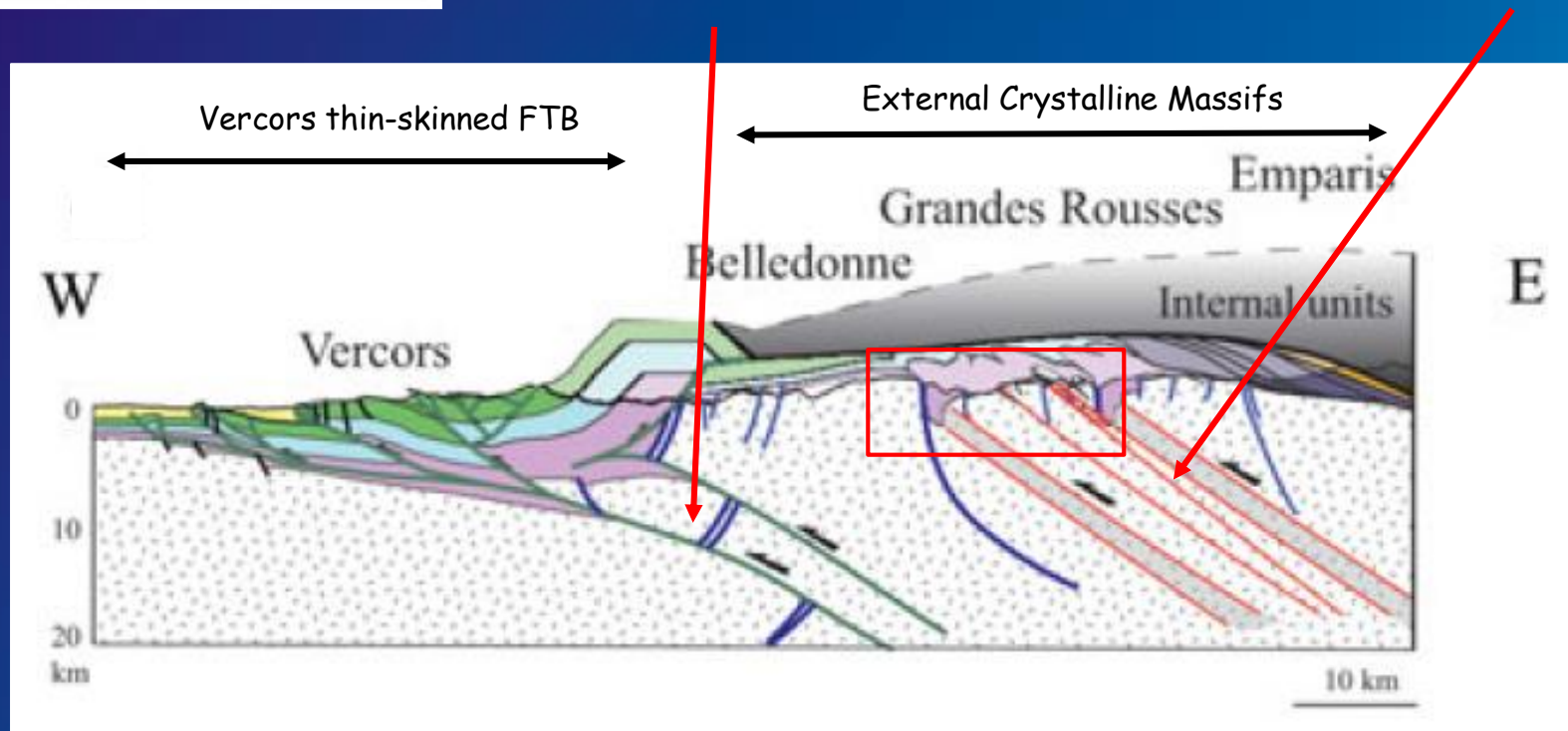


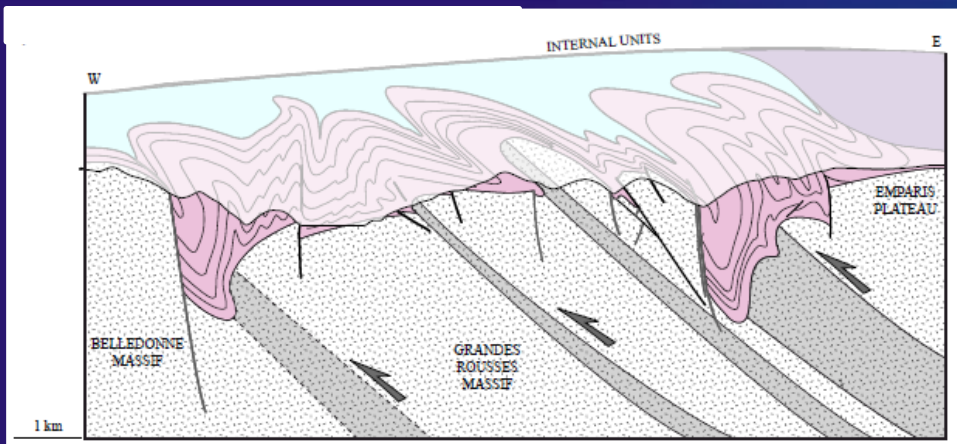


Oisans section : 2 styles of basement deformation in the External Crystalline Massifs

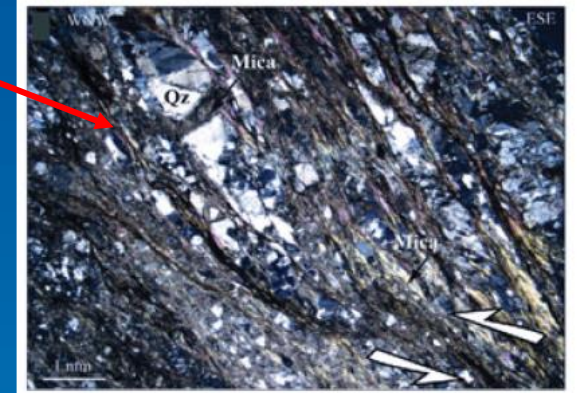
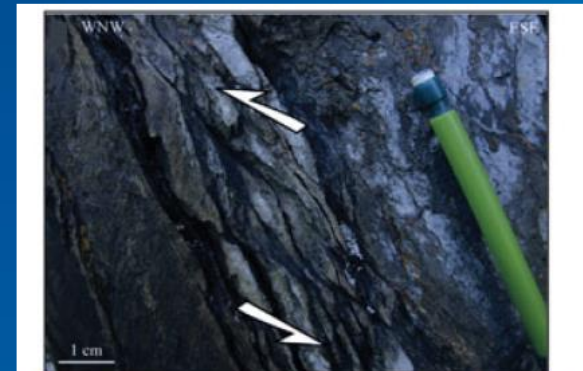
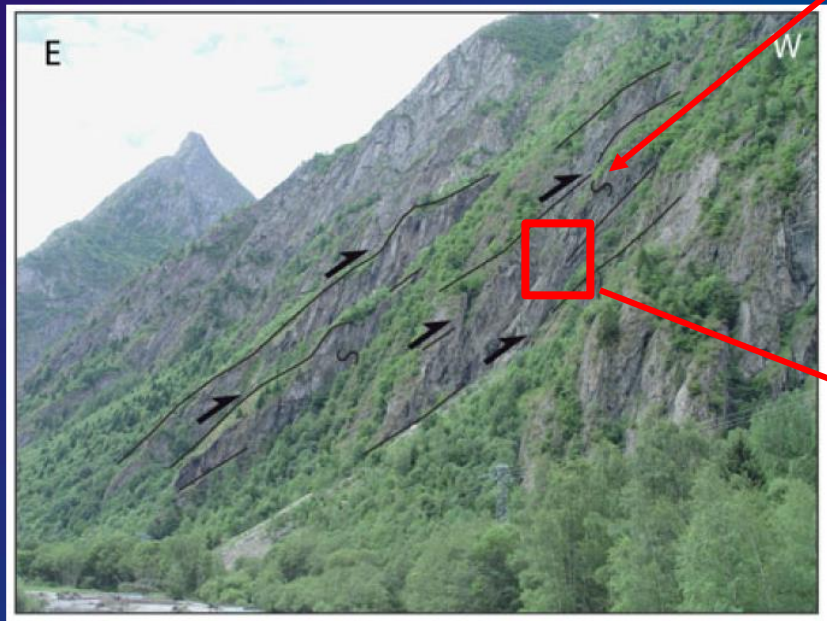
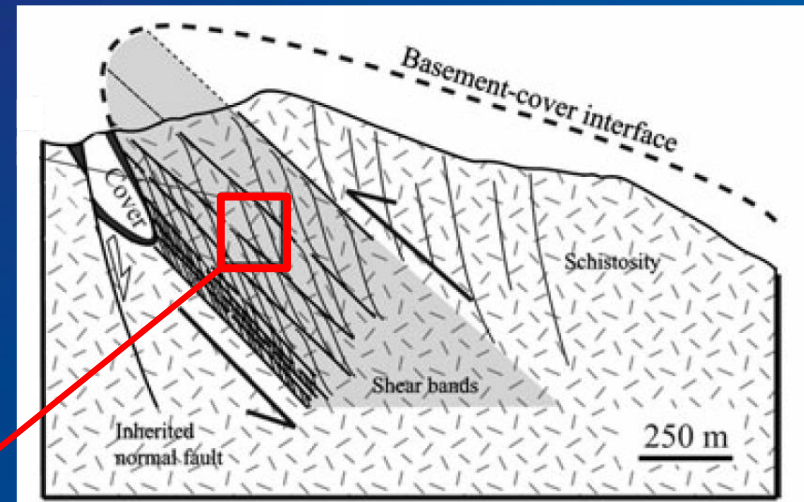
Deformation is localized on
the frontal ramp and the
shallow décollement of the
Vercors FTB is activated

Basement is shortened by
distributed underplating
under the Penninic units.





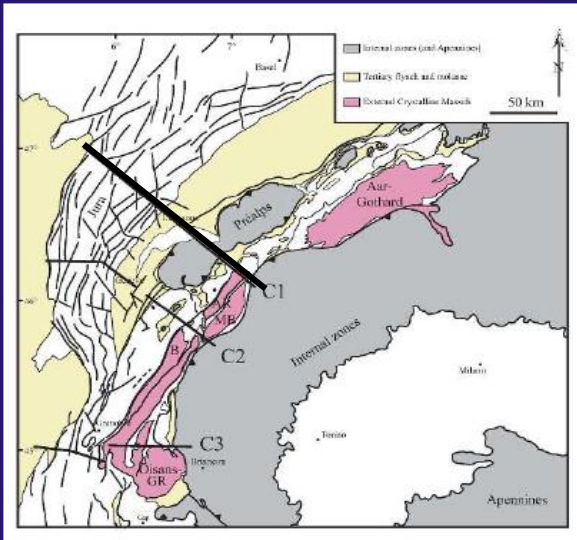
(Bellahsen et al., 2012; Lacombe and Bellahsen, 2016)



Fractured Qz clasts
Mylonitic deformation related to high white micas content

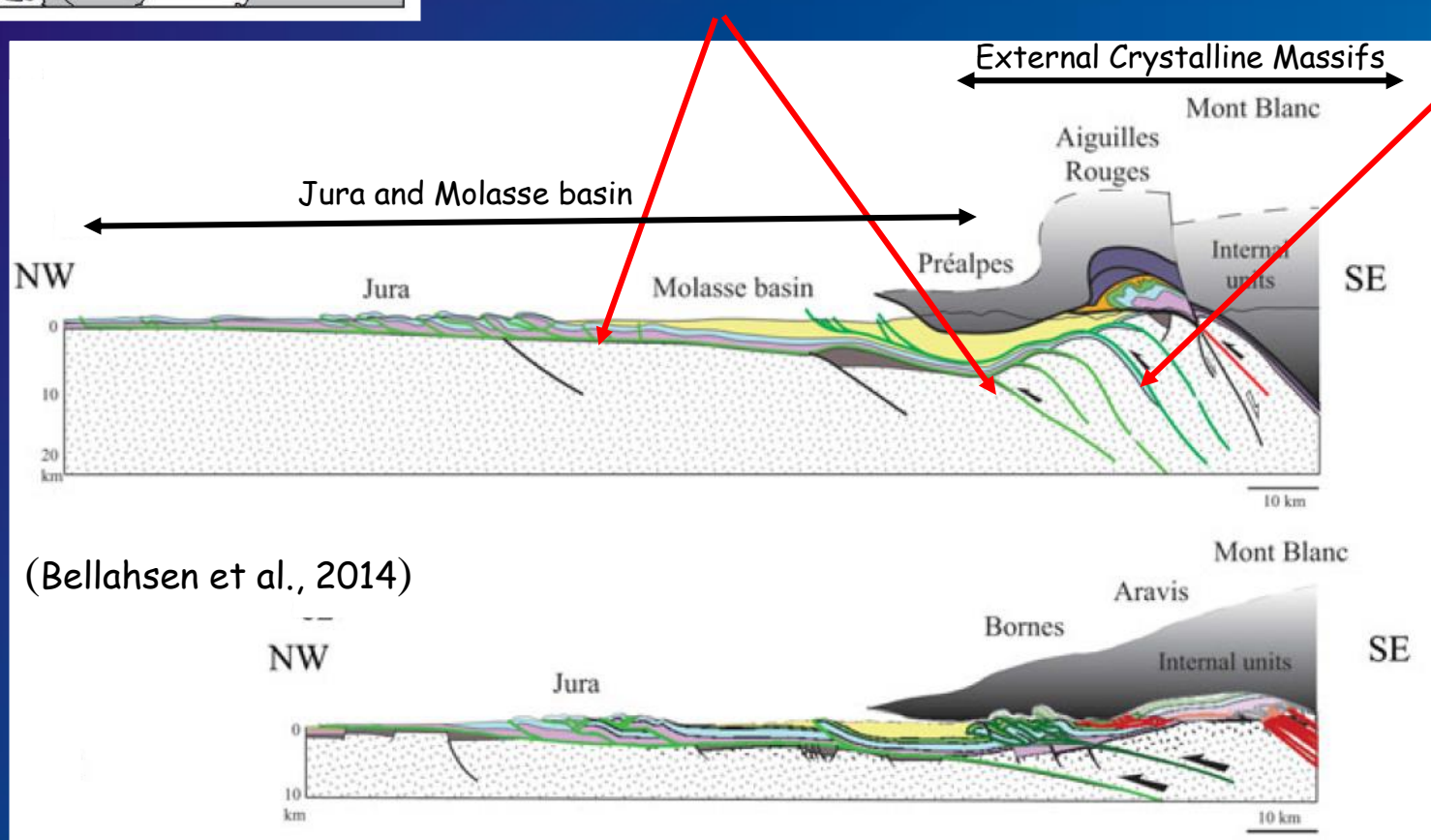
- *Non reactivation of inherited Tethyan normal faults
- *Basement « folding » closely associated with top-to-the-W distributed low-angle brittle-ductile Alpine shear zones (GS facies : 3-4 kb / 330-350°C, 25 Ma Ar-Ar)
- Efficient crustal thermal weakening during collisional burial

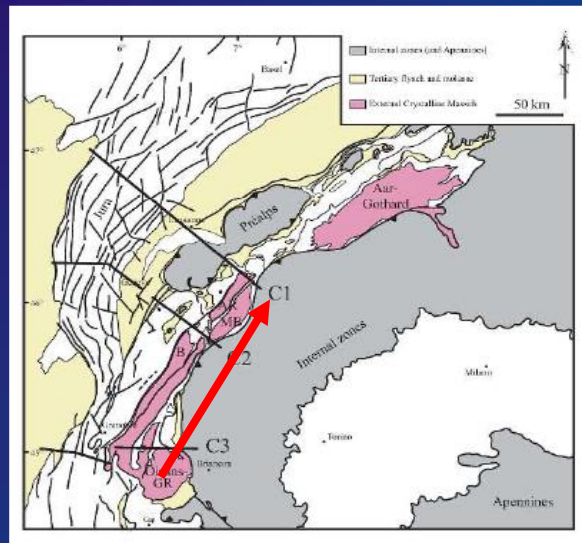
Mont Blanc-Aiguilles Rouges section : Again, 2 styles of basement deformation in the External Crystalline Massifs



Accretion of a wide cover domain in frontal parts (Jura and Molasse Basin) with activation of large basement thrusts.

Basement shortened by localized thrust stacking and underplating below the Penninic units



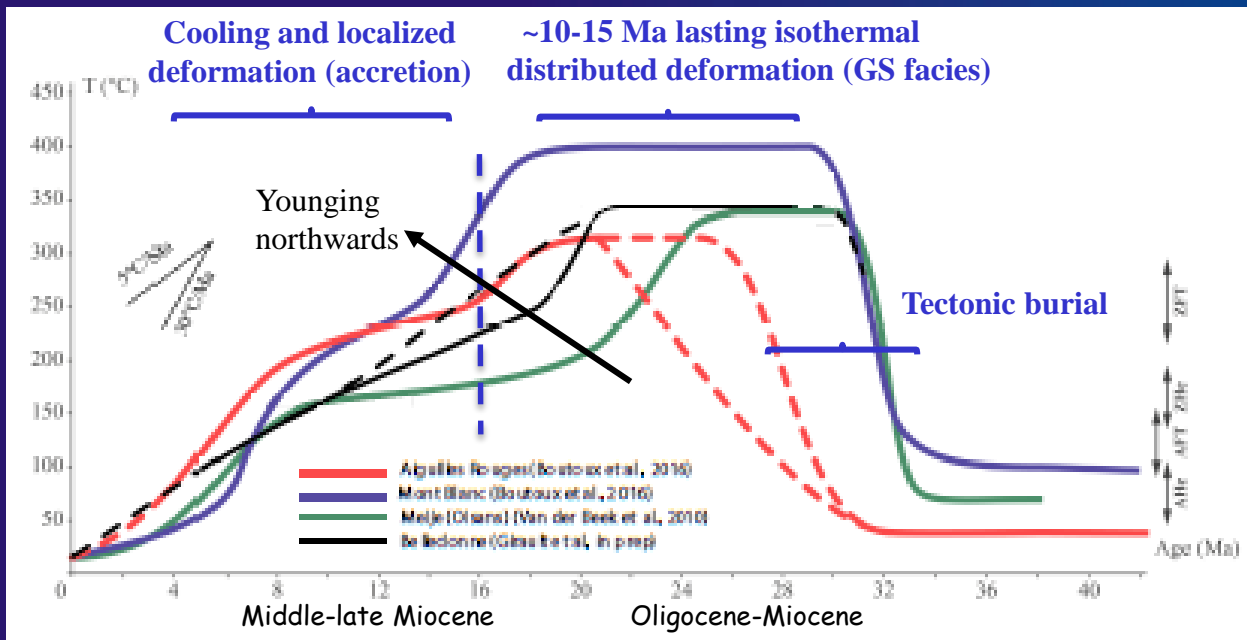


Localization, style of basement-involved deformation and shortening (%) vary along the strike of the western Alpine arc. Shortening increases across the external zone from the Oisans section (ECM : 16%) to the Mont Blanc section (ECM : 30-38%).

Significance in terms of crustal rheology :

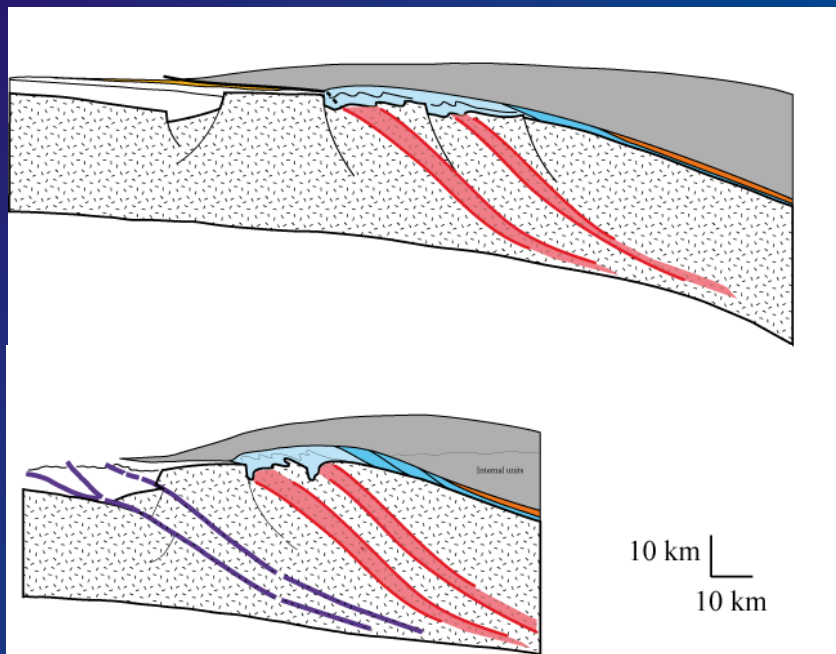
Along the Mont Blanc section, basement shortening remains localized, leading to stacking of basement slices, while it is more distributed along the Oisans section.

→ the more buried and thermally weakened crust at the latitude of the Mont Blanc (400°C, 5kb) is more prone to localized shortening at the orogen-scale.



RSCM, metamorphism and low-T thermochronology

(Bellahsen et al., 2014; Boutoux et al., 2016; Girault et al., in prep)



Basement shortening :

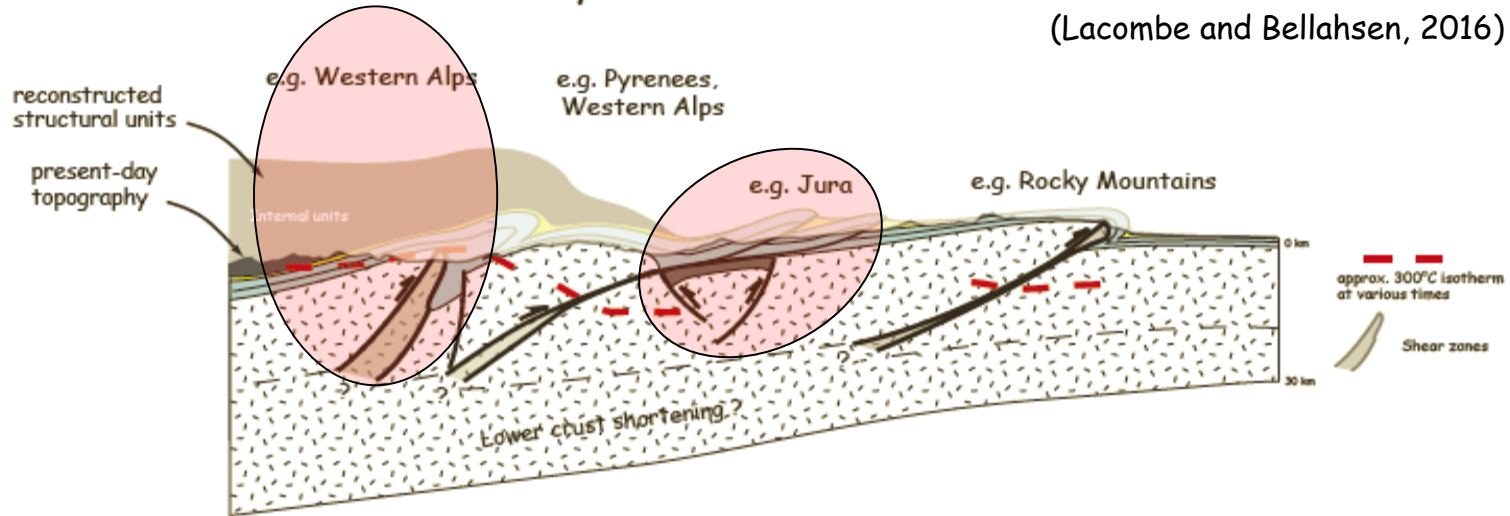
- distributed shearing or stacking of crustal slices during a long-lasting (~10-15 Ma) T°C peak (330-400°C) related to burial (10-20 km) under the Penninic nappes = underplating without orogenic wedge widening

- frontal accretion/exhumation thanks to localized crustal thrust ramps = later stage of orogenic wedge widening

Consistent westward sequence of basement shortening and exhumation

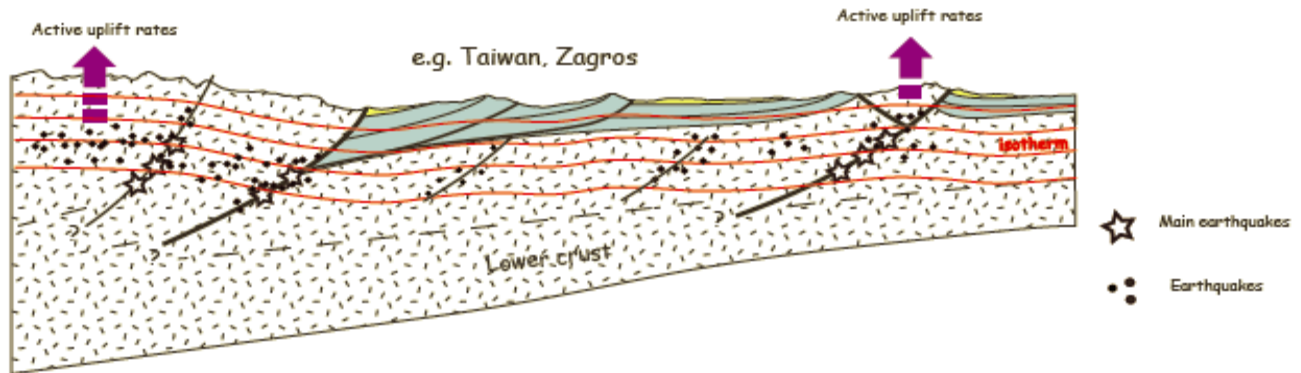
Tertiary fold-thrust belts

(Lacombe and Bellahsen, 2016)



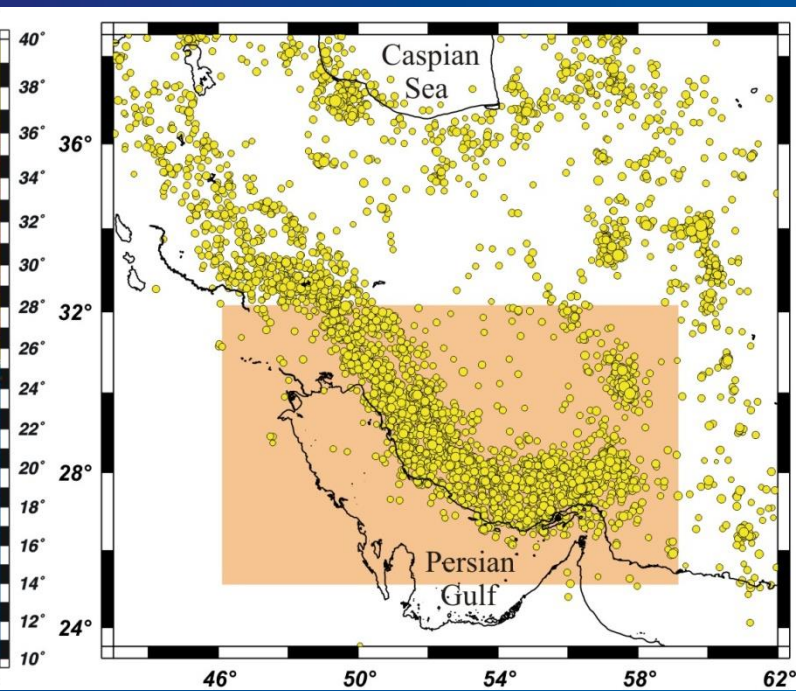
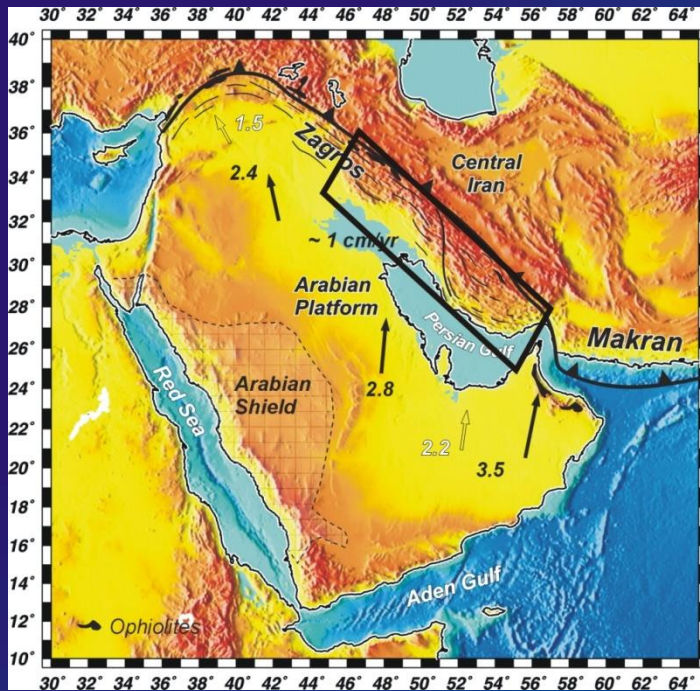
Active fold-thrust belts

e.g. Sierras Pampeanas



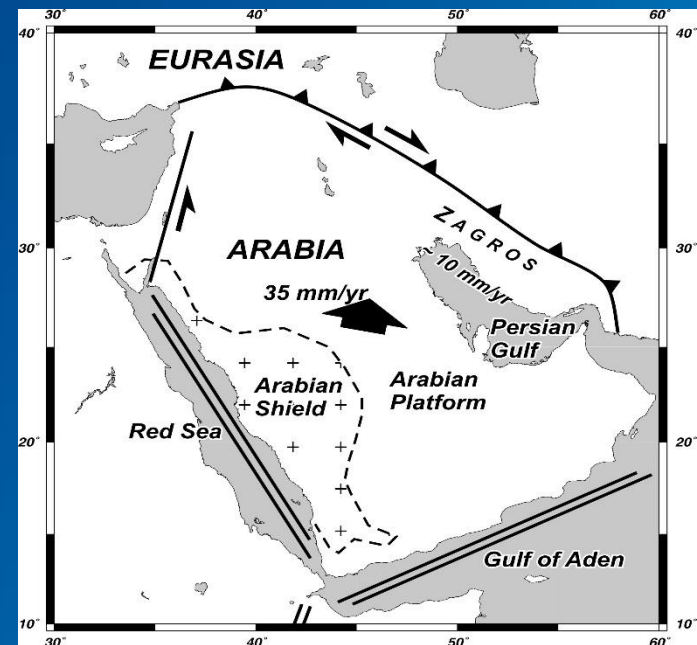
In young but no longer active orogens (Western Alps), evidence for basement involvement in shortening come mainly from structural and seismic studies

**The Zagros :
Superimposed thin-skinned and thick-skinned
tectonic styles**



The Zagros belt results from the collision between Arabia and Central Iran, beginning in (Oligo ?)-Miocene times and continuing today.

About one third of the 22-25 mm/yr Arabia-Eurasia convergence is currently accommodated in the Zagros (Vernant et al., 2004)



Based on available information of Geological Survey of Iran and
 National Institute of Cartography and Surveying
 Compiled by: A. Haghayegh and A. Akhavanfar
 Second edition 1989

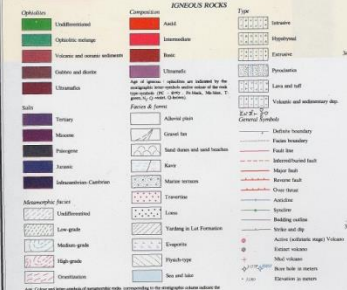
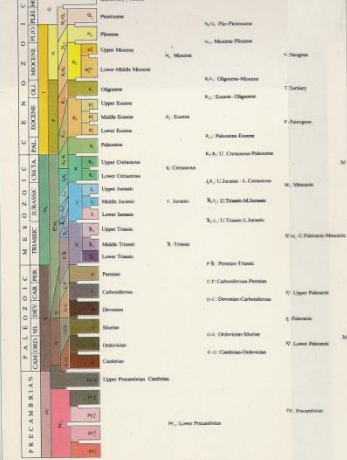
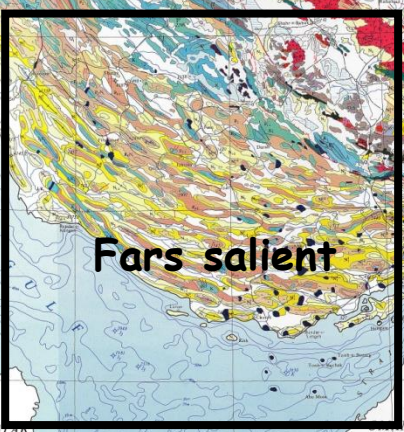


TABLE OF ROCK UNITS

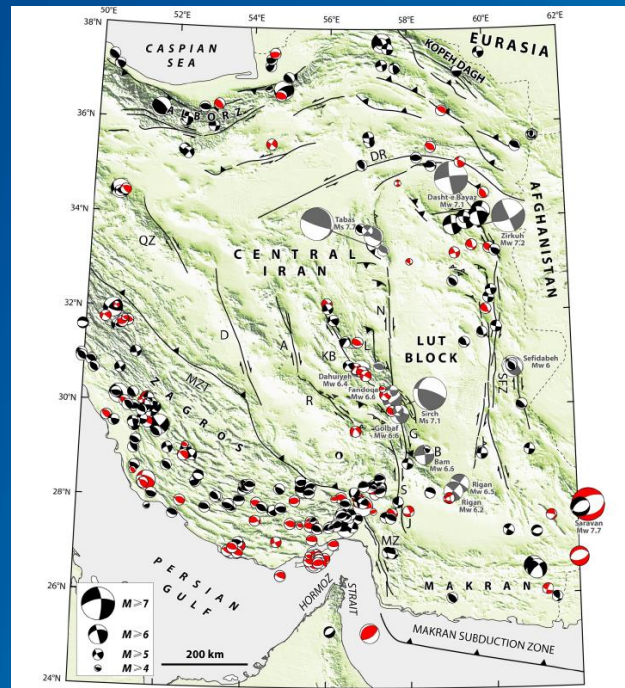
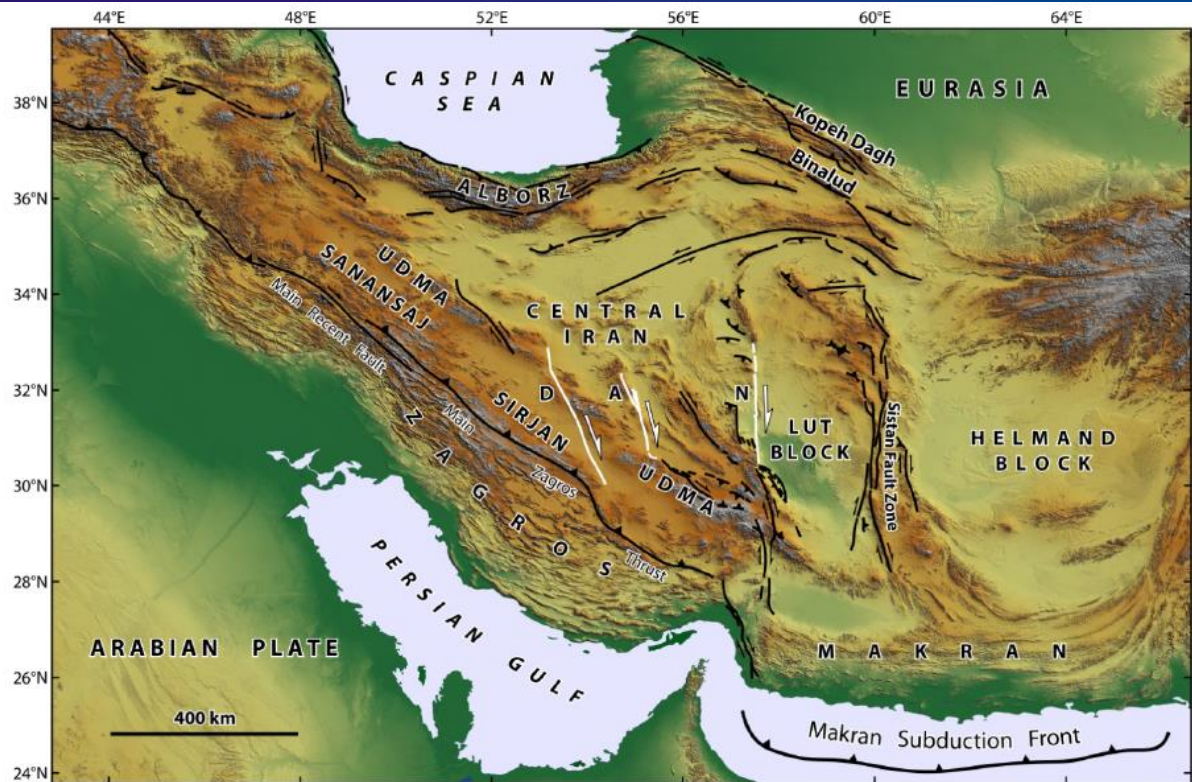
| Province | Zone (NW) | Unit Name | Age (North) | Exp. Depth (m) |
|----------|-----------|---|--------------|----------------|
| Hydrus | Zagros | 101. Hama F. (a, b, c) | Upper Eocene | 1000-1500 |
| | | 102. Hama F. (d, e, f, g, h, i, j, k, l, m, n, o, p, q, r, s, t, u, v, w, x, y, z) | Upper Eocene | 1000-1500 |
| | | 103. Hama F. (aa, ab, ac, ad, ae, af, ag, ah, ai, aj, ak, al, am, an, ao, ap, aq, ar, as, at, au, av, aw, ax, ay, az) | Upper Eocene | 1000-1500 |
| | | 104. Hama F. (ba, bb, bc, bd, be, bf, bg, bh, bi, bj, bk, bl, bm, bn, bo, bp, bq, br, bs, bt, bu, bv, bw, bx, by, bz) | Upper Eocene | 1000-1500 |
| | | 105. Hama F. (ca, cb, cc, cd, ce, cf, cg, ch, ci, cj, ck, cl, cm, cn, co, cp, cq, cr, cs, ct, cu, cv, cw, cx, cy, cz) | Upper Eocene | 1000-1500 |
| | | 106. Hama F. (da, db, dc, dd, de, df, dg, dh, di, dj, dk, dl, dm, dn, do, dp, dq, dr, ds, dt, du, dv, dw, dx, dy, dz) | Upper Eocene | 1000-1500 |
| | | 107. Hama F. (ea, eb, ec, ed, ee, ef, eg, eh, ei, ej, ek, el, em, en, eo, ep, eq, er, es, et, eu, ev, ew, ex, ey, ez) | Upper Eocene | 1000-1500 |
| | | 108. Hama F. (fa, fb, fc, fd, fe, ff, fg, fh, fi, fj, fk, fl, fm, fn, fo, fp, fq, fr, fs, ft, fu, fv, fw, fx, fy, fz) | Upper Eocene | 1000-1500 |
| | | 109. Hama F. (ga, gb, gc, gd, ge, gf, gg, gh, gi, gj, gk, gl, gm, gn, go, gp, gq, gr, gs, gt, gu, gv, gw, gx, gy, gz) | Upper Eocene | 1000-1500 |
| | | 110. Hama F. (ha, hb, hc, hd, he, hf, hg, hh, hi, hj, hk, hl, hm, hn, ho, hp, hq, hr, hs, ht, hu, hv, hw, hx, hy, hz) | Upper Eocene | 1000-1500 |
| Hydrus | Zagros | 111. Hama F. (ia, ib, ic, id, ie, if, ig, ih, ii, ij, ik, il, im, in, io, ip, iq, ir, is, it, iu, iv, iw, ix, iy, iz) | Upper Eocene | 1000-1500 |
| | | 112. Hama F. (ja, jb, jc, jd, je, jf, jg, jh, ji, jj, jk, jl, jm, jn, jo, jp, jq, jr, js, jt, ju, jv, jw, jx, jy, jz) | Upper Eocene | 1000-1500 |
| | | 113. Hama F. (ka, kb, kc, kd, ke, kf, kg, kh, ki, kj, kk, kl, km, kn, ko, kp, kq, kr, ks, kt, ku, kv, kw, kx, ky, kz) | Upper Eocene | 1000-1500 |
| | | 114. Hama F. (la, lb, lc, ld, le, lf, lg, lh, li, lj, lk, ll, lm, ln, lo, lp, lq, lr, ls, lt, lu, lv, lw, lx, ly, lz) | Upper Eocene | 1000-1500 |
| | | 115. Hama F. (ma, mb, mc, md, me, mf, mg, mh, mi, mj, mk, ml, mm, mn, mo, mp, mq, mr, ms, mt, mu, mv, mw, mx, my, mz) | Upper Eocene | 1000-1500 |
| | | 116. Hama F. (na, nb, nc, nd, ne, nf, ng, nh, ni, nj, nk, nl, nm, nn, no, np, nq, nr, ns, nt, nu, nv, nw, nx, ny, nz) | Upper Eocene | 1000-1500 |
| | | 117. Hama F. (oa, ob, oc, od, oe, of, og, oh, oi, oj, ok, ol, om, on, oo, op, oq, or, os, ot, ou, ov, ow, ox, oy, oz) | Upper Eocene | 1000-1500 |
| | | 118. Hama F. (pa, pb, pc, pd, pe, pf, pg, ph, pi, pj, pk, pl, pm, pn, po, pp, pq, pr, ps, pt, pu, pv, pw, px, py, pz) | Upper Eocene | 1000-1500 |
| | | 119. Hama F. (qa, qb, qc, qd, qe, qf, qg, qh, qi, qj, qk, ql, qm, qn, qo, qp, qq, qr, qs, qt, qu, qv, qw, qx, qy, qz) | Upper Eocene | 1000-1500 |
| | | 120. Hama F. (ra, rb, rc, rd, re, rf, rg, rh, ri, rj, rk, rl, rm, rn, ro, rp, rq, rr, rs, rt, ru, rv, rw, rx, ry, rz) | Upper Eocene | 1000-1500 |

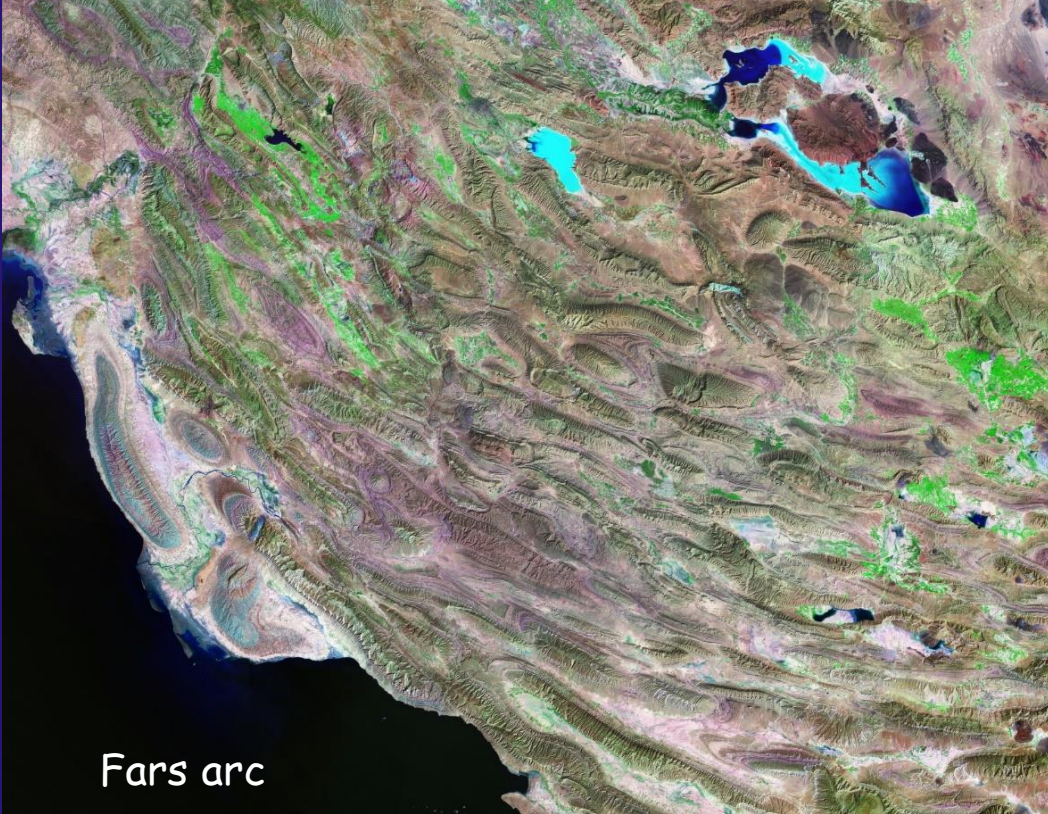
Lurestan salient

Dezful recess

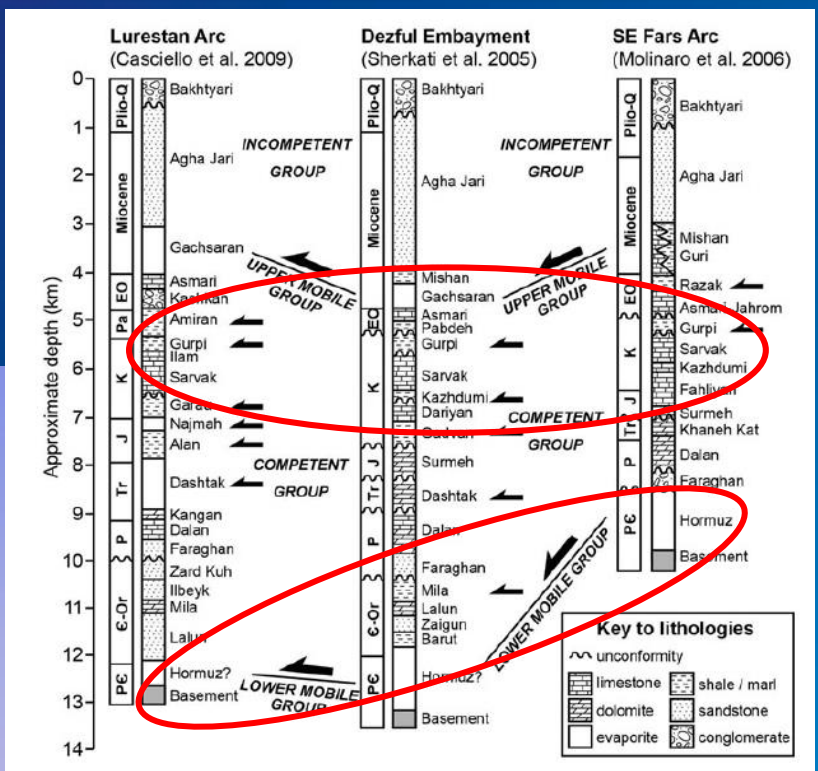


Fars salient

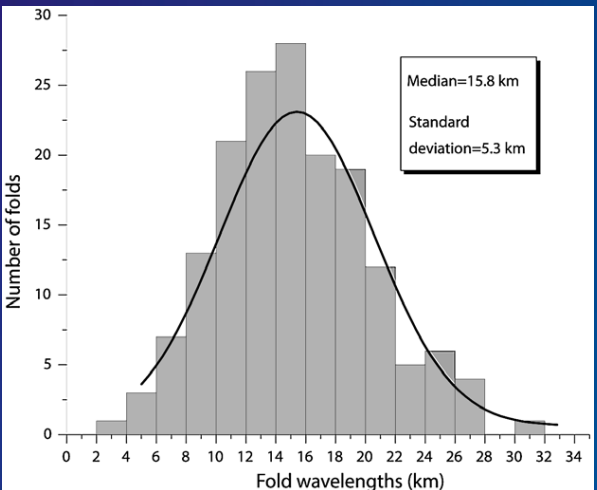




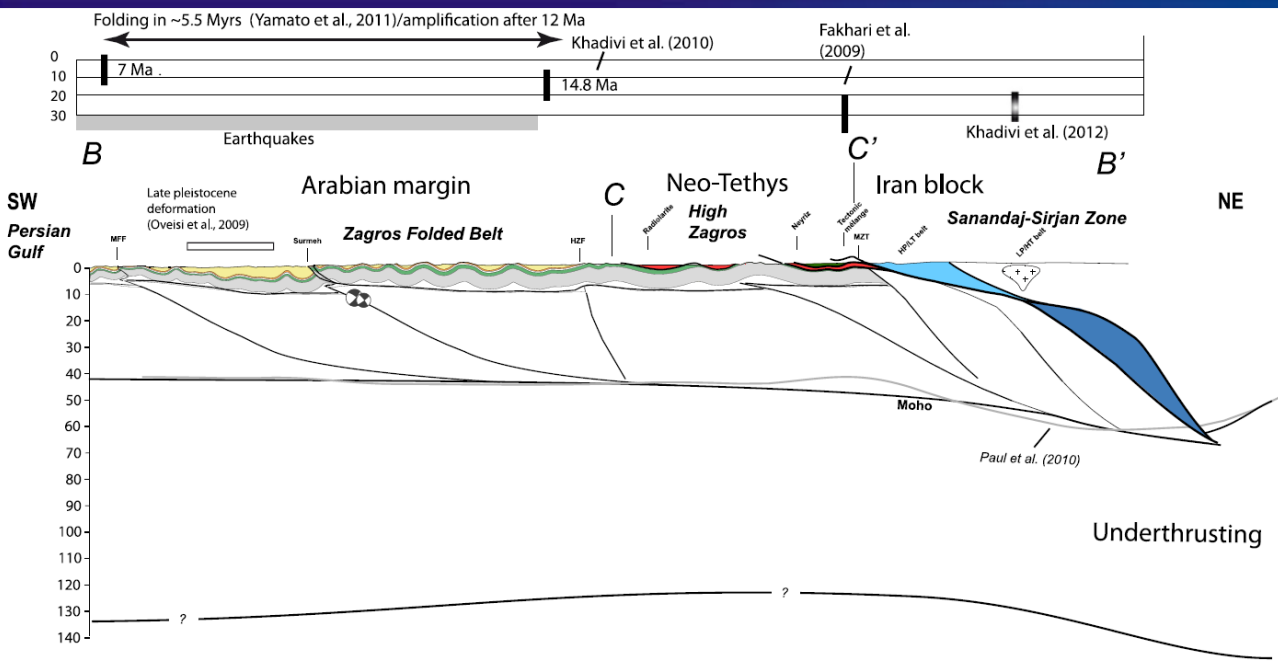
Fars arc



World-class folds and salt diapirs

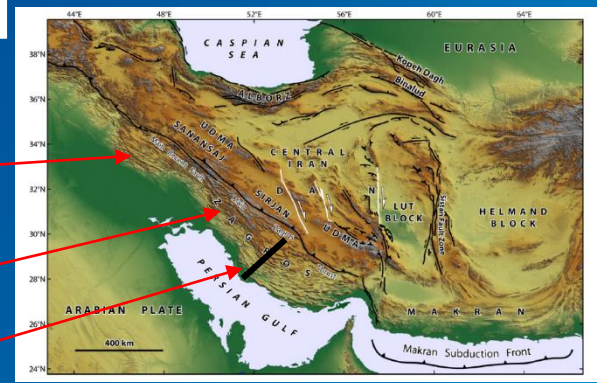
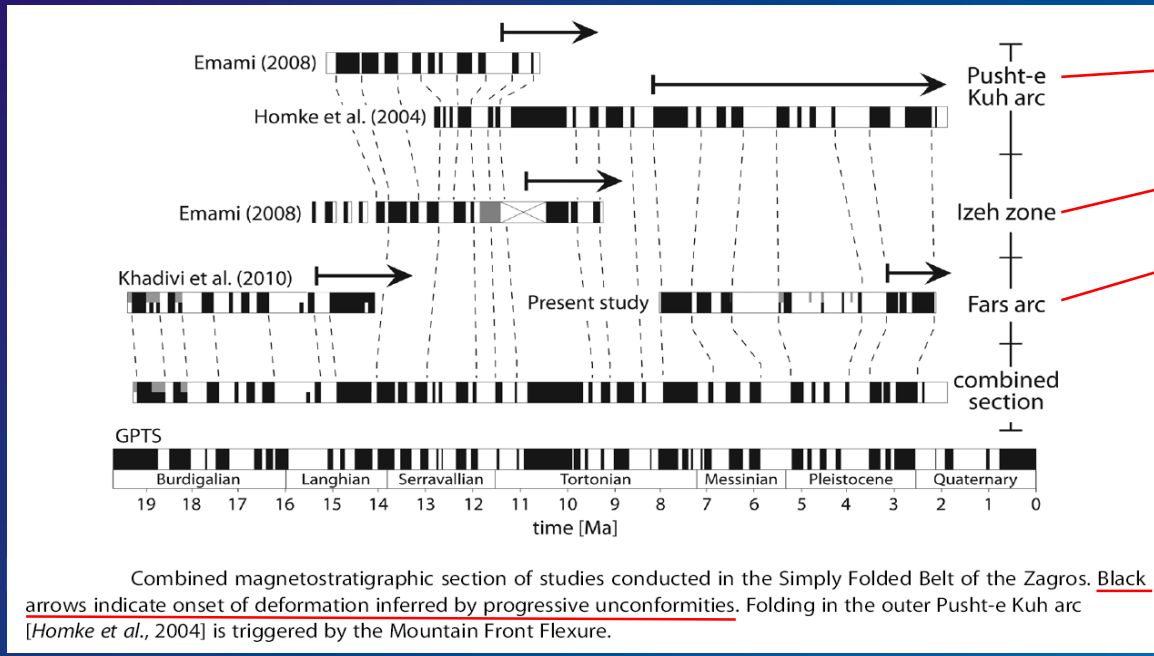


(Mouthereau et al., 2007, 2012)

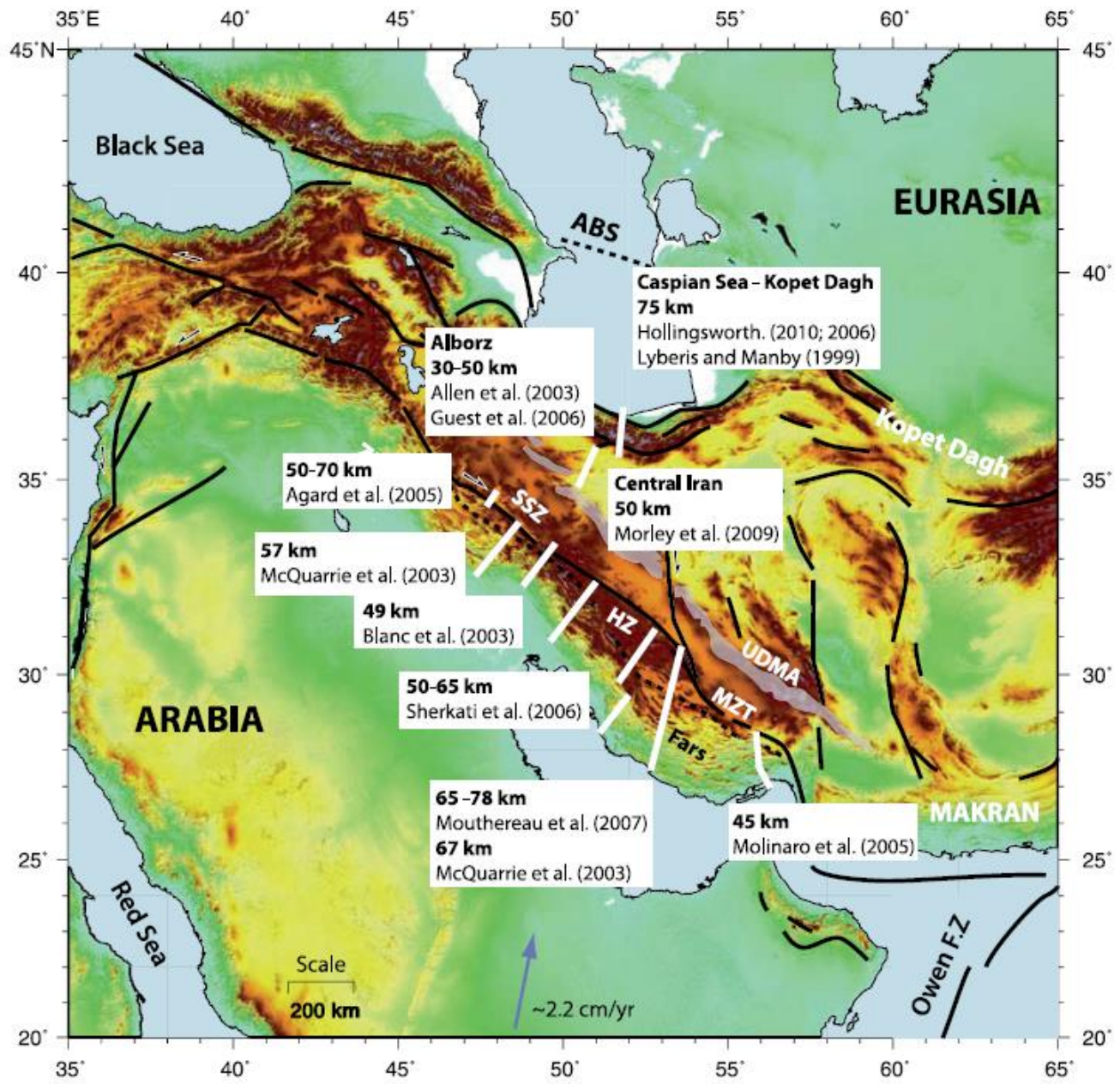


Evidence for outward sequence of folding in the Zagros belt by magnetostratigraphic dating of syn-folding formations

Ruh et al. 2014



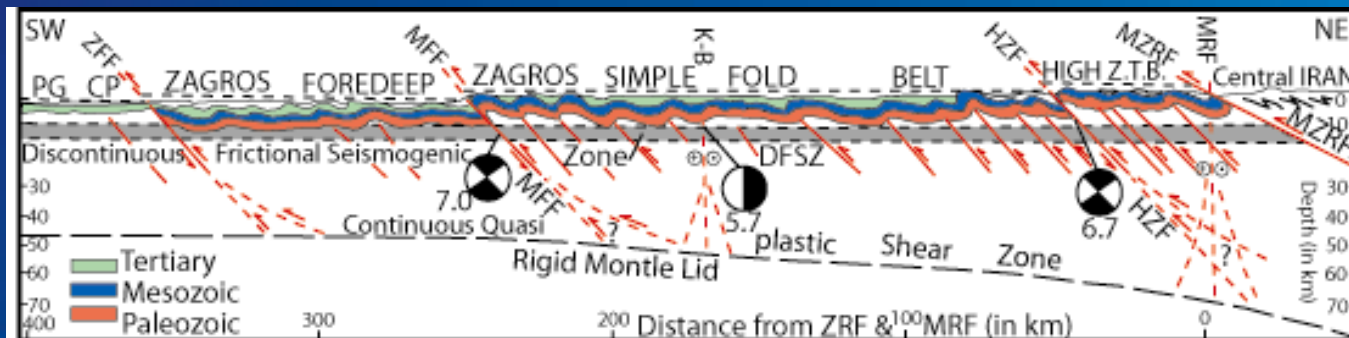
Combined magnetostratigraphic section of studies conducted in the Simply Folded Belt of the Zagros. Black arrows indicate onset of deformation inferred by progressive unconformities. Folding in the outer Pusht-e Kuh arc [Homke et al., 2004] is triggered by the Mountain Front Flexure.

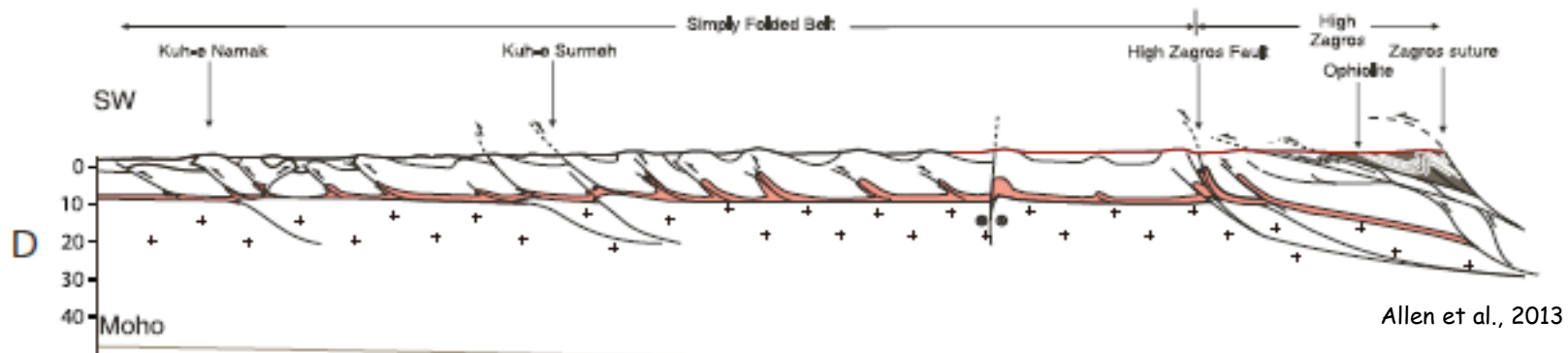
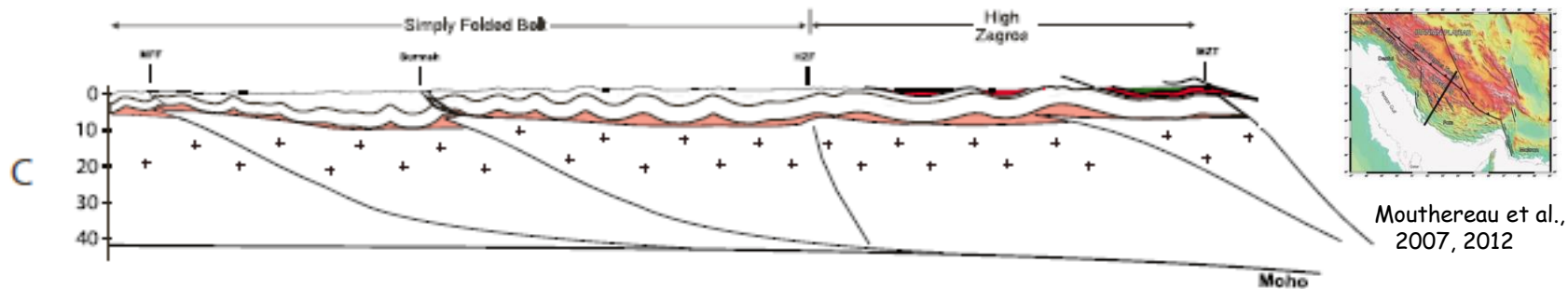
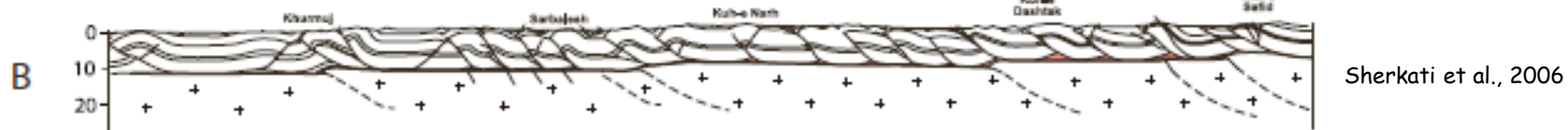
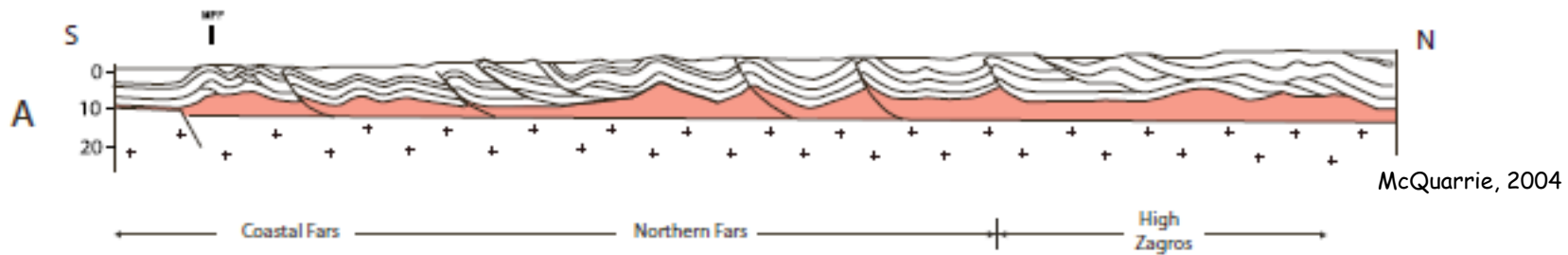


(Mouthereau et al., 2012)



(Berberian, 1995)

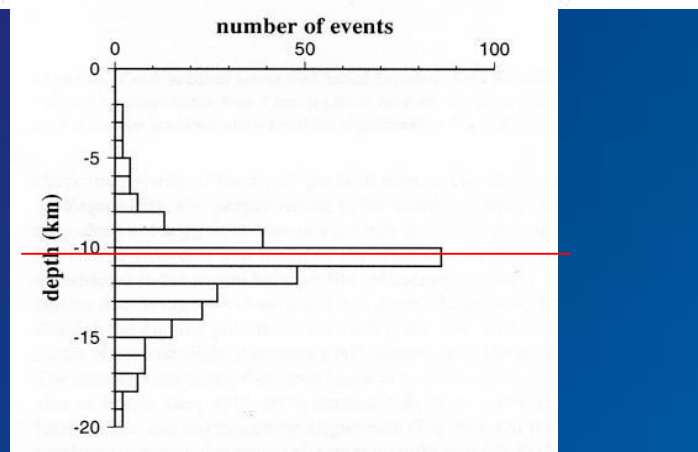
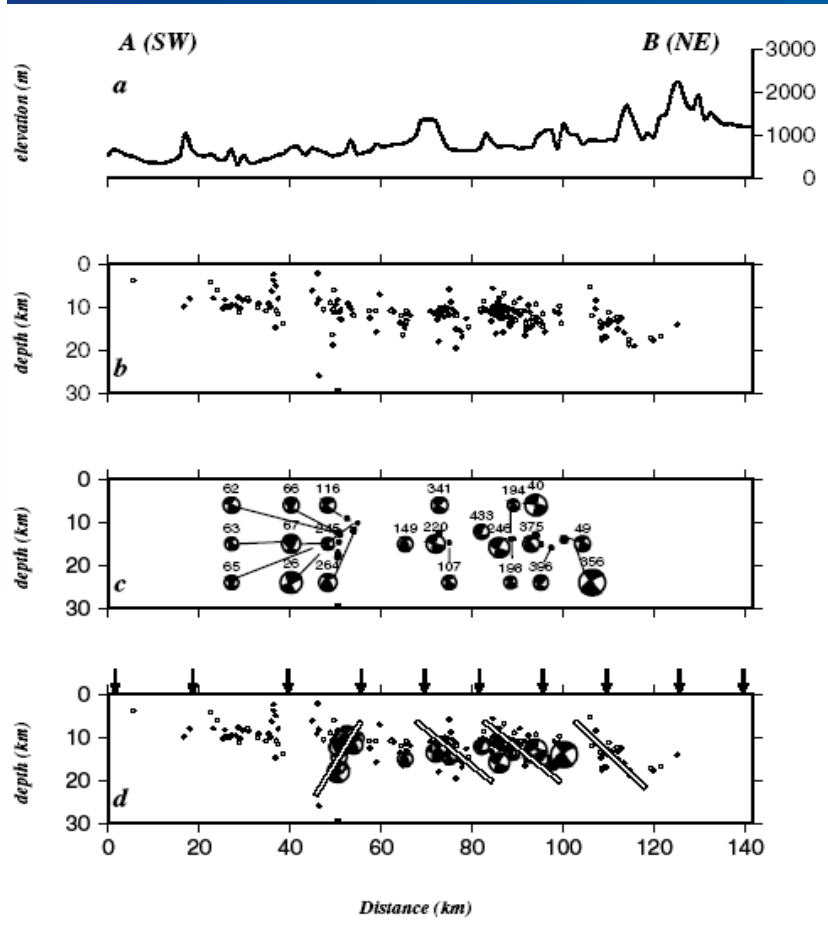
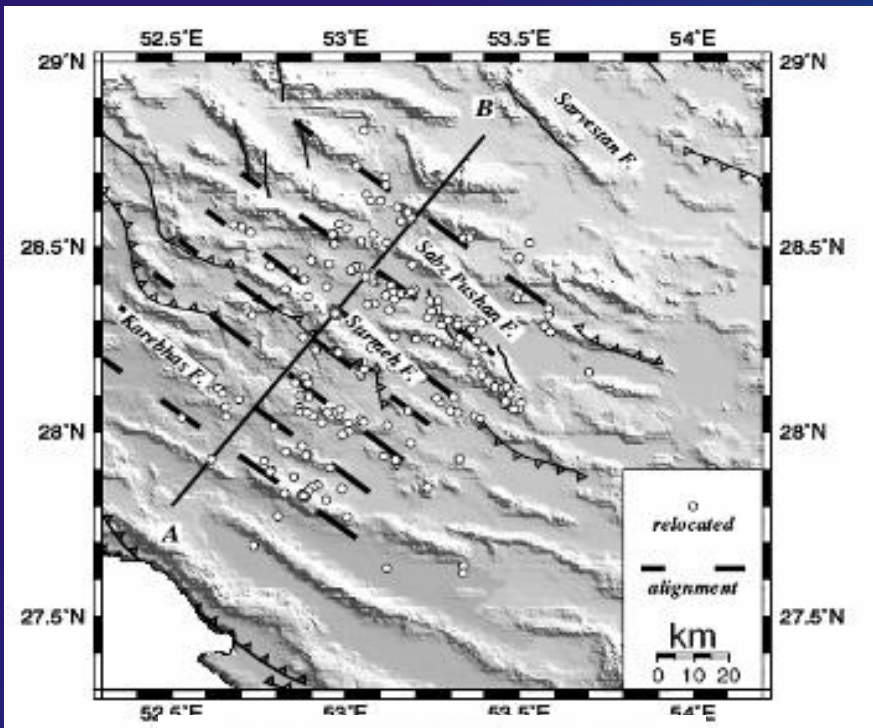




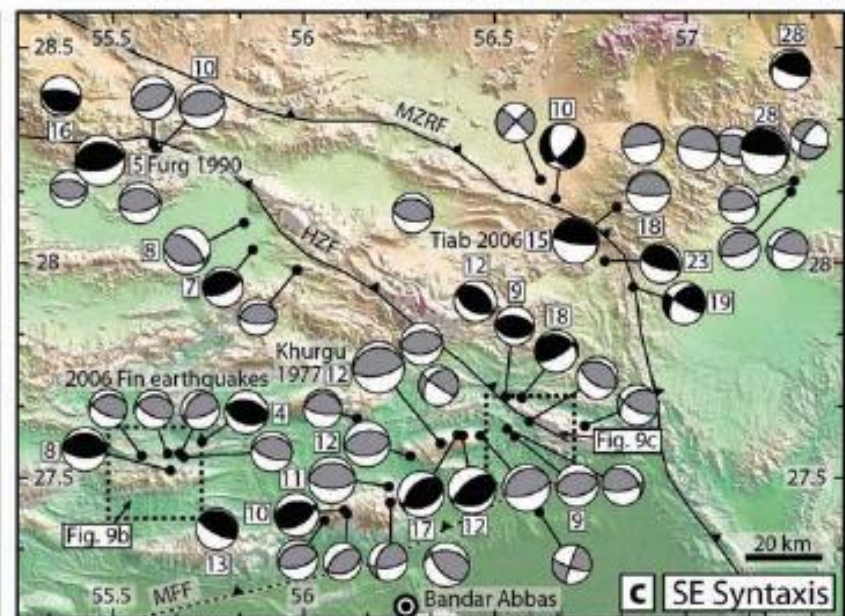
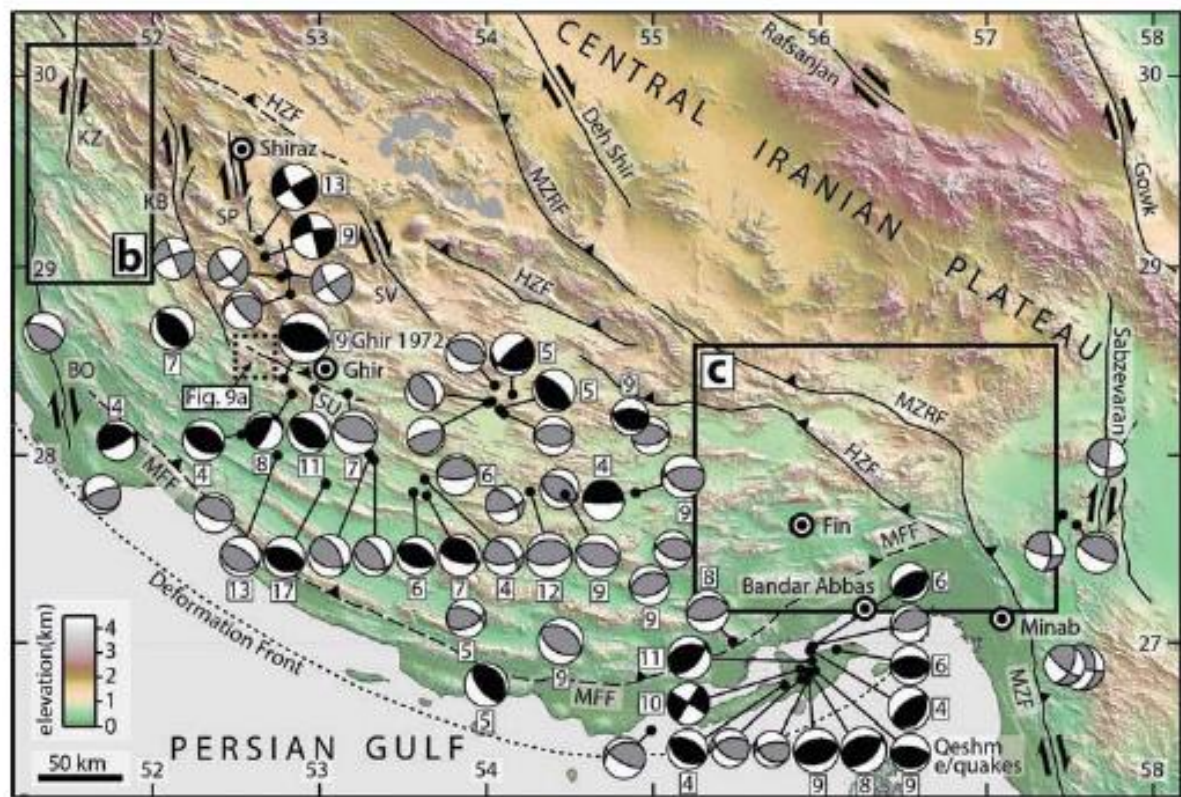
(Lacombe and Bellahsen, 2016)

Changing interpretations through time of the structural style of the Zagros Simply Folded belt (Fars)

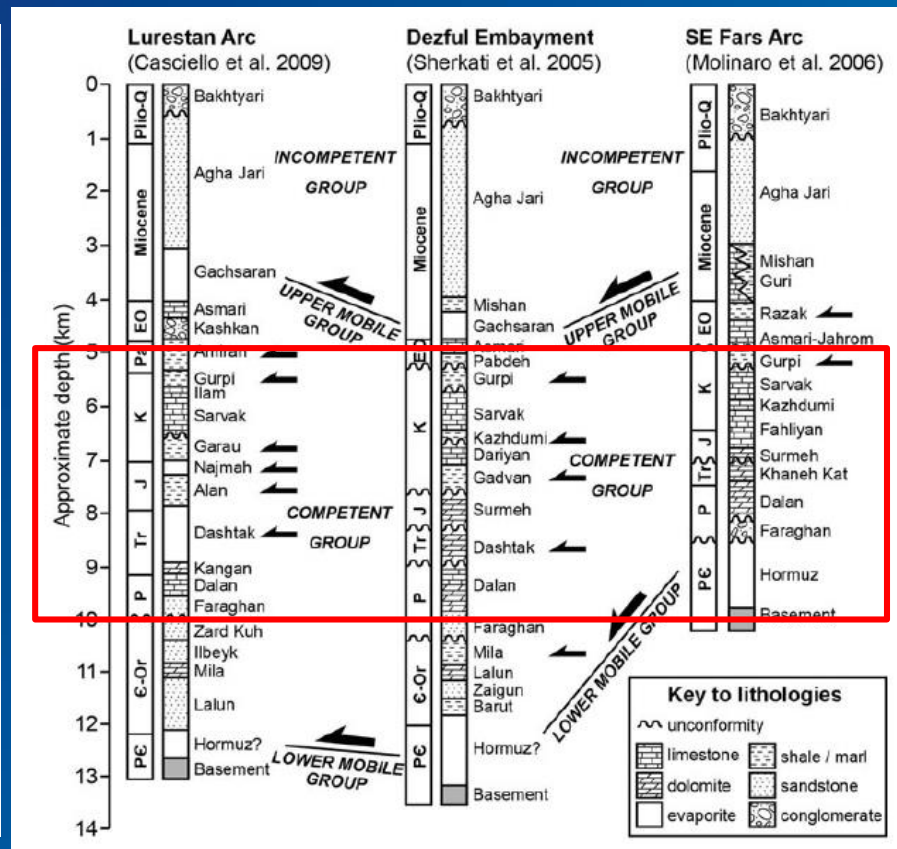
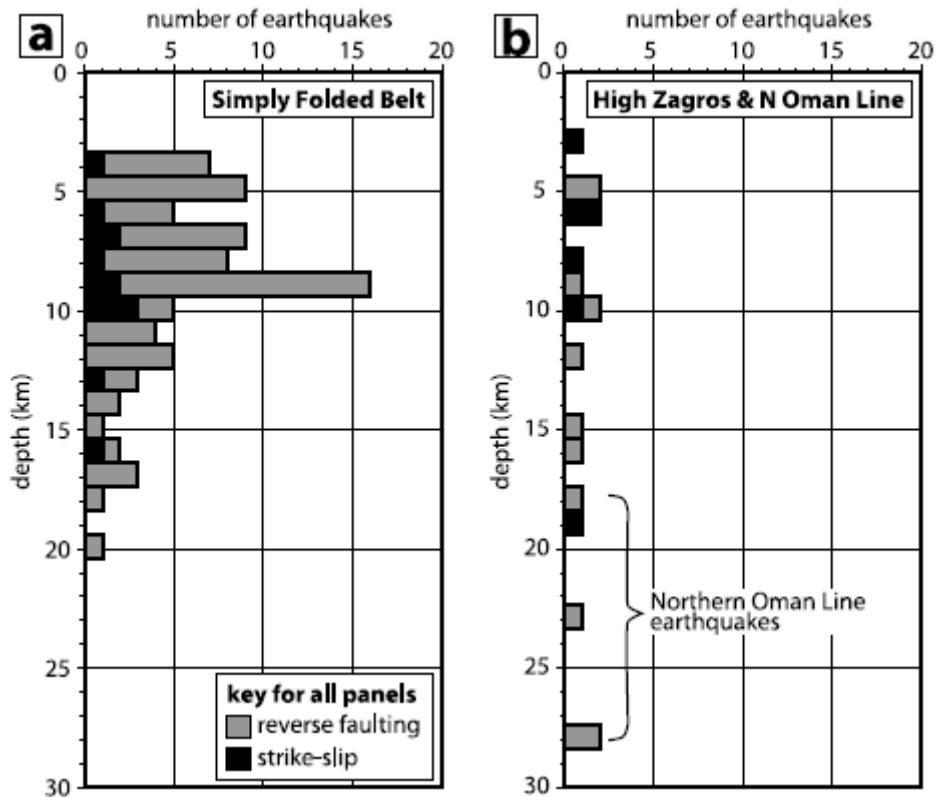
Localization of basement faults using microseismicity



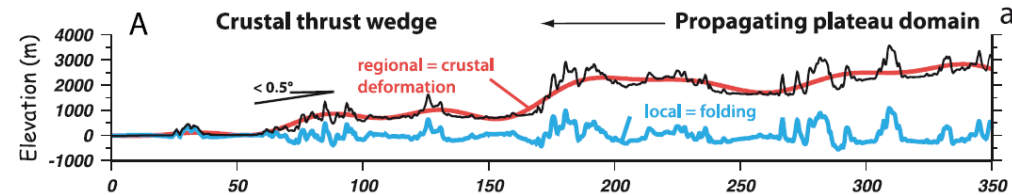
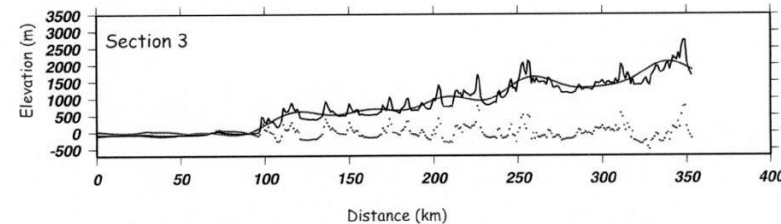
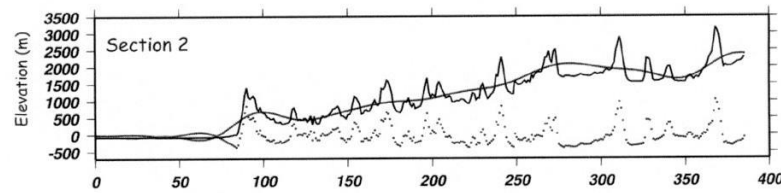
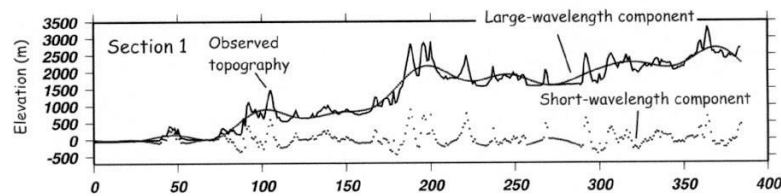
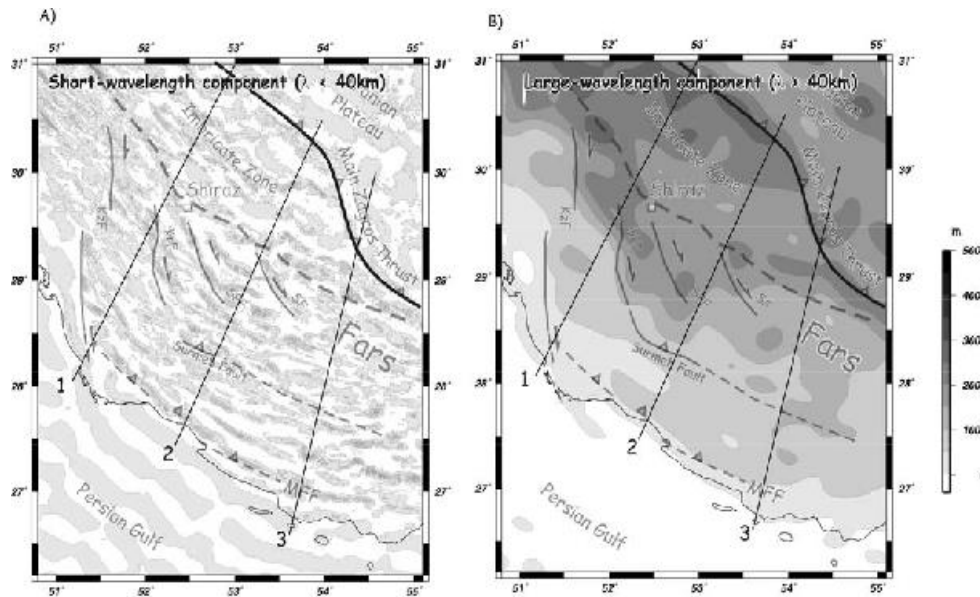
(Tatar et al. 2004)



(Nissen et al., 2011)

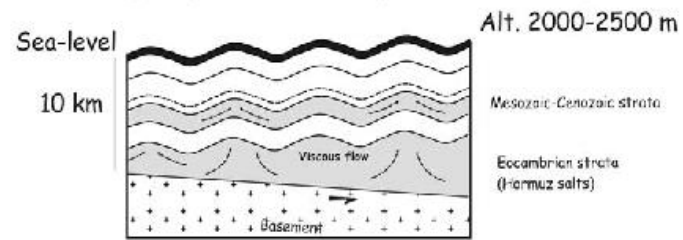


Analysis of topography

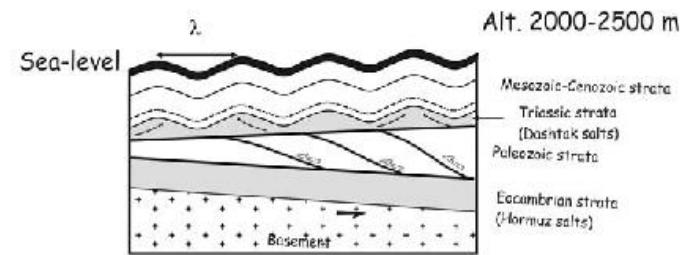
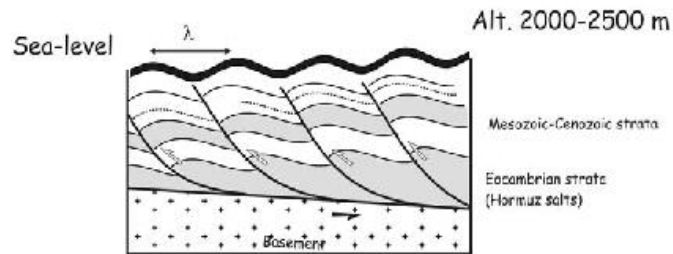


(Mouthereau et al., 2006, 2012)

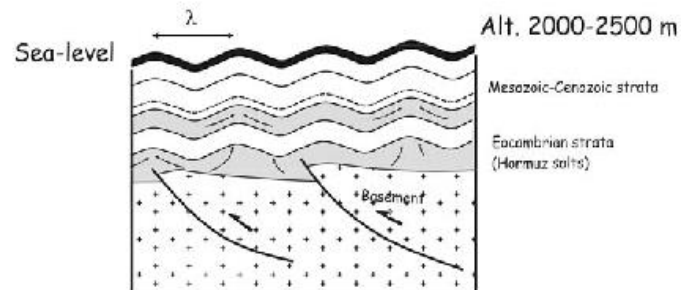
A) Wedge taper controlled by ductile thickening of salt

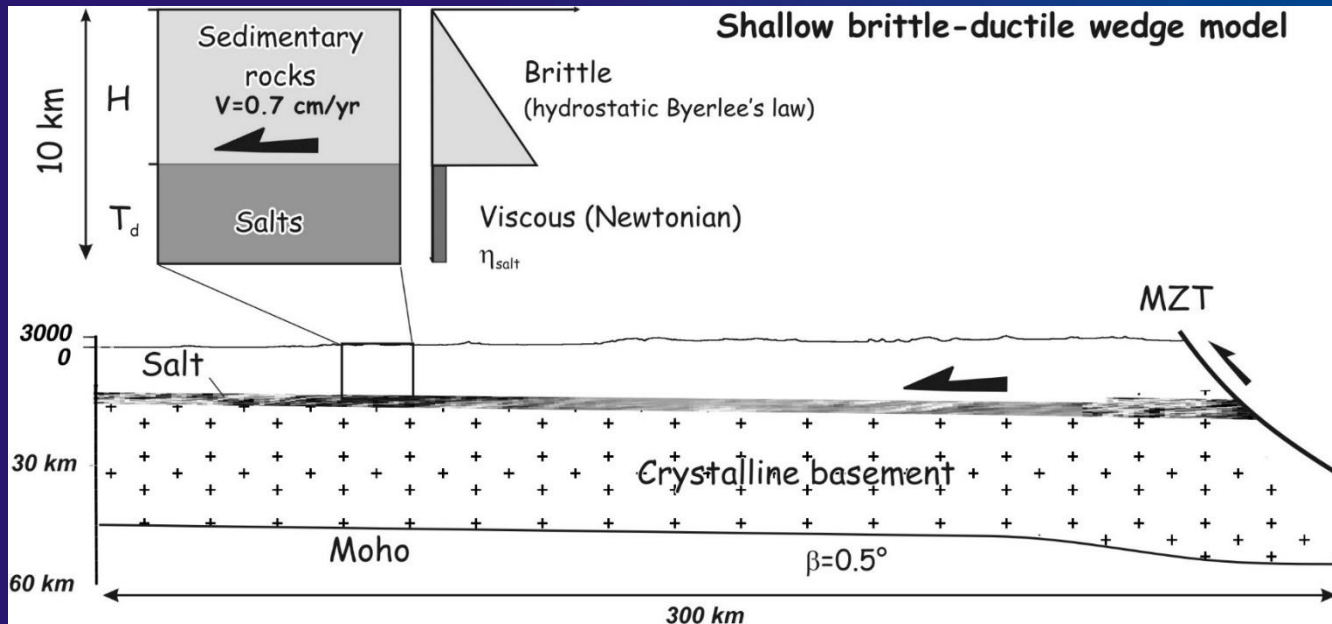


B) Wedge taper controlled by frictional behavior of sedimentary rocks

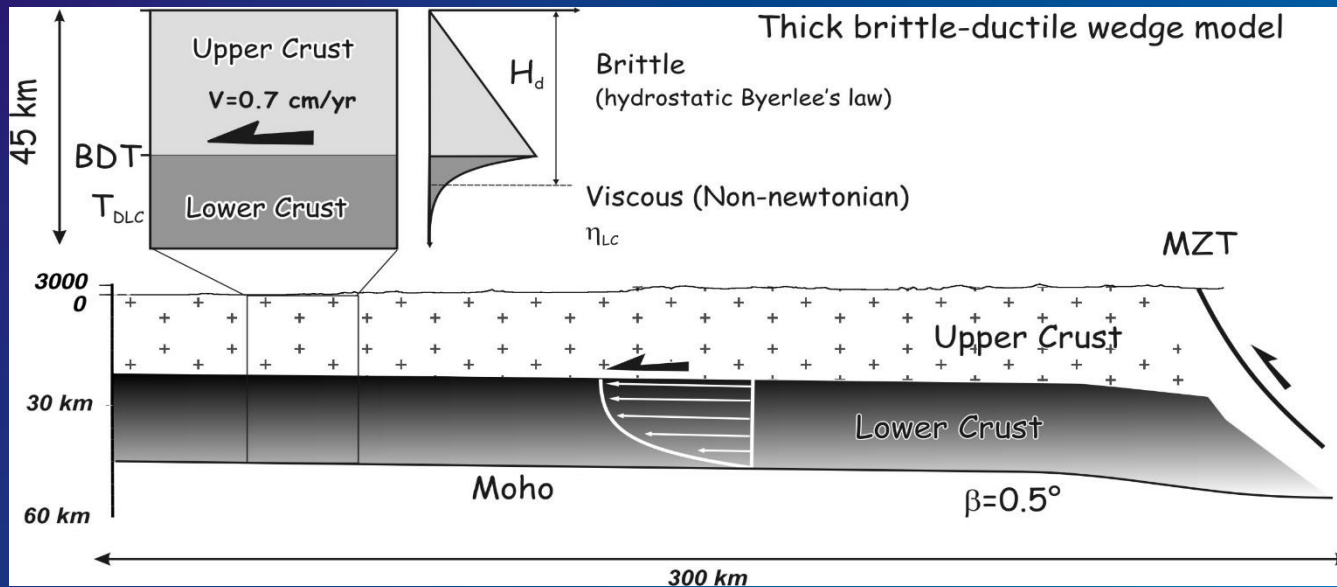


C) Wedge taper controlled by basement-involved faulting

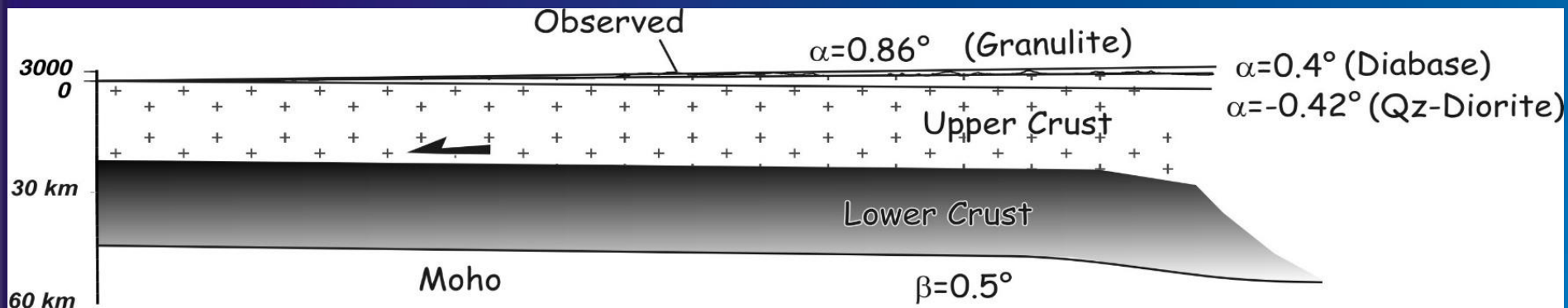




Critical wedge
analytical
modelling of
the Zagros
belt



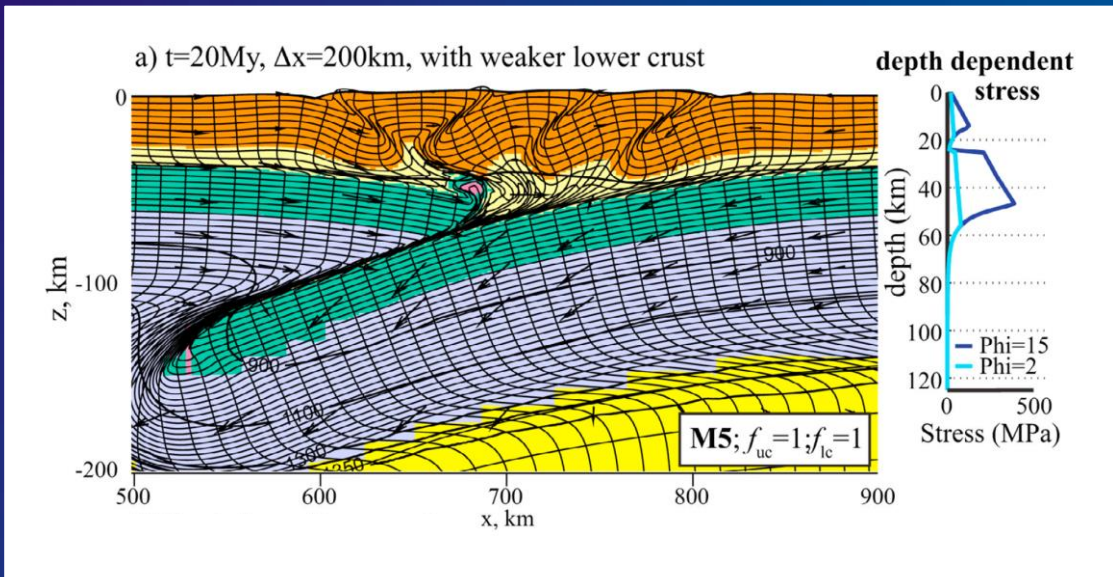
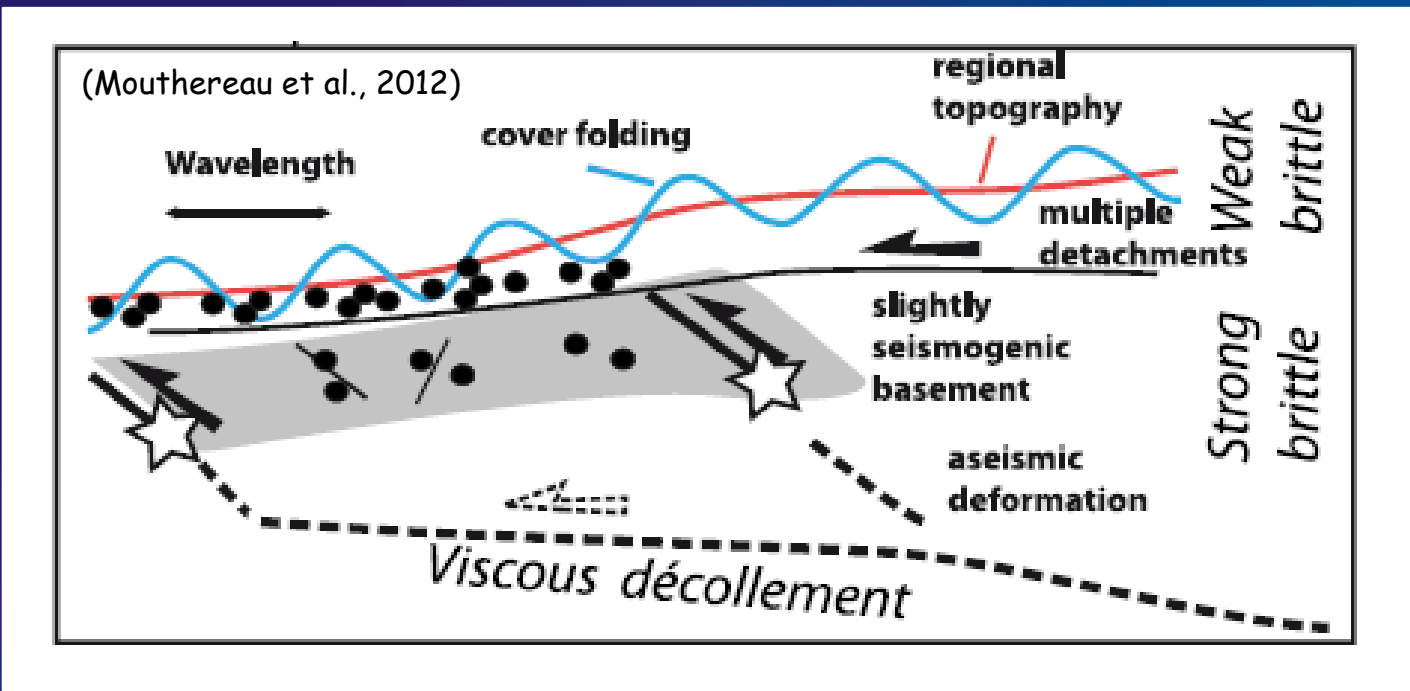
(Mouthereau et al., 2006)



(Mouthereau et al., 2006)

Salt is unable to sustain topography.

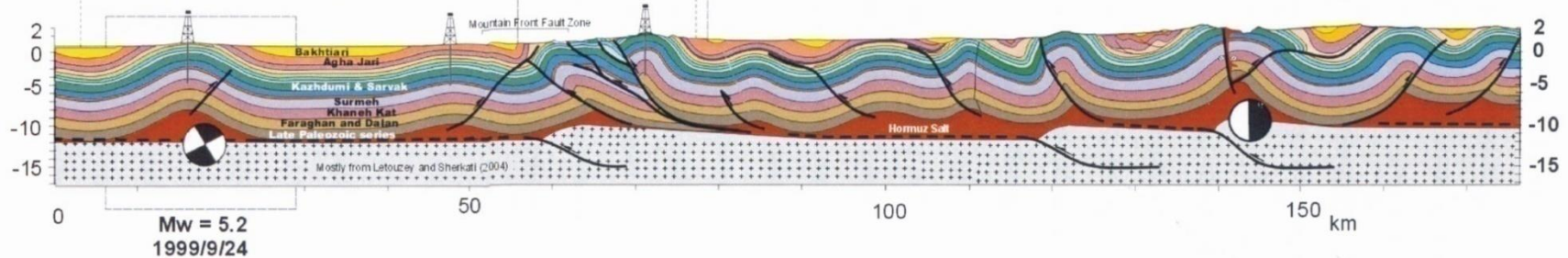
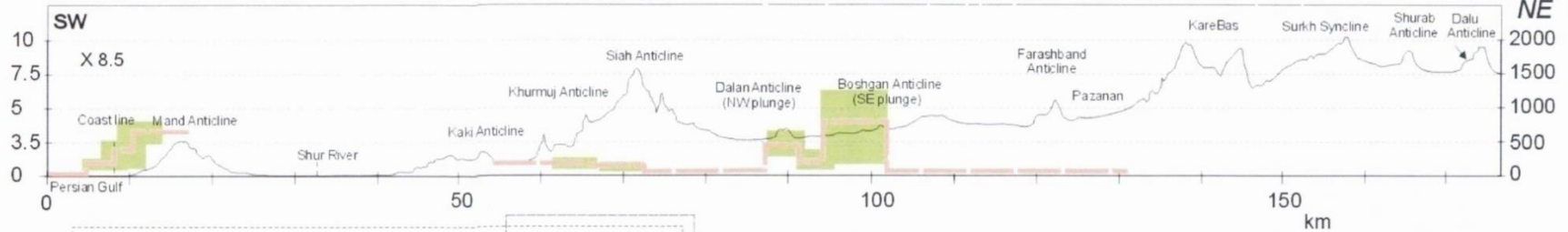
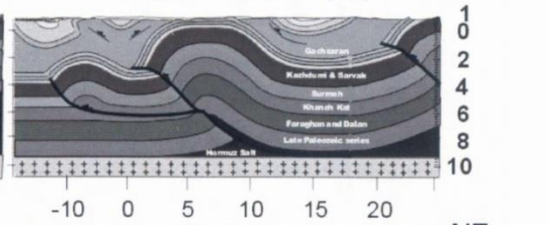
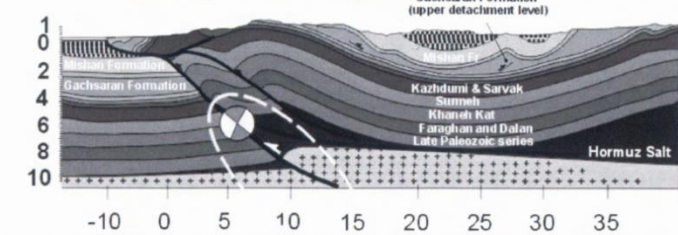
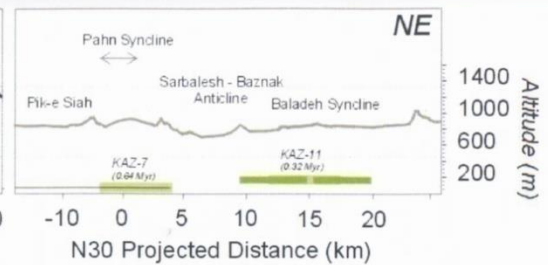
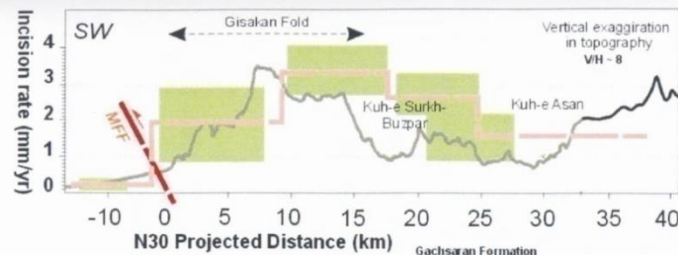
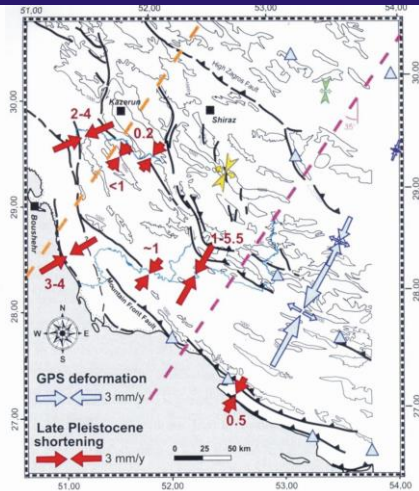
Only a model of critically-tapered brittle-viscous wedge involving the crystalline basement reproduces the observed topographic slopes across the Fars



2D thermomechanical modelling approach

- the Zagros = broad orogenic domain involving forelandward propagation of thick-skinned thrusts
- well captured by an orogenic system with weak upper and lower crusts, which leads to deformation being accommodated on a few thick-skinned crustal-scale thrusts with moderate displacement and by distributed thickening of the crust.

(Jammes and Huisman, 2012)



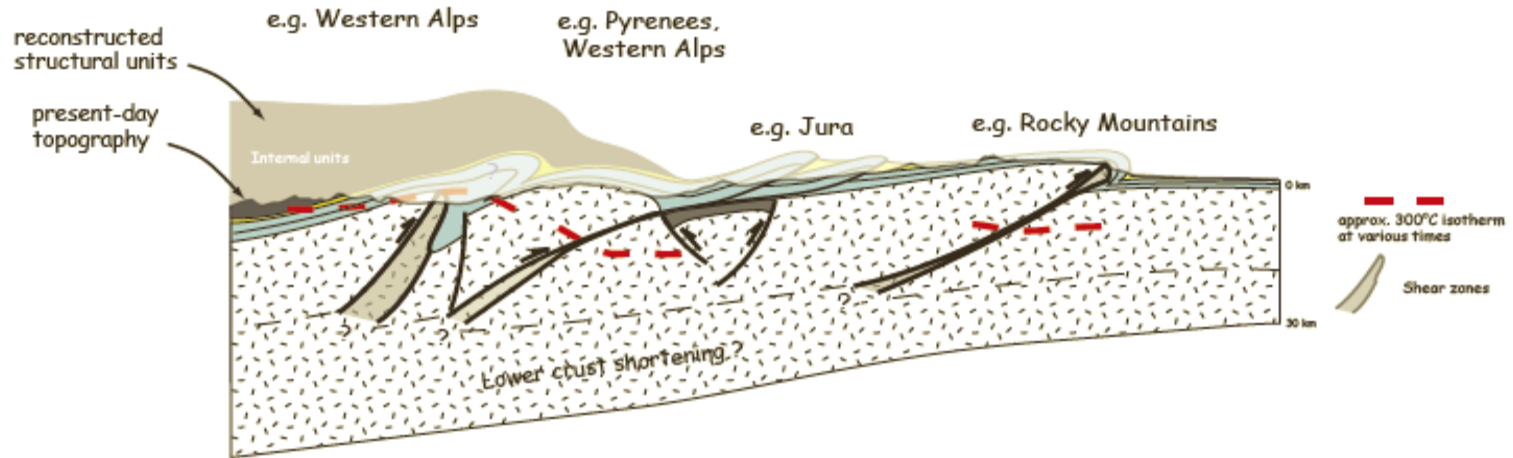
(Oveisi, 2007)

Outer folds accommodate most of current shortening in the Zagros. Their growth over the last My can be accounted for either by thin-skinned tectonics, or by the activity of underlying basement faults.

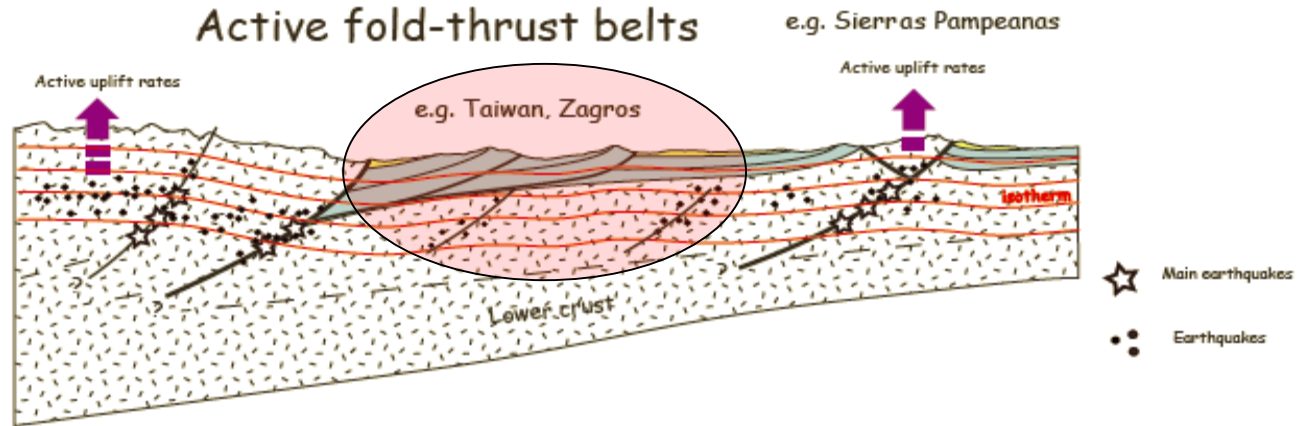
Cover and basement are mostly decoupled :
this is in agreement with superimposed thin- and thick-skinned tectonics styles.

Tertiary fold-thrust belts

(Lacombe and Bellahsen, 2016)



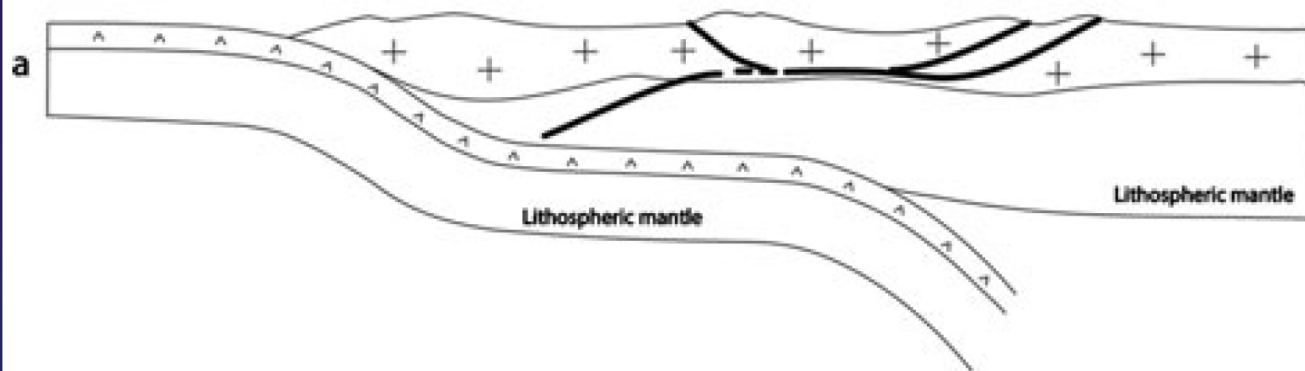
Active fold-thrust belts



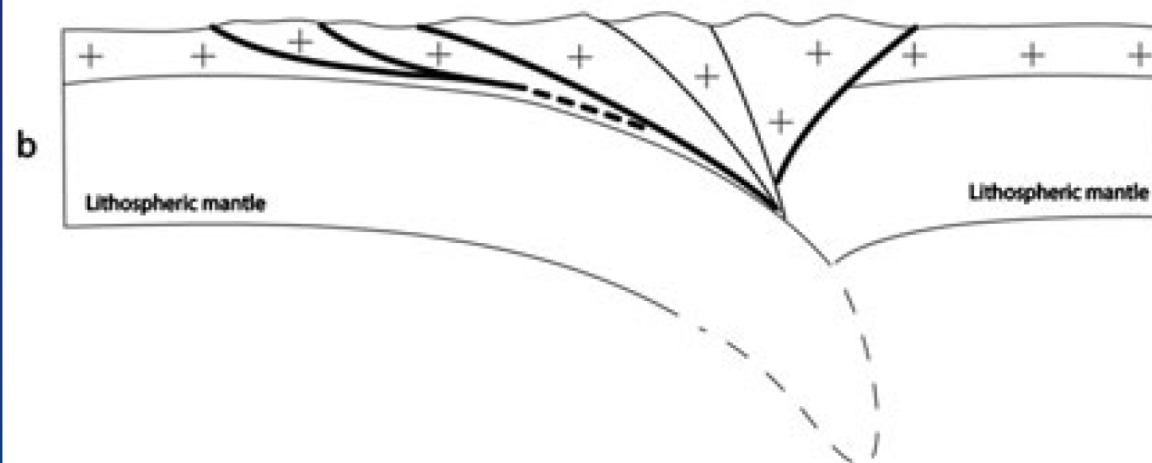
In active orogens (Zagros), evidence for basement involvement in shortening come from seismological, geodetic and morphological evidence (+ structural and seismic analyses)

**Thick-skinned tectonic style :
the Laramide belt**

Basement-involved shortening in the upper plate above an oceanic flat-slab subduction zone

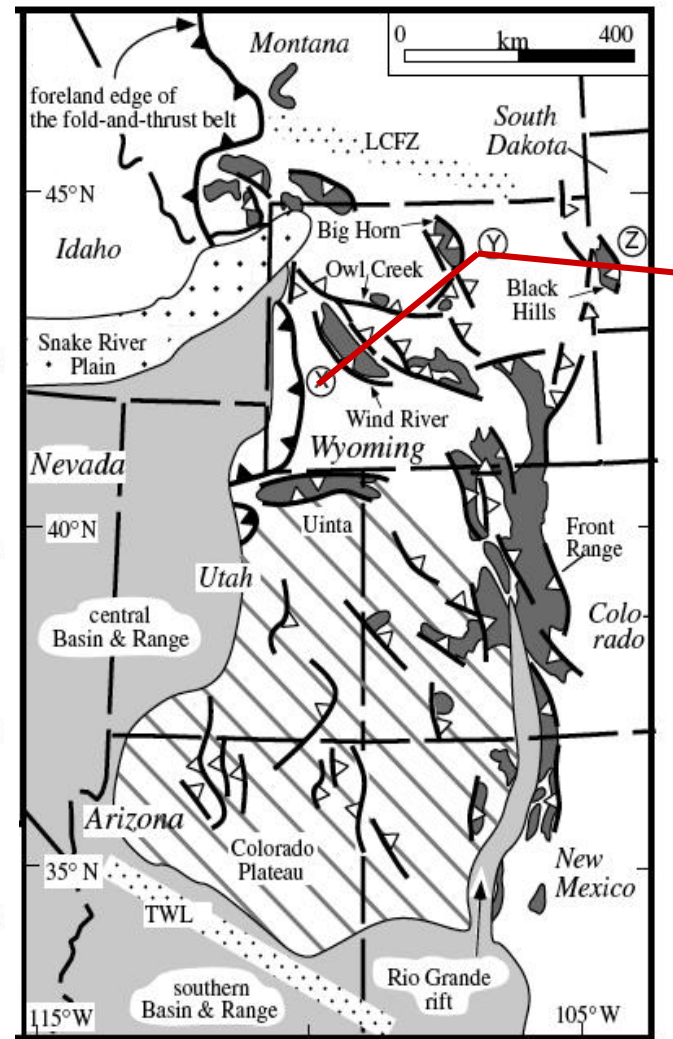
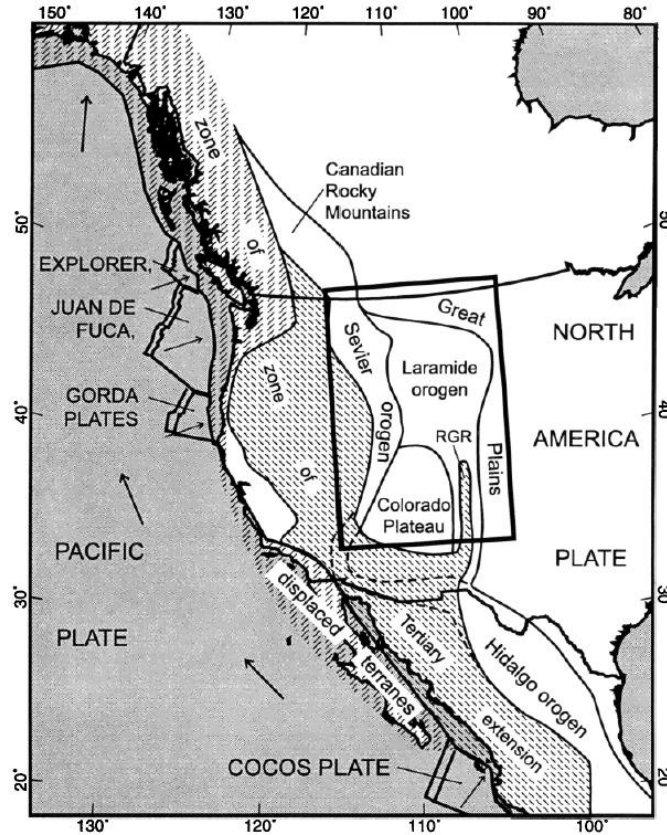


'Classical' basement-involved shortening in the lower/upper plate



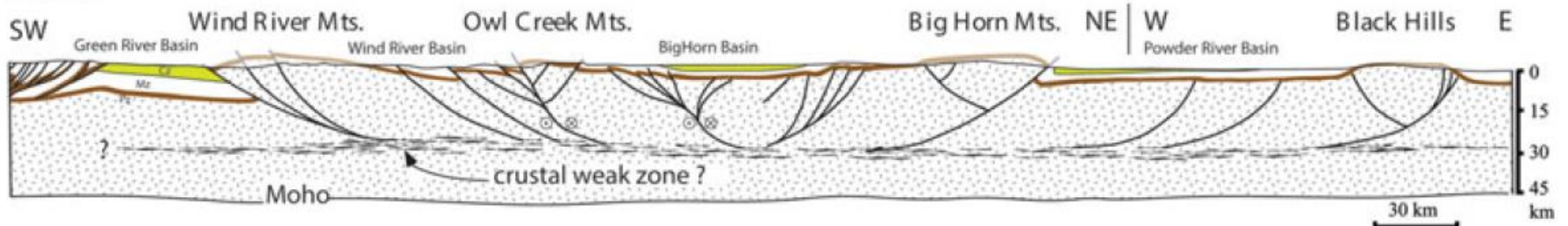
(Marshak et al., 2000;
Lacombe and Bellahsen, 2016)

The Laramide belt exhibits a network of anastomosing basement-cored anticlines and uplifts separated by broad basins. The basement arches are bounded by moderate-dipping crustal thrusts, likely resulting from the reactivation of Precambrian normal faults.



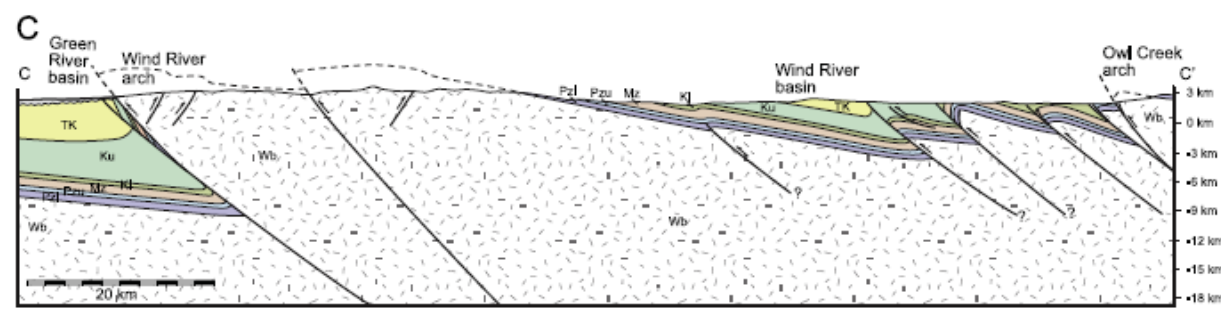
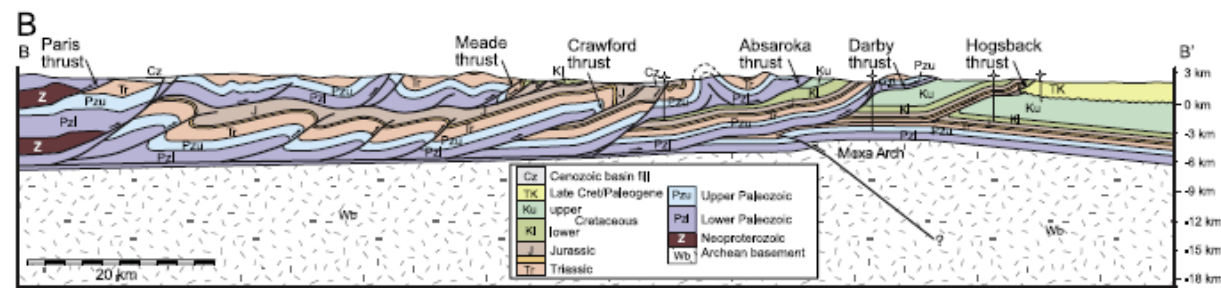
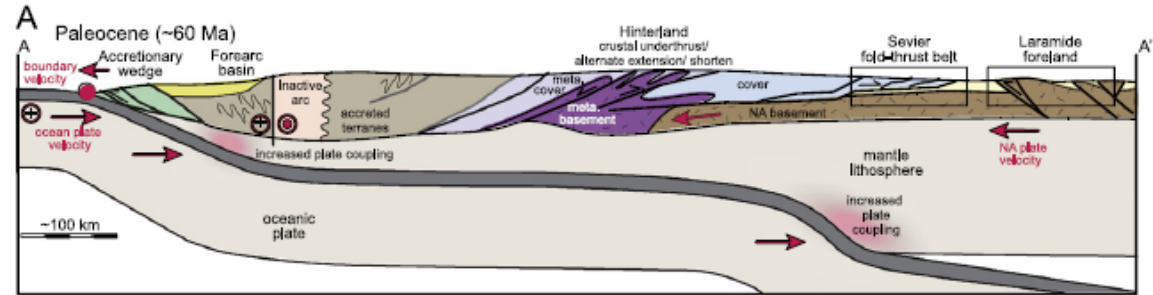
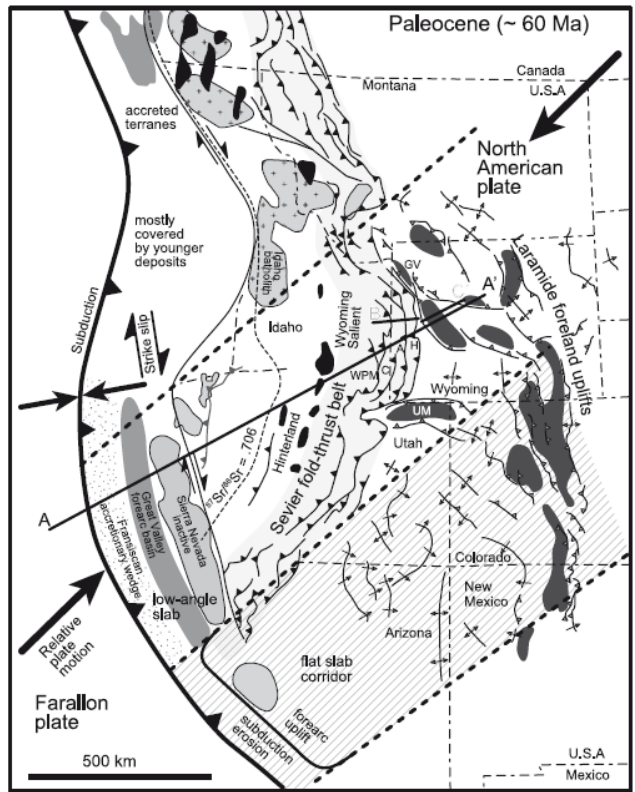
SEVIER
THIN-SKINNED
THRUST BELT

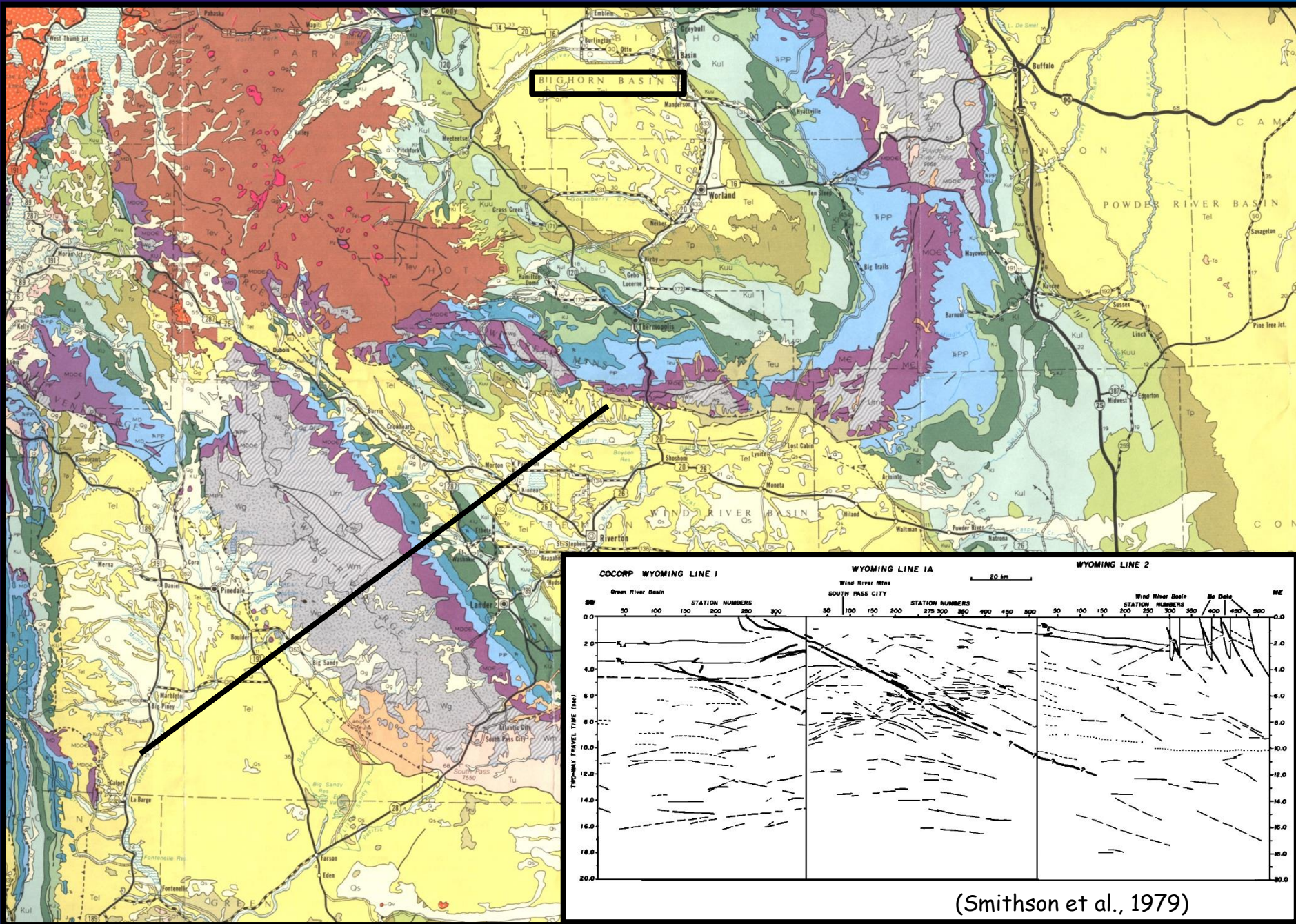
LARAMIDE THICK-SKINNED THRUST BELT



The Laramide belt consists of the deformed and disrupted foreland of the former Sevier orogeny.

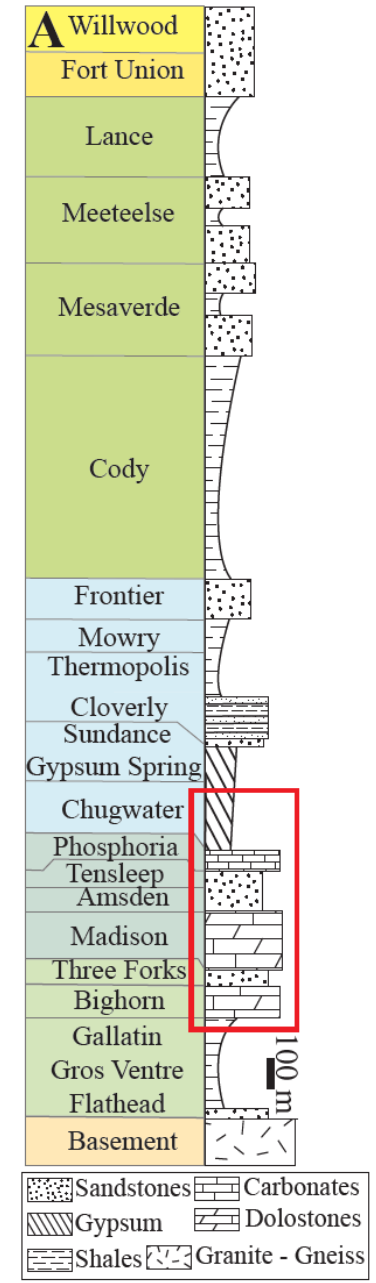
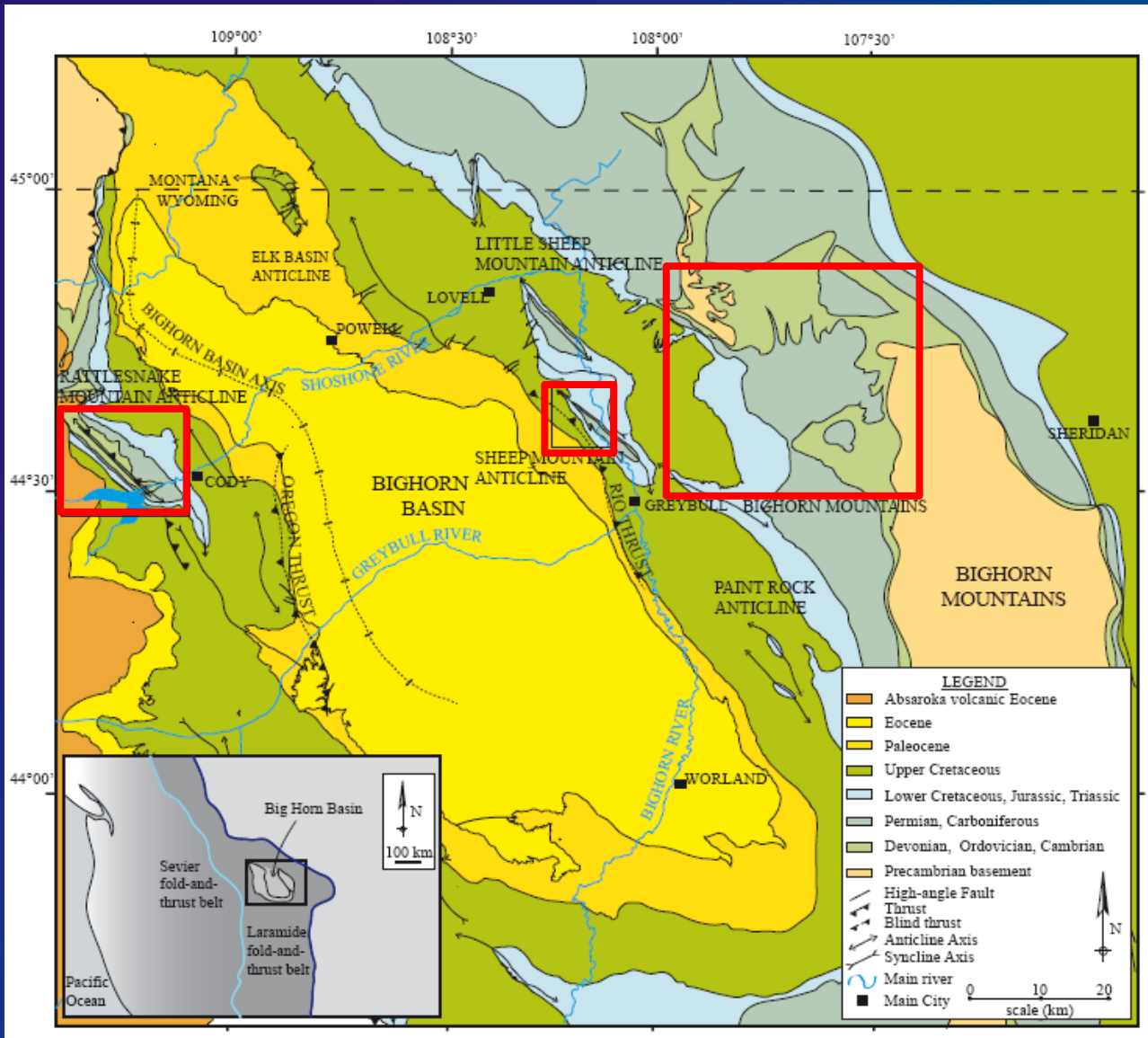
It formed in response to the long-lasting subduction of the Farallon plate at the expense of the North American cratonic upper plate during late Cretaceous-Paleogene.

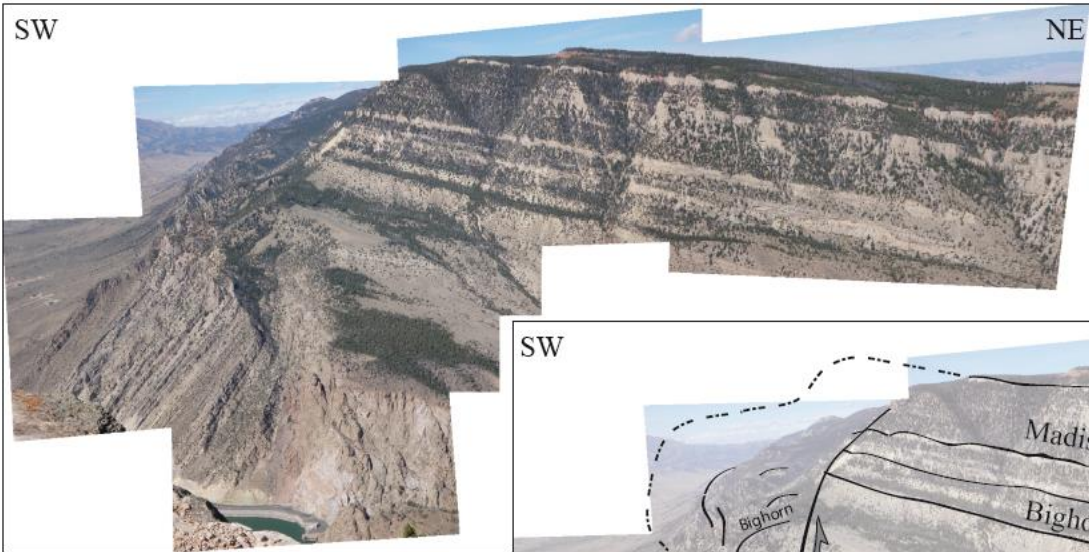




(Smithson et al., 1979)

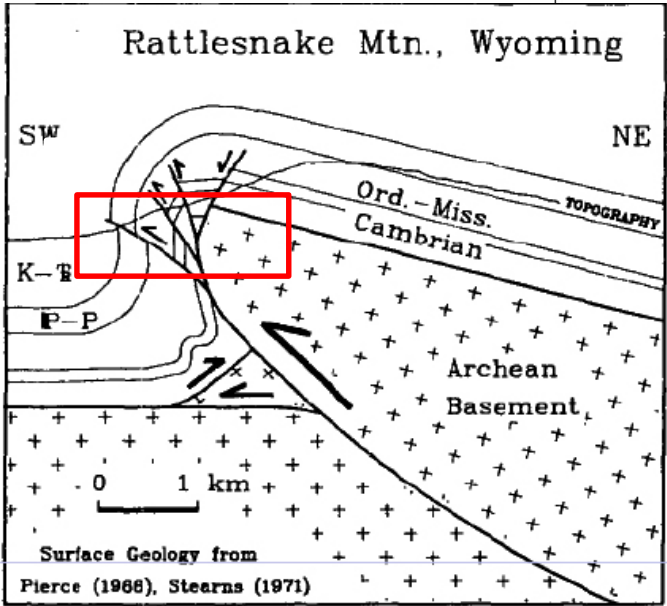
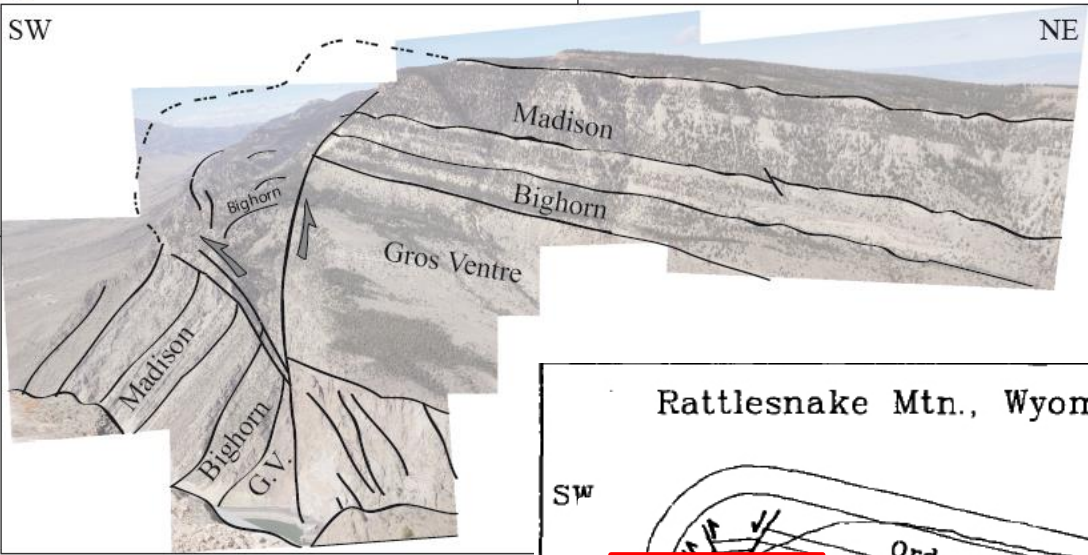
The Bighorn basin and its surrounding basement-cored anticlines and arches





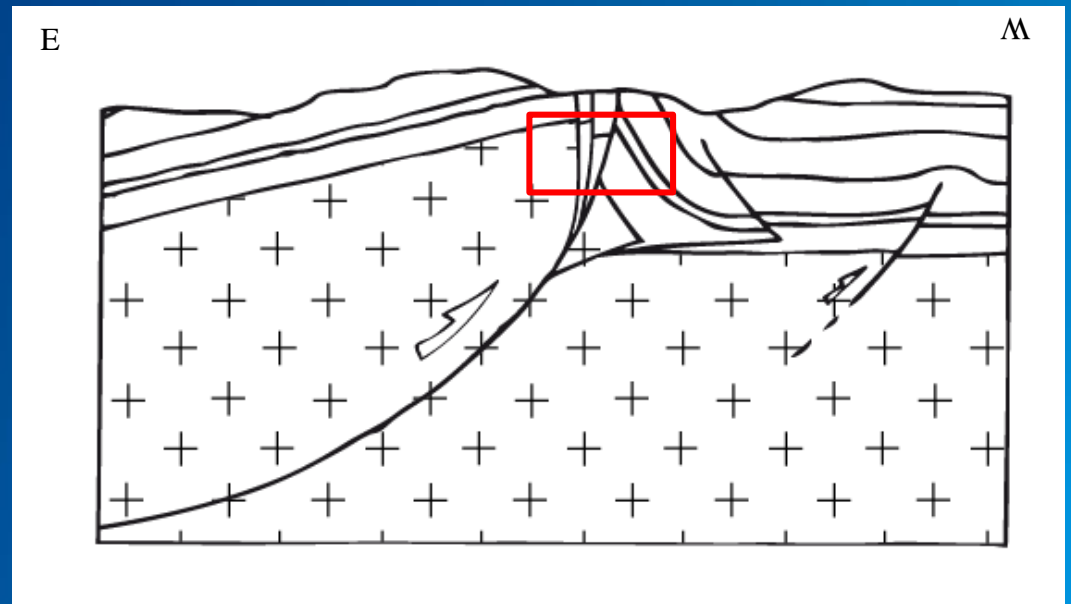
Rattlesnake Mountain
basement-cored anticline

(Beaudoin et al., 2012)



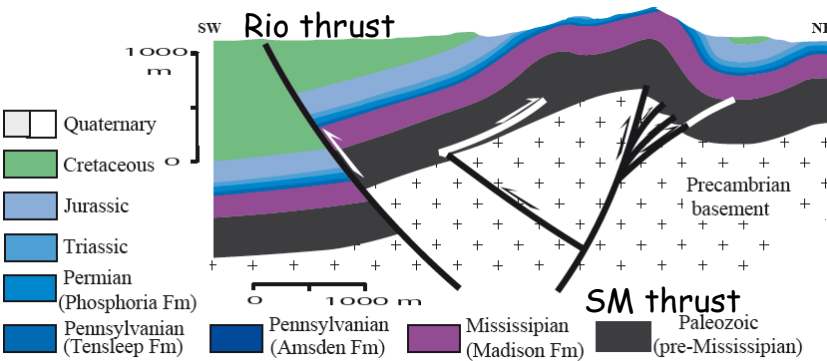
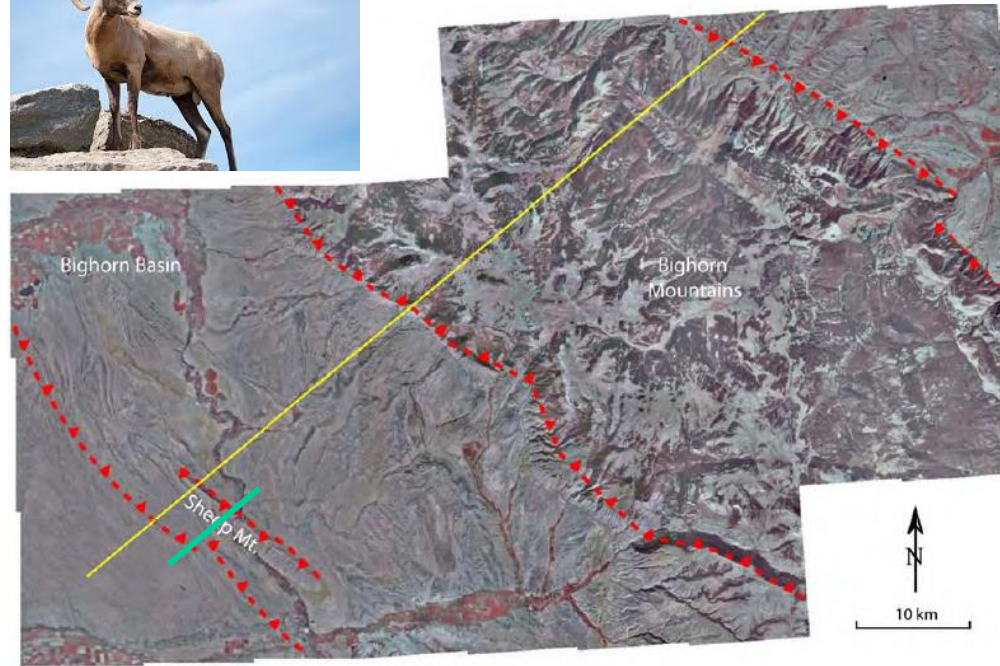
Erslev, 1986)



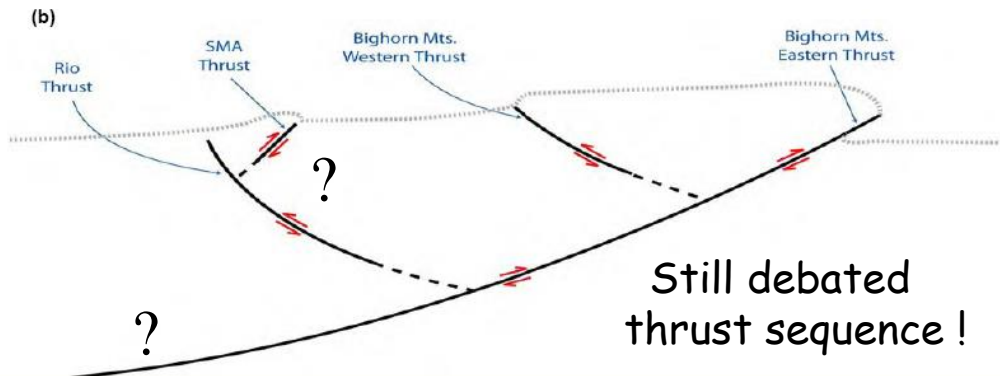




Sheep Mountain basement-cored anticline



(Amrouch et al., 2010)



Still debated thrust sequence !



Western Big Horn basement arch

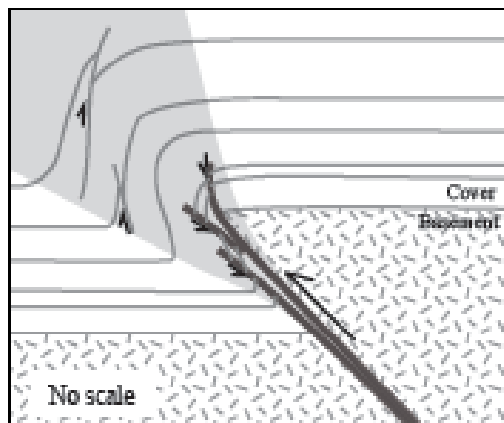
The mechanical response of the basement rocks / the overall fold geometry depend on :
P-T conditions during deformation; nature and orientation of pre-deformation basement fabrics;
competence of cover rocks; degree of coupling of folded strata with basement blocks.

Basement can be deformed through : slip on closely spaced fractures; flexural slip on pre-existing foliation oriented sub-parallel to bedding; slip on foliation favorably oriented for simple shearing parallel to the fault.

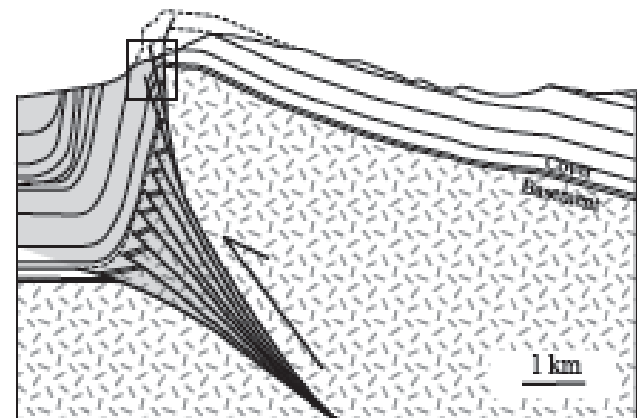
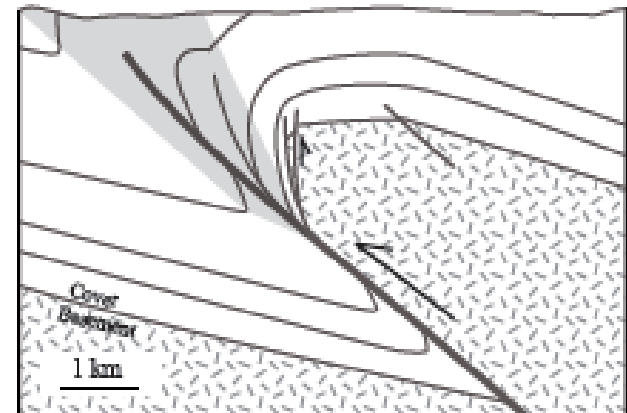
Most outcropping basement rocks are mainly
brittly deformed at shallow depth (about 2.5 to
5 km) and at a temperature of about 70-120°C)

Laramide cover folding is not related to true
basement « folding » but is instead associated
with distributed damaging of basement rocks by
pervasive fluid-assisted faulting/fracturing
and/or cataclasis ahead of the propagating thrust.

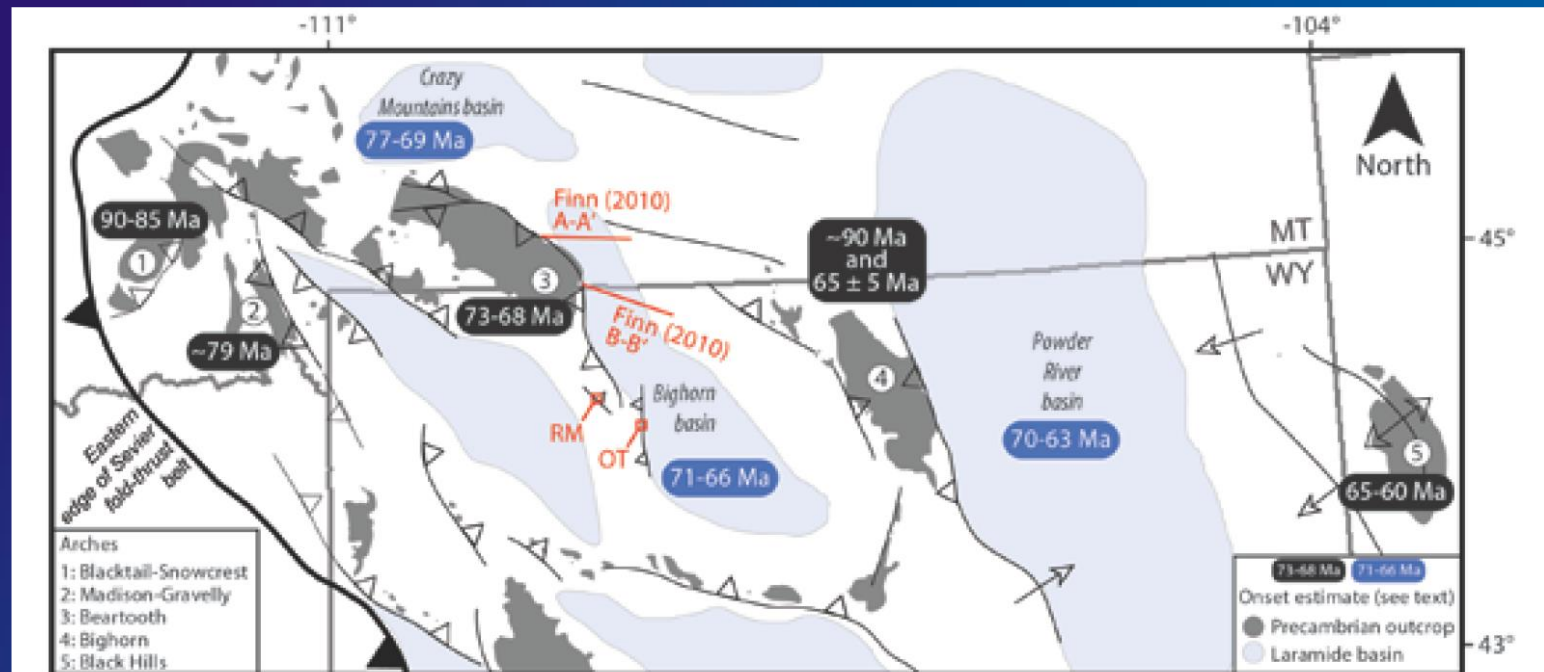
Tri-shear model



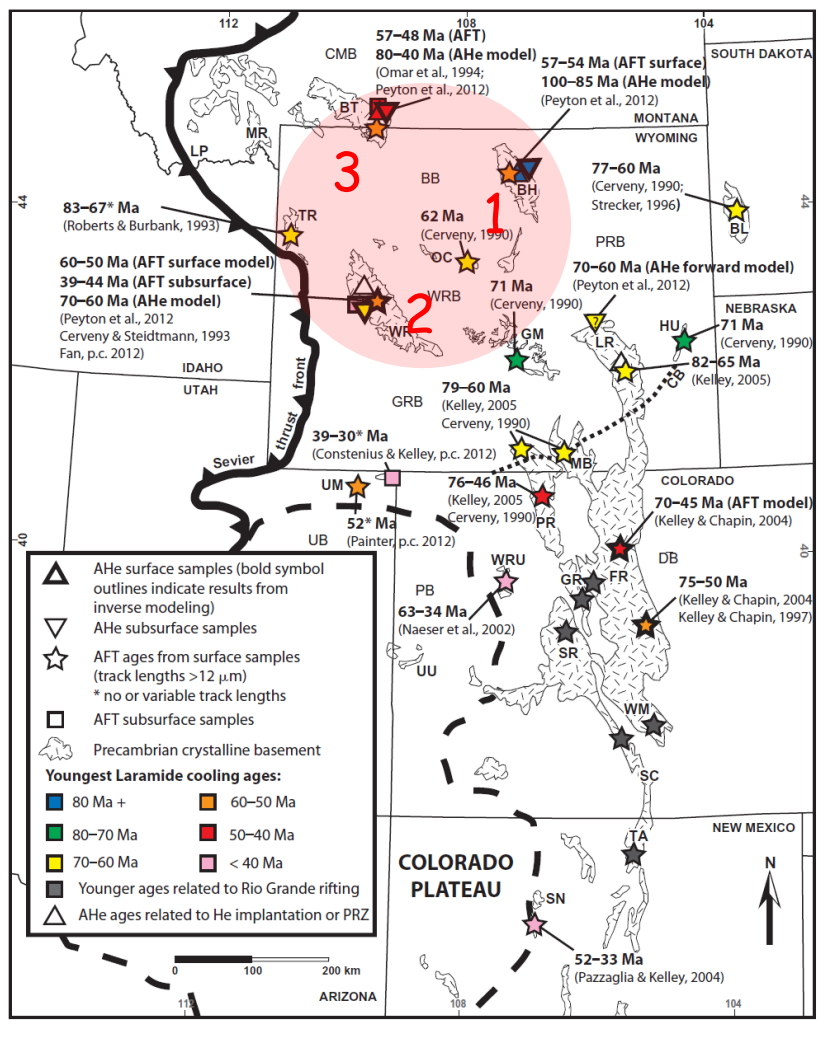
(Lacombe and Bellahsen, 2016)



In northern Wyoming - Montana, thermochronology and stratigraphy seemingly support an eastward sequence of thick-skinned Laramide deformation

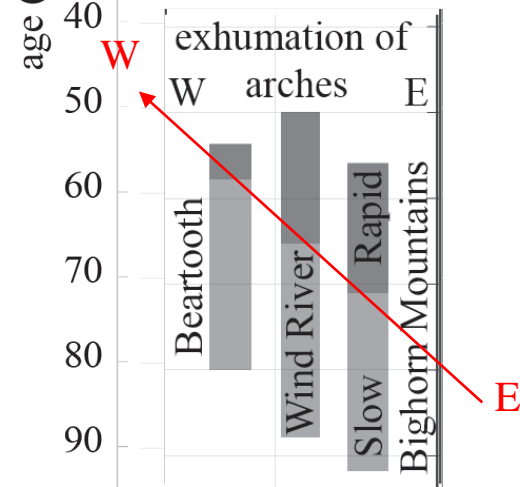


Map showing structural arches and basins
RM—Rattlesnake Mountain anticline; OT—Oregon thrust.



(Peyton et al., 2012)

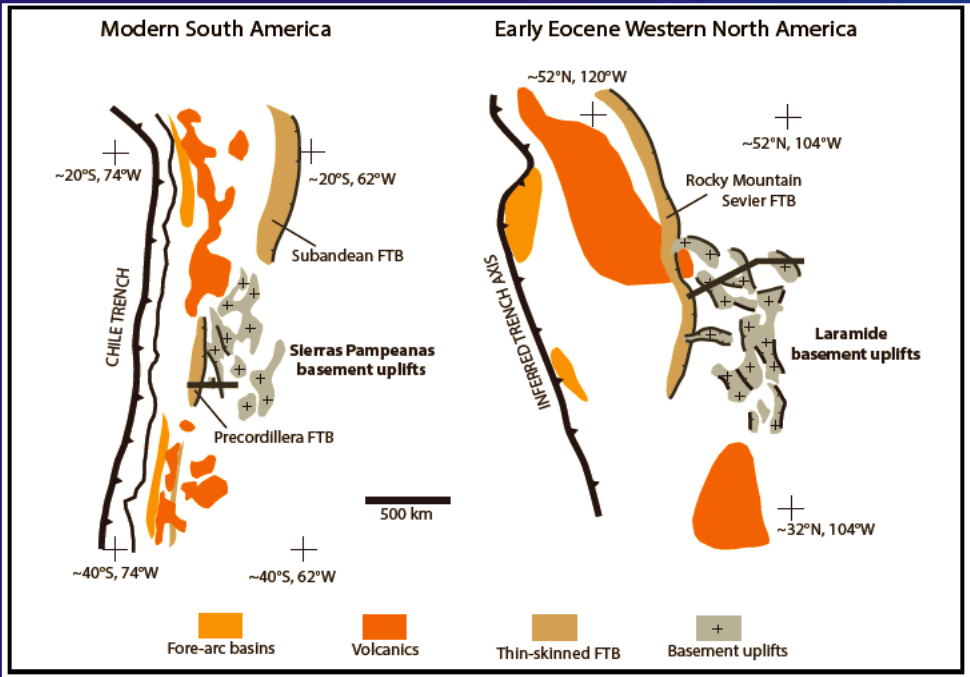
Arches around BHB cooled/exhumed slowly, then rapidly in a rather westward sequence



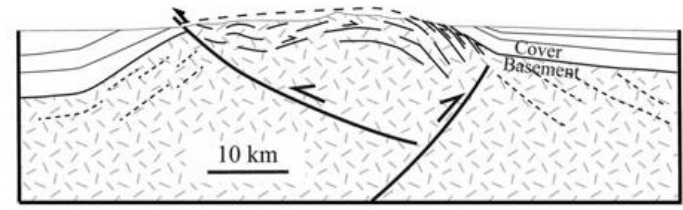
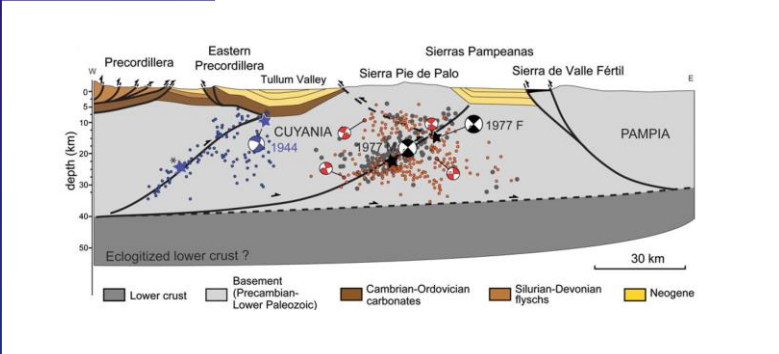
(Fan and Carrapa, 2014; Stevens et al., 2016; Beaudoin et al., 2018, 2019)

The Laramide arches were exhumed first at slow rate then at higher rate in an overall eastward (cratonward) sequence of deformation, but a westward sequence of uplift is documented in/around the Bighorn basin.

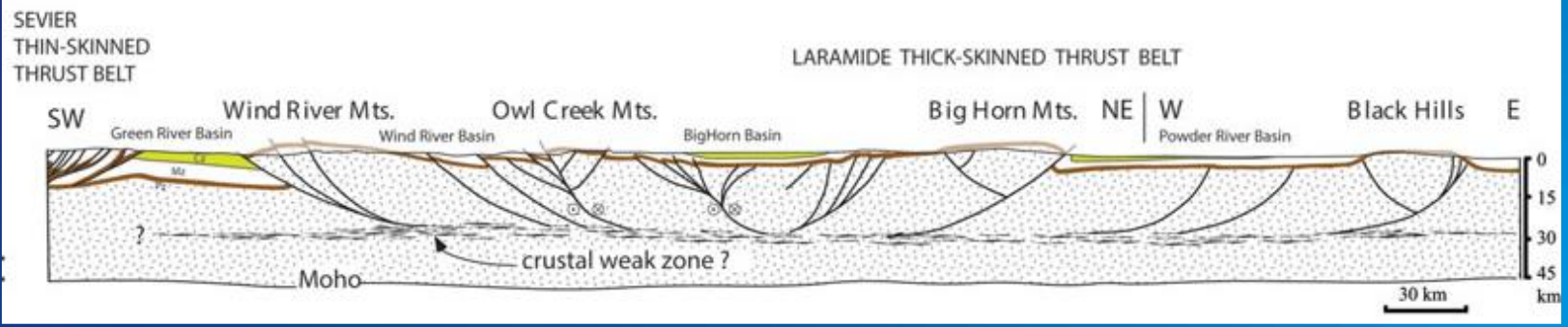
This somewhat erratic sequence is probably linked to the heterogeneous and complex stress transmission and accommodation of shortening through the crystalline basement that displays inherited weaknesses and anisotropies.



(Jordan and Allmendinger, 1986;
 Lacombe and Bellahsen, 2016;
 Bellahsen et al., 2016)

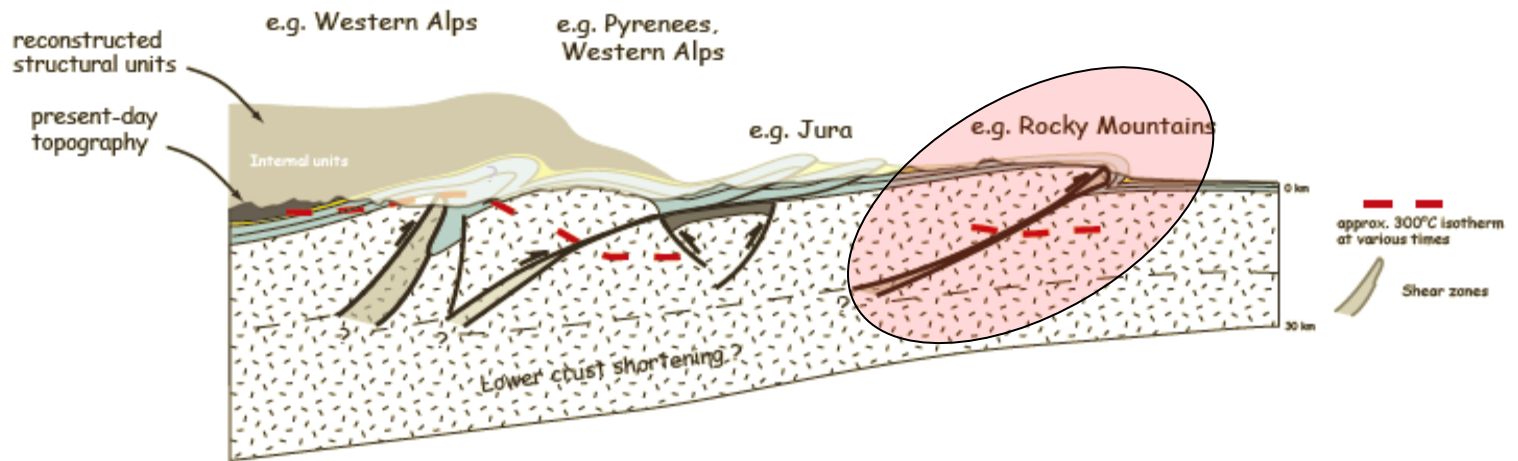


Mode of basement deformation in the Sierra Pie de Palo



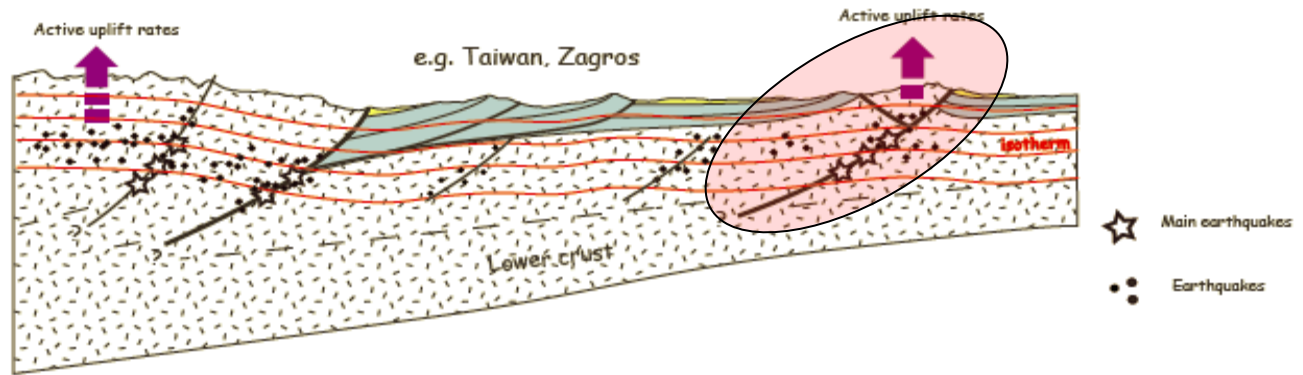
Tertiary fold-thrust belts

(Lacombe and Bellahsen, 2016)



Active fold-thrust belts

e.g. Sierras Pampeanas



In the upper plate setting of flat slab subduction (Laramide, Sierras Pampeanas), evidence for basement involvement in shortening come from structural, seismic, seismological, and morphological studies

Fold-and-thrust belts, and more generally fold-and-thrust belt / foreland basin systems are beautiful and exciting playgrounds, and targets of great interest for the study of various geological processes, including mountain building, deformation, kinematics and rheology of the lithosphere, vertical movements, thermicity, interaction between deep and surface processes, mass transfer, resource exploration, ...



Thank you for your attention